NEW ZEALAND GEOTECHNICAL SOCIETY INC

JUNE 2021 issue 101

NZ GEOMECHANICS NEWS

Bulletin of the New Zealand Geotechnical Society Inc.

ISSN 0111-6851

SCOTT BASE
REDEVELOPMENT PROJECT

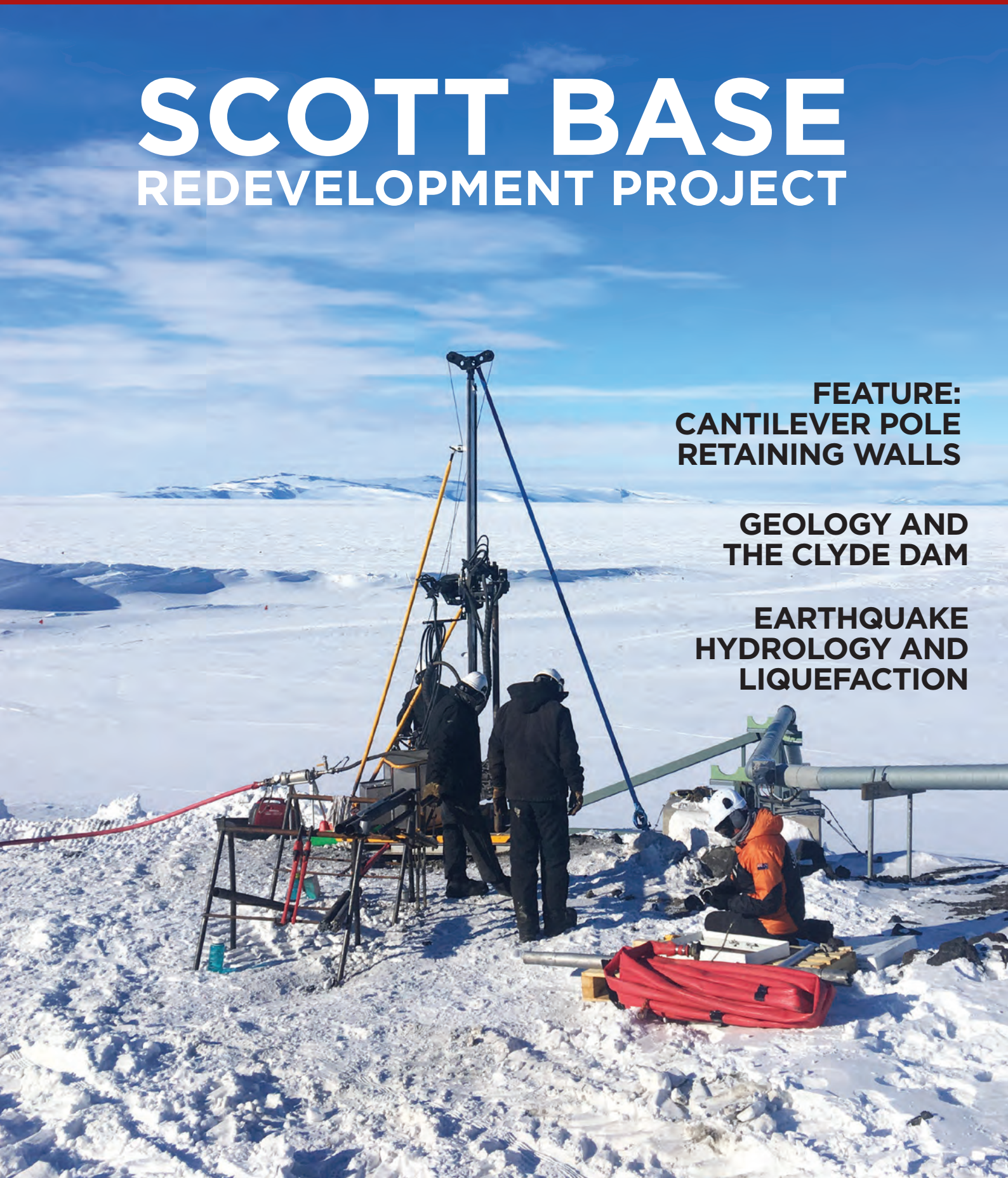

FEATURE:
CANTILEVER POLE
RETAINING WALLS

GEOLOGY AND
THE CLYDE DAM

EARTHQUAKE
HYDROLOGY AND
LIQUEFACTION

RETAINING YOUR BUSINESS IS OUR BUSINESS

Design	Construct	Perform	Improve
	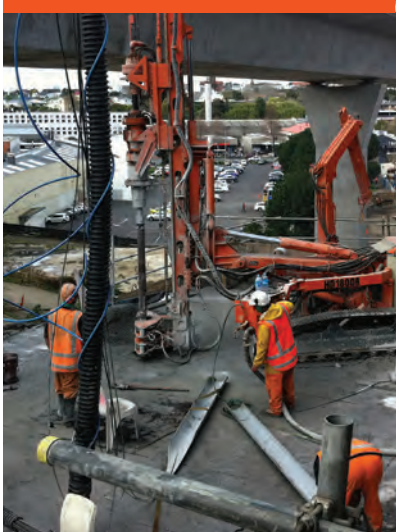	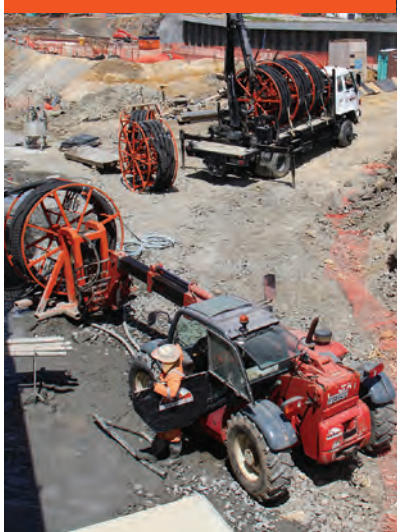	

For over more than 40 years, Grouting Services has delivered some of New Zealand's most significant Ground Anchoring, Soil Nailing, Micro-Piling and Post-Tensioning contracts.

With ground anchor technology advancing all the time, our association with Samwoo means our New Zealand clients will continue to have access to world-leading technology including:

- Removable compressive distributive anchors (SW-RCD)
- Removable distributive tension anchors (SW-SMART)
- Permanent compressive distributive anchors (SW-PCD)
- Permanent tensile frictional anchors (SW-PTF)

We have successfully completed some 5000m of removable anchors and the level of enquiry continues to rise as the sustainable benefits of this technology are realised - once a construction project is completed, there is nothing left in the ground that will obstruct future developments on adjoining properties.

Samwoo's anchor technology is economical, efficient and another way for Grouting Services to remain at the forefront of our industry.

If you're interested in working with us or finding out more about the results we've achieved for our clients call 09 837 2510 or visit our website.

Our multidisciplinary operation specialises in the fields of ground anchoring, soil nailing, drilling, post-tensioning and grouting. The combination of capability and depth of technical expertise makes us a market leader and supports our reputation for providing value engineered solutions to our customers.

GROUND ANCHORING	SOIL NAILING	GROUTING
POST-TENSIONING	SEISMIC UPGRADE	DRILLING

We're proud to be the sole distributor in New Zealand for Samwoo Anchor Technology, BluGeo GRP60 Bar, OVM Prestressing Systems, Tighter (Kite) Earth Anchors and Grout Grippa Grout Sock (Australasia).

GROUTING SERVICES

09 837 2510 www.groutingservices.co.nz

Your remote monitoring specialists

We specialise in the hire, supply and installation of cost-effective telemetry systems for geotechnical, environmental and structural instrumentation...and much more!

- **Eliminate manual data collection**
- **Automate reporting**
- **Minimise risk**
- **Maintain continuity of work**
- **Increase your data frequency**
- **Know what's happening on your sites in near real-time**
- **Stay notified if set parameters are exceeded via automatic notifications**

We have adaptable systems that can be tailored to suit your project...no matter how small or large.

Get in touch to find out how we can help you to work smarter!

t **0508 223 444**
e **enquiry@geotechnics.co.nz**
w **www.geotechnics.co.nz**

GEOTECHNICS

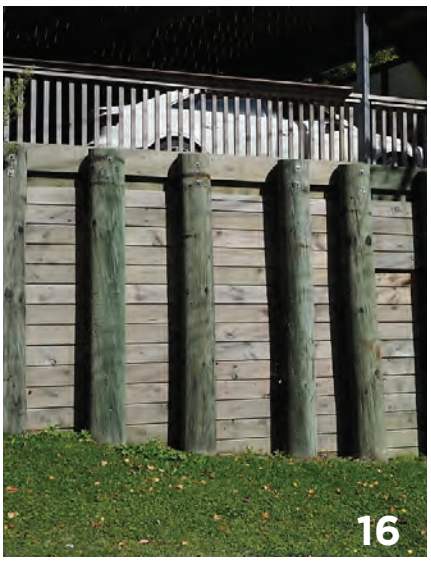

CONTENTS JUNE 2021

COVER IMAGE:
Matthew Jordan, Antarctica New Zealand

From the Chair

Ross is Auckland Council's geotechnical and geological practice lead, which involves managing all aspects of geotechnical and geological risk. This ranges from emergency management and geohazard studies to geotechnical design, standards and policy.

Ross Roberts
Chair, Management Committee

CONSTRUCTION SECTOR ACTIVITY

As the end of my two-year term as NZGS Chair approaches it seems appropriate to return to the topic of my first Chair's Corner where I discussed the pipeline of work for our sector. Back then (December 2019) the National Construction Pipeline Report (MBIE, 2019) anticipated continued growth in residential and infrastructure sectors until at least 2024, with a peak in the non-residential building sector in 2021 (Fig 1a).

The pandemic has thrown these forecasts into disarray and it is now much harder to predict what the future will hold for us. Issues such as national debt levels, employment vulnerability and supply chain disruption make forecasting significantly more challenging.

The latest MBIE forecasts in December 2020 suggested a very significant drop in residential construction, a smaller drop in non-residential, and a slight increase in infrastructure (Fig 1b). Overall this forecast a startling 30% drop in building and construction from the high in 2019. However, more recent data showing strength in residential consents suggests that these predictions are overly-conservative. The number of dwellings consented throughout 2020 and in the first three months of 2021 were at record highs (Fig 2). A useful comparison is total consents in the first three months of each year:

- Jan to Mar 2019 = 8,774
- Jan to Mar 2020 = 8,746
- Jan to Mar 2021 = 10,372

These numbers suggest a very strong residential construction sector and are supported by anecdotal reports of a skills shortage in the geotechnical sector across the country.

We are likely to be living with significant uncertainty for some time yet, and there are clouds on the horizon in the form of overseas inflationary pressures, skills and supply chain shortages, but for now the future appears to be bright.

NZGS MANAGEMENT COMMITTEE

The NZGS management committee includes six elected members and a range of co-opted and ex-officio members. Because of a quirk in our NZGS rules, all six elected roles are up for renewal this term.

The call for nominations to stand for election onto the NZGS National Management committee is scheduled to occur during June. I strongly encourage all members who are passionate about their profession to submit a nomination. Each committee member takes on a portfolio of work which can be tailored to their skills and experience. The ideal committee includes individuals from a range of backgrounds and interests – the only re-requisites are enthusiasm and a willingness to put in the time required. Working on the committee is extremely rewarding. Please get in touch with me if you would like to find out more about what is involved.

I would like to extend my thanks to the current committee for all their hard work, particularly over the last year when finding time for NZGS activities has been particularly challenging.

NZGS SYMPOSIUM

The 21st NZGS Symposium was held at the Dunedin Conference Centre in March. After a six-month delay caused by the pandemic it was wonderful to finally meet up with friends from around the country. The event was a great success with quality technical talks, fantastic keynotes beamed in from around the world, and many opportunities to socialise.

On behalf of all the delegates I would like to extend my thanks to our wonderful sponsors who stood behind the event and ensured it could continue despite all the uncertainty of 2020, and our organising committee who put in countless hours to run the event.

OCCUPATIONAL REGULATION

In response to the Royal Commission of Inquiry into Building Failure Caused by the Canterbury Earthquakes, the Ministry of Business, Innovation and Employment (MBIE) reviewed the occupational regulation of engineers in 2013 and 2014. Since then, progress has been disappointing with several rounds of consultation undertaken by MBIE and Engineering New Zealand and little sign of a conclusion. Despite this I encourage all our members to engage with MBIE this time around. It is understandable that there will be some 'consultation fatigue' after such a drawn-out process. However, the latest proposal from MBIE (out for consultation as I write) do appear to be the start of genuine change and may well signal that progress is finally being made.

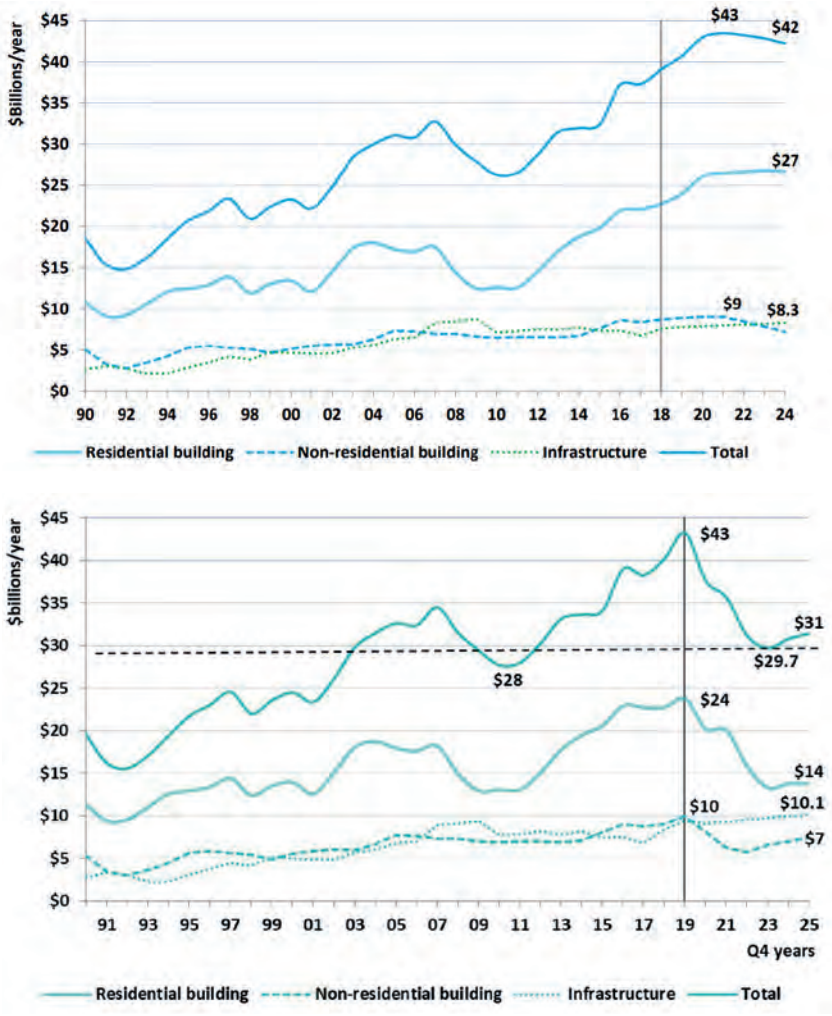

FIGURE 1 – All building and construction in New Zealand Top: previous forecast to 2024 (MBIE, Dec 2019). Bottom: current forecast to 2025 (MBIE, Dec 2020)

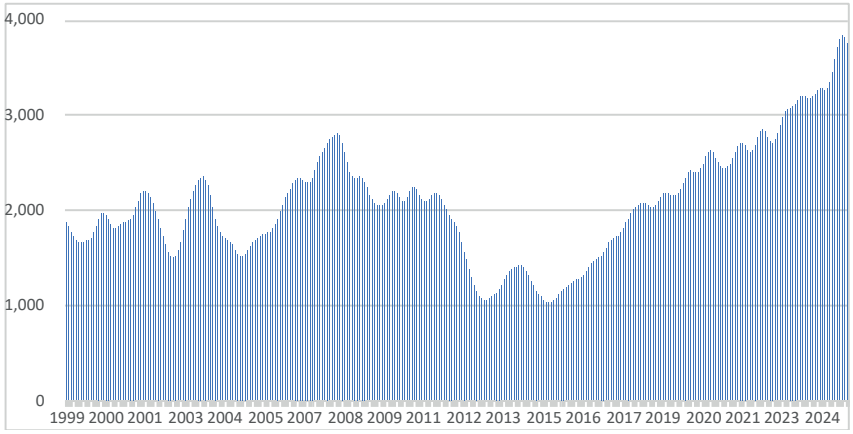

FIGURE 2 – New dwellings consented, monthly average by year, January 1995–March 2021 (Stats NZ https://www.stats.govt.nz/information-releases/building-consents-issued-march-2021)

OTHER NZGS ACTIVITIES

The committee and all our supporting volunteers have plenty of projects to keep us busy. With so much going on it has become challenging to keep track of it all and report it in sufficient detail to our members. We hope to improve this over the coming months and have started by creating a new Activities section on the NZGS website for logged-in users. This summarises all our major activities and projects, with progress updates and contact details if you want to find out more.

BRANCHES

Branch activities, after a year where face-to-face contact has been challenging, are starting to ramp up again and we're looking forward to a series of great talks.

There are some big changes afoot in some of our branches. In the Waikato both Kori Lentfer and Andrew Holland are stepping down after 12 and 10 years in the role respectively. Jerry Spinks has stepped down from his role in Wellington, and Christoph Kraus has stepped up to take his place alongside Shirley Wang, Aimee Rhodes and Safia Moniz. Perhaps most excitingly of all, a new branch has been set up by Frances Neeson in Gisborne, which is a great indication of the growth in the area.

I'd like to thank all our branch coordinators for their hard work; without their efforts the NZGS would be far less useful and fun. I'd also like to welcome our new branch coordinators and wish them all the best. If you'd like to see more activities in your region please contact the management committee or your branch coordinator and offer to help out. We're always keen to welcome new volunteers!

WEBINARS

Following the success of our webinars last year we are starting the process of developing a series of webinars for the coming twelve months. We are also able to arrange for international speakers to present to us all online. Please contact the NZGS committee lead if you have any suggestions for either individual presenters or topics of interest.

TECHNICAL INTEREST GROUPS

We are considering setting up technical interest groups modelled on the success of our Young Professionals Group. These would operate in a similar manner to the current branches but would comprise members across the country who

share an interest in a particular topic. Suggestions for these groups include "Central and local government employees", "Registered Professional Engineering Geologists", or "Ground improvement". To be successful these groups need to have a large enough membership to be vibrant but be small enough that their topics are not of general interest to most NZGS members and might therefore not be discussed in our other forums. If you would like to set up and coordinate one of these groups please contact me.

CONFERENCES AND EVENTS

Great progress is being made on the development of a one-day symposium on climate change in geotechnics hosted jointly by NZGS and Engineering New Zealand. Scheduled for 30 September this year, the event will be hosted in multiple centres to minimise travel and cost. Led by Jen Smith (NZGS Committee member) and Tania Williams (Engineering NZ general manager) this event is bound to be very popular and will provide great value. Save the date now!

We are also working on a series of future international conferences that we would like to host in New Zealand over the next eight years. Watch this space for more news soon.

YOUNG PROFESSIONALS ACTIVITIES

Our Young Professionals' Group is going from strength to strength under the stewardship of Helen Hendrickson. She has received great support from Miles Buob who is leading the development of a series of short training modules aimed at helping new graduates with implementing their university learning into professional practice.

We have also appointed three Young Professionals to support our linkages with the three international societies that we represent in New Zealand. They will report to the committee through Helen, and work closely with our Australasian Vice Presidents for each of the international societies. These new representatives are:

- Sarah Barrett to represent IAEG
- Nima Taghipouran to represent ISSMGE
- Romy Ridl to represent ISRM

BUILDING CODE ADVOCACY AND STANDARDS

I have continued to work with MBIE representing the geotechnical profession on their Building Code Advisory Panel (CAP – formerly known as BCTRAG). This group meets quarterly to raise technical issues and recommend improvements for MBIE to consider. If you have any issues that you'd like raised with MBIE please contact me.

We are also working with MBIE on updates to NZS4431 and will soon be involved in NZS3604, and are assisting MBIE and Engineering New Zealand with the scoping of a series of projects implement the key recommendations from the Seismic Risk Working Group. Key among these are updates to B1/VM4 (foundation design) and the possibility of removing retaining walls from B1/VM4 and putting this content instead into a new Verification Method covering slope stability, retaining walls and rockfall protection.

EARTHQUAKE GEOTECHNICAL ENGINEERING MODULES

We are working closely with Engineering NZ and MBIE to finalise the Earthquake Geotechnical Engineering modules. These were originally published in "preliminary draft" form and are now almost ready for final publication. We expect that Modules 2-6 will be published later this year. Module 1 is also nearly complete, but as discussed at our Symposium its publication status is not yet fully determined. I am working very closely with MBIE, Engineering New Zealand and our sister societies NZSEE and SESOC on this rather challenging topic. We expect more information to be available on this in the very near future.

INTERNATIONAL REPRESENTATION

The NZGS is represented on numerous international technical committees. These are summarised on our website, and short progress reports are presented later in this edition of Geomechanics News.

NEW ZEALAND GEOTECHNICAL DATABASE STRATEGIC PLAN

A joint MBIE/EQC project is being developed to provide a plan for the NZGD. The system is considered a very successful model and has buy-in from many stakeholders. However, it was identified in 2019 that, in part due to its age and part through limited investment, the NZGD had some age-related technical deficiencies that limited its value and needed a strategic vision so as to set the direction for future development and governance. I have been working with Engineering NZ to help scope this project and ensure that the voices of NZGS members are heard.

CONCLUSION

My two years as chair have been dominated by the impact of Covid-19 on our society and profession. Despite the many challenges this posed, the NZGS and the sector as a whole appear to be busy and largely successful. We have a huge work programme, and some compromises will have to be made if we're to make real progress on the most important issues. The activities described above are only a part of what we're working on, and more information on all is available on the NZGS website.

Our current priorities are our training courses, branch events and webinars, the Earthquake Geotechnical Engineering Modules, and our liaison role with MBIE. We are truly grateful for your ongoing support and would welcome any offers from members who would like to become more involved to help us drive the other projects forward.

LET MAGNUMSTONE DRIVE YOUR DESIGN!

WALL OPTIONS

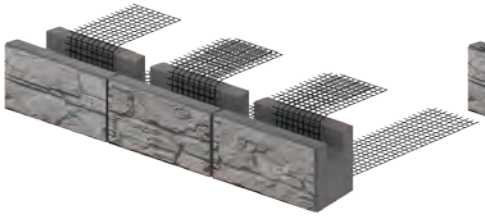

POSITIVE CONNECTION

MagnumStone allows for the ultimate geogrid positive connection.

GEOGRID WALL

Geogrid reinforcement with the MagnumStone system is typically very cost effective.

GRAVITY WALL

Gravity walls are built with the large MagnumStone blocks that use a tongue -and-groove system.

PLANTER WALL

It's unique internal drainage system makes it the prime choice for environmentally friendly and sustainable wall solutions.

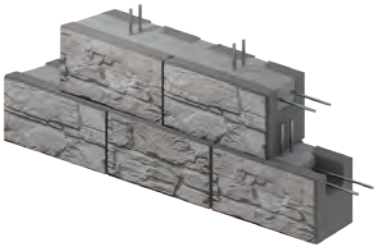

CANTILEVERED WALL

MagnumStone provides the permanent form for reinforcing steel and concrete, making installation easy.

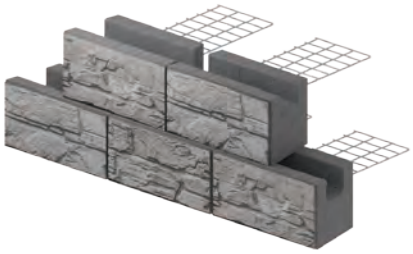

STEEL GRID

The MagnumStone steel grid solution provides designers with a great option.

SOIL NAILED

Soil nailing could be one of the fastest growing solutions for retaining wall structures.

CIRTEX®
GAIN MORE GROUND

WWW.CIRTEX.CO.NZ

Room for improvement

IN THIS ISSUE we have contributions from practitioners who see a need for improvement in how some things are done. They are seeking to raise our awareness of limitations in everyday practices. They are not alone. The following quote is from Jackie Stewart, whom some (at least) of us remember as a Formula 1 race car driver and three times World Champion between 1965 and 1973:

> *It is not always possible to be the best, but it is always possible to improve your own performance*

The contributors to this issue are not just commenting on the issues they see, but offering solutions. They epitomise the objectives of challenge – to openly acknowledge deficiencies and encourage change and adaptation leading to improved performance. While they are targeting professional issues and concerns, the simple fact is that none of us is perfect and there is ALWAYS room for improvement in everything we do, both personally and professionally.

Great results come from individual thoughts and actions. In engineering geology, the scale of rock mass weathering, RQD and GSI are examples of ideas that brought about huge improvements in technical approach and that have in turn fostered further change.

But the power of the group or team is equally important and is the best opportunity most of us will ever have to participate in creating improvements to techniques or project outcomes. I was recently reminded of one such example.

When Clyde Power Project (the Clyde dam landslides stabilisation project) was underway and the site was crowded with geologists, engineers, drill rigs and tunnellers trying to build reliable geological models for the designers, we initiated regular team meetings at which the senior staff shared their observations and thoughts (and those of their team members). From this we built a picture of variabilities and similarities in the ground conditions that helped each of us develop those models much more quickly and much more robustly than would have been possible working in isolation. And we did it without GSI, LiDAR or fancy 'sophisticated' software that tries to think for you.

These are all examples of the tools now available to help us do our jobs better. And there are new technological developments and future developments that will provide further assistance. None of them should fully replace the field observations and data assessments that we all do every day, and that we can all learn to do better. Use the new tools wisely but don't rely on them, and always remember the words of Jackie Stewart: *it is always possible to improve your own performance.*

Don and Gabriele

Don Macfarlane has worked as an applied engineering geologist for nearly 40 years and has accumulated some knowledge, a fair bit of wisdom and a few brickbats along the way.

His real interest is dams and associated issues (seismic hazard, slope instability) but any good geohazard affecting an engineering structure will do. These days he is a Consultant with AECOM in Christchurch.

NZ Geomechanics News **co-editor**

Gabriele is a Senior Lecturer in Geotechnical Engineering at the University of Canterbury. Gabriele's research interests include earthquake geotechnical engineering and related problems; constitutive modelling for geomaterials; development of advanced laboratory and field testing devices; geo-hazard reconnaissance and mitigation; reuse and recycling of industrial granular wastes as sustainable geomaterials.

NZ Geomechanics News **co-editor**

WE'RE OFTEN TOLD

WE'RE THE BEST AT WHAT WE DO

CALL US AND WE'LL PROVE IT

EXTRACTING THE PAST

shaping the future

PHILLIP FALCONER
0274 304 554

JOSH KENDRICK
0272 855 004

EMAIL: OFFICE@PERRYGEOTECH.CO.NZ

37 GLENLYON AVENUE, P.O. BOX 9376,
TAURANGA 3142, NEW ZEALAND

WWW.PERRYGEOTECH.CO.NZ

PERRY
GEOTECH

LETTER TO THE EDITOR

28 April 2021

To New Zealand Geotechnical Society members,

Understanding Expansive Soils within the New Zealand Building Code Framework: A Structural Engineer's View

I AM AN Auckland structural engineer from Markplan Consulting. Our company has been involved in the design of tens of thousands of raft/waffle slabs on expansive soils, over the past 25 years. Our director, Mark Smith, was heavily involved in raft slab inception in the NZ industry (in the mid-late 1990's) alongside the likes of Firth. I have worked for Markplan Consulting for the last 12 years and in that time, I have been responsible for developing our design methodologies for raft slabs on expansive soils. As such, I have a good general understanding of the interaction of structural raft slab foundations with expansive soils (by no means an expert in geomechanics).

I have read the recent paper by Tonkin and Taylor (T+T) in the NZ Geomechanics News (June 2020) regarding the shrink-swell test, and found this very interesting. Markplan Consulting carry out many projects with large housing developers in Auckland, and we see many subdivisional geotechnical investigations and reports. The T+T paper helps explain why we are seeing such a large variability in specified soil classes within a single subdivision, and sometimes even within the same building footprint. I am also aware of the further work that T+T have done in this domain and that has been presented at the recent NZGS Symposium. It is concerning that there appears to be significant flaws in the testing methodology, and it seems to me that the New Zealand geotechnical community (and Australia for that matter) has a considerable issue to resolve.

Aside from the issues noted by T+T, I would like to draw your attention to other concerns, which I believe to be causing considerable confusion with structural engineers and with geotechnical engineers, in regards to expansive soils in NZ. These are code/design issues, that do not exactly require a high level of geotechnical expertise, but do require the geotechnical community to assist and progress further industry understanding or change. Some members may already be aware of these issues, and may even be implementing the recommendations that I propose here.

My concerns relate to the November 2019 update to the NZBC, which refers to expansive soils within B1/AS1 amendments to NZS3604. This update is mentioned in the T+T paper, and symposium presentation. Many structural and geotechnical engineers that I have spoken to about the NZBC update are of the understanding that MBIE have made a deliberate decision to revert back to the site soil classes as outlined in the superseded version of AS2870:1996, rather than utilise the Class H split to H1 and H2 outlined in AS2870:2011. I strongly believe that this has been an unconsidered and unintended change. This is based on the following logic:

- AS2870:1996 (now superseded) outlined soil classes and characteristic surface movement (y_s values) as Class S (<20mm), Class M (20-40mm), Class H (40-70mm), and Class E (>70mm).
- BRANZ report SR120A (2008), which is mentioned in the T+T paper, references AS2870:1996, which was the active version at the time. One of the main design recommendations of this report was to effectively increase the return periods adopted for foundation design, by way of scaling factors which were outlined in the report.
- In 2010, the Department of Building and Housing (now MBIE), produced the Simple Housing Acceptable Solution (SH/AS1), as part of the NZBC. SH/AS1 made reference to expansive soils and the soil classes as per AS2870:1996, which at the time was the current version. This reference to expansive soils and soil classes, also applied scaling factors from SR120A to the upper limit y_s values of each soil class to account for a 500-year return period, similar (but slightly varied) to the recommendations of SR120A. To my knowledge, these scaled y_s values were not (prior to 2019) referenced in any other NZBC documentation except SH/AS1, and I had never seen these referenced in any geotechnical assessment of expansive soils, nor any structural foundation design.
- Shrink-swell index (I_{SS}) ranges corresponding to each soil class (as noted in SR120A) were also referenced in SH/AS1, although these do not appear to be scaled in any way. SH/AS1 also had prescribed solutions for concrete slab foundations on expansive soils, however the scope of SH/AS1 was limited (to simple housing), and the prescribed slab foundations did not allow for typical raft/waffle type slabs that are common within the New Zealand industry.
- In 2011, AS2870:2011 was published in Australia. Important changes that affected the day-to-day design of raft slabs were: the split of soil Class H into Class H1 and Class H2; and an adjustment of some soil class y_s value ranges. AS2870:2011 outlined soil classes and y_s values as Class S (<20mm), Class M (20-40mm), Class H1 (40-60mm), Class H2 (60-75mm), and Class E (>75mm).
- As AS2870 was a referenced document in NZS3604 and the NZBC at the time, it stands to reason that this new version effectively made the soil class references in SH/AS1 out of date. Certainly, geotechnical and structural engineers in NZ began referencing the updated AS2870, especially the new soil classes and corresponding y_s values (with no reference to increased y_s values by way of scaling factor). SH/AS1 was never updated to align with AS2870:2011.

- In 2018, MBIE decided to revoke the Simple Housing Acceptable Solution due to its low uptake. However, MBIE noted that some of the content was applicable to other residential buildings; specifically, the reference to soil classes and the corresponding scaled y_s values and I_{SS} values. Therefore, in the November 2019 NZBC update, this information was transferred to B1/AS1. Unfortunately, this was simply a transfer of existing information, and it appears to have been made with no consideration for the changes to AS2870 in 2011. I believe that this was an oversight, and that there was no specific intention to differ from the soil classes in AS2870:2011. I also note that the references to AS2870 within B1/AS1 specifically refer to AS2870:2011. This transfer of information also included the prescribed slab foundations from SH/AS1, but these solutions did not allow for typical raft/waffle slab construction and are limited in their use.

Unfortunately, it appears that many structural and geotechnical engineers have not understood the error regarding soil class references, and it has caused much confusion since the 2019 NZBC update. One reason that this error is such an issue is because it has effectively rendered large parts of AS2870 obsolete. AS2870 has prescribed methods for foundation designs, with much of the information tabulated based on soil class; these now do not align with the soil classes within the NZBC.

For example, if a geotechnical engineer was to provide expansive soil information as per the current NZBC, they may note that the soil class for a specific site is Class H with an upper limit characteristic surface movement of 78mm. The shrink-swell testing for the site (ignoring the issues that the T+T paper raises), may actually have provided a calculated site y_s value of say 48mm, which is slightly higher than the Class M limit (but most often, we see geotechnical reports refer to a soil class and its corresponding upper limit, rather than the actual calculated site y_s value). As Class H does not exist in AS2870:2011, and since 78mm is greater than the upper limit of Class H2, in this case if a structural engineer was to use a prescribed foundation solution from AS2870:2011, they must use a solution for Class E soils, despite the calculated site y_s value being toward the lower bound of Class H1. Of course, this would give a foundation solution that works, but it would be at a significant unnecessary cost.

Purely based on this logic, I would suggest that B1/AS1 be updated to reflect the soil classes of AS2870:2011. However, there is another concern that I believe would also need to be addressed, specifically in regards to the scaling factors that have been applied to the corresponding y_s values of each soil class within B1/AS1.

BRANZ SR120A recommends that a 300-year return period be adopted for serviceability limit state (SLS) design of foundation on expansive soils (with a scaling factor of 1.0 applied to y_s values), and a 1000-year return period for ultimate limit state (ULS) design (with a scaling factor of 1.2). The information on expansive soils that has been added to B1/AS1 (November 2019), explicitly states that a 500-year return period for SLS design has been adopted (with a scaling factor of 1.11), deliberately differing from the SR120A recommendation of 300-year return period. As this is a clearly noted decision, this point is not debated.

I believe that the scaling factors have been applied within B1/AS1 incorrectly, and that this was incorrect from the outset of the Simple Housing Acceptable Solution in 2010. This is based on the following logic:

- SR120A states that a 300-year return period would require a scaling factor of 1.0 (i.e. no change to the soil class y_s values of AS2870).
- Considering standard probability/risk and return period philosophies, it would be expected that a 500-year return period event would be greater (worse) than a 300-year return period event. Therefore, if we were to consider a 500-year return period for design, our foundation solution would be expected to be more robust (stronger/stiffer) than if we were designing for a 300-year return period.
- SR120A repeatedly states that scaling factors should be applied to the calculated (site) y_s values (there is no reference to scaling of soil class limits/ranges); i.e. it is implied that if a geotechnical engineer was to carry out a shrink-swell test for a specific site, and calculate y_s values by the methods noted in AS2870, then it is this value that should be multiplied by the scaling factor. It would be expected that this scaled site y_s value would be compared to the unaltered ranges of y_s values for each soil class, and then a soil class determined accordingly.
- For example, if a geotechnical engineer calculated a (unscaled) site y_s value for a specific site of 38mm using the methods noted in AS2870:2011, and compared this to the soil class ranges of AS2870:2011, a soil class of Class M would be determined (based on Class M y_s values = 20-40mm, as per AS2870:2011). However, considering the conversion to a 500-year return period by using a scaling factor of 1.11, the scaled site y_s value becomes 42mm; this would result in a Class H1 soil being determined (y_s values = 40-60mm). In this case if a structural engineer was to use a prescribed foundation solution from AS2870:2011, a Class H1 solution would be adopted which would be more robust than the Class M foundation solution that would have otherwise been adopted if no scaling factor was applied to the calculated site y_s value.

- From what I have seen, I believe that many geotechnical engineers are not applying scaling factors to their calculated site y_s values. This may be because they consider that the scaling factors have been applied correctly to the soil class ranges in B1/AS1. Running through another example similar to above, but with the B1/AS1 values considered, if a geotechnical engineer calculated a (unscaled) y_s value for a specific site of 42mm using the methods noted in AS2870, and compared this to the soil class ranges noted in B1/AS1, a soil class of Class M would be determined (based on maximum Class M y_s value = 44mm, in B1/AS1). If this calculated site y_s value was compared to the y_s values in AS2870:2011, a soil class of Class H1 would be determined (y_s values = 40-60mm). The intended effect of increasing from a 300-year return period to a 500-year return period and increasing robustness, has in fact resulted in a less robust solution.
- Based on the above, I consider that the scaling factor utilised within B1/AS1 has effectively been applied to the "wrong side of the equation", and is having the opposite effect than intended. As a result, I believe that we may effectively be designing for a return period closer to 100 years (1.00/1.11 = 0.90, which is close to the scaling factor for 100-year return period = 0.88, as per BRANZ SR120A). This error erodes any redundancy that may exist in foundation designs, and that may otherwise help to counteract the flaws of the shrink-swell testing noted by the T+T paper.
- I am aware that some geotechnical engineers are applying scaling factors to their calculated site y_s values. However, these values are currently typically compared to the soil classes outlined in B1/AS1, therefore the scaling factors are essentially applied to "both sides of the equation" and therefore cancel each other out. The net effect is that the solution is no different than if scaling factors were never introduced (i.e. a 300-year return period is effectively adopted).

Recent discussions that I have had about these concerns with geotechnical engineers have been variable. Most have generally understood the concerns that I have raised to some degree, but many have not been willing to provide information for foundation design purposes outside of what is now being dictated by the NZBC. This is causing issues for structural engineers when attempting to design foundations as per AS2870:2011, as in some cases it is now technically not applicable, or can result in under-designed or over-designed foundations.

Based on what has been outlined herein, the following solution is proposed:

- B1/AS1 of the NZBC be updated by MBIE, to refer to the soil classes outlined by AS2870:2011, with no scaling factors applied to the corresponding characteristic surface movements.
- When assessing expansive soils at a specific site, geotechnical engineers are to apply a scaling factor to the calculated characteristic surface movement before determining a soil class for the site.

In the interim, before this information may be updated in the NZBC, I recommend that geotechnical engineers provide soil class information in two forms:

- one set of information for characteristic surface movement values and soil classes to reference B1/AS1, in order to align with the NZBC (albeit that the NZBC information has flaws);
- and another set of alternative information, for scaled site characteristic surface movement values and corresponding soil classes in reference to AS2870:2011 (which itself is a referenced document within the B1/AS1).

This will allow structural engineers to select how they specify foundation solutions; either to align with B1/AS1, or to AS2870:2011. This will alleviate the confusion and discrepancy that currently exists, and will provide solutions that are more aligned with the intent of B1/AS1, AS2870:2011, and BRANZ SR120A.

To conclude, I believe that the confusion surrounding the NZBC November 2019 updates (to B1/AS1) regarding expansive soils has been caused due a transfer of previous information without consideration of the updated version of AS2870:2011. The situation is worsened due to scaling factors originally being applied to the characteristic surface movement limits of each soil class in error, when they should only be applied to the calculated site characteristic surface movements.

I believe that if the geotechnical community can understand and agree with these issues, then change to the NZBC can be easier. At least in the interim, if the industry is on the same page, then it can be justifiable to provide additional design parameters that are more in line with the intent, which will allow foundation designers to adopt methods that are suitable for the New Zealand industry.

Mitchell Rooney
(Senior Structural Engineer at Markplan Consulting)
BE (Civil), CPEng, CMEngNZ

027 700 2544

(09) 415 9793 ext. 205
mitchell@markplan.co.nz

ABSEIL ACCESS
CIVIL · INFRASTRUCTURE · ENVIRONMENTAL

GEOTECHNICAL DIVISION

ABSEIL ACCESS

ROCK ANCHORS

ROCKFALL NETTING

CATCHFENCES

DESIGN & BUILD

SLOPE STABILISATION

WWW.ABSEILACCESS.CO.NZ

WELLINGTON 15 Bute Street, Te Aro +64 4 801 5336
NEW PLYMOUTH 26 Gilmour Street, +64 6 751 0910
CHRISTCHURCH 26 Thackers Quay, +64 3 384 0336
NELSON 19 Fountain Place, +64 27 488 2849

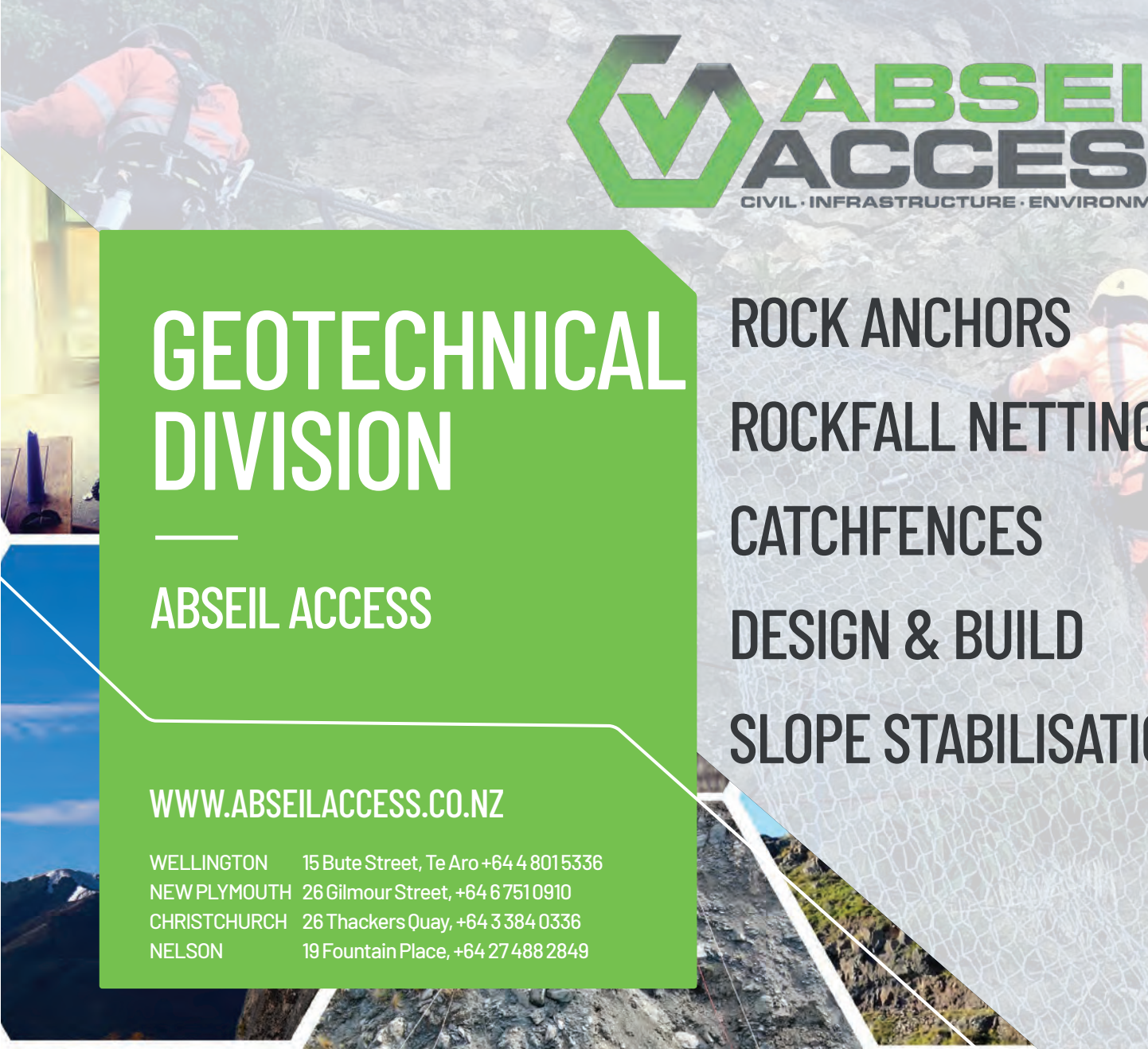

MINISTRY OF EDUCATION
TE TĀHUHU O TE MĀTAURANGA

NZ Geotechnical Society Inc.
c/o Engineering New Zealand
PO Box 12-241
Wellington 6013
Via email: secretary@nzgs.org

Kia ora

The use of the New Zealand Geotechnical Database on school projects

The Ministry of Education has a large property portfolio distributed of nearly 2,100 state schools throughout New Zealand. Significant investment in the upgrade and construction of new school buildings and schools has seen the New Zealand Geotechnical database (NZGD) become an integral part of our information systems. Accordingly, the Ministry requires all geotechnical practitioners working on school projects to upload all relevant geotechnical information to the NZGD.

A recent review of our schools has shown that some practitioners are not following our requirement to upload the geotechnical information. While we have been in contact with the specific practitioners to request they upload the data retrospectively, we would appreciate if you can bring this to the attention of the New Zealand Geotechnical Society members.

The Ministry will continue to monitor school sites in the NZGD to ensure information is being uploaded. The NZGD is a valuable tool not only to the Ministry, but to the wider industry, and the successful use of it by all will help inform better decision making regarding the use of the land.

Further information on our requirements to use the NZGD can be found in our *Structural and Geotechnical Requirements* document that was updated in 2020.

The Ministry is looking to geotechnical practitioners to lead the way by addressing the timely uploads to the NZGD.

Ngā mihi

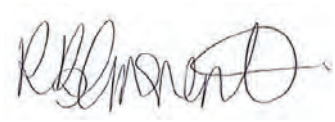

Renelle Gronert
Senior Manager - School Design

WSP Materials
Testing Laboratories

WSP laboratories have a proud history dating back more than 65 years. WSP have a network of eleven IANZ (International Accreditation New Zealand) accredited laboratories. We provide specialist independent testing and analysis of engineering construction materials.

Through collaboration, our multi-disciplinary team of highly trained and motivated technicians have the capability to deliver large projects in a short timeframe.

WSP laboratories provide a wide range of site investigation and laboratory services, including:

- Specialised geomechanics testing (eg triaxial)
- Instrumentation installation and monitoring
- CPT (Cone Penetration Testing) services CPTu, seismic including SCPTu and temperature cones for geothermal areas
- Field investigations and soils classification

Contact us for more information:

New Zealand Laboratories Manager:
Daniel Grebenar
t. +64 9 415 4664
t. +64 27 231 3442
e. daniel.grebenar@wsp.com

Laboratory Manager Hamilton:
Sarah Amoore
t. +64 7 856 2870
t. +64 274 721 598
e. sarah.amoore@wsp.com

Our full capabilities and services can be viewed at:
wsp.com/en-NZ/sectors/laboratories-services

Cantilever Pole Retaining Walls

John Wood, retired civil engineer

John Wood

John Wood has recently retired as a consulting civil engineer specialising in bridge design, structural investigation, soil-structure interaction and earthquake engineering. Before setting up his consulting engineering practice in 1986, he was Head of the Ministry of Works, Central Laboratories.

His work included peer reviews of seismic strengthening proposals and seismic risk assessment for hydro power stations. He carried out bridge strengthening design and peer review for the New Zealand Transport Agency, and research into the earthquake performance of underground structures, reinforced earth retaining walls and bridge abutments.

John is a Life Member and past President of the New Zealand Society for Earthquake Engineering. He holds post-graduate degrees in structural and civil engineering from both the University of Canterbury and California Institute of Technology.

ABSTRACT

Cantilever timber pole walls are one of the most commonly used forms of retaining wall construction used in New Zealand for low to moderate retained heights. Pole walls in New Zealand have mainly been designed using the isolated pile theory (Broms) or by continuous embedded wall theory.

These commonly used design analysis methods have limitations and do not accurately represent the pole-soil interaction and displacement behaviour. In particular, the Broms method for estimating the pole lateral force capacity in cohesionless soils assumes rotation of the pole about the toe instead of the correct depth at a significant height above the toe. This simplification gives an unconservative lateral load capacity. Simplifying the analysis by assuming that the poles behave as a continuous wall is unnecessary and may introduce errors that are difficult to quantify. Although soil strength parameters are unlikely to be accurately known for design of small wall structures it is nevertheless desirable to eliminate analysis errors as far as possible and deal with the soil uncertainty by adopting moderately conservative soil strength parameters.

The pole foundation soil-interaction design should be based on pile theory that has been verified by testing. Pile design methods suitable for cantilever wall design have been presented by Guo (2008) for cohesionless soils, Motta (2013) for cohesive soils and by Zhang (2018), for the mixed friction and cohesion case. The Guo and Motta methods are based on elastic-plastic soil response and give force versus displacement equations for loading from zero up to the ultimate hyperbolic loads. These allow serviceability displacements and the pile top lateral force capacity based on soil yield at the toe to be determined.

Although the empirical equations of Guo, Motta, and Zhang are more complex than the simple Broms equation for cohesionless soils and the Pender (1997) equations based on Broms theory for cohesive soils they are not difficult to set up on a spreadsheet. Design charts are presented in this paper that enable the equations to be evaluated at sufficient accuracy for most design applications in both types of soils and for the mixed friction and cohesion case.

Limiting force profiles in cohesionless soils are a function of the effective vertical stress which is difficult

FIGURE 1. Typical timber pole wall construction

to evaluate in the vicinity of the wall face. Plots of the variation with distance from the face are presented accompanied by recommendations on a correction factor simplification that is satisfactory for design applications.

The strength enhancement of the concrete encasement used on timber poles embedded in the ground should be considered in design. Information is presented in the paper that allows the encasement strengthening effect to be predicted with sufficient accuracy for wall design.

1. INTRODUCTION

Cantilever timber pole walls are one of the most common forms of retaining wall construction used in New Zealand for low to moderate height applications (1.0 m to 3.5 m). Timber facing materials are used in conjunction with the poles to form an economical wall constructed from sustainable locally processed materials (see Figure 1). Construction is straightforward with the poles usually installed in drilled holes backfilled with concrete. Drilled holes have diameters ranging from 400 mm to 600 mm and these can be drilled with light machinery, or portable power augers. The construction width of less than 1.0 m is less than conventional concrete cantilever or gravity wall construction. This is advantageous on sites with existing development.

For more heavily loaded or higher walls steel section poles can be used and these may be driven rather than installed in bored holes. Tied-back timber poles are sometimes used for walls higher than 3.0 m.

The embedment pole depth is usually of the same order of the wall height above the ground level in front of the wall so the ratio of the embedment length, L divided by the diameter, B is approximately 5. With this aspect ratio the pole behaves as a rigid element deforming by rotating about a point that is usually between 0.6L to 0.8L below the ground surface. Failure in the soil surrounding the encased pile is the preferred failure mechanism. The pole section at ground level is a critical location; failure in this section may lead to limited deformation prior to failure and should be avoided at specified design loads.

Timber design in New Zealand is carried out in accordance with NZS3603:1993, Timber Structures Standard but there is no design standard covering the geotechnical aspects of the design required for the embedded section of a pole wall. MBIE-NZGS, 2017 provides some guidance by way of a design example for a cantilever timber pole wall.

Pole walls in New Zealand have mainly been designed using the isolated pile theory presented by Broms, 1964a, 1964b (Pender, 1997) or by continuous embedded wall theory (McPherson and Bird, 2020; MBIE-NZGS, 2017). These two methods are summarised below.

1.1 BROMS METHOD

The best-known approach to estimating the ultimate lateral load capacity of a pile is that of Broms. He considers separately piles in cohesive soils and those in cohesionless soils. In each case Broms gives a simple method of estimating the maximum lateral pressure that the soil can mobilise and from these evaluates the capacity of the pile for lateral load applied at the top of the pile. The approach is intended to account for the three-dimensional interaction between the pile and the surrounding soil. For a short rigid pile, it is assumed that the maximum moment does not reach the ultimate capacity of the pile section and that failure occurs in the surrounding soil.

For piles in overconsolidated cohesive soil with undrained shear strength, s_u - constant over the depth, Broms assumed that the soil provides no resistance between the ground surface and a depth of 1.5 pile diameters, and that the ultimate lateral soil pressure

against the pile at greater depths was $9s_u$. Davis and Budhu, 1986 suggested that a uniform depth of 600 mm may be a more appropriate depth for the depth of zero resistance rather than 1.5 diameters.

For piles in cohesionless soils Broms proposed a maximum lateral pressure of $3K_p$ times the vertical effective stress in the soil adjacent to the pile (K_p is the Rankine passive pressure coefficient). For cohesionless soils the soil resistance extends to the ground surface in contrast to the cohesive soil case. Broms derived a simple expression for the lateral load capacity of a short rigid pile in cohesionless soils by assuming that the pile rotated about its toe.

Pender, 1997 extended the Broms analyses to cover piles in soft clay where the undrained shear strength increases linearly with depth from zero at the ground surface. However, this case is not applicable to the short piles considered in the present application as short piles would be unsatisfactory in this type of soil.

Broms provided design charts for the pile lateral load capacity in a cohesive soil; however, Pender, 1997 presented a complete set of equations which are more convenient for spread sheet calculation.

1.2 CONTINUOUS WALL METHOD

Pole spacing for cantilever walls usually ranges from 1.5 to 4 times the embedded diameter of the pole including the concrete encasement. For poles spaced at four times the embedment diameter or less, the below-ground soil pressure bulbs are assumed to provide continuous pressure along the wall and calculations are carried out using conventional continuous embedded wall theory (as used for sheet pile walls). One analysis approach adopted by Pender, 2000 is to assume a rotation point at some depth and use iteration to vary this depth to satisfy both horizontal force and moment equilibrium equations. For cohesionless soils he assumed that both the active and passive pressures were calculated using the Rankine active and passive pressure coefficients. For short-term loading of saturated clays, he assumed a passive pressure resistance based on $2s_u$.

In the example given in MBIE-NZGS, 2017 active and passive pressure coefficients for long-term loading (drained soil for static loads) of a clay soil were estimated using NAVFAC - DM7, 2011 charts (assuming zero cohesion). These charts were derived assuming logarithmic spiral failure surfaces and for passive pressures give coefficients significantly greater than given by the Rankine assumption. For short-term loading (earthquake load case) of the clay soil the passive pressure resistance was based on $2s_u$. The MBIE-NZGS analysis was simplified by assuming rotation about the toe of the wall.

1.3 LIMITATIONS OF CURRENTLY USED METHODS

Shortcomings of the present methods commonly used for estimating the lateral capacity of pole foundations used in cantilever pole wall design are summarised below.

Failure Mechanism

The failure mechanism for piles spaced at 1.5B or greater involves flow of the soil on the soil-pile interface. In contrast there is no flow mechanism for a continuous embedded wall section and the failure develops on passive pressure slip lines. Assuming continuous wall behaviour for piles at moderate spacing misses some of the intricacies of the true behaviour and this may lead to unnecessary error in the design analysis.

Passive Pressure Estimation

There is limited published load test information for continuous walls and there is uncertainty on how to estimate passive pressure coefficients above and below the rotation point. In contrast empirical formulae for the limiting pressures on isolated piles have been developed from a wide range of pile tests. One advantage of the continuous wall assumption is that the wall can be modelled using two-dimensional numerical analysis which partially overcomes the uncertainty in estimating passive pressures. However, the complexity of numerical analysis makes it unsuitable for pole wall design.

Rotation Point

In the Broms method for cohesionless soil and in some applications of the continuous wall theory it is assumed that the rotation point is at the toe of the pole. This assumption can lead to significant error and in the case of the Broms analysis an unconservative prediction of the load capacity. With the availability of automatic iteration capability in spread sheets, it is straightforward to simultaneously solve the equations of horizontal force and moment equilibrium to give the correct depth of the point of rotation. There is no need to make the simplifying assumption of rotation about the toe.

Definition of Ultimate Capacity

The load versus displacement curve for lateral loading of a pile has a hyperbolic shape resulting in large deflections at the ultimate load. Broms and the continuous wall theory assume that the limiting passive pressures on the pile or wall develop over the total pile length. This assumption implies that the capacity is the hyperbolic or maximum capacity. A better approach is to base the ultimate capacity on the load required to produce yield in the soil at the toe of the pile or wall.

Displacements

The present methods do not give a load versus displacement curve although sometimes displacement estimates are based on elastic soil assumptions (Winkler or elastic continuum). To satisfy both serviceability and ultimate limit state (ULS) requirements it is important to have a reliable method of computing a load versus deflection curve for the load increasing from zero to the ULS.

Load Testing

Broms verified his load capacity methods using a number of test results. Over the past 50 years since the publication of the Broms methods there have been a large number of published results for lateral loading of rigid piles. Alternative methods using limiting pressure predictions based on this more recent test information are now available.

Pile Spacing

Pile spacing effects have been studied in a number of recent test and analytical investigations resulting in the publication of empirical equations for estimating the lateral load capacity reduction resulting from interaction of the pressure bulbs between adjacent piles. With the availability of these equations there is no need to assume continuous wall behaviour.

Gravity Stresses

The Broms and simplifications of the continuous wall methods assume that the gravity or effective vertical stress that determines the limiting force profile on the pole are based on the ground surface in front of the wall. The soil depth step at the wall face increases the gravity stresses in both the front and back of the wall face. On the back face the vertical stress is sometimes assumed to be based on the ground level behind the wall but this assumption overestimates the vertical stress near the pole.

2. ULTIMATE LATERAL FORCE CAPACITY OF RIGID PILES IN COHESIONLESS SOIL

In the present application the pile is assumed to be rigid and fail by rotation about a point on the pile below the mid embedment depth. Failure is expected to occur in the soil rather than in the pile. A number of definitions of a rigid pile have been proposed. These include:

1. Kasch et al, 1977 proposed that length to diameter ratio , L/B be used to classify the rigidity of a pile with a rigid pile having $L/B < 6$.
2. Guo and Lee, 2001 defined a pile as rigid when the pile-soil relative stiffness, E_P/G_s exceeds a critical ratio $(E_P/G_s)c = 0.052(L/r_0)^4$, where E_P is the effective Young's modulus of the pile, defined as $E_P = (EI)_P/(\pi r_0^{\,4}/4)$; $(EI)_P$ is the pile bending rigidity; G_s is the shear modulus of the soil; L is the pile embedded length, and r_0 is the outer radius of the pile.
3. Poulos and Davis, 1980 considered that a pile was rigid if the stiffness ratio $(EI)_p/(E_s L^4)$ was greater than 10^{-2} where E_s is the Young's modulus for the soil.
4. Carter and Kulhawy, 1992 suggest that a pile is rigid when $L/B \leq 0.07\ (E_P/E_s)^{0.5}$

Poles used in low to moderate height timber wall construction (height less than 3.5 m) are usually encased in concrete below ground with an overall encasement diameter of 0.4 to 0.6 m. L/B ratios are usually < 6. The $(EI)_p/(E_s L^4)$ ratio is typically > 3×10^{-2} (assuming composite action between the timber and the concrete encasement). Concrete encased poles generally satisfy all of the above four criteria.

Extensive theoretical studies, in-situ full-scale tests and laboratory model tests have been carried out on laterally loaded rigid piles in cohesionless soils (Brinch Hansen, 1961; Broms, 1964; Petrasovits and Awad, 1972; Meyerhof et al., 1981; Poulos and Davis, 1980; Scott, 1981; Fleming et al., 2009; Prasad and Chari, 1999; Dickin and Nazir, 1999; Laman et al., 1999; Guo, 2008; Zhang et al., 2005; Zhang 2009; Chen et al., 2011). The following analysis methods have been proposed (Moussa and Christou, 2018).

LFP Method

An ULS method based on an assumed profile of limiting soil resistance per unit length along the pile or a limiting force profile (LFP). The analysis is reduced to a simplified two-dimensional analysis. Many of these LFP methods (Brinch Hansen, 1961; Broms, 1964; Petrasovits and Awad, 1972; Meyerhof et al., 1981; Prasad and Chari, 1999) do not consider the soil deformation and therefore do not provide the displacements associated with the ULS. To resolve this issue, Guo, 2008 established elastic-plastic solutions for analysing laterally loaded rigid piles, assuming a modulus of subgrade reaction that was either constant or linearly increasing with depth together with a LFP that linearly increased with depth. His solutions enable the nonlinear response of piles and displacement-based capacity to be estimated and gave satisfactory agreement with model pile test results presented by Prasad and Chari, 1999 and the experimental and numerical analysis results presented by Laman et al, 1999.

Winkler Spring

A Winkler spring model (Scott, 1981; Pender, 1993) can be used to estimate the displacement and load capacity of a rigid pile. The soil surrounding the pile is modelled as a bed of independent springs. Displacement of individual springs has no effect on the other springs and this greatly simplifies the mathematical analysis. This model neglects the soil continuity or shear coupling between the springs and is difficult to apply when there is significant soil nonlinearity. It is a simple method that may give acceptable results for the serviceability limit state (SLS).

P-Y Curve

A refinement of the Winkler spring method is the *p-y* curve analysis which was originally developed by McClelland and Focht, 1956. The reaction of the soil is related to the lateral movement of the pile by means of a nonlinear load transfer function. Methods to estimate the *p-y* curves have been developed by many authors (Reece, 1977; Scott, 1981; Murchison

and O'Neill, 1984; Lam and Martin, 1986). Empirical expressions have been derived from test results to give the initial stiffness and the ultimate force as a function of depth and from these values a hyperbolic force versus displacement or *p-y* curve can be developed for node points on the pile. The method does not lead to closed-form solutions; however, software programs are available to generate the *p-y* curves and to perform a nonlinear analysis (Rollins et al, 2003). The complexity of numerical procedures are not justified in many circumstances related to the present application for cantilever pole walls.

Strain Wedge

The strain wedge method overcomes some the limitations of the *p-y* curve method by taking into account the three-dimensional nature of the soil-pile interaction near the top of the pile (Norris, 1986; Ashour et al, 1998). While traditional nonlinear *p-y* characterization provides reasonable assessment for a wide range of loaded piles, it has been found that the *p-y* curve (or the Winkler modulus of subgrade reaction) depends on pile properties (width, shape, bending stiffness, and pile-head conditions) as well as soil properties. The strain wedge model allows the assessment of the nonlinear *p-y* curve response of a laterally loaded pile based on the relationship between the three-dimensional response of a flexible pile in the soil to its one-dimensional beam on elastic foundation parameters. The model employs stress-strain-strength behaviour of the soil as established from triaxial testing. The determination of strain wedge depth and the value of the subgrade reaction modulus below the strain wedge add considerable complexity. The method is more applicable to long piles than short rigid piles.

Elastic Continuum

Continuum methods (Poulos and Davis, 1980; Pender 1983; Carter and Kulhawy, 1992) can be used to model the continuity of the soil, its nonlinearity, and the boundary conditions in a similar manner to the discrete Winkler spring or *p-y* spring models. The method envisages the soil to be a continuous elastic medium in which stresses and displacements spread outward and diminish with distance from the point of application. It gives closed form expressions for load capacities and deflections of axially and laterally loaded piles. However, only a few solutions are available for rigid piles and these do not adequately represent the ULS of a pile in a nonlinear cohesionless soil.

Finite Element

Finite element methods (FEMs) can provide rigorous results including the consideration of material nonlinearity and heterogeneity (Trochanis et al, 1991; Yang and Jeremi, 2002, 2005). Results need to be validated against simplified analysis methods before using in design. Development of an accurate FEM model is time consuming and requires detailed soil parameters that are usually not available for the design of low or moderate height cantilever pole walls.

When a pile is laterally loaded calculation of the soil yield stress against the pile requires the assumption of a plastic mechanism in the soil surrounding the pile. Near the surface the mechanism is three-dimensional since both vertical and horizontal movements of the soil occur. At depths greater than several pile diameters from the surface the mechanism is essentially two-dimensional with most of the displacement in the horizontal plane. The solution of this plasticity problem is complex and no exact analytical solutions are available although Reese et al, 1974 have presented an approximate solution.

Rigorous estimation of the lateral load resistance of rigid piles in cohesionless soil requires advanced modelling techniques such as the FEM method and consideration of the three-dimensional nature of the problem. However, the scope of most pole retaining wall projects, the available geotechnical information, or the budget, often do not justify an advanced approach. A simplified, yet accurate design analysis procedure is required when advanced calculations are not justified. Of the analysis methods summarised above, the LFP method is considered to be the most suitable for the present application. Simplifications in the method give closed form analytical solutions that can be expeditiously applied in design.

Various versions of the LFP method have been proposed and number of these were compared to find the most suitable for the present application. A summary of the methods considered is given below. Evaluation of their suitability was undertaken by comparing for each method calculated lateral load capacities with test results and calculated pole embedment depths for a typical pole wall.

2.1 BRINCH HANSEN, 1961

Brinch Hansen considered the soil failure behaviour at shallow, moderate and large depths. At shallow depths, the failure was based on the difference between the passive and active pressures developed on a rough wall translated horizontally. At moderate depths, the resistance was estimated by considering the equilibrium of a Rankine passive wedge having the same width as the shaft diameter. The sides of the wedge were acted on by at-rest soil pressures. At large depths, the failure stress was calculated assuming failure to take place on a horizontal plane and was based on the solution for a deep strip foundation. The following equation was developed for the soil failure pressure, p_u acting on the pile at an arbitrary depth:

$$p_u = \sigma_{vo} K_q + c K_c \qquad (1)$$

Where σ_{vo} is the vertical overburden stress, K_q the earth pressure coefficient for overburden pressure, c the

soil cohesion and K_c the earth pressure coefficient for cohesion.

The failure pressure was assumed to act uniformly across the pile diameter and the failure force per unit length assumed to be the failure pressure multiplied by the diameter. The depth of the rotation point was obtained by adjusting this depth by trial and error to simultaneously satisfy force and moment equilibrium equations. A convenient analysis procedure used by Brinch Hansen was to take moments about the load application point assumed to be at an eccentricity of *e* above the ground. The failure pressure was assumed to change sign at the rotation point (see Figure 2).

2.2 BROMS, 1964 (SIMPLE METHOD)

Broms assumed that the lateral earth pressure which develops at failure was equal to $3K_p$. The accuracy of this assumption was established by comparisons with test data and Broms indicated that these comparisons showed that the assumption yielded results on the safe side. For short rigid piles it was assumed that the failure pressure extended from the ground surface to the point of rotation. At a depth z below the ground surface the assumed LFP (or limiting soil reaction per unit length) was given by:

$$P_u = 3\, B\, \gamma'\, z\, K_p \qquad (2)$$

Where *B* is the pile diameter, γ' the effective unit weight of the soil and K_p the Rankine passive earth pressure coefficient. Broms assumed that the high negative earth pressures develop close to the toe of the pile and that this pressure could be replaced by a concentrated load. The ultimate lateral resistance was determined by satisfying moment equilibrium assuming rotation about the toe. This gave the lateral capacity for a force applied at the top of the pile, H_u as:

$$H_u = \frac{0.5\,\gamma'\, B\, L^3 K_p}{(e+L)} \qquad (3)$$

Where *L* is the pile length below ground level and *e* the height of the applied lateral load above ground (or eccentricity).

Although the Broms analysis procedure provides a simple closed form equation for the lateral load capacity, comparisons with other methods indicate that it overestimates the capacity of short rigid piles in cohesionless soils. A shortcoming is the assumption that the rotation point is at the toe of the pile. Other methods indicate that the rotation point is at a depth of between 0.6*L* to 0.8*L* below ground level.

2.3 BROMS MODIFIED

A modification to the Broms method has been suggested by others (Chen and Kulhawy, 1994). In this modified analysis the Broms conventional or *Simple* method assumption of the ultimate pressure being $3K_p$ is used but the depth of the rotation point is obtained by satisfying both the horizontal and moment equilibrium equations. Instead of a concentrated force at the toe, the ultimate negative pressure distribution below the rotation point is also based on the three times Rankine passive pressure assumption (see Figure 2). Simultaneous solution of the two equilibrium equations can be carried out by a trial-and-error procedure. The Solver add-in on Excel can be used to expedite this operation.

A closed form solution for the modified Broms method is available from a more general analysis for both cohesive and cohesionless soils presented by Zhang, 2018. The solution for cohesionless soil is presented in terms of a general ultimate lateral resistance coefficient *K*. For the Broms *Modified* analysis $K = 3\,K_p$. (Zhang also indicated that the solution is applicable to the LFP method of Petrasovits and Award, 1972 who assumed that $K = 3.7\,K_p - K_a$. Where K_a is the Rankine active pressure coefficient.) The Zhang analysis involves simultaneous solution of horizontal and moment equilibrium equations and results in complex closed form expressions for the ultimate lateral resistance and the rotation depth. The following simplified expressions for the dimensionless ultimate lateral capacity, f_ϕ and depth of the rotation centre, z_{rd} were presented by Zhang as being of sufficient accuracy for engineering design.

$$f_\phi = 0.13r^{3.2} \qquad (4)$$

$$z_{\mathrm{rd}} = \sqrt{2} + 0.069r + 0.018r^2 \qquad (5)$$

Where
$f_\phi = H_u/[k(L+e)^2]$, $z_{\mathrm{rd}} = z_r/L$, $r = L/(e+L)$, $k = KB\gamma'$, z_r = depth of the rotation centre.

2.4 MEYERHOF AT AL, 1981

Meyerhof et al assumed that the lateral earth pressure which develops at failure is equal to the Rankine passive pressure minus the Rankine active pressure with this pressure difference increased by a pile shape factor. At depth z below the surface the assumed LFP was given by:

$$P_u = B\, \gamma'\, z\, (K_p - K_a)\, s_{bu} \qquad (6)$$

Where s_{bu} is a pile shape factor based on the theory of pressure on a convex circular wall. It is a function of the pile length to diameter ratio (*L/B*) and the soil friction angle ϕ. Plotted values are presented by Mayerhof et al. For *L/B* = 5 and $\phi = 35°$, s_{bu} is approximately 2.6.

The ultimate pressure was assumed to increase linearly from the surface to reach a maximum value at the rotation point then drop to zero. Below the rotation point a negative pressure was assumed to increase linearly from zero to a maximum at the pile toe. A plot of the force per unit length is shown in Figure 2 where it is compared with the force per unit length assumed in

the Brinch Hansen, Broms *Simple* and Broms *Modified* analyses. The Mayerhof et al plot is based on a *L/B* ratio of 5 and the plots for all methods are for an eccentricity ratio of *e/L* = 0.1. The *L/B* ratio affects the s_{bu} pile shape factor in the Mayerhof et al analysis but does not directly affect the results for the other analyses. The plots are shown in dimensionless form with the force per unit length divided by $K_p^2\ \gamma\ 'BL$. (In other methods described below the LFP is related to K_p^2 and expressing the dimensionless force in terms of this factor is convenient for comparisons.)

The Mayerhof et al lateral resistance was determined by satisfying both horizontal and moment equilibrium. The ultimate capacity for the lateral force is given approximately by:

$$H_u = P_u\ L^2\ F_b\ r_b \qquad (7)$$

Where F_b is the lateral resistance factor for weight and has a value of 1.25, and r_b is the reduction factor for the moment resulting from applying the load at an eccentricity e above the ground, $r_b = 1/(1 + 1.4\ e/L)$.

In Meyerhof et al, 1981 more general lateral resistance solutions are given for both rigid walls and piles in a soil comprising of two layers with both cohesive and cohesionless properties.

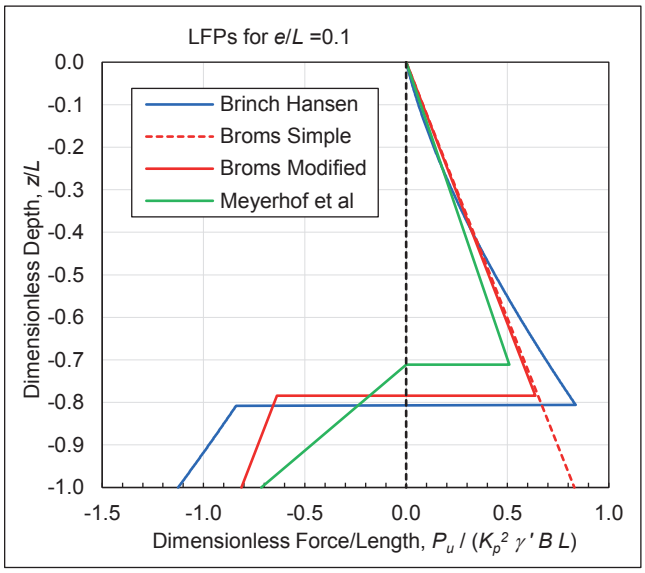

FIGURE 2. Comparison of LFPs for Brinch Hansen, Broms and Meyerhof et al methods.

2.5 PRASAD AND CHARI, 1999

Prasad and Chari developed a LFP based on measurements they made on a rigid model pile in sand (uniform and cohesionless) prepared at various relative densities in a steel drum. From the test results the maximum earth pressure was found to occur at a depth of 0.6 times the depth of the point of rotation. They found that maximum pressure, p_m at this depth could be calculated by:

$$p_m = \left[10^{(1.3tan\emptyset+0.3)}\right]0.6\ z_r\ \gamma' \qquad (8)$$

Where z_r is the depth of the rotation point below the ground surface.

Based on the test results the maximum pressure at $0.6z_r$ was assumed to decrease linearly to zero at the rotation point then become negative and increase linearly to reach a maximum value at the toe of 1.7 times the peak value above the rotation point (see Figure 3). In the other methods described above, the LFP has a value greater than zero at the rotation point which is not theoretically correct. With zero displacement at the rotation point the pressure must also be zero.

From soil pressure measurements Prasad and Chari found that average pressure across the pile section could be taken as 0.8 time the peak measured value. By considering force and moment equilibrium for the LFP shown in Figure 3, the rotation depth was found to be:

$$z_r = [-(0.567L + 2.7e) + (5.307L^2 + 7.29\ e^2 + 10.541\ e\ L)^{0.5}]/2.1996 \qquad (9)$$

For *e/L* = 0 the above expression gives the dimensionless rotation depth, z_r/L = 0.79 and for *e/L* = 0.1, z_r/L = 0.77.

The ultimate lateral force capacity was given as:

$$H_u = 0.24\left[10^{(1.3tan\emptyset+0.3)}\right] z_r\ \gamma'\ B(2.7z_r - 1.7L) \qquad (10)$$

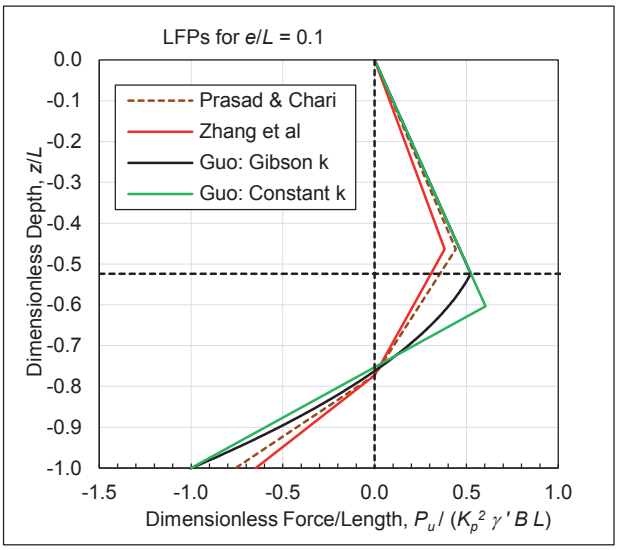

FIGURE 3. Comparison of LFPs for Prasad & Chari, Zhang et al and Guo methods

The ultimate lateral force capacity given by the Prasad and Chari equation corresponded to the point where the load versus pile-head displacement becomes linear or substantially linear after following a curved path. (This definition was used by Meyerhof et al, 1981 and Chari and Meyerhof, 1983.) Prasad and Chari indicated that beyond

this point there is only a marginal increase in load and for practical purposes that the soil around the pile within the failure wedge can be considered to have yielded.

2.6 ZHANG ET AL, 2005

Zhang et al, 2005 considered that the soil resistance to lateral movement of a rigid pile could be divided into two components; the frontal normal reaction and the side friction reaction. Based on pressure measurements that were made in lateral load pile tests carried out by Adams and Radhakrishna, 1973; Chari and Meyerhof, 1983; Joo, 1985; Meyerhof and Sastry, 1985, and Prasad and Chari, 1999 they concluded that the best fit to the ultimate frontal pressure was given by:

$$p_u = K_p^2 \gamma' z \tag{11}$$

Where z is the depth below ground surface.

No measured data were available to determine the side shear resistance. They assumed that the ultimate shear stress resistance was the same as the vertical shear resistance given by API, 1991 as:

$$\tau_u = K_r \gamma' z \tan\delta \tag{12}$$

Where K_r is the ratio of horizontal to vertical effective stress and δ is the interface friction between the pile and soil.

For values of K_r and δ they recommended the guidelines given by Kulhawy et al, 1983, and Kulhawy, 1991. For drilled shafts and concrete surround with a rough contact surface against the soil, as generally used in pole wall construction, these guidelines give K_r = (0.9 to 1.0) K_o and δ = 1.0ϕ. Where K_o is the at rest pressure coefficient and ϕ the soil friction angle.

Zhang et al assumed that the LFP for both the frontal soil resistance and side shear resistance followed the profile given by Prasad and Chari, 1991 (as shown in Figure 3). That is, they assumed that the maximum positive pressure occurred at a depth of 0.6 times the rotation depth and that the negative peak value at the pile toe was 1.7 times the positive peak pressure. The Zhang et al LFP is compared with those proposed by Guo and Prasad and Chari in Figure 3. Both the Prasad and Chari and Zhang et al dimensionless LFPs are a function of the soil friction angle which has been taken as 35° for the plots shown in Figure 3. (Since the LFPs are made dimensionless by dividing by K_p^2 the changes in the dimensionless LFPs with friction angle are small. In the case of Zhang et al the dimensionless normal pressure force does not change with the friction angle but the shear resistance force is a function of K_o which depends on the friction angle.)

Based on horizontal and moment equilibrium considerations the depth of the rotation point z_r was as given by Prasad and Chari (see above) and the ultimate pile head lateral force capacity was given by:

$$H_u = 0.3\left(\eta K_p^2 + \xi K \tan\delta\right) z_r \gamma' B (2.7 z_r - 1.7L) \tag{13}$$

Where η and ξ are pile shape functions. For a circular pile they are 0.8 and 1.0 respectively (Briaud and Smith, 1983).

2.7 AGUILAR ET AL, 2019

By using the principle of minimum potential energy and assuming that the soil stiffness increased linearly with depth Aguilar et al, 2019 derived the horizontal displacement function for a rigid rotating pile as:

$$u(z) = -\frac{H}{n_h L^4}(36e + 24L)z + \frac{H}{n_h L^3}(24e + 18L) \tag{14}$$

Where n_h is the subgrade reaction modulus (FL^{-3} units).

By setting u = 0 in the above displacement function the dimensionless rotation depth z_r/L is equal to 0.75 for a load eccentricity ratio e/L = 0, and z_r/L = 0.74 for e/L = 0.1. These depths are significantly less than given by Prasad and Chari.

Aguilar et al give the pile head ultimate force capacity as:

$$H_u = \frac{P_m L^2}{6(L + 2e)} \tag{15}$$

Where P_m is the maximum force per unit length at the toe.

With reference to the Prasad and Chari earth pressure profile Aguilar et al give the maximum force per unit length at the toe as:

$$P_m = 0.45 \gamma' L B \, 10^{(1.3 \tan\emptyset + 0.3)} \tag{16}$$

Aguilar et al indicate that the above expression comes from a statistical analysis of comparisons between the Prasad and Chari theoretical predictions and test results. However, Prasad and Chari give a significantly higher pressure force at the toe $(P_m = 1.7 \gamma' 0.6 z_r B \, 10^{(1.3 \tan\emptyset + 0.3)})$, that is a value of 1.7 times the peak value at a depth of 0.6 z_r).

At low values of e/L the Prasad and Chari ultimate lateral force capacity is approximately 10% higher than given by Aguilar et al.

Aguilar et al considered two failure criteria. The first of these was the *Meyerhof* criterion used by Prasad and Chari (see above) and the second was based on a hyperbolic fit to the experimental results or the *nominal resistance*. They suggested that the *nominal resistance* was a factor of 1.5 times the *Meyerhof* capacity. The

expression for H_u above is for the *Meyerhof* capacity.

Aguilar et al mentioned the importance of estimating displacements under serviceability conditions and proposed using their deflection equation given above for this purpose. To apply the method values of the soil subgrade reaction n_h are required but for elastic response these can be estimated from published values (Terzaghi, 1955). It is a simple approach suitable for the present application.

2.8 GUO, 2008

Guo determined the soil interaction forces on laterally loaded rigid piles in cohesionless soil by assuming elastic-plastic soil behaviour as shown schematically in Figure 4. The nonlinear response of the pile was characterised by slip depths or points where the soil commenced to yield that progressed down from the ground surface and upwards from the pile-toe. Expressions for critical slip depths were developed corresponding to soil yield at the toe and at the rotation point. At toe-yield the force per unit length at the pile toe just attains the limiting yield value of P_u. Prior to and at this state, the pile force profile from soil interaction follows the positive LFP (plastic soil interaction) down to a depth above the rotation depth of z_o, below this depth it is governed by elastic interaction. This results in a pile force profile similar to that adopted by Prasad and Chari, 1999 (see Figures 3 and 5). Further increase in load beyond the toe-yield state results in a portion of the pile negative LFP progressing upwards from the toe (at depth L) to a depth of z_1 below the rotation point (see Figure 5). With further increase in the load the depths z_o and z_1 approach each other and merge with the depth of rotation z_r which is strictly unachievable. At this stage, the pile force profile follows the positive LFP down from the ground surface and the negative LFP up from the toe to the rotation point. This fully plastic or ultimate limit (although unachievable) was adopted by some investigators including Brinch Hansen, 1961 and Petrasovits and Award, 1972.

Guo developed solutions for both a *Constant* subgrade modulus and a linearly increasing modulus with depth (*Gibson k*). The solutions were in reasonable agreement with data measured in tests by Prasad and Chari, 1999 and other numerical predictions (Laman et al, 1999).

Guo assumed that within the elastic soil range the pile force per unit length was given by:

$$P = k_o\, z\, B\, u \text{: for } Gibson \text{ modulus} \qquad (17)$$

$$P = k_c\, B\, u \text{: for } Constant \text{ modulus} \qquad (18)$$

Where k_o is the soil modulus for *Gibson* modulus (FL^{-4} units), k_c is the soil modulus for *Constant* modulus (FL^{-3} units), B the pile outside diameter, z the depth below the surface and u the pile lateral displacement.

Upon reaching the plastic state the net limiting force per unit length (LFP) on the pile is given by:

$$P_u = A_r\, z\, B \qquad (19)$$

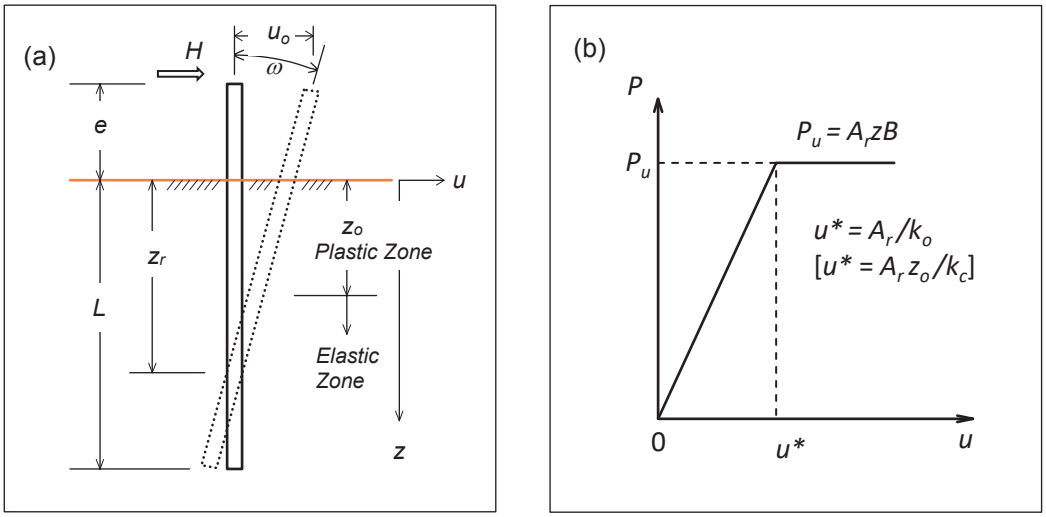

FIGURE 4. (a) Pile-soil system. (b) Soil load versus displacement model. Value of u^* in [ ] is for *Constant k*. Other value is for *Gibson k*. From Guo 2008.

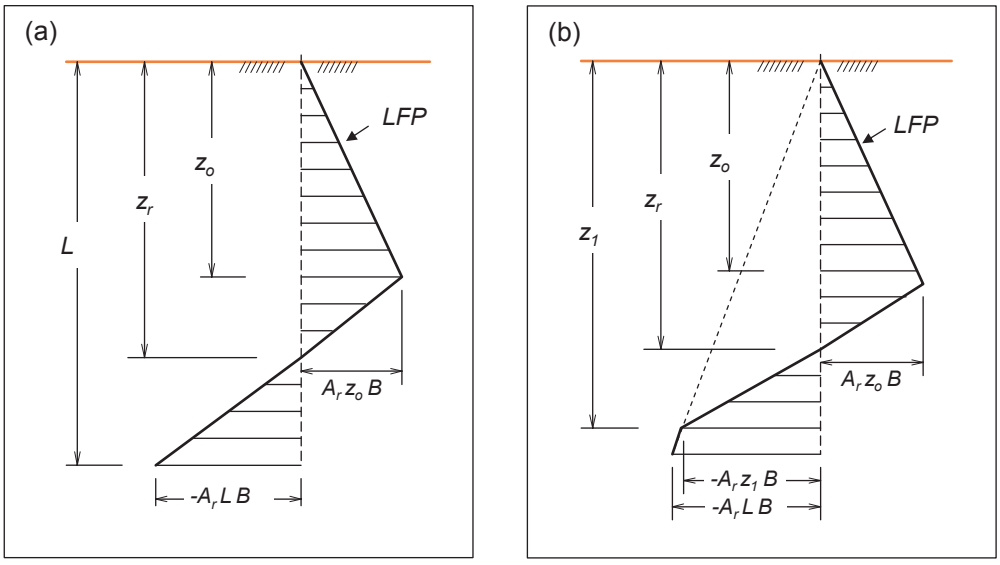

FIGURE 5. (a) Toe-yield state. (b) Post-toe yield state. From Guo, 2008.

Where $A_r z$ is the pressure on the pile surface (FL^{-2} units) contributed by radial and shear stresses around the pile surface.

Based on the tests carried out by Prasad and Chari, 1999 (and other experimental work), Guo assumed that A_r was given by:

$$A_r = \gamma' K_p^2 \quad (20)$$

Where γ' is the soil effective unit weight.

The displacement of a rigid pile varies linearly with depth and is given by:

$$u = \omega z + u_o \quad (21)$$

Where ω is the rotation (in radians) and u_o the displacement at the ground surface. Above a depth of z_o, called the slip depth, the pile displacement reaches a local threshold given by:

$$u^* = \omega z_o + u_o \quad (22)$$

For the *Gibson k* assumption, the threshold displacement is given by:

$$u^* = A_r / k_o \quad (23)$$

The unknown rotation ω and displacement u_o given in the above equations were determined by solution of the equilibrium equations for pile force and moment. Prior to toe-yield, relevant dimensionless solutions in terms of the pile head lateral force H and slip depth z_o are given for the *Gibson k* assumption by:

$$\frac{H}{A_r B L^2} = \frac{1 + 2\,z_o/L + 3\left(\frac{z_o}{L}\right)^2}{6\left[(2 + z_o/L)\left(\frac{2e}{L} + \frac{z_o}{L}\right) + 3\right]} \quad (24)$$

$$\frac{u_o\,k_o}{A_r} = \frac{3 + 2\,[2 + (z_o/L)^3]\,e/L + \left(\frac{z_o}{L}\right)^4}{[(2 + z_o/L)(2e/L + z_o/L) + 3](1 - z_o/L)^2} \quad (25)$$

$$\omega = \left[\frac{A_r}{k_o\,L}\right] \frac{-2(2 + 3\,e/L)}{[(2 + z_o/L)(2e/L + z_o/L) + 3](1 - z_o/L)^2} \quad (26)$$

$$\frac{z_r}{L} = \frac{-u_o}{\omega L} \quad (27)$$

The depth of the maximum moment in the pile, z_m for $z_m < z_o$ is given by:

$$\frac{z_m}{L} = \sqrt{\frac{2H}{A_r B L^2}} \quad (28)$$

Guo, 2008 also presents a maximum moment depth for $z_m > z_o$. This case results in a complex expression which is not relevant for the present application.

The maximum moment, M_m for $z_m < z_o$ is given by:

$$M_m = \left(\frac{2z_m}{3} + e\right) H \quad (29)$$

At toe-yield $z_o = \bar{z}_o$ where $\bar{z}_o$ is given by the solution of the cubic equation:

$$\bar{z}_o^3 + (2e + L)\bar{z}_o^2 + (2e + L)\bar{z}_o - (e + L)L^2 = 0 \quad (30)$$

This cubic equation can be solved by trial and error which can be expedited using the Excel Solver add-in.

Force, displacement, and rotation solutions for *Constant k* are:

$$\frac{H}{A_r B L^2} = \frac{z_o/L}{2(2 + z_o/L + 3\,e/L)} \quad (31)$$

$$\frac{u_o\,k_c}{A_r L} = \frac{(2 + 3\,e/L)\,z_o/L}{(2 + z_o/L + 3\,e/L)\,(1 - z_o/L)^2} \quad (32)$$

$$\omega = \left[\frac{A_r z_o}{k_c\,L}\right] \frac{(z_o/L)^2 + 3\,(z_o/L - 2)\,e/L - 3}{(2 + z_o/L + 3\,e/L)\,(1 - z_o/L)^2} \quad (33)$$

$$\frac{z_r}{L} = \frac{-u_o}{\omega L} \quad (34)$$

The equations for z_m and M_m for $z_m < z_o$ are the same as for the *Gibson k* equations. At toe yield $\bar{z}_o$ for *Constant k* is given by:

$$\bar{z}_o/L = -(1.5\,e/L + 0.5) + 0.5\sqrt{5 + 12\,e/L + 9(e/L)^2} \quad (35)$$

In contrast to the *Gibson k* case, a direct solution is obtained for $\bar{z}_o$ from this equation without iteration.

The slip depths and rotation depths at toe-yield are plotted for both the *Gibson* and *Constant k* cases in Figures 6 and 7 respectively. For *Gibson k* the second order polynomial trend lines shown on the plots are sufficiently accurate for design purposes and eliminate the need to solve the cubic equation. The trend lines give the slip depth and rotation depths as:

$$\bar{z_0}/L = 0.1358(e/L)^2 - 0.2062e/L + 0.543 \quad (36)$$

$$z_r/L = 0.0679(e/L)^2 - 0.1031e/L + 0.7715 \quad (37)$$

(36) and (37): only accurate for $e/L < 0.5$

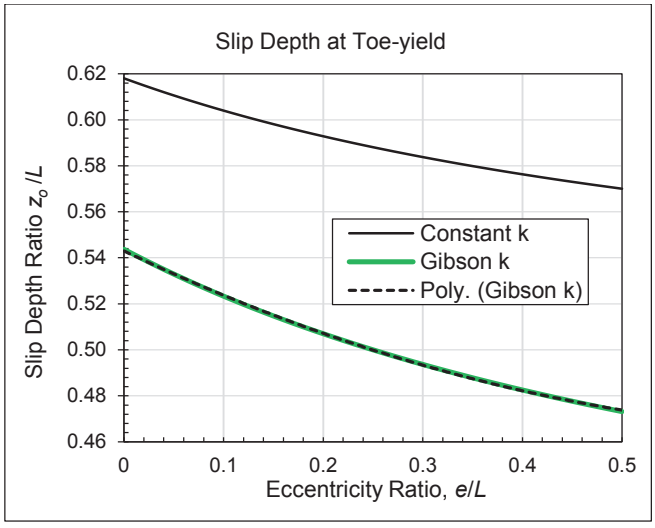

FIGURE 6. Slip depth ratio at toe-yield for *Constant k* and *Gibson k*. Trend line is shown for *Gibson k* case.

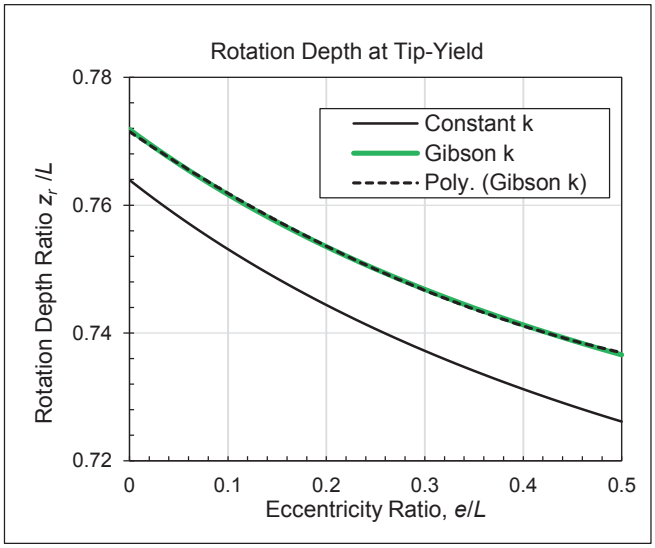

FIGURE 7. Rotation depth ratio at toe-yield for *Constant k* and *Gibson k*. Trend line is shown for *Gibson k* case.

Equations (23) to (37) for both the *Gibson* and *Constant k* are only valid up to toe-yield. Guo, 2008 also presents force, displacement, and rotation equations for horizontal forces greater than the toe-yield and up to the ultimate load when yield commences at the rotation point (unachievable in theory because of the large associated rotation). For the present application, the response beyond toe-yield is not of particular interest although displacements for forces beyond this point are shown in Figures 8 and 9.

Force versus displacement functions (in dimensionless terms) generated from Guo's equations for *Gibson* and *Constant k* are shown in Figures 8 and 9 respectively. For comparison, the Prasad and Chari ultimate lateral loads, H_u are shown for each of the corresponding *e/L* curves plotted in Figure 8 for the *Gibson k* case. The Gibson k lateral toe-yield forces are approximately 16% higher than the Prasad and Chari ultimate forces over the *e/L* range of 0 to 0.4.

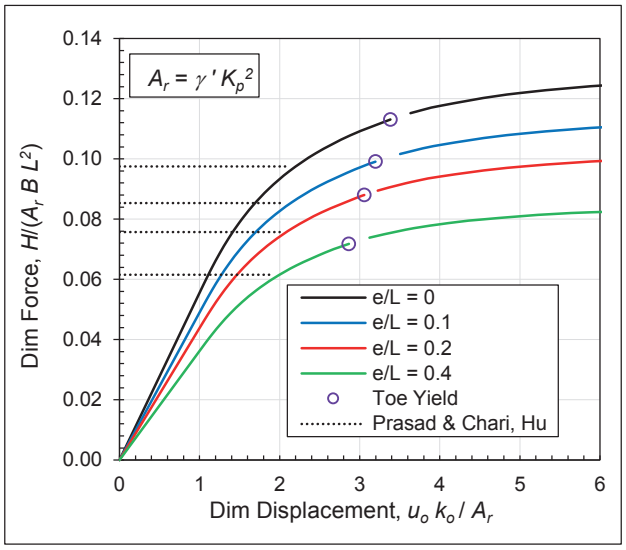

FIGURE 8. Force versus displacement for *Gibson k*.

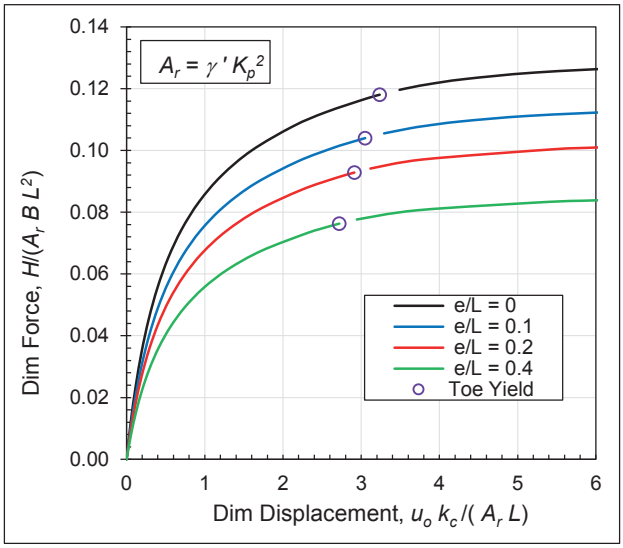

FIGURE 9. Force versus displacement for Constant k

Guo validated his theoretical solutions with results from tests on model piles carried out by Prasad and Chari. Figure 10 shows a comparison between the Guo predictions with results for a model steel pile with embedded depth of 612 mm, outside diameter of 102 mm and the load applied at 150 mm above the soil surface (*e/L* = 0.25). The soil was a well graded sand with relative density D_r = 0.75 (unit weight of 18.3 kN/m^3 and friction angle of 45.5º). (By curve fitting Guo derived an A_r value of 739 kN/m^3 which was used in the comparison. This value is about 15% higher than the A_r calculated from the unit weight and friction angle.) For the comparison, the *Gibson k* displacements have been made dimensionless by dividing by the average k_c value over the depth of the pile rather than k_o which was used in Figure 8.

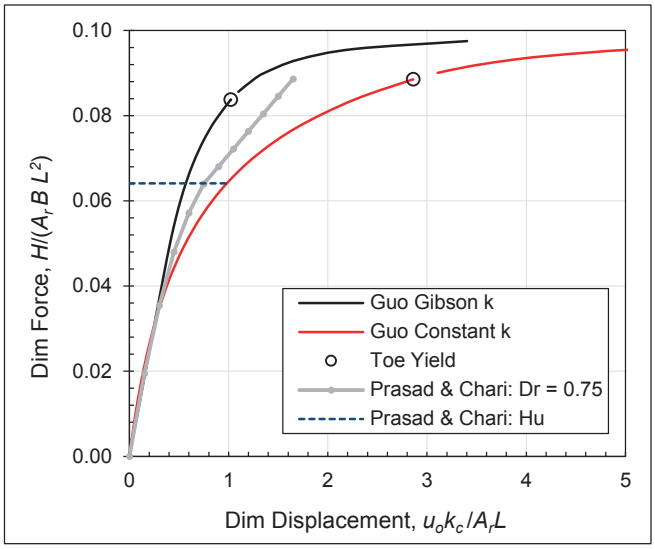

FIGURE 10. Comparison of Guo theory with Prasad & Chari model pile test for sand with D_r = 0.75.

Figure 10 shows reasonable agreement between the theoretical load versus displacement curves and the test results, with the test results lying between the *Gibson* and *Constant k* curves. The assumption of an elastic-plastic soil rather than more realistic stress-strain behaviour is the main reason why closer agreement is not expected.

The Guo dimensionless pile head lateral force at toe-yield versus the eccentricity ratio *(e/L)* is plotted in Figure 11 for both the Gibson and Constant k soils. A polynomial trend line for the Gibson k dimensionless pile head lateral force at toe-yield is given by:

$$H_{yd} = \frac{H_y}{\gamma' B L^2 K_p^2} = -0.046(e/L)^3 + 0.1236(e/L)^2 - 0.1447(e/L) + 0.1126 \quad (38)$$

Where H_y is the horizontal force capacity at toe-yield.

This trend line equation can be used to estimate the pile-toe yield load to sufficient accuracy for design (only accurate for *e/L* < 0.5).

Griffiths continue to lead the way with technological advances to improve safety, efficiency and service.

Introducing New Zealand's first dual head sonic drilling rig:

- A small, lightweight rig with exceptional power
- High efficiency and extremely fast penetration speeds
- Versatile - sonic and wire line coring on the same rig
- Improved core quality and outstanding recovery rates

Contact Mel Griffiths:
mel@griffithsdrilling.co.nz
Phone 04 5277 346

GRIFFITHS DRILLING
RESULT DRIVEN GEOTECHNICAL SPECIALISTS

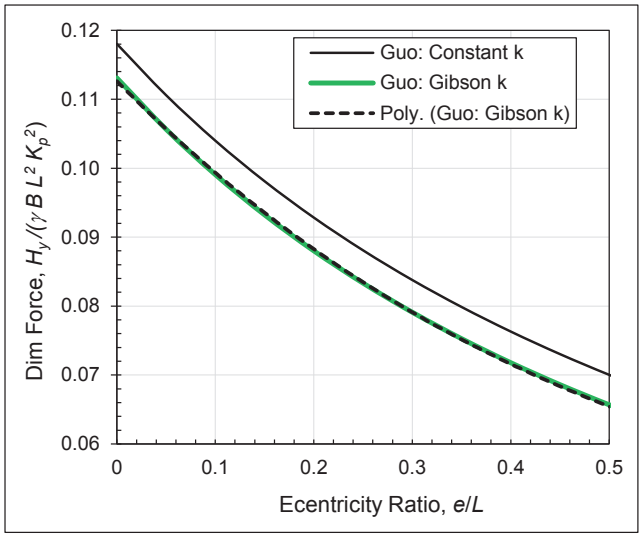

FIGURE 11. Pile head force at toe-yield from Guo method for *Gibson* and *Constant k* soils. Trend line is shown for *Gibson k*.

The Guo method provides greater pile response detail than the other LFP methods investigated (including those summarised above and several others) in that it considers soils with both *Constant* and *Gibson k* stiffness properties. It also provides displacement response curves from initial pile head lateral loading up to the ULS force (yield at the rotation point). In particular, the response curve up to the toe-yield load provides the design information required for the present application. The assumption of elastic-plastic soil behaviour may limit the accuracy of the estimated displacements for some soils.

Comparisons of solutions from the Guo method with other LFP methods and test results are presented in the following sections. It was concluded that the Geo method is the most satisfactory of the simplified LFP methods for the present application. Solutions can be obtained by evaluating Equations (24) to (37) on a spread sheet or by using the results plotted in Figures 6 to 9, and 11.

2.9 COMPARISON OF LFP METHODS

The ultimate pile head lateral force capacity for *e/L* ratios from 0 to 0.5 was calculated for each of the LFP methods discussed above. Average dimensionless ultimate force capacity over this *e/L* range is shown in Figure 12 for soil friction angles of 30° and 35°. The toe-yield capacity for the Guo methods was used in the comparison. For the Meyerhof et al, Prasad and Chari, Zhang et al, and Aguilar et al methods the capacities shown are the *Meyerhof* capacities. Broms, 1964 compared the ultimate capacity from his *Simple* method with a number of test results and indicated that his method gave conservative results so this may indicate a capacity equivalent to the *Meyerhof* capacity. The Broms *Modified* and Brinch Hansen methods are based on a force profile that reaches yield at the rotation point and it is unclear whether they correspond to the *Meyerhof* capacity. The Broms *Modified* method is based on an LFP of $3K_p^2$ and this is probably a conservative assumption (see Zhang et al, 2005).

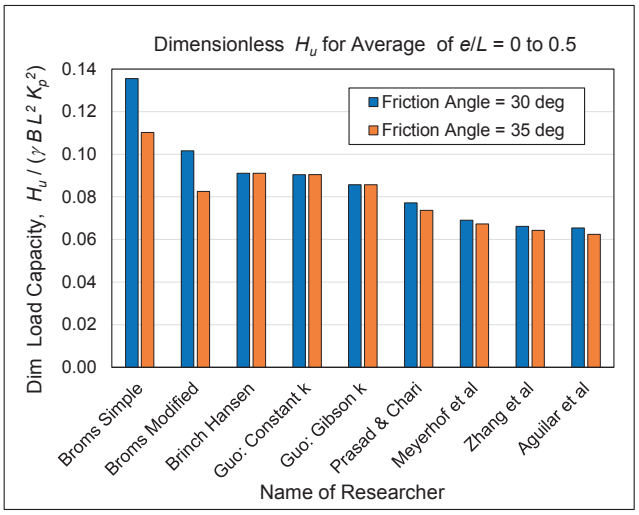

For the 30° soil friction angle the dimensionless force capacities range from 0.065 (Aguilar et al) to 0.14 (Broms Simple). This is a very wide range; a factor of greater than 2 between the lowest and highest capacity estimates, and indicates that the Broms Simple method, which gives the highest capacity, is probably unconservative.

With the exception of the two Broms methods, the dimensionless capacities are almost independent of the friction angle. This is because the LFPs in other than the Broms methods are essentially a function of K_p^2 (with minor variations) and the capacity has been made dimensionless by dividing by K_p^2.

A further comparison of the LFP methods was made by calculating the pole embedment depth required by each method for a typical 3 m high vertical pole wall assumed to be loaded by gravity loads including a live load on the assumed level surface behind the wall. The parameters assumed in the analysis are summarised in Table 1.

The active pressure from the wall backfill and surface live load was assumed to act on the pole down to the

Table 1. Typical Pole Wall: Analysis Input Parameters

Parameter	Value	Comment
Soil friction angle	35°	Both wall backfill and pole foundation
Soil unit weight	18 kN/m^3	Both wall backfill and pole foundation
Friction angle on pole/soil interface	35°	
Friction angle on back-face of wall	23.3°	Active pressure on back-face
Surface live load	5 kPa	Assumed to be factored
Pole diameter	0.6 m	Includes concrete encasement
Pole spacing	1.5 m	Spacing / diameter = 2.5
Load factor on active pressure	1.3	
Strength reduction on passive pressure	0.65	Gives effective factor of safety = 2.0
Pole spacing reduction factor	0.8	See Section 4 below
Vertical stress increase factor	1.2	See vertical Section 3 below

Table 2. Typical Pole Wall: Comparison of Pole Embedment Depths

Method	Embed Depth, *L* m	Rotation/ EmbedDepth z_r/L	Eccent Ratio *e/L*	Max Moment in Pole kN m
Meyerhof et al	3.15	0.71	0.109	84.2
Zhang et al	3.10	0.77	0.091	76.2
Aguilar et al	3.05	0.74	0.111	-
Prasad & Chari	2.90	0.77	0.119	74.2
Brinch Hansen	2.75	0.81	0.123	76.2
Broms: *Modified*	2.75	0.78	0.138	81.0
Guo: *Gibson k*	2.70	0.76	0.154	74.0
Guo: *Constant k*	2.65	0.75	0.167	75.5
Broms: *Simple*	2.40	1.00	0.120	74.1
Average	**2.83**	**0.79**	**0.126**	**76.9**

rotation point but was assumed to remain constant with depth below the level of the ground in front of the wall. For calculating the passive LFP the ground was assumed to be horizontal and at the level in front of the wall. A factor of 1.2 was applied to the vertical stress to make allowance for the increase in stress resulting from the additional height of soil behind the wall (see Section 3).

The lateral force capacity of the poles was approximately 64 kN. The depth of the point of rotation varied between the methods with a corresponding variation in the applied load (from the active pressure on the pole) and this changed by a small amount the ultimate lateral resistance required by each method.

Main results from the wall analysis are summarised in Table 2.

The typical wall analysis gave embedment depths between 2.4 to 3.15 m. That is, a factor of 1.3 between the smallest to greatest depth. A significant variation but perhaps not as great as the comparison of the pile head ultimate force capacities might indicate (Figure 12).

2.10 COMPARISON OF LFP METHODS WITH PILE TEST RESULTS

Ultimate pile head lateral force capacities predicted by the LFP methods discussed above were compared with the lateral force capacities observed in reported pile tests for short rigid piles in cohesionless soils (mainly sands). For this comparison only tests with *L/B* and *e/L* ratios less than 9 and 0.5 respectively were selected. Forty-one laboratory tests, nine field tests, and two centrifuge tests satisfied these limits and were used in the comparison. A summary of the selected tests including pile dimensions and the main soil parameters is given in Table 3. (The length and eccentricity ratio limits were based on the expected range in the present application.)

Ratios of the calculated lateral capacity divided by the observed capacity were computed for the LFP methods investigated. Average values of this ratio, the standard deviation of the average and the coefficient of variation are listed in Table 4. The observed capacities were

Type of Test	No of Tests	Pile Length/ Diameter m	Soil Friction Angles	Soil Unit Weights kN/m3	Tests Performed By	Test Information Source
Laboratory	37	0.198 to 0.912/ 0.076 & 0.152	38° to 49°	15 to 18	Agaiby et al, 1992	EPRI TR-104601, Chen & Kulhawy, 1994
Field	4	0.25/ 0.10 0.31/ 0.08 0.31/ 0.10	41°	17.1	Ivey et al, 1968	
Laboratory	1	0.90/ 0.102	40°	14.6	Joo, 1985	
Laboratory	3	0.612/ 0.102	35° to 46°	16.5 to 18.3	Prasad & Chari, 1999	Zhang et al, 2005
Field	1	6.0/ 0.90	35°	17	Adams & Radhakrishna, 1973	Prasad & Chari, 1999
Field	1	5.49/ 0.61	42°	16.5	Bhushan et al, 1981	
Field	1	9.75/ 2.44	39°	7.5	Anderson, 1997	Aguilar et al, 2019
Field	1	5.5/ 1.22	30°	11.8	Thiyyakkandi, 2016	
Field	1	6.4/ 0.914	34°	11	Ismael & Klym, 1978	
Centrifuge	2	9.05/ 1.09 9.05/ 1.22	36°	16.3	Georgiadis et al, 1992	Qin & Guo, 2014

Method	Ave Ratio Obs/ Cal H_u	Sta Dev of Ave Ratio Obs/Cal	Coeff of Variation of Ave Ratio Obs/Cal
Meyerhof et al	0.75	0.26	0.35
Aguilar et al	0.89	0.25	0.27
Broms: *Modified*	0.89	0.28	0.31
Zhang et al	0.91	0.24	0.27
Prasad & Chari	1.06	0.28	0.26
Petrasovits & Awad	1.08	0.34	0.31
Broms: *Simple*	1.19	0.36	0.31
Guo: *Gibson k*	1.25	0.33	0.26
Brinch Hansen	1.43	0.43	0.30
Zhang (Barton)	1.48	0.39	0.26

thought to be based on approximately the Meyerhof capacity or approximately a factor of 1.5 less than the ULS or hyperbolic capacity. Capacities given in Chen and Kulhawy, 1994 (EPRI project) were labelled lateral or moment limits and it was stated that this limit was approximately the load at which initial failure occurred and that it did not correspond to the ULS. Ratios between the hyperbolic (ULS) and the lateral or moment limits given by Chen and Kulhawy for the tests that were considered in the present comparison were mostly between 1.2 and 2.1. There is some uncertainty in how the observed capacity was assessed so the information presented in Table 4 is illustrative of the relative magnitude of calculated/observed ratios for the methods rather than the absolute values.

The Zhang (Barton), 2018 and the Petrasovits and Awad, 1972 methods listed in Table 4 are not discussed in detail above. Both are similar to the Broms *Modified* method with the LFP reaching a maximum positive value and a corresponding negative value at the rotation point. In the Zhang method, the LFP is defined by $P_u = z\, K_p^2 \gamma' B$ (FL^{-1} units) which Zhang indicated was used by Barton, 1982. In Petrasovits and Awad the LFP is defined by, $P_u = z\,(3.7K_p^2 - K_a)\,\gamma' B$.

The average ratio of observed to calculated values shown in Table 4 indicates that all methods except the Mayerhof, Brinch Hansen and Zhang methods give satisfactory agreement with test results. The Broms *Simple* method gives better agreement than expected but many of the tests involved soils with friction angles greater than 35° (see Table 3). In soils with friction angles lower than this value it is expected to give unconservative capacities. Zhang, 2018 indicated that his method (using the Barton LFP) gave the *hyperbolic* capacity which is approximately 1.5 times greater than the *Mayerhof* capacity calculated by the other methods except for Guo's methods. Therefore, it also gives capacities that are in satisfactory agreement with the test results.

The Guo *Gibson k* method gives values that on average are approximately a factor of 1.25 times the observed test values. However, the capacity for this and the Guo *Constant k* methods are based on the LFP reaching the soil yield pressure at the pile-toe and

YOUR NUMBER ONE ROCK STAR

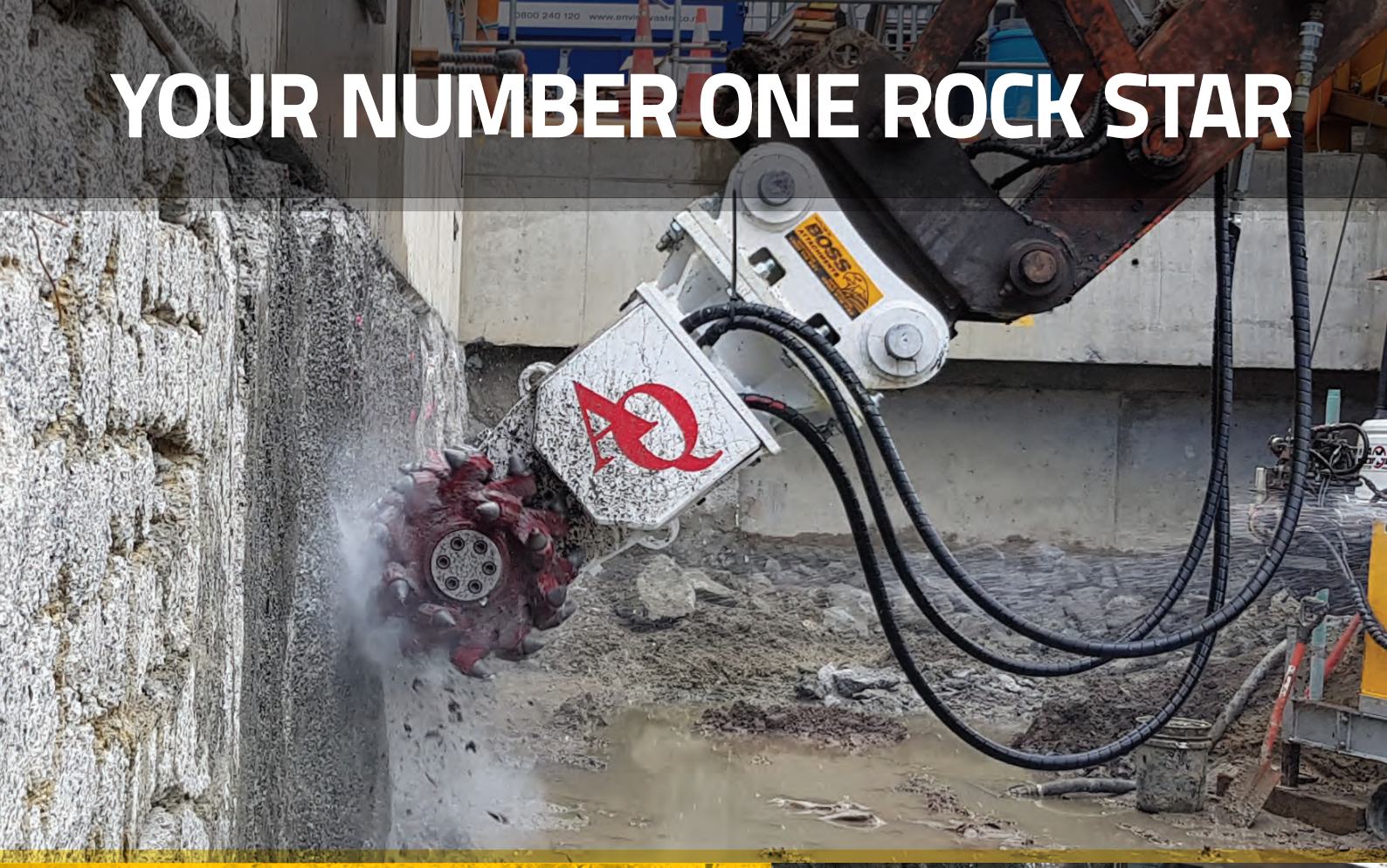

THE **PROVEN** ALTERNATIVE TO **BLASTING** OR **BREAKERS**

Antraquip Milling Heads operate with little or no micro cracking of the area outside the excavation line.

AQ ANTRAQUIP®

Built to work harder and last longer the Antraquip range can provide customer engineered solutions for any rock or concrete cutting project.

Models available to handle in excess of 200mpa in igneous rock.

NZ project details available on request

FREEPHONE 0800 278 742
paul@bossattachments.co.nz www.bossattachments.co.nz

BOSS ATTACHMENTS

BOS1695-19

this capacity is thought to be significantly higher than the *Meyerhof* capacity. It is unclear how the *Meyerhof* capacity could be determined from the Guo response curves shown in Figures 8 and 9 which have significant curvature for lateral force values greater than 0.5 times the pile-toe yield capacity. Equations given in Guo, 2008 for the case when both the positive and negative LFPs reach yield at the rotation point (force versus displacement curve approaches an asymptotic value) enable the *hyperbolic* capacities to be estimated and these are approximately 1.15 and 1.10 times the toe-yield capacities for *Gibson* and *Constant k* soils respectively (for *e/L* values between 0 to 0.4). If it is assumed that the *Meyerhof* capacity is approximately a factor of 0.7 times the *hyperbolic* capacity then the Guo Gibson k average observed/calculated test result ratio reduces to approximately 1.0 (1.25*1.1*0.7) for the Meyerhof capacity.

3. GRAVITY STRESSES NEAR WALL FACE

The LFP in all the methods discussed above is a function of the vertical effective stress in the soil assumed to be given by $z\,\gamma$ '. The lateral load capacity calculations are based on the ground having an approximately level surface near the pile with *z* being the depth below this level. In all the tests used for the comparison with the calculated capacities the ground surface was level. However, in the case of a pole retaining wall there is a step in the surface at the wall face with the depth of the pole toe below the ground in front of the wall being approximately the same as the height of the wall face. The wall ground surface geometry is therefore significantly different from that assumed in the pile head lateral force capacity calculation methods.

In the case of a wall the passive soil resistance against the pole above the rotation point is usually based on the depth below the ground in front of the wall. In contrast, the passive resistance below the rotation point is sometimes based on the depth below the ground surface adjacent to the top of the wall. This approach results in the calculated vertical stresses near the rotation point differing by a factor of approximately two over a short horizontal distance either side of the pole. This is an approximation that needs to be investigated in more detail since an increase in the vertical stress in the soil above the assumed value in front of the wall will increase the LFP on the pole above the pole rotation point, whilst a decrease in assumed vertical stress in the soil behind the wall will decrease the LFP on the pole below the rotation point.

As part of the present study the vertical stresses near the face of a 3 m high wall with level ground in front and behind the wall were calculated using an elastic plane strain finite element model. Vertical stress contours calculated by the model are shown in Figure 13. A soil unit weight of 20 kPa was used in the analysis and this resulted in the steps between the contours on the plot being approximately 13.5 kPa. The vertical wall boundary was unrestrained. This approximately simulates an active pressure state on the wall face.

At a depth of approximately the wall height below the ground surface in front of the wall there is significant variation in the vertical stresses on a horizontal plane extending both in front of the wall and into the backfill for a distance of the wall height (3 m). At a depth of 3 m below the surface in front of the wall and at distance of 3 m in front of the wall, the vertical stress is 67 kPa or a factor of 1.11 times the vertical stress at a large distance in front of the wall face (60 kPa = 3 x 20).

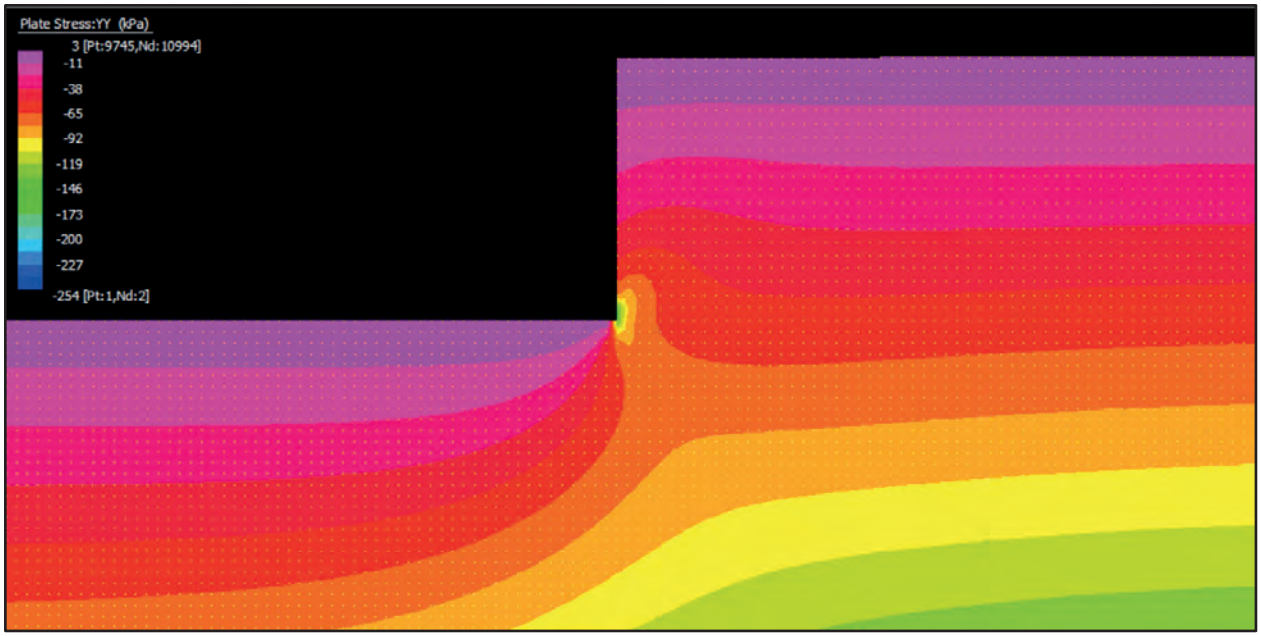

At this same depth and at a distance of 3 m behind the wall face, the stress is 112 kPa or a factor of 0.93 the vertical stress at a large distance behind the wall face (120 kPa = 6 x 20). On a horizontal plane at a depth of 1.5 m below the surface in front of the wall these factors are lower but are still significant being 1.07 in front of the wall and 0.95 behind the wall.

Figure 14 shows a plot of the vertical stresses near the wall face at a depths below the surface in front of the wall between 0.35 and 1.35 times the wall height. The horizontal distance from the face is shown in terms of pole diameters with the diameter taken as 0.6 m which is typical for a 3 m high wall. The positive direction is taken to be in the direction from the face into the backfill. The vertical stresses are plotted as the ratio of the FEA stress divided by the gravity stresses at large distances from the wall. The large distance stress is based on the depth below the ground in front of the wall and behind the wall for the stresses in front of the wall and behind the wall respectively.

Figure 14 shows that at two pole diameters in front of the wall the vertical stress ratio is between 1.27 and 1.4 with the ratio in the shallower depths (above 0.7 of the wall depth) being approximately 1.4. At two pole diameters behind the wall face the stress ratio is approximately 0.87 for depths greater than 0.35 of the wall depth. Figure 15 is a modification of Figure 14 with the FEA vertical stresses on either side of the wall shown as the ratio of the stress divided by the gravity stress at a large distance from the front of the wall. Figure 15 is relevant for the case when the analysis of the pole lateral capacity is based on the assumption that the ground surface is horizontal and at the level in front of the wall. Both Figures 14 and 15 show that at two pole diameters in front of the wall the gravity stress ratio over the upper section of the pole is approximately 1.4. This ratio drops to about 1.2 at three pole diameters from the wall so the impact on the passive LFP is rather uncertain. Figure 15 shows that the stress ratio in the backfill region at the pole toe (depth ratio approximately 1.0) at two pole diameters from the face is between 1.5 and 2.1 and increases to between 1.6 and 2.2 at three pole diameters. These stress ratios in both directions from the wall face indicate that the pole lateral load capacity will be significantly greater than calculated assuming the ground to be horizontal at the level in front of the wall. A correction could be applied by increasing A_r (or the effective unit weight of the foundation soil) by a factor of between 1.2 to 1.4. (A factor of 1.2 was used in the wall example described in Section 2.9 and Table 1.)

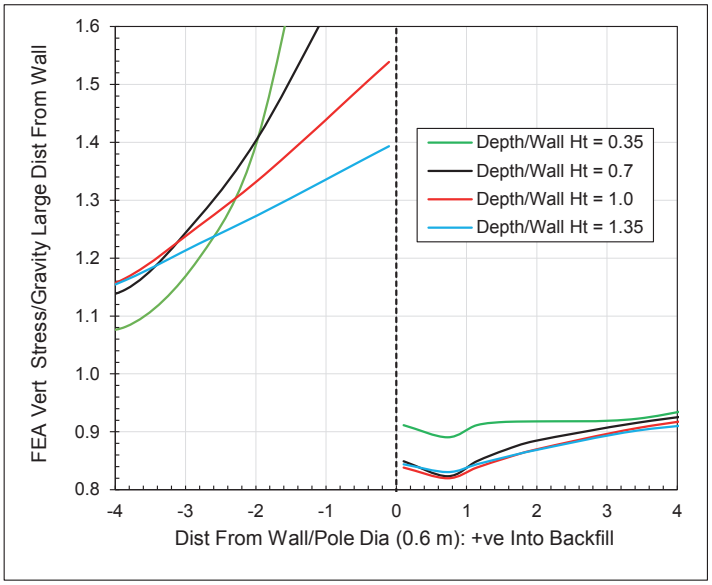

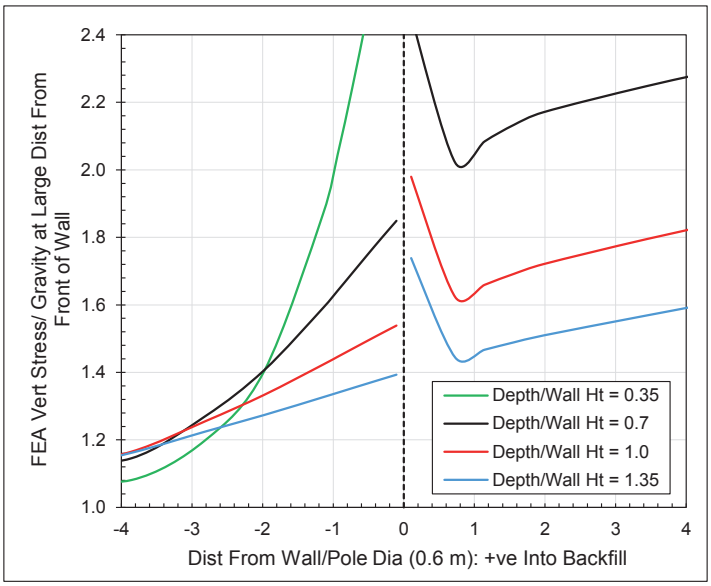

In the Broms *Modified* analysis (effectively a trial-and-error analysis) the LFPs above and below the rotation point can independently adjusted by scaling the passive resistance in the two regions. In the 3 m wall example described in Table 1, changing the LFPs by factors of 1.4 and 0.87 above and below the rotation point respectively, increased the Broms *Modified* lateral load capacity compared to the same wall without LFP modifications by approximately 30%. The modified LFPs reduced the required depth of embedment of the poles by approximately 12%. (These changes were based on using the total height to the top of the wall for calculating the LFP below the rotation point.) Although it is possible to modify the Guo analyses to allow for variations in vertical stress in the soil foundation near the wall face this adds complexity to the method which is not justified for the present application. As suggested above, assuming horizontal ground at the level in front of the wall and increasing the A_r by a factor of between 1.2 to 1.4 is a satisfactory approach for the present application.

4. PILE SPACING EFFECTS

For timber pole retaining walls the ratio of the pole centreline horizontal spacing, *S* divided by the embedded pole diameter (*S/B* ratio) is typically between 1.5 and 4.0. The spacing adopted is dependent on both the pole lateral resistance and the strength of the timber facing elements. For walls with a height of 3 m the spacing is likely to be at the lower end of this range. Below *S/B* ratios of 4.0 there is significant interaction between the stresses in the soil arising from the lateral loading of individual poles.

The lateral load behaviour of piles in groups is commonly analysed using the *p-y* method in which pile interaction is taken into account using a *p*-multiplier which is applied to the ultimate lateral load resistance of a single pile. A summary of relevant research on pole spacing effects is given below.

4.1 GEORGIADIS ET AL, 2013

Georgiadis et al used lower and upper bound finite element limit analysis and analytical upper bound plasticity methods to investigate the limiting lateral resistance of piles in a single pile row embedded in an undrained cohesive soil. Numerical analyses and analytical calculations were presented for various pile spacings and pile-soil adhesion factors. The numerical results were in good agreement with each other and also with the theoretical upper bounds produced by the analytical calculations. An empirical equation was proposed for the calculation of the ultimate undrained lateral bearing capacity factor.

4.2 PHAM ET AL, 2019

Pham et al investigated the ultimate lateral resistance for pile groups consisting of various arrangements of four piles, as well as two piles, three piles, four piles, and an infinite number of piles arranged in a row (relevant to the present application) against ground movement for various direction of the ground movement. They used a two-dimensional rigid-plastic finite element method to determine the total ultimate lateral resistance of the pile groups, but also the load bearing ratio of the piles in the group. The group effect was further investigated by considering the failure mode of the ground around the piles.

Although the study was based on pile resistance to ground movement, rather than loads applied to the piles as in the Georgiadis et al study, the results were similar for both types of loadings.

4.3 CHEN AND CHEN, 2008

Chen and Chen used elasticity theory and the concept of a fictitious pile to develop a rigorous analysis of the interaction factors between two piles subjected to horizontal loading and bending moment applied to the pile at the ground surface. By assuming the displacement compatibility between fictitious piles and the extended soil, the problem was reduced to a Fredholm integral equation of the second kind, which could be solved readily with numerical procedures. Close agreement was obtained between their results and other numerical results presented for the horizontal influence factors of single piles. They found that the conventional interaction factor approach, which ignores the pile stiffening effect, would generally yield satisfactory results, but may overestimate considerably the interaction effect when the piles are long and flexible.

4.4 ROLLINS ET AL, 2003

Static lateral load tests were conducted on three single piles and four pile groups at centre-to-centre spacings of 3.0, 3.3, 4.4 and 5.6 pile diameters. The pile groups had three to five rows with three piles in each row and the test piles consisted of steel piles of outside diameter 0.32 m and 0.61 m. Fifteen cycles of loading were applied at each deflection increment to evaluate the effect of cyclic loading and gap formation on lateral resistance. The load carried by each pile was measured along with deflection, rotation, and strain along the length of the pile to allow comparisons between the behaviour of the pile group and the single pile (Rollins et al, 1998). In addition, comparisons were made between the measured and calculated values using three computer programs based on the *p-y* method (Rollins et al, 2006).

The lateral resistance of the piles in the group was found to be a function of row location within the group, rather than location within a row. Contrary to expectations based on elastic theory, the piles located on the edges of the group did not consistently carry more load than those located within the group. The front row piles in the groups carried the greatest load, while the second and third row piles carried successively smaller loads for a given displacement. However, the fourth and fifth row piles, when present, carried about the same load as the third-row piles. Average lateral load resistance was a function of pile spacing. Little decrease in lateral resistance was observed for the pile group spaced at 5.6 pile diameters; however, the lateral resistance consistently decreased for pile groups spaced at 4.4, 3.3 and 3.0 pile diameters. Group reduction effects typically increased as the load and deflections increased up to a given deflection but then remained relatively constant beyond this deflection.

The Rollins et al pile tests were carried out in clay soils but they concluded that their *p*-multiplier curves for estimating pile interaction effects appeared to give reasonable estimates of the behaviour of pile groups in sand based on available full-scale and centrifuge testing (McVay et al, 1995). They also suggested that the curves were not significantly affected by the pile diameter or pile head boundary condition.

4.5 MOKWA AND DUNCAN, 2005

In discussing a paper by Ilyas et al, 2004 related to centrifuge tests on the lateral resistance of pile groups, Mokwa and Duncan presented results of their review study on the behaviour of the response of pile-groups to lateral loads (Mokwa and Duncan, 1999; Mokwa and Duncan, 2001). On the basis of the results of these studies, which summarized 29 separate field tests in varying soil conditions, Mokwa and Duncan developed a design chart to estimate values of the *p*-multiplier factor that were based on pile spacing and pile location within a group.

4.6 LIN ET AL, 2015

Lin et al carried out an experiment on a fully instrumented model to investigate the soil-structure interaction on single short, stiff pile laterally loaded at the head. The pile had a steel pipe section with diameter 102 mm, wall thickness 6.4 mm, and a length of 1.52 m. It was installed in well-graded sand and subjected to increasing lateral load. The pile and surrounding soil were fully instrumented using advanced sensors, including flexible shape acceleration arrays, thin tactile pressure sheets, and in-soil null pressure sensors. The sensors attached to the pile were used to develop the compressive soil-pile interaction pressures and the lateral displacement along the pile length. The tactile pressure sheet sensors provided the soil-pile interaction compressive pressures on the circumference of the pile at a specific depth and along the length of the pile. The null pressure sensor measurements were used to develop the distribution of horizontal stress changes in the soil around the pile as the lateral pile displacement increased.

Theoretical analysis of the nonlinear interaction of piles laterally loaded in cohesionless soils is complex. Finite element analysis can be used to study this problem but numerical results for the range of pile geometries relevant to the present study have not been published. The experimental study of Lin et al is therefore informative for the present application.

Figure 16 shows the pressures measured in the soil surrounding the pile at the ultimate lateral load of 3.8 kN reached at the end of a test. Contours are soil pressures with labels in kPa. Of interest for the present application is the pressure drop in the lateral direction (x-direction). At a lateral distance of 2.5 pile diameters the pressure in the soil has dropped from a peak value of greater than 50 kPa on the leading face to approximately 5 kPa. This indicates that there would be negligible interaction effect for piles spaced on centrelines of greater than 5.0 diameters in cohesionless soils.

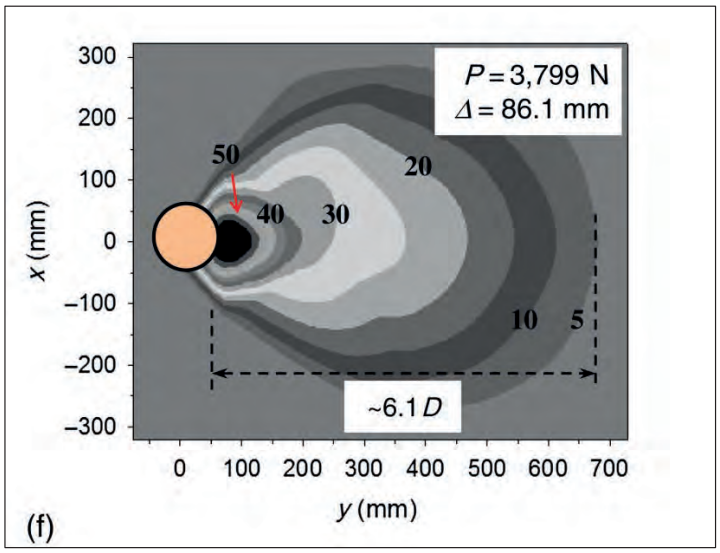

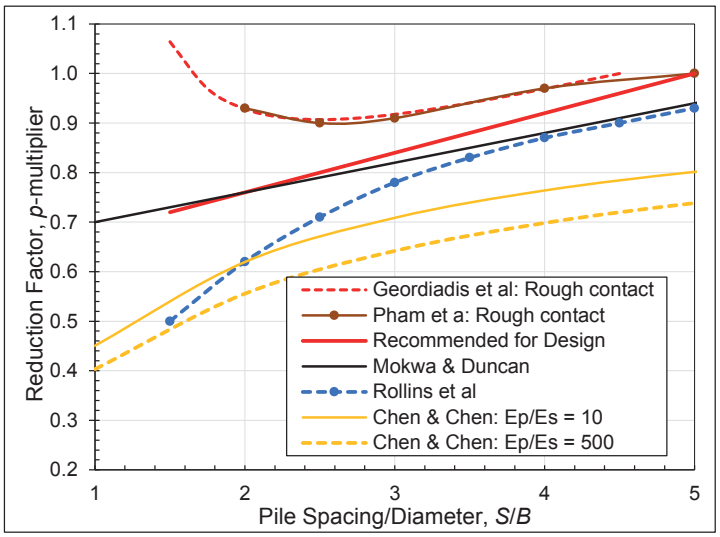

4.7 COMPARISON OF *P*-MULTIPLIER INTERACTION CURVES

A comparison of *p*-multipliers from the results of the investigations mentioned above is shown in Figure 17. The curves from Pham et al and Georgiadis et al are for piles with full adhesion (perfectly rough) and are based on theoretical finite element and plasticity theory. The Rollins et al curve and the *p*-multiplier proposed by Mokwa and Duncan are from pile test results and apply to the leading row of multi-row pile groups.

The *p*-multipliers from the test results are significantly lower than the values obtained by Pham et al and Georgiadis et al indicating greater pile–soil–pile interaction effects. The test values are applicable to the entire pile length, and one of the reasons for this difference could be that the reduction in the limiting earth pressure, due to group effects, is not constant with depth, as implied by the adoption of constant *p*-multipliers. The theoretical *p*-multipliers are applicable to the lower part of piles, where the flow around failure mechanism assumed is predominant. The depth below the surface where two-dimensional plane strain failure occurs, is likely to increase with the decrease of pile spacing, which could explain the large discrepancies at small pile spacings. Other factors that may contribute to the differences are the different soil types and the different geometrical characteristics of the tests. The tests were for multiple rows and interaction between the leading and second row would result in lower *p*-multipliers.

Chen and Chen reduction factors based on elasticity theory are shown in Figure 17 for pile to soil Young's moduli ratios, E_p/E_s of 10 and 500. They are based on an assumed row of 5 piles (interaction was computed by superposition of the influence coefficients between two piles) and for $L/B \geq 10$ (the only length to diameter ratio presented by Chen and Chen). Although elastic solutions are not relevant for the present application, they provide a lower bound for the *p*-multiplier reduction factors.

For the present design application, a recommended curve is shown in Figure 17. It generally follows the Mokwa and Duncan curve (a straight line) but with the *p*-multiplier reducing to 1.0 at S/B = 5 instead of at a ratio of 6.

5. ULTIMATE LATERAL FORCE CAPACITY OF RIGID PILES IN COHESIVE SOIL

Significant research effort has focused on the determination of the limiting lateral load, P_u distribution with depth for single piles in clay (Matlock, 1970; Reese and Welch, 1975; Stevens and Audibert, 1980; Murff and Hamilton, 1993; Jeanjean, 2009; Georgiadis and Georgiadis, 2012). This research established that P_u increases with depth in the upper part of the pile, where a wedge-type failure occurs, up to a maximum value and remains constant in the lower part of the pile. In this lower part failure take place with a flow-around mechanism. Randolph and Houlsby, 1984 developed lower and upper bound plasticity solutions for the calculation of the maximum load per unit length, and proposed the following lower bound equation, expressed in terms of the single-pile lateral bearing capacity factor, N_p:

$$N_p = \frac{P_u}{s_u B} = \pi * 2\arcsin(\alpha) + 2\cos(arcsin\,(\alpha)) + 4\left[cos\left(\frac{\arcsin(\alpha)}{2} + sin\frac{\arcsin(\alpha)}{2}\right)\right] \quad (39)$$

Where s_u is the undrained shear strength, B is the pile diameter and α is the pile soil adhesion factor (limiting interface shear stress/undrained shear strength). Martin and Randolph, 2006 showed that the above expression gives the theoretically exact solution for all practical purposes.

The above equation gives N_p values of 9.14 and 11.94 for perfectly smooth and full adhesion on the pile-soil interface respectively.

Some of the models that have been developed to describe the limiting lateral force per unit length down the full depth of the pile are described below.

5.1 REESE MODEL

In the Reese model (Reece 1958; Reece et al 1974), the soil behaviour is divided into either shallow or deep failure. For shallow failure, a three-dimensional passive wedge is assumed to exist in front of the pile. By summing the wedge forces in the horizontal direction, the soil resistance against the shaft was obtained. This procedure gave an N_p of 2 if the failure wedge occurs with a vertical inclination of 45^o without shear forces between the shaft and soil. For the deep failure, at depths greater than 3B Reece undertook a simplified plasticity analysis and estimated an N_p of 12. The N_p between ground surface and 3B depth was obtained by linear interpolation, to give the N_p profile shown in Figure 18.

5.2 BRINCH HANSEN MODEL

As discussed above for cohesionless soils, Brinch Hansen, 1961, considered the soil behaviour at shallow, moderate, and large depths. He considered soils with both friction and cohesion components and developed equations and corresponding charts using simplified plasticity theory based on horizontal translation of a rough wall and deep strip foundations. For a purely cohesive soil (zero friction angle) the variation of N_p with depth calculated using his equations is shown in Figure 18. The value of N_p at a depth of 3B is 6.2.

The yield stress was assumed to act uniformly across the shaft diameter and is multiplied by the shaft diameter to obtain the yield or lateral force per unit length.

5.3 BROMS MODEL

Broms, 1964b employed classical plasticity theory for determining values for N_p and examined a number of different shaft shapes and surface roughness. The resulting N_p values ranged from 8.28 for a smooth square shaft to 12.56 for a rough flat plate. The value for a smooth circular shaft was 9.14 which agrees with the value calculated from the Randolph and Houlsby, 1984, equation given above. As a simplification, he assumed that N_p = 9 below a depth of 1.5B and N_p = 0 above that depth (see Figure 18).

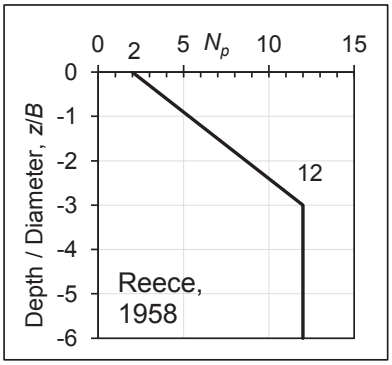

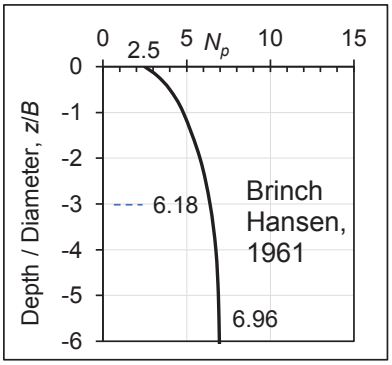

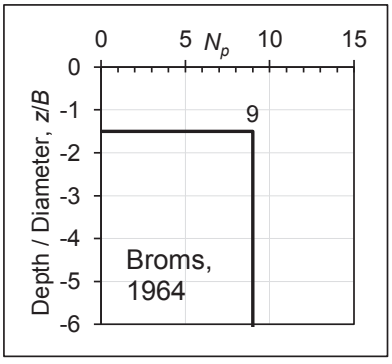

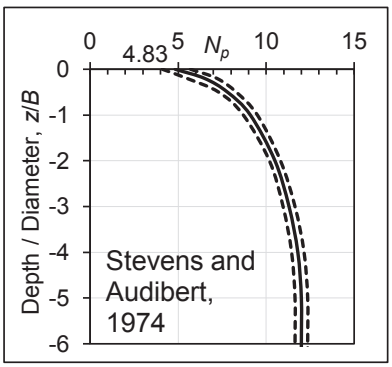

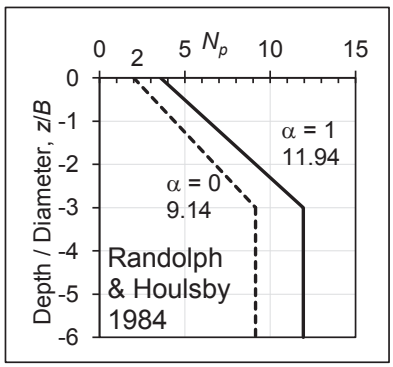

5.4 STEVENS AND AUDIBERT MODEL

By comparing available *p-y* curves (Matlock, 1970; API, 1977) Stevens and Audibert, 1979 back figured a profile of N_p with depth from instrumented driven pile load test data. Their observed N_p range versus depth is shown in Figure 18. They recommended the profile shown within the observed range. No equation was given to represent this profile. For $z/B > 4$, $N_p = 12$.

5.6 RANDOLPH AND HOULSBY MODEL

Randolph and Houlsby, 1984 considered a wedge failure at shallow depth and used plasticity theory for N_p at large depths. Their N_p profiles for smooth and rough shafts are shown in Figure 18. At the ground surface, a yield stress of $3s_u$ was obtained from a passive stress of $2s_u$ in front of the shaft and allowance for side shear. As described above, at depth they considered the soil as a perfectly plastic cohesive material. The rough shaft N_p limiting value of 11.9 at depth is relevant to the present study because drilled holes backfilled with pole concrete surround are likely to be perfectly rough.

5.7 PENDER MODEL

Pender, 2000 found that the assumption made by Broms of an unsupported depth of 1.5*B* was too conservative for the short piles used in pole wall design. To determine an appropriate depth, he used the pressure distribution shown in Figure 19 that has a N_p value of 5 at the ground surface increasing to 12 at a depth of 3*B*. His conclusion was that a depth of 250 mm of zero resistance was appropriate for short piles used in pole wall design.

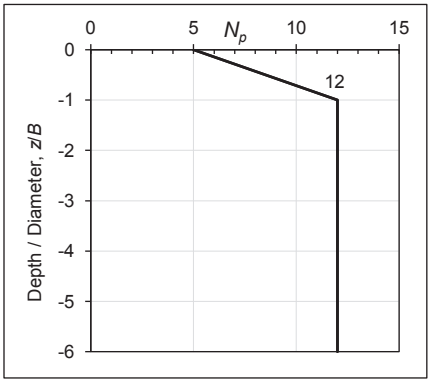

FIGURE 19. N_p profile used by Pender, 2000.

5.8 ULTIMATE LATERAL FORCE CAPACITY IN COHESIVE SOIL (UNDRAINED)

The pile head lateral force capacity, H_u is calculated from the cohesive LFP by limit equilibrium analysis of the horizontal forces and moment in a similar manner to that described for cohesionless soils. This requires the simultaneous solution of force and moment equilibrium equations with unknown variables the depth of rotation and the lateral force.

Solutions for the assumed LFP shown in Figure 20 are presented in Pender, 1997; Motta, 2013, and Zhang, 2018. The solution for this LFP is readily applied to the case when there is zero resistance in a top layer of depth z_t below the ground surface by reducing the pile depth below the ground surface of L by z_t and increasing the eccentricity e by z_t (effectively an artificial ground surface at depth z_t)

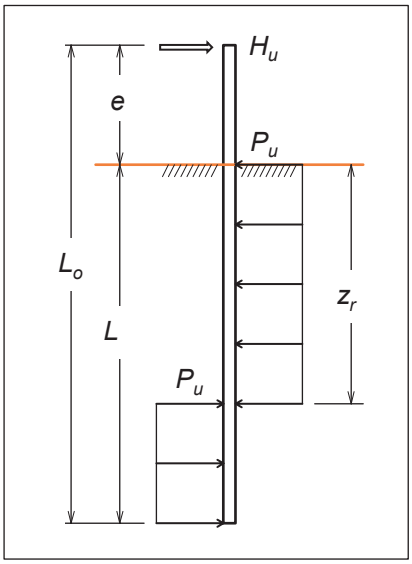

FIGURE 20. Assumed LFP for analysis. From Zhang, 2018.

Compact forms of the solution are given by Zhang, 2018. Minor rearranging of his solution gives the dimensionless ultimate lateral load capacity H_{ud} as:

$$H_{ud} = \frac{H_u}{P_u L} = 1 - 2R + \sqrt{4R(R-1)+2} \qquad (40)$$

Where $P_u = s_u B N_p$ the limiting force on the pile per unit length, $R = L_o/L = 1 + e/L$

The dimensionless rotation depth z_r/L is given by:

$$z_r/L = e/L + \sqrt{(e/L)^2 + e/L + 0.5} = 0.5(1 + H_{ud}) \qquad (41)$$

The depth to the maximum bending moment in the pile, z_m and maximum moment, M_m are determined from calculating the depth of zero shear force in the pile and are given by Pender, 1997 as:

$$\frac{z_m}{L} = \frac{H_u}{P_u L} = H_{ud} \qquad (42)$$

$$M_{md} = \frac{M_m}{P_u L^2} = H_{ud}\left(\frac{e}{L} - \frac{H_{ud}}{2}\right) \qquad (43)$$

The depth z_m is taken from the effective soil surface (surface level reduced by depth z_t of any layer of zero resistance). If a zero-resistance surface layer is assumed, the force eccentricity e above actual ground level is increased by z_t.

By assuming elastic-plastic soil response Motta, 2013

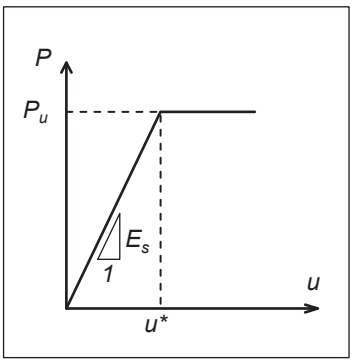

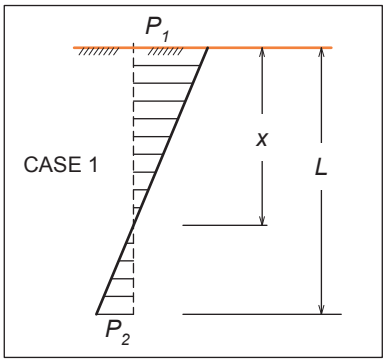

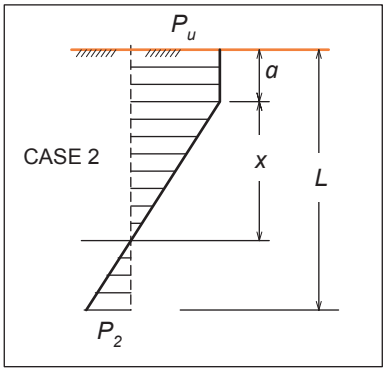

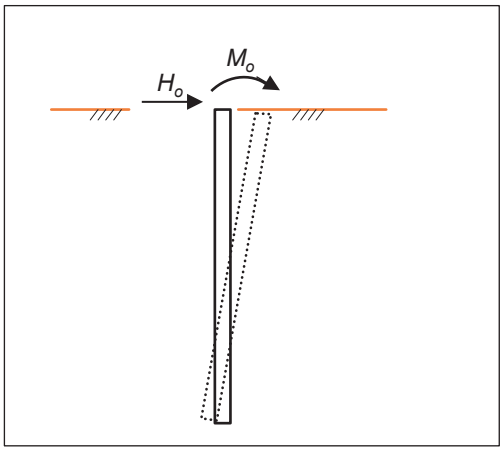

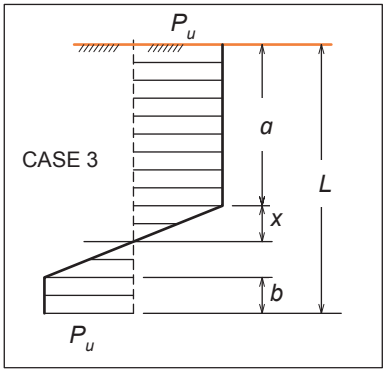

presented lateral force versus displacement curves. Defining an elastic stiffness or modulus of the soil-reaction as E_s (FL^{-2} units) the limiting deflection is given by:

$$u^* = P_u/E_s \tag{44}$$

After the soil yields the soil force on the pile was assumed to be constant with increasing soil deflection (see Figure 21). Motta defined three cases of soil-pile interaction as shown in Figure 22.

In Case 1 the soil remains elastic over the pile depth. With increasing deflection Case 2 is reached with yield in the soil down to depth *a* at distance *x* above the rotation point. With further deflection yield in the soil is reached at the pile toe and Case 3 commences with yield progressing from the toe up to the rotation point. (The soil-pile interaction to reach limiting forces on the pile is similar to the interaction described above for cohesionless soils.)

From equations presented by Motta the pile top lateral force required to initiate soil yield at the pile toe, H_y can be calculated from the following expression:

$$H_{yd} = \frac{H_y}{P_u L} = -\frac{(3e_d + 1)}{2} + \frac{\sqrt{(3e_d + 1)^2 + 2}}{2} \tag{45}$$

Where $e_d = (e + z_t)/L_e$ and L_e is the length of pile excluding the ineffective soil depth z_t

The pile ground level displacement, u_y at toe yield can be calculated by:

$$u_{yd} = \frac{u_y E_s}{P_u} = \frac{1 + H_{yd}}{\sqrt{3 - 6H_{yd} - 3H_{yd}^2 - 12e_d H_{yd}}} \tag{46}$$

Solutions for the dimensionless ultimate lateral load, load at toe yield and the depth of the rotation point as functions of eccentricity ratio e_d (e/L) are shown in Figure 23. Ultimate loads are shown for three cases; z_{td} = 0 (no limiting force reduction in the top layer), z_{td} = 0.1 (no resistance in top layer of depth 0.1*L*) and for a top

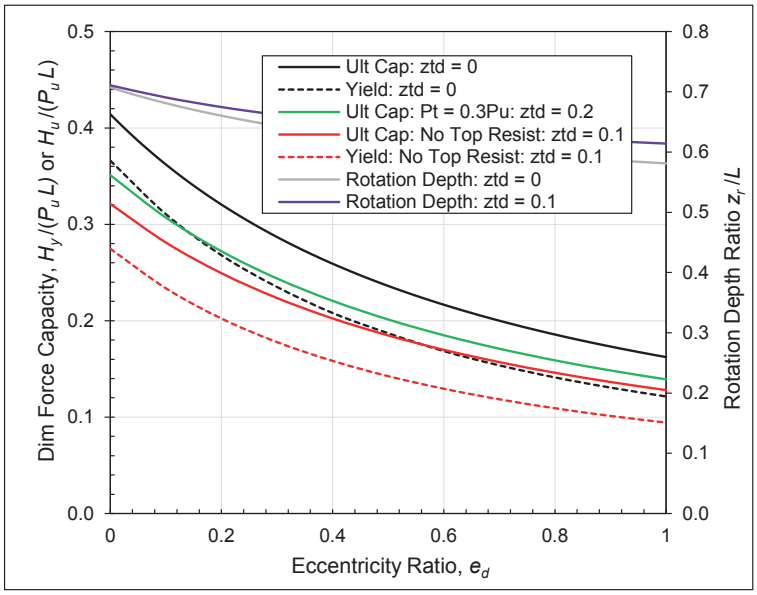

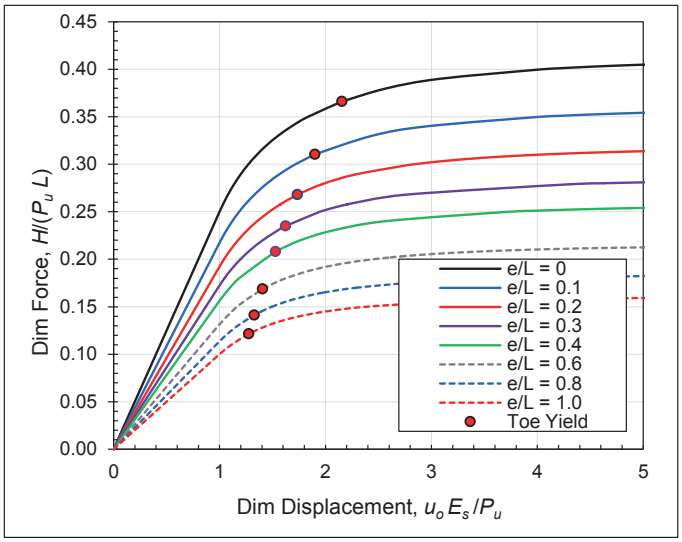

layer with a limiting force profile increasing from $0.3P_u$ at the surface to $1.0P_u$ at a depth of z_{td} = 0.2, where $z_{td} = z_t/L$. The dimensionless ultimate and yield forces, and the eccentricity ratio are plotted in terms of L the length of the pile from ground surface to the toe with the eccentricity, e taken as the height of the horizontal force above ground level. Yield loads and rotation depths are only shown for the first two cases because yield loads and rotation depths cannot be readily calculated for the case where P_u varies with depth (there is no available closed form equation). The rotation depth for the z_{td} = 0.1 case is calculated from the actual ground surface (rather than the effective surface).

For the two cases where pile toe yield capacities were calculated the ultimate load capacities are approximately 20% higher than the yield capacities over the e_d range of 0 to 1.0. Reducing the resistance to zero in a top layer of dimensionless depth z_{td} = 0.1 reduces the ultimate capacity by approximately 22%. The ultimate capacity for this case is on average 8% less than the case with the variable LFP in the z_{dt} = 0.2 top layer so it gives a conservative estimate for the more realistic case of a variable LFP in the top layer.

Ultimate and yield capacities for values of $z_t > 0$ can be estimated from the z_t = 0 curves by using appropriate values of e and L in the dimensionless parameters. (For z_t = 0.1 an e_d value = (0.1+e)/0.9 and an effective length of 0.9L would be used to estimate H_u and H_y from the z_t = 0 curve.)

Dimensionless pile head lateral force versus ground level (u_o) displacement curves, calculated from displacement equations given by Motta, 2013, for e/L ratios from 0 to 1.0 are shown in Figure 24.

5.9 COMPARISON OF CAPACITIES USING THE BROMS LFP WITH PILE TEST RESULTS

Ultimate capacities predicted by the constant LFP or *Broms* method discussed above for cohesive soil were compared with lateral load test results published in Chen and Kulhawy, 1994 for short rigid piles in clay soils. For this comparison only tests with L/B and e/L ratios less than 9 and 1.1 respectively were selected. Forty-three laboratory tests and seven field tests satisfied these limits and were used in the comparison. A summary of the selected tests including pile dimensions and the soil shear strength is given in Table 5.

Zhang, 2018 calculated ultimate capacities using the limiting force of $9s_uB$ recommended by Broms and compared these capacities for a range of 58 laboratory and field tests, including tests on piles with L/B and e/L ratios greater than considered in the present study. However, he assumed that the soil provided resistance over the total pile length and did not use the 1.5B ineffective top layer recommended by Broms, 1964b. The average ratio of calculated ultimate capacity divided by the test capacity (H_u/Q_u) over the 50 tests considered in the present study was 1.09. The test load capacities were taken as the *hyperbolic* (or ULS load) as presented in Chen and Kulhawy, 1994. For the present study, corresponding ultimate capacities were calculated assuming a N_p value of 11 (based on full soil adhesion) instead of 9, and assuming ineffective top layer depths of zero, 0.5B and 1.0B. Results from these analyses and the analysis based on Zhang's assumptions for the relevant 50 tests are summarised in Table 6.

Overall, there is reasonable agreement between analyses based on the constant LFP (*Broms* method) and the test results but the level of agreement was sensitive to the assumption made regarding the depth of the top layer with ineffective resistance. The N_p value of 9 and

WE'VE GOT IT COVERED...

ROCKFALL PROTECTION SYSTEMS

INCLUDING PRODUCTS FROM:

GEOFABRICS
GEOBRUGG
AVAROC
G.T.S ELITE

PLUS...

EROSION CONTROL
TEMPORARY SOLUTIONS
ANCHOR SYSTEMS
EXPLOSIVES

We minimise your risks!

AVALON

// ROPE ACCESS SERVICES

PO BOX 5187, 94 HIGH STREET, FRANKTON, HAMILTON 3204

P 07 846 1686 **E** admin@avalonltd.co.nz **W** avalonltd.co.nz

CONSULT // DESIGN // DELIVER

Type of Test	No of Tests	Pile Length, m	Pile Diameter, m	Soil Shear Strength, kPa	Tests Performed By
Laboratory	46	0.267 to 1.050	0.051 to 0.175	1.62 to 7.06	Mayne et al, 1995
Field	3	6.1 4.57 4.57	0.91 0.91 0.76	44 45 44	Bierschwale et al, 1981
Field	1	10.95	1.83	55	Dunnavant & O'Neil,1985
Field	1	4.40	0.95	14	Baguelin et al, 1973
Field	1	5.20	0.67	98	Harris et al, 1985
Field	1	0.31	0.10	75	Ivey et al, 1968

Adopted Variation of Broms Method	N_p	Top Layer Ineffective Depth in Dia. Units	Ave Ratio Obs/ Cal H_u	Sta Dev of Ave Ratio Obs/Cal
Zhang, 2018	9	0	1.09	0.26
Broms, 1964	9	1.5*B*	0.40	0.14
Present Study	11	0	1.33	0.42
	11	0.5*B*	0.99	0.27
	11	1.0*B*	0.71	0.20

ineffective layer depth of 1.5*B* recommended by Broms gives load capacities less than 50% of the average of the test capacities (based on the *hyperbolic*, ULS). The average *L/B* ratio for the test piles was 4.4 so reducing the effective length by 1.5*B* has a significant impact on the load resistance. For longer piles the reduction in resistance would obviously be less.

For the present application, using an N_p of 11 (based on a rough soil-pile interface) and assuming that the depth of ineffective layer is 0.5*B* appears acceptable and gives good agreement with the average of the test load capacities. A top ineffective depth of 0.5*B* would correspond to about 300 mm or about 0.1*L* for typical pole walls that have *L/B* ratios of about 5.

5.10 COMPARISON OF DEPTHS OF EMBEDMENT REQUIRED FOR TYPICAL POLE WALL

A further comparison of the assumptions made in application of the constant LFP assumption was made by calculating the pole embedment depth required by three of the N_p and z_t combinations listed in Table 6 for a typical 3 m high vertical pole wall assumed to be loaded by gravity loads including a live load on the assumed level surface behind the wall. The parameters assumed in the analysis are summarised in Table 7.

Active pressure from the wall backfill and surface live load were assumed to act only above ground with no load from these pressures transferred to the pole in the cohesive soil foundation. The ground in front of the wall was assumed to be horizontal.

The length of pole embedment was based on the toe yield capacity using the Motta yield equations. Using this approach ensures that deflections are unlikely to exceed acceptable limits; however, it is necessary to consider the overstrength of the foundation up to the ultimate capacity of the soil to design the pole above ground and the composite section pole with concrete encasement below ground.

The total factored load on the wall (pressures from backfill and surcharge) was 42 kN and acted at an eccentricity of 1.08 m above ground level. The analysis procedure was to determine the required total embedment of the pole to achieve the required capacity at the commencement of toe yield (42 kN) and then to calculate the ultimate capacity using the yield embedment length. In all three cases investigated the soil ultimate capacity was approximately a factor of 1.3 greater than the yield capacity. Main results from the wall analysis are summarised in Table 8.

The below ground bending moment diagram and a flexural capacity curve (ULS) for the encased timber pole using N_p = 11 and z_t = 0.3 m is shown in Figure 25. The

Parameter	Value	Comment
Wall height	3 m	
Backfill and foundation soil friction angle	35^o	
Backfill unit weight	18 kN/m^3	
Friction angle on back-face of wall	23.3^o	Active pressure on back-face
Surface live load	5 kPa	Assumed to be factored load
Foundation soil shear strength	50 kPa	
Pole diameter including encasement	0.6 m	Encasement > 50 mm thick
Pole spacing	1.5 m	Spacing / diameter = 2.5
Load factor on active pressure	1.3	
Strength reduction on soil shear strength	0.65	Gives effective factor of safety = 2.0
Pole spacing reduction factor	0.8	See pole spacing section above
Thickness of concrete surround	50 mm	
Concrete compressive strength	20 MPa	
Concrete modulus of elasticity	22 GPa	
Timber pole flexural design stress	17.4 MPa	Characteristic stress of 38 MPa
Timber section strength reduction factor	0.8	
Timber pole modulus of elasticity	7.4 GPa	
Encased strength / bare pole strength	1.56	See details in following section

N_p Value	Ineffective Layer Depth, z_t m	Required Total Pole Length Below Ground, L m	Max Dim Moment Below Ground, M_{md}	Required Timber Pole Dia, mm
11	0.3	2.0	0.120	350
9	0.3	2.3	0.120	360
11	0.6	2.5	0.098	370

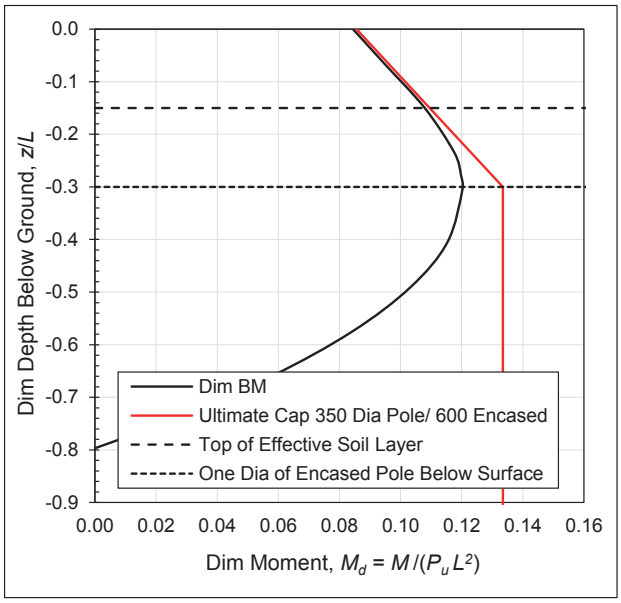

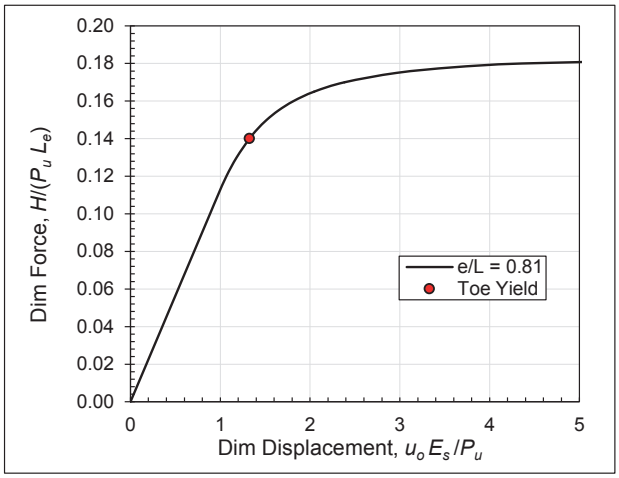

moments shown in dimensionless form in Table 8 and Figure 25 were calculated by dividing the moment by the limiting force per unit length and the square of the total pile length below ground ($M_d = M/(P_u L^2)$). The capacity curve for the pile is based on a 350 mm diameter timber pole section at ground level increasing linearly to a fully composite pile section at a depth of 600 mm (one diameter of the composite section) below the ground surface. It is assumed that the 50 mm thick concrete surround commences at ground level.

The force versus displacement plot for the example using N_p = 11 and z_t = 0.3 m is shown in Figure 26. The length, L_e (1.7 m) used in the dimensionless factors is the embedment depth below the ineffective top layer of soil. The total eccentricity including the ineffective layer was 1.38 m giving an effective e/L_e of 0.81.

6. DISPLACEMENTS IN COHESIVE AND COHESIONLESS SOILS

For most soils including clay and sand, pile head force versus displacement curves are assumed to follow a hyperbolic curve as show in Figure 27 and defined by the equation (Lam and Martin, 1986):

$$\frac{H}{H_u} = \frac{u/u_c}{1 + u/u_c} \tag{47}$$

Where H_u is the ultimate force capacity and u_c the displacement at 0.5 of the ultimate force.

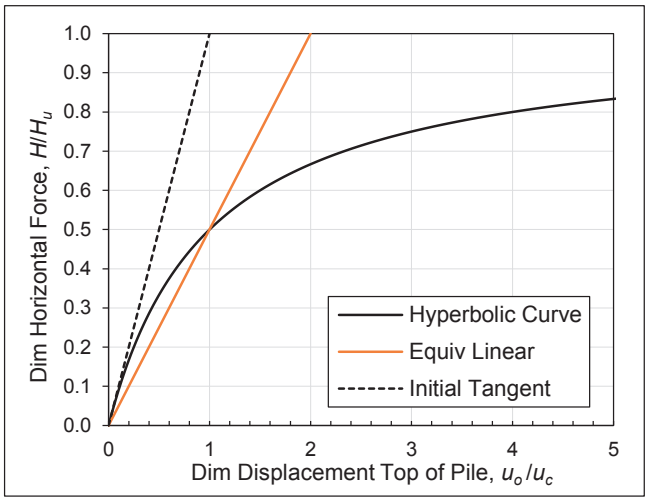

FIGURE 27. Typical pile top force versus displacement for clay.

Comparison of Figures 26 and 27 shows significant differences with the elastic portion being greater in Figure 26 which is based on an elastic-plastic assumption.

6.1 COHESIVE SOILS

The initial stiffness E_i of the pile force versus displacement curve for a cohesive soil is given by Lam and Martin, 1986 as:

$$E_i = \frac{P_u}{u_c} \tag{48}$$

Displacement u_c is given by:

$$u_c = 2.5\varepsilon_c B \tag{49}$$

Where ε_c is the strain amplitude at one-half the peak deviatoric stress in an undrained compression test. It usually ranges from 0.005 to 0.025. In the absence of laboratory data, a value of 0.01 is suggested by Lam and Martin.

In the example for clay presented in the previous section the limiting force per unit length, P_u is expected to vary over the top half of the pile increasing to a value of 330 kN/m ($s_u N_p B$) at the toe. Using this value gives an initial elastic modulus, E_i of 22 MPa (u_c = 15 mm). For the complete pile length, adopting an equivalent linear value of one-half of the initial stiffness value would appear to be appropriate for predicting the serviceability displacement (at a load of approximately toe yield capacity/1.3). From Figure 27 and making allowance for pile interaction (a reduction to stiffness of approximately 0.8) the pile top ground level displacement at toe yield was estimated as 41 mm. (The rotation depth below ground surface was estimated to be 1.31 m.) Making allowance for the load factor of 1.3 the serviceability limit state (SLS) deflection at the top of the wall was estimated to be 105 mm at a corresponding wall rotation of 1.8°. The wall top SLS displacement is significant but within acceptable limits.

6.2 COHESIONLESS SOILS

The tangent stiffness E_t of the pile force versus displacement curve for cohesionless soil is given by Lam and Martin, 1986 as:

$$E_t = k_1 z \tag{50}$$

Where E_t is the force per unit length per unit deflection and varies linearly with depth z. k_1 is a coefficient for sands which varies with relative density or friction angle (FL^{-3} units). Values of k_1 are plotted in Figure 28. The initial tangent values are from Reese et al, 1974 and the secant values from Terzaghi, 1955.

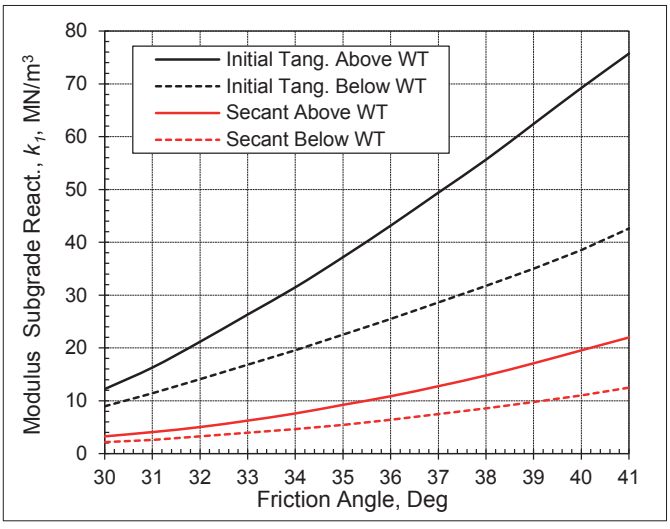

FIGURE 28. Subgrade modulus values for sand.

DENNY AVE LEVEL CROSSING GRADE SEPARATION, PERTH WESTERN AUSTRALIA

STONE STRONG
SYSTEMS NEW ZEALAND

0800 820 8070
www.stonestrong.co.nz

PHOTO COURTESY OF Downer
Relationships creating success

Parameter	Value	Comment
Foundation soil friction angle	35°	
Pole diameter including encasement, B	0.6 m	Encasement > 50 mm thick
Pole embedment below ground level, L	2.8 m	
Calculated eccentricity ratio, e/L	0.138	
Reduced pressure coefficient, A_r	153 kN/m	Soil strength and pole spacing reductions
Initial tangent modulus, k_i	37 MPa/m	From Figure 28 (Lam & Martin, 1986)
Adopted Guo k_o modulus, $(k_o = k_i/B)$	20.6 MPa/m^2	Initial tangent modulus reduced by factor of 3
Dimensionless ground level displacement	3.1	At toe yield. From Figure 8 $(u_o\, k_o/A_r)$
Ground level displacement at toe yield, u_o	24 mm	
Dimensionless rotation depth, z_r/L	0.76	From Figure 7
Pole rotation angle at toe yield	0.011 rad	0.63°
Displacement at top of wall at toe yield	60 mm	45 mm at SLS

The displacement of the typical pole wall example described in Table 1 was calculated using the Guo analysis for Gibson *k*. A summary of the analysis is given in Table 9.

To obtain the displacement at toe-yield the initial tangent stiffness should be reduced by a factor of between 2 and 4. A reduction of 4 gives approximately the Terzaghi secant value (see Figures 27 and 28.) For the present example, a reduction factor of 3 was used.

Making allowance for the load factor of 1.3 the SLS deflection at the top of the wall was estimated to be 45 mm at a corresponding wall rotation of 0.5°. The wall top SLS displacement is clearly within acceptable limits.

7. ULTIMATE CAPACITY OF RIGID PILES IN C-ϕ SOIL

Zhang, 2018 presents a solution for the ultimate capacity of a laterally loaded rigid pile in a *c*-ϕ soil. He expressed the ultimate capacity in dimensionless form by:

$$f_1 = f_c + kqf_\emptyset, \quad (51)$$

or alternatively:

$$f_2 = f_\emptyset + qkf_c \quad (52)$$

Where:

$f_1 = H_u/(q_u L_o)$ the dimensionless ultimate capacity in the *c*-ϕ soil

$f_2 = H_u/(kL_0^2)$ the dimensionless ultimate capacity in the *c*-ϕ soil

$f_c = H_u/(q_u L_o)$ the dimensionless ultimate capacity of the pile in a cohesive soil

$f_\emptyset = H_u/(kL_o^2)$ the dimensionless ultimate capacity of the pile in a cohesionless soil

$$kq = \frac{kL_0}{q_u}$$

$$qk = \frac{q_u}{kL_o}$$

$$L_o = L + e$$

$$k = \gamma' KB$$

$$q_u = N_p s_u B$$

K is the ultimate lateral coefficient for cohesionless soil. ($K = K_p^2$ in the Guo analysis.)

Complex expressions are given for z_{rd} (z_r/L) the dimensionless rotation centre. For design purposes the depth of the rotation centre can be estimated from Figure 29. This figure shows how the rotation centre varies depending on the *kq* ratio for the soil between the limiting cases for a purely cohesionless soil with *kq* = 0 and a purely cohesive soil with *kq* = a large value (*qk* = 0).

Dimensionless ultimate capacities f_1 and f_2 are plotted as a function of the eccentricity ratio in Figures 30 and 31 respectively. Either of the two figures can be used but Figure 30 is more convenient for a cohesive soil and Figure 31 for cohesionless soils with small s_u values. These capacities are hyperbolic values based on the assumed ultimate pressure diagram shown in Figure 32. The *f*ϕ and f_c components used in the calculation of f_1 and f_2 are computed using the z_r rotation depth calculated from moment equilibrium for the combined cohesionless and cohesive components shown in Figure 32.

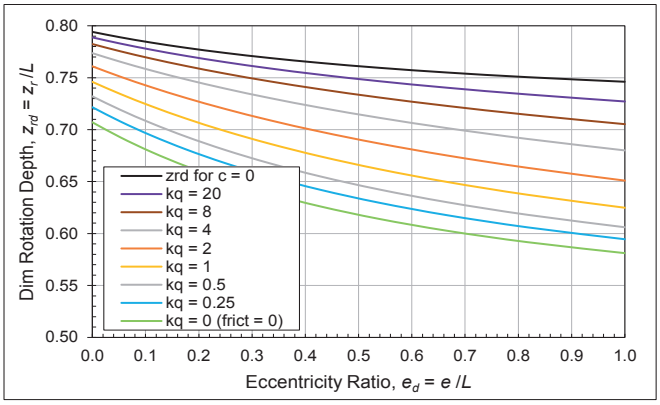

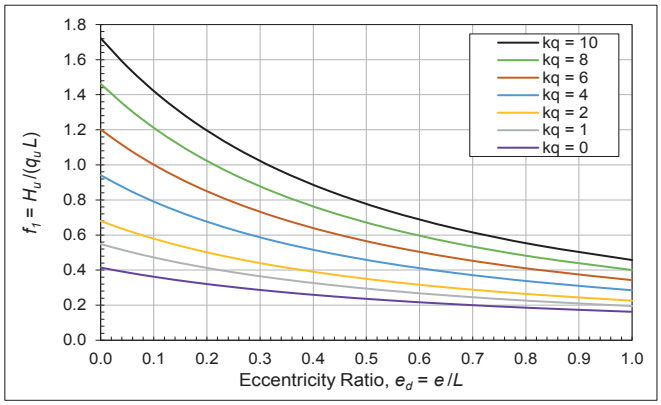

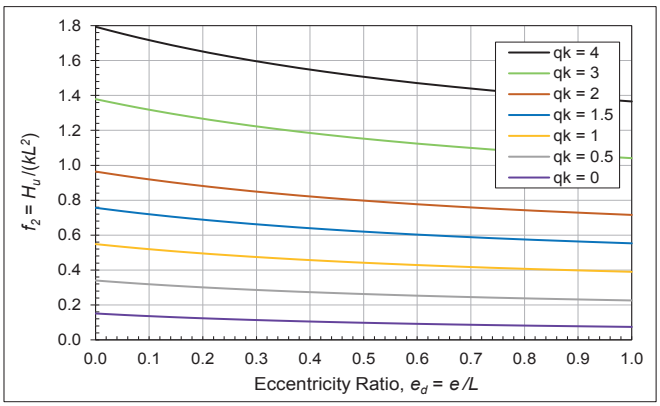

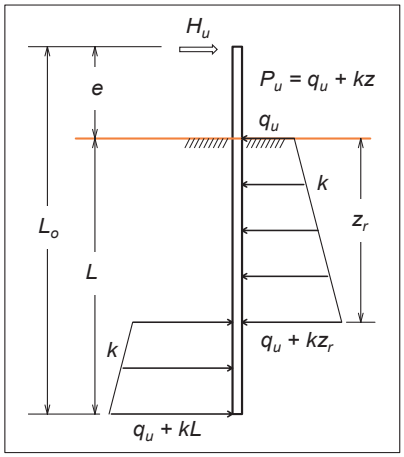

Parameter	Value	Comment
Embedment depth for pile below ground, L	3 m	
Pile diameter in ground, *B*	0.6 m	Includes concrete encasement
Load eccentricity, *e*	1.0 m	Above ground level
Foundation soil friction angle, ϕ	35^o	
Foundation soil unit weight, γ '	18 kN/m^3	
Foundation soil shear strength, s_u	10 kPa	
N_p factor for cohesive resistance	9	
Cohesionless resistance factor, *K*	K_p^2 = 13.62	
Strength reduction for cohesionless resistance, Φ_ϕ	0.65	
Strength reduction for soil shear strength, Φ_c	0.65	
Pole spacing reduction factor, S_p	0.8	
Zhang, L_o factor	4.0 m	$L_o = L + e$
Zhang *k* factor (no correction for gravity stress)	76.5 kN/m^2	$= \gamma' K_p^2 B \Phi_\phi S_p$
Zhang q_u factor	28.1 kN/m	$= N_p s_u B \Phi_c S_p$
Zhang *qk* factor	0.092	$qk = q_u / kL_o$
Zhang *kq* factor	10.90	$kq = kL_o / q_u$

Parameter	Value	Comment
Dimensionless rotation depth, z_r / L	0.750	
Dimensionless load capacity, f_1	0.973	$f_1 = H_u / (q_u L)$
Load capacity in force units	87 kN	Hyperbolic capacity (exact analysis)
Load capacity assuming soil with only cohesion	23 kN	s_u = 10 kPa
Load capacity assuming soil with friction only	63 kN	$\phi = 35^o$
Sum of cohesion and friction components	86 kN	Only 2% less than exact analysis
Dimensionless depth for maximum moment	0.40	z_m / L
Dimensionless maximum moment (reduced)	0.072	$M_{md} = M_m / (k L^3)$: M_m = 150 kN m
Dimensionless ground level moment (reduced)	0.042	Ratio max mom / ground level mom = 1.7

To illustrate an application of the *c*-ϕ theory the analysis of a pile with a 3 m depth of embedment that might be used for a pole wall was carried out. The input parameters are summarised in Table 10. Ultimate forces per unit length for the cohesionless and cohesive soil components were assumed to be those illustrated in Figure 32. No ineffective layer below the ground surface with zero soil resistance was used. Soil strength properties used in the example would be appropriate for highly weathered greywacke rock (Pender, 1977).

Results of the analysis are summarised in Table 11.

The depth of the maximum moment z_m is calculated by finding the depth of zero shear in the pile and is given by:

$$z_m = -\frac{q_u}{k} + \sqrt{\left(\frac{q_u}{k}\right)^2 + \frac{2H_u}{k}} \quad (53)$$

The maximum moment is given by:

$$M_m = H_u(e + z_m) - q_u z_m^2/2 - kz^3/6 \quad (54)$$

and in dimensionless form the maximum moment, M_{md} is given by:

$$M_{md} = \frac{M_m}{kL^3} \quad (55)$$

The *c*-ϕ analysis is based on the LFP shown in Figure 32. It could be modified for minor variations such as assuming there was no cohesion in an upper soil layer.

Results using the Zhang LFP assumption and analysis method suggests that a good approximation (slightly conservative) can be obtained by adding the capacities from separate zero cohesion and zero friction analyses. This finding suggests that more complex LFP's could be analysed using the separate components although the rotation depths will be different for the two cases. (For the above example, the dimensionless rotation depths for separate analyses of the cohesive and cohesionless components were 0.64 and 0.77 respectively – see Figure 29.) Calculating the lateral force capacity at toe yield requires a more detailed analysis to obtain an exact result but reducing the hyperbolic capacity by 20% would give an approximate toe yield capacity. Alternatively, determining the pile head lateral force capacity at toe yield by adding the separate cohesion and cohesionless components at toe yield would be satisfactory for design application.

The example discussed above indicates that a small amount of cohesion can result in a significant increase in the lateral force capacity. The low cohesion of 10 kPa used in the example increased the capacity of the friction only case by approximately 40%. It is customary to neglect small amounts of cohesion in predominantly cohesionless soils because cohesion is less readily assessed and can be variable. However, in foundations in highly weathered rock making a conservative allowance for cohesion is usually considered an acceptable approach. (Pender, 1977 completed laboratory tests to determine friction and cohesion parameters for highly and completely weathered Wellington greywacke. Friction angles for the highly weathered material were in the range of 32^o to 38^o and the cohesion in the range of 80 to 130 kPa.)

In cohesive soils full consolidation may occur under long-term loading, so calculations in terms of drained shear strength based on both cohesion and friction might be appropriate for this case. (Where live load represents a substantial portion of the load on the wall, static design for cohesive soils should be on a short-term undrained basis.)

8. EFFECT OF GROUND WATER IN COHESIONLESS SOILS

The effective unit weight of the soil should be used when calculating the lateral force capacities of poles in cohesionless soils. If the water table is below the toe of the pole an estimated bulk unit weight should be used for the effective unit weight. If the water table is at the ground surface in front of the wall the soil effective unit weight should be taken as the submerged unit weight. For typical sands and gravels the submerged unit weight will be approximately one-half of the bulk unit weight of the soil above the water table leading to an approximate 50% reduction in the lateral force capacity.

If water is expected in the backfill then it should be included as a pressure on the facing. Pole walls will often have open joints in timber facing and are well drained if good drainage practise is followed so it will seldom be

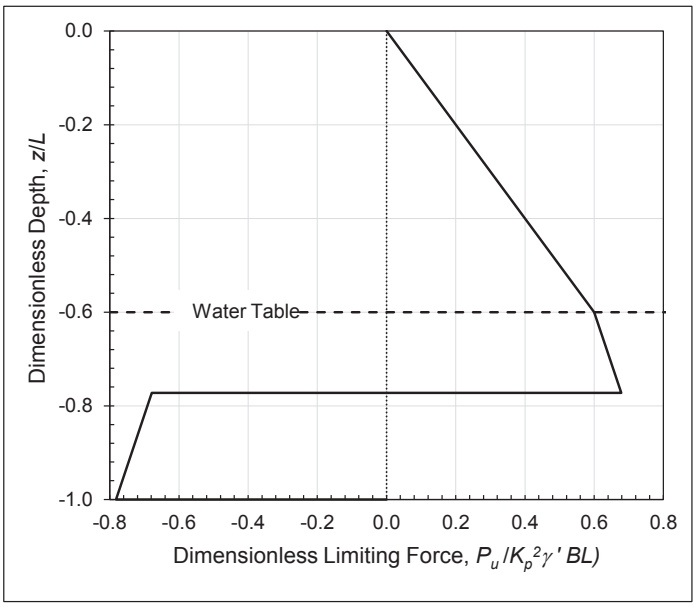

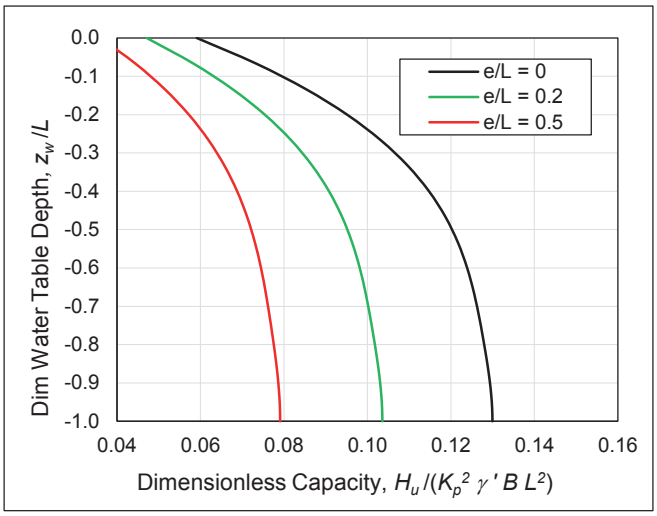

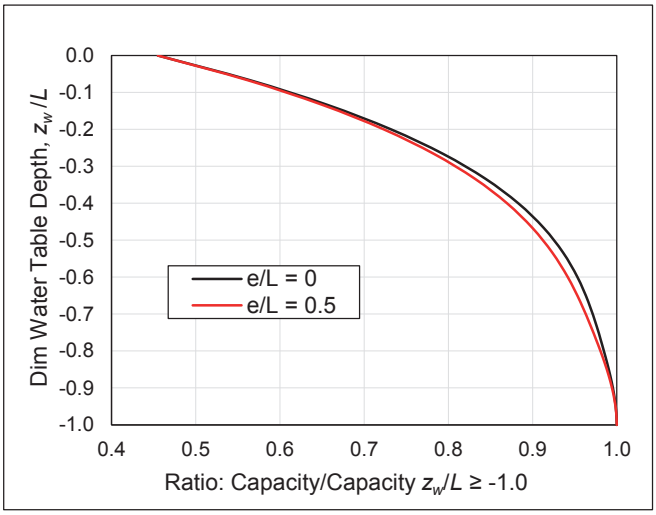

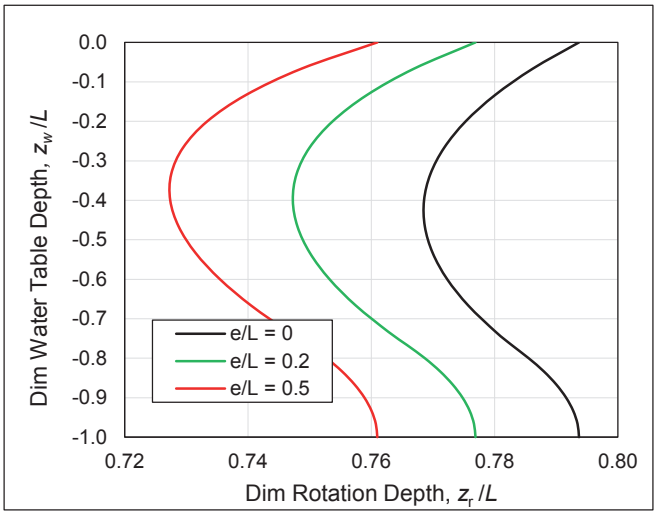

necessary to include a water pressures load against the wall facing.

In higher pole walls the water table level could be located at some height between the ground surface in front of the wall and the toe of the pole. To estimate the lateral force capacity for this intermediate case an analysis was carried out on a 3 m long pole with an 0.6 m embedded diameter located in a cohesionless soil with bulk unit weight of 18 kN/m^3 (buoyant unit weight of 8.2 kN/m^3) and friction angle of 35^o. The hyperbolic lateral force capacity was calculated assuming a Guo A_r factor of $\gamma' K_p^2$. At the hyperbolic ultimate capacity, the LFP reaches both negative and positive soil yield at the rotation point. This profile enables a simple analysis to be undertaken whereas the analysis becomes more complex for the case when yield initially commences at the pole toe (recommended capacity for design). The LFP at the hyperbolic ultimate capacity for the assumed pole and soil properties for the water table located at a depth of 0.6*L* is shown in Figure 33.

The ultimate hyperbolic capacity plotted as a function of the water table depth, z_w below ground level for the 3 m long pole with eccentricity ratios e/L = 0, 0.2 and 0.5 is shown in Figure 34. Depths and capacities are plotted in dimensionless form to enable the results to be used for other geometries and soil properties than used in this particular example. (In the dimensionless force divisor, γ' is the bulk unit weight.) The capacity ratio obtained by dividing the capacity at each particular water table depth by the capacity for the case with the water table at the pole toe or deeper is shown in Figure 35. As indicated in the figure the capacity ratio is insensitive to the e/L ratio. For depths of water greater than z_w/L of 0.7 the capacity is less than 5% below the case with water at the toe level or deeper. Thus, in practical design, when the water table depth is close to

the pole toe depth the water table capacity reduction can be ignored.

Although the above analysis is for the hyperbolic capacity the influence of the water table depth on the Guo toe yield capacity is expected to be similar.

The influence of the water table depth on the rotation point depth is shown in Figure 36. Although the rotation depth z_r is sensitive to the e/L ratio, for a particular ratio the rotation depth varies by less than 5% from the case with water at the surface or below the toe.

9. COMPOSITE ACTION

Cantilever timber pole retaining walls are usually constructed by drilling an oversize hole, installing the poles, and then backfilling the annulus between the pole and the soil with unreinforced concrete. In low to moderate height retaining walls the maximum bending moments in the poles occur at depths of between 0.5 to 1.5 m below ground level. The maximum moments in the embedded section are typically 1.5 times greater than the bending moments at ground level and the question arises as to whether the composite action between the timber pole and concrete encasement is effective in providing a strength increase to offset this increase. The maximum practical height that can retained using cantilever timber pole walls is increased if the timber section can be designed for the bending moment at ground level or at least for a moment intermediate between the maximum and ground level moments.

The strength of the adhesion or bond between the timber pole and concrete is a key issue in deciding whether composite action is effective. Unfortunately, this is an area where there is little published information. Observations of concrete encased timber poles removed from the ground indicate that the adhesion is generally good with the concrete surround usually intact and the concrete difficult to remove from the timber.

The adhesion might be reduced by differential shrinkage between the pole and concrete. However, the concrete effectively seals the timber at depths greater that about 300 mm below the surface so that timber shrinkage is likely to be small or at least less than the shrinkage of the concrete. Shrinkage of the concrete will depend on the moisture in the soil. In dry soil conditions concrete shrinkage will be significant. Generally, the soil will reduce the rate of shrinkage and in ideal conditions the rate of increase in the tensile strength of the concrete may be sufficient to prevent radial cracking caused by circumferential shrinkage. Even if radial cracking occurs is unlikely to be extensive at depths below the surface greater than a few hundred millimetres. In addition, moderate radial cracking is unlikely to result in a significant reduction to the adhesion between the concrete and timber.

At the point of maximum moment in the embedded pole section the shear force on the section is zero. Therefore, in the vicinity of the maximum moment the adhesion bond does not need to be large to resist the interface shearing action.

PARAMETER	VALUE	UNITS	COMMENT
Minimum diameter timber poles	250	mm	Varied from 250 to 400 mm
Maximum diameter timber poles	400	mm	
Thickness of concrete surround	50	mm	Can be varied but kept constant for present analyses
Characteristic stress for poles	38	MPa	From NZS 3603
Load duration factor	0.6		From NZS 3603. Gravity more critical than EQ load
Timber pole design stress	17.4	MPa	Characteristic stress using NZS 3603 reduction factors
Timber modulus of elasticity	7.4	GPa	Characteristic value reduced by 0.85 steaming factor
Concrete compressive strength	20	MPa	Typical value after ageing (used to estimate modulus)
Concrete modulus of elasticity	22	GPa	From NZS 3101
Concrete modulus reduction factor	0.5 – 0.75		Allows for non-linear response and creep.
Section strength reduction factor	0.8		Based on reduction used for timber poles
Axial load on pole	Zero		Typically, the axial load is small in retaining walls

PARAMETER	VALUE		UNITS	COMMENT
Diameter of timber pole	300		mm	
Thickness of concrete surround	50		mm	
Concrete modulus reduction	0.5	0.75		Uncertain parameter. 0.5 is conservative
Distance NA from centre of pole	42	54	mm	By trial and error to give zero axial force
Area of concrete in compression	23,247	21,966	mm^2	
Area of timber in compression	22,910	19,416	mm^2	
Area of timber in tension	47,776	51270	mm^2	
Tensile strain in timber outer fibre	0.0024			
Comp. strain in concrete outer fibre	-0.0019	-0.0017		
Force from timber in compression	-93	-66	kN	
Force from concrete in compression	-270	-327	kN	
Force from timber in tension	363	393	kN	
Reduction factor for moment	0.8			
Moment from timber in compression	5	3	kN m	Moments reduced by reduction factor
Moment from concrete in compression	23	26	kN	
Force from timber in tension	33	39	kN	
Total reduced moment capacity	61	67	kN	
Capacity Ratio: Composite/Timber	1.65	1.81		

9.1 COMPOSITE SECTION ANALYSIS

In the present project the enhanced strength of timber pole sections acting compositely with concrete surround was estimated based on the overriding assumptions that the concrete acts in compression but provides no resistance in tension, there is no slippage on the concrete/timber interface and plane sections remain plane. The analysis can be simplified by adopting one or other of the following assumptions.

(a) The concrete in compression is linearly elastic (stress proportional to strain).

(b) The concrete is non-linear and becomes stressed to a uniform level given by the Whitney Stress Block assumption used in the ultimate strength calculations for reinforced concrete sections.

Trial analyses indicated that assumption (a) was more correct for typical encased pole sections than the second assumption. The strain was more critical in the timber with tensile failure in the outer fibres at a maximum concrete compression strain of about 0.0015. (The usual non-linear failure assumption for concrete is a strain of 0.003). The

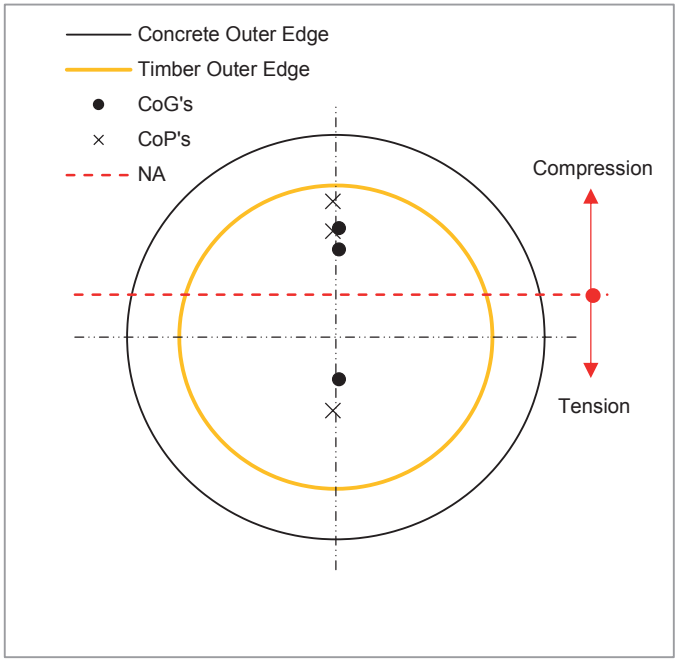

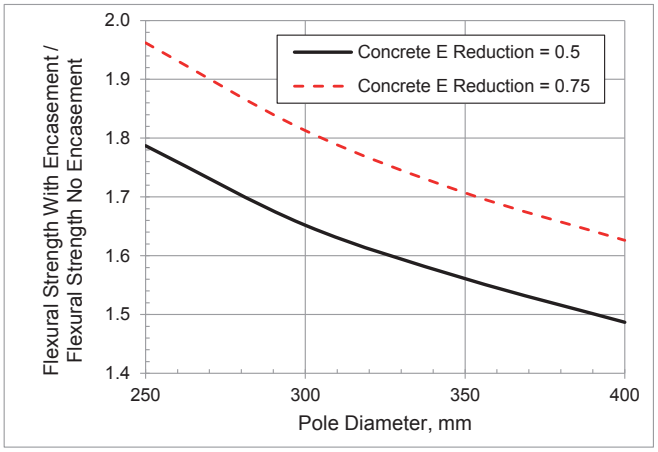

first assumption was adopted for the results presented below with checks made using the second assumption.

The main dimension and strength parameters used in the analysis are summarised in Table 12.

The analysis procedure was to vary the location of the neutral axis by trial and error to give zero net force on the section. The moment capacity was then calculated by taking the moments of the timber compression and tension force plus the moment of the concrete compression force about the neutral axis. The total moment from these forces was reduced by a strength reduction factor to be consistent with the reduction made for a timber pole acting alone. The reduced composite flexural strength was then compared with the flexural strength of the timber pole acting without the concrete to give a moment enhancement ratio for the composite section.

A summary of the main numerical results for a 300 mm diameter pole is given in Table 13.

A summary of the moment capacity ratio results for the range of pole diameters considered is shown in Figure 38.

The results show that the flexural strength enhancement from the concrete is significant and is likely to increase the basic strength of the timber section acting alone by at least a factor of 1.5. Provided there is good adhesion between the concrete and timber and good quality control to ensure that the assumed thickness of concrete is achieved it seems reasonable to make use of this enhancement in the design of retaining walls. The neglect of concrete in tension and the use of a concrete modulus reduction factor of 0.5 are conservative assumptions so the actual composite strength is likely to be greater than shown by the present results.

Composite section design should be based on the moment calculated at one pole diameter, including the casing, below ground level to make allowance for the composite section to fully develop. In the example in the previous section the maximum bending moment occurred at a depth of approximately 1.2 m below ground surface and was a factor of 1.34 greater than the moment at a depth of 0.6 m (one pole diameter) below ground.

10. CONCLUSIONS

(a) Commonly used design analysis methods for cantilever poles walls have limitations and do not accurately represent the pole-soil interaction and displacement behaviour. In particular, the Broms method for estimating the pole lateral force capacity in cohesionless soils assumes rotation of the pole about the toe instead of the correct depth at a significant height above the toe. This simplification gives an unconservative lateral load capacity. Simplifying the analysis by assuming that the poles behave as a continuous wall is unnecessary and may introduce errors that are difficult to quantify. Although soil strength parameters are unlikely to be accurately known for design of small wall structures it is nevertheless desirable to eliminate analysis errors as far as possible and deal with the soil uncertainty by adopting moderately conservative soil strength parameters.

(b) The pole foundation soil-interaction design should be based on pile theory that has been verified by testing. Pile design methods suitable for cantilever wall design have been presented by Guo, 2008 for cohesionless soils and Motta, 2013 for cohesive soils. Both these methods are based on elastic-plastic analysis and give force versus displacement equations

for loading from zero up to the ultimate hyperbolic loads. These allow serviceability displacements and the pile top lateral force capacity based on soil yield at the toe to be determined.

(c) Zhang, 2018 has presented an analysis procedure for a soil with both friction and cohesion properties. Although this method is presented for a particular LFP that may not apply in all design applications, typical pole capacity calculations showed that the addition of results from separate analyses for the friction and cohesion components gave an acceptable prediction of the total load capacity. The Zhang method is applicable to the analysis of poles in highly weathered rock materials which have both friction and significant cohesion properties.

(d)The Goa, Motta and Zhang pile load capacity analyses are based on isolated pile theory but there is sufficient load testing and other theoretical analyses that give satisfactory capacity reduction factors to allow for the interaction of the soil pressures for piles in groups, or in the case of a wall, for piles in a single row of multiple piles.

(e) Although the empirical equations of Goa, Motta, and Zhang are more complex than the simple Broms equation for cohesionless soils they are not difficult to set up on a spread sheet. Design charts are presented in this paper that enable the equations to be evaluated at sufficient accuracy for most design applications in both types of soils and for the mixed friction and cohesion case.

(f) Limiting force profiles in cohesionless soils are a function of the effective vertical stress which is difficult to evaluate in the vicinity of the wall face. Plots of the variation with distance from the face are presented accompanied by recommendations on a correction factor simplification that is satisfactory for design applications.

(g) The strength enhancement of the concrete encasement used on timber poles embedded in the ground should be considered in design. Information is presented in the paper that allows the encasement strengthening effect to be predicted with sufficient accuracy for wall design.

11. REFERENCES

Adams J I, and Radhakrishna H S. 1973. The Lateral Capacity of Deep Augured Footings", Proc. 8th Int. Conf. Soil Mech. Found. Eng., Moscow, USSR.

Agaiby S W, Kulhawy F H and Trautmann C H. 1992. Experimental Study of Drained Lateral and Moment Behavior of Drilled Shafts Using Static and Cyclic Loading. Electric Power Research Institute. EPRI Report TR-100223, Palo Alto, Calif.

Aguilar V, Stallings J M, Anderson J B, and Nowak A J. 2019. Simplified Method for Laterally Loaded Short Piles in Cohesionless Soil. Transport Research Record Vol267(3) pp 605-616.

American Petroleum Institute (API). 1977. Recommended Practice for Planning, Designing and Constructing Fixed Offshore Platforms. API Recommended Practice 2A (RP2A), 9th ed., Washington, D.C.

American Petroleum Institute (API). 1991. Recommended Practice for Planning, Designing and Constructing Fixed Offshore Platforms. API Recommended Practice 2A (RP2A), 19th ed., Washington, D.C.

Anderson J B. 1997. A Laterally Loaded Pile Database. University of Florida.

Ashour M, Norris G, and Pilling P. 1998. Lateral Loading of a Pile in Layered Soil Using the Strain Wedge Model. J. of Geotech. and Geoenviron. Eng., ASCE, 124(4), pp-303-315.

Baguelin F, Goulet G, and Jezequel J. 1973. Experimental Study of Behavior of Laterally Loaded Pile, Proceedings. 5th European Conf. on Soil Mech. and Found. Eng. (1), Madrid, pp 317-324.

Barton Y. 1982. Laterally Loaded Model Piles in Sand: Centrifuge Tests and Finite Element Analyses. PhD Thesis. University of Cambridge, Cambridge, UK.

Bhushan K, Lee L J, and Grime D B. 1981. Lateral Load Tests on Drilled Piers in Sand, Drilled Piers and Caissons, Proc. of a session sponsored by the Geotech. Eng. Div. and the ASCE National Convention, St. Louis, Missouri, pp 114-131.

Bierschwale M W, Coyle H M, and Bartoskewitz R E. 1981. Lateral Load Tests on Drilled Shafts Founded in Clay, Drilled Piers and Caissons. Ed. MW O'Neill, ASCE, New York, pp. 98-113.

Briaud J-L, and Smith T D. 1983. Using the Pressuremeter Curve to Design Laterally Loaded Piles. Proc., 15th Offshore Technology Conf., Houston, Paper 4501, pp 495–502.

Brinch Hansen J. 1961. The Ultimate Resistance of Rigid piles against Transversal Forces. The Danish Geotechnical Institute, Copenhagen, Denmark, Bulletin No.12, pp 5-9.

Broms B. 1964a. The Lateral Response of Piles in Cohesionless Soils. J. of Soil Mech. and Found. Eng. Div., ASCE, 90 (3), pp 123-156.

Broms B. 1964b. Lateral Resistance of Piles in Cohesive Soils. J. of the Soil Mech. and Found. Div., ASCE, Vol. 90 (2), pp 27–64.

Carter J P, and Kulhawy F H. 1992. Analysis of Laterally Loaded Shafts in Rock. J. Geotech. Eng., ASCE, Vol 118 (6) pp.839-855.

Chari T R, and Meyerhof G. 1983. Ultimate Capacity of Rigid Single Piles under Inclined Loads in Sand. Canadian Geotech. J., Vol. 20 (4), pp 849–854.

Chen S L, and Chen L Z. 2008. Note on Interaction Factor for Two Laterally Loaded Piles. J. of Geotech. and Geoenviron. Eng., ASCE, 134(11), pp 1685-1690.

Chen Y-J, and Kulhawy F H. 1994. Case History Evaluation of the Behaviour of Drilled Shafts Under Axial and Lateral Loading. Prepared by Cornell University for Electric Power Research Institute. EPRI TR-104601, Research Project 1493-04. Palo Alto, Calif.

Chen Y-J, Lin S W, and Kulhawy F H. 2011. Evaluation of Lateral Interpretation Criteria for Rigid Drilled Shafts", Can. Geotech J., 48(5), pp 634-643.

Davis T G, and Budhu M. 1986. Nonlinear Analysis of Laterally Loaded Piles in Heavily Overconsolidated Clays. Geotechnique Vol 35 (6), pp 527-538.

Dickin E A, and Nazir R B. 1999. Moment-carrying Capacity of Short pile Foundations in Cohesionless soil. J. of Geotech. and Geoenviron. Eng., ASCE, 125(1), pp 1-10.

Dunnavant T W, and O'Neill M W. 1985. Performance, Analysis, and Interpretation of Lateral Load Test of 72-Inch-Diameter Bored Pile in Overconsolidated Clay, Report UHCE 85-4. Univ. of Houston, Houston, 49 p.

Fleming W G K, Weltman A J, Randolph M F, and Elson W K. 2009. Piling Eng., Taylor and Francis, London, UK.

Georgiadis K, and Georgiadis M. 2012. Development of p–y Curves for Undrained Response of Piles Near Slopes. Comput. Geotech., Vol 40, pp 53–61.

Georgiadis K, Sloan S W Lyamin A V. 2013. Undrained Limiting Lateral Soil Pressure on a Row of Piles. Comput. and Geotech., Vol 54, pp 175-184.

Georgiadis M, Anagnostopoulos C, and Saflekou S. 1992. Centrifuge Testing of Laterally Loaded Piles in Sand", Can. Geotech. J., 29(2), pp 208-216.

Guo W D, and Lee F H. 2001. Load Transfer Approach for Laterally Loaded Piles. International J. for Numerical and Analytical Methods in Geomechanics 25(11), pp1101-1129.

Tonkin+Taylor

We're looking for groundbreaking geotechnical specialists!

Who do we need?

Tonkin + Taylor is looking for geotechnical specialists to help deliver a visionary, resilient future for Aotearoa New Zealand, its wonderfully diverse culture, people and communities. We promise that life will never be dull!

For 62 years, we've been helping to create a country and infrastructure that is envied the world over. Our clients range from local and central Government to businesses and private developers.

Our Geotechnical Team has helped to shape Auckland's City Rail Link, Downtown and America's Cup infrastructure projects, anchor projects for Christchurch, such as the Justice Precinct and to build back a better Kaikoura following 2016's devastating earthquake.

There are plenty more exciting projects in our portfolio, so if your appetite is whet, read on!

Who do we need?

- Geotechnical Engineers and Engineering Geologists at all levels, predominantly in Auckland and Melbourne

What's in it for you?

- A highly competitive salary and great benefits
- Flexible working arrangements, including variable start times and working from home
- A workplace that welcomes diversity in all its forms
- A fantastic working environment, learning from people who are leaders in their field
- The potential to work on projects across NZ and the Pacific (bubbles permitting)
- A "family/whānau first" ethos. We understand that they take priority!

APPLY NOW, or if you would like any more information about this position, please contact Ronny Bilkhu Rbilkhu@tonkintaylor.co.nz

We particularly encourage speakers of Te Reo Māori or Pasifika languages to apply.

To find out more about Tonkin + Taylor, go to www.tonkintaylor.co.nz

Guo W D. 2008. Laterally Loaded Rigid Piles in Cohesionless Soil. Canadian Geotechnical J., 45(5), pp 676-697.

Harris M C, Papanicolas D, and Rogers W G. 1985. Behavior of Test Piles Subjected to Lateral Loading, Proceedings. 38th Canadian Geotech. Conf., Edmonton, pp 399-406.

Ilyas T, Leung C F, Chow Y K, and Budi S. 2004. Centrifuge Model Study of Laterally Loaded Pile Groups in Clay. J. of Geotech. and Geoenviron. Eng., ASCE 130 (3) pp 1090-024.

Ismael N F, and Klym T W. 1978. Behavior of Rigid Piers in Layered Cohesive Soils. J. Geotech. Eng. Div., ASCE, 104(8), pp 1061–1074.

Ivey D L, Koch K J and Raba C F. 1968. Resistance of a Drilled Shaft Footing to Overturning Loads, Model Tests and Correlation with Theory. Research Report 105-2, Texas Transportation Institute, Texas A & M University, College Station. 20p.

Jeanjean P. 2009. Re-assessment of p–y Curves for Soft Clay from Centrifuge and Finite Element Modelling. Proceedings of 41st Offshore Technology Conference. Houston, p. 2081–2103 [OTC 20158].

Joo J S. 1985. Behaviour of Large-Scale Rigid Model Piles under Inclined Loads in Sand. Memorial University of Newfoundland.

Kasch V R, Coyle H M, Bartoskewitz R E, and Server W G. 1977. Design of Drilled Shafts to Support Precast Panel Retaining Walls. Research Rep. No. 211-1, Texas Transportation Institute, Texas A&M Univ., College Station, Texas.

Kulhawy F H. 1991. Drilled Shaft Foundations. Foundation Eng. Handbook., 2nd Ed., Chap. 14, H-Y Fang ed., Van Nostrand Reinhold, New York.

Kulhawy F H, Trautmann C H, Beech J F, O'Rourke T D, McGuire W, Wood W A, and Capano C. 1983. Transmission Line Structure Foundations for Uplift-compression Loading." Rep. No. EL-2870, Electric Power Research Institute, Palo Alto, Calif.

Lam I P, and Martin G R. 1986. Seismic Design of Highway Bridge Foundations. Report No. FHWA/RD-86/102. Vol II, Design Procedures and Guidelines. Department of Transportation, Federal Highway Administration, Virginia, USA.

Laman M, King G J W, and Dickin E A. 1999. Three-dimensional Finite Element Studies of the Moment-carrying Capacity of Short Pier Foundations in Cohesionless Soil. Comp. and Geotech., Vol 25(3), pp 141-155.

Lin H, Ni L, Suleiman M T, and Raich A. 2015. Interaction Between Laterally Loaded Pile and Surrounding Soil. J. Geotech. Geoenviron. Eng., ASCE, 141(4) 04014119-1 04014119-11.

Martin C M, and Randolph M F. 2006. Upper-bound Analysis of Lateral Pile Capacity in Cohesive Soil. Geotechnique 56(2), pp 141–5.

Matlock H. 1970. Correlations for Design of Laterally Loaded Piles in Soft Clay. Proceedings of the 2nd Offshore Technology Conference. Houston, pp 577–94 [OTC 1204].

Matlock H, and Reese L C. 1960. Generalized Solutions for Laterally Loaded Piles. J. Soil Mech. and Found. Div., 86(5), pp 63–91.

Mayne P W, Kulhawy F H, and Trautmann C H. 1995. Laboratory Modeling of Laterally Loaded Drilled Shafts in Clay. J. of Geotech and Geoenviron. Eng., ASCE, 121(12), pp 827-835.

MBIE-NZGS. 2017. Earthquake-resistant Retaining Wall Design: Module 6. New Zealand Ministry of Business Innovation and Employment and New Zealand Geotechnical Society.

McClelland B, and Focht J A. 1958. Soil Modulus for Laterally Loaded Piles. Trans. of ASCE, Vol. 123(1), pp. 1049–1063.

McPherson A R, and Bird G D. 2020. Simplified Structural Design Guide Timber Pole Retaining Walls. Published by Structural Eng. Society New Zealand. Draft document dated 20 August 2020.

McVay M, Casper R, and Shang T. 1995. Lateral Response of Three-row Groups in Loose to Dense Sands at 3D and 5D Pile Spacing. J. of Geotech. Eng., ASCE Vol. 121(5), pp 436-441.

Meyerhof G, and Sastry V. 1985. Bearing Capacity of Rigid Piles Under Eccentric and Inclined Loads. Canadian Geotech. J., Vol. 22(3), pp 267–276.

Meyerhof G, Mathur S K, and Valsangkar A J. 1981. Lateral Resistance and Deflection of Rigid Walls and Piles in Layered Soils. Can. Geotech. J., Vol 18, pp 159-170.

Mokwa R L, and Duncan J M. 2005. Discussion of "Centrifuge Model Study of Laterally Loaded Pile Groups in Clay" by T Ilyas, C F Leung, Y K Chow, and S Budi. J. of Geotech and Geoenviron. Eng., ASCE 131 (10) pp 1305-1308.

Mokwa R L, and Duncan J M. 1999. Investigation of the Resistance of Pile Caps to Lateral Loading. Report of Research Performed under Sponsorship of the VA Transportation Research Council, Charlottesville, Vagina, USA, VTRC 99-CR.

Mokwa R L, and Duncan J M. 2001. Laterally Loaded Pile Group Effects and P-Y Multipliers. ASCE Geotechnical Special Publication (GSP No. 113.), Foundations and Ground Improvement, ASCE, Reston, Vagina, USA, pp 728–742.

Motta E. 2013. Lateral Deflection of Horizontally Loaded Rigid Piles in Elastoplastic Medium. J. Geotech. Geoenviron. Eng., ASCE, Vol 139(3), pp 501–506.

Moussa A and Christou P. 2018. The Evolution of Analysis Methods for Laterally Loaded Piles Through Time. Advances in Analysis and Design of Deep Foundations, Sustainable Civil Infrastructures. Abu-Farsakh M et al eds. Springer International Publishing AG, pp 65-94.

Murchison J M, and O'Neill M W. 1984. Evaluation of p-y Relationships in Cohesionless Soils. Analysis and Design of Pile Foundations. ASCE, J.R. Meyer, ed. National Convention, San Francisco, pp 174-191.

Murff J D, and Hamilton J M. 1993. P-Ultimate for Undrained Analysis of Laterally Loaded Piles. J. Geotech. Eng., ASCE, Vol 119(1), pp91–107.

NAVFAC DM7: 2011. Soil Mechanics, Foundations and Earth Structures: NAVFAC DM 7. Naval Facilities Eng. Command. USA.

Norris G. 1986. Theoretically Based BEF Laterally Loaded Pile Analysis. Proceedings 3rd International Conference on Numerical Methods in Offshore Piling, pp. 361–386.

NZS 3603: 1993 (and Amendments). Timber Structures Standard. Standards New Zealand.

Pender M J. 1977. Friction and Cohesion Parameters for Highly and Completely Weathered Wellington Greywacke. Report 2-77/7, Central Laboratories, Ministry of Works and Development, 32 p.

Pender M J. 1993. Aseismic Pile Foundation Design Analysis. Bulletin of the NZ Society for Earthquake Eng., Vol 26(1), pp 49-161.

Pender M J. 1997. Ultimate Lateral Capacity of Piles Embedded in Soil. J. of New Zealand Structural Eng. Society. Vol 10(2), pp 53-60.

Pender M J. 2000. Ultimate Limit State Design of Foundations. NZ Geotechnical Society Short Course. University of Auckland.

Petrasovits G, and Awad A. 1972. Ultimate Lateral Resistance of a Rigid Pile in Cohesionless Soil. Proceedings 5th European Conference on Soil Mech. and Found. Eng., Madrid, Vol.3, pp 407-412.

Pham Q N, Ohtsuka S, Isobe K, and Fukumoto Y. 2019. Group Effect on Ultimate Lateral Resistance of Piles Against Uniform Ground Movement. Soils and Foundations, Vol 59, pp 27-40.

Poulos H G, and Davis E H. 1980. Pile Foundation Analysis and Design, John Wiley and Sons, New York.

Prasad Y V S N, and Chari T R. 1999. Lateral capacity of Model Rigid Piles in Cohesionless Soils. Soils and Foundations, Vol 39(2), pp 21-29.

Qin H Y, and Guo W D. 2014. Nonlinear Response of Laterally Loaded Rigid Piles in Sand. Geomech. and Eng., Vol 7(6), pp 679-703.

Randolph M F, and Houlsby G T. 1984. The Limiting Pressure on a Circular Pile Loaded Laterally in Cohesive Soil. Geotechnique, Vol 34(4), pp 613–23.

Reece L C. 1958. Discussion of Soil Modulus for Laterally Loaded Piles. Trans., ASCE 123, pp 1071 – 1074.

Reese L C, and Welch R C. 1975. Lateral Loading of Deep foundations in Stiff clay. J. Geotech. Eng. Div., ASCE, Vol 101(7), pp 633–49.

Reese L C. 1977. Laterally Loaded Piles: Program Documentation. Proceedings, ASCE, Vol. 103(GT4), pp. 287-305.

Reese L C, Cox W R, and Koop F D. 1974. Analysis of Laterally Loaded Piles in Sand. In Offshore Technology in Civil Eng. Hall of Fame Papers from the Early Years, pp. 95–105.

Rollins K, Olsen R, Egbert J, Olsen K, Jensen D, and Garrett B. 2003. Response, Analysis and Design of Pile Groups Subjected to Static and Dynamic Lateral Loads. Civil & Environmental Eng. Department Brigham Young University. Report prepared for Research Division of Utah Department of Transportation.

Rollins K M, Olsen K G, Jensen D H, Garrett B H, Olsen R J, and Egbert J. 2006. Pile Spacing Effects on Lateral Pile Group Behavior: Analysis. J. Geotech. Geoenviron. Eng., ASCE, Vol 132(10), pp 1272–83.

Rollins KM, Peterson K T, Weaver T J. 1998. Lateral Load Behavior of Full-scale Pile Group in Clay. J. Geotech. Geoenviron. Eng., ASCE, Vol 124(6), pp 468–78.

Scott R F. 1981. Foundation Analysis. Prentice Hall, Englewood Cliffs, New Jersey.

Stevens J B, and Audibert J M E. 1980. Re-examination of p-y Curve Formulation. Proceedings 11th Offshore Technology Conference. Houston, p.397–03 [OTC 3402].

Terzaghi K V. 1955. Evaluation of Coefficient of Subgrade Reaction. Geotechnique, Vol 5, pp 295-326.

Thiyyakkandi S, McVay M, Lai P, and Herrera R. 2016. Full-Scale Coupled Torsion and Lateral Response of Mast Arm Drilled Shaft Foundations. Canadian Geotech. J., Vol. 53(12), pp 1928–1938. https: //doi.org/10.1139/cgj-2016-0241.

Trochanis A M, Bielak J, and Christiano P. 1991. Three-dimensional Nonlinear Study of Piles. J. Geotech. Eng., ASCE, Vol 117(3), pp 429–447.

Yang Z, and Jeremi B. 2002. Numerical Analysis of Pile Behaviour Under Lateral Loads in Layered Elastic–plastic Soils. Int. J. Numer. Anal. Methods Geomech. Vol 26(14), pp 1385–1406.

Yang Z, and Jeremi B. 2005. Study of Soil Layering Effects on Lateral Loading Behavior of Piles. J. Geotech. Geoenviron. Eng., ASCE, Vol 131(6), pp 762–770.

Zhang W. 2018. Ultimate Lateral Capacity of Rigid Pile in c-f Soil. China Ocean Eng., Vol. 32(1), pp 41–50.

Zhang L. 2009. Nonlinear Analysis of Laterally Loaded Rigid Piles in Cohesionless Soil. Comput. Geotech., Vol 36(5), pp 718-724.

Zhang L, Silva F, and Grismala R. 2005. Ultimate Lateral Resistance to Piles in Cohesionless Soils. J. Geotech. Geoenviron. Eng., ASCE, Vol 131(1), pp 78-83.

APPENDIX – SYMBOL NOTATION

a	Depth of plastic soil below ground level for cohesive soil
$A_r z$	Pressure on the pile surface at depth z in cohesionless soil (FL^{-2} units): for Guo, $A_r = \gamma' K_p^2$
B	Pile outside diameter of embedded length in ground
c	Soil cohesion
e	Height of applied load above ground surface (eccentricity)
e_d	Dimensionless eccentricity (or eccentricity ratio) = e/L
$(EI)_p$	Pile bending rigidity
E_i	Initial stiffness of pile versus displacement curve for cohesive soil (FL^{-2} units, Lam and Martin)
E_p	Effective Young's modulus for pile = $(EI)_P/(\pi r_0^{\,4}/4)$
E_s	Young's modulus for soil
E_t	Tangent stiffness of force versus displacement curve for cohesionless soil (FL^{-2} units, Lam and Martin)
f_1	Dimensionless ultimate capacity of pile in c-ϕ soil = $H_u/(q_u L_o)$

f_2 Dimensionless ultimate capacity of pile in c-ϕ soil = $H_u/(kL_o^2)$
F_b Mayerhof lateral resistance factor for weight = 1.25
f_c Dimensionless ultimate capacity of pile in cohesive soil = $H_u/(q_uL_o)$
f_ϕ Dimensionless ultimate capacity of pile in cohesionless soil = $H_u/(kL_o^2)$
G_s Shear modulus for soil
H Lateral load applied at pile head
H_u Ultimate lateral load applied at pile head
H_{ud} Dimensionless ultimate lateral load: for cohesionless soil = $H_u/(K\gamma' BL^2)$: for cohesive soil = $Hu/(s_u BN_p L)$
H_y Lateral pile head load at yield of pile toe soil
H_{yd} Dimensionless pile toe yield load: for cohesionless soil = $H_y/(K\gamma' BL^2)$: for cohesive soil = $H_y/(P_uL)$
K Ultimate lateral resistance coefficient: for Guo analysis = K_p^2
k Limiting resistance factor for cohesionless soil = $K\gamma' B$
k_1 Soil modulus coefficient for cohesionless soil: function of soil density (FL^{-3} units, Lam and Martin)
K_a Rankine active pressure coefficient
K_c Brinch Hanson earth pressure coefficient for cohesion
k_c Soil modulus for Constant modulus with depth (FL^{-3} units)
k_o Soil modulus for Gibson modulus (linear increase with depth, FL^{-4} units)
K_o Soil at rest pressure coefficient
K_p Rankine passive pressure coefficient
K_q Brinch Hanson earth pressure coefficient for overburden pressure
kq Friction/cohesion ratio used for c-ϕ soil = kL_o/q_u
K_r Ratio of horizontal to vertical effective stress
L Pile length below ground level
L_e Effective pile length below ground level = $L - z_t$
L_o Depth from top to toe of pile = $L + e$
M Bending moment in pile
M_d Dimensionless bending moment in pile: for cohesionless soil = $M/(kL^3)$: for cohesive soil = $M/(P_u L^2)$
M_m Maximum bending moment in pile
M_{md} Maximum dimensionless bending moment in pile: for cohesionless soil = $M_m/(kL^3)$: for cohesive soil = $M_m/(P_uL^2)$
n_h Soil subgrade reaction modulus (FL^{-3} units)
N_p Pile lateral bearing capacity factor in cohesive soil
P Soil resistance per unit length acting on the pile (FL^{-1} units, within elastic range)
p_m Maximum soil pressure on pile
P_m Maximum soil resistance force per unit length at pile toe
p_u Limiting soil pressure on pile (FL^{-2} units)
P_u Limiting soil resistance per unit length of pile: for cohesive soil = $s_u BN_p$: for cohesionless soil = $K\gamma' Bz$ (FL^{-1} units)
qk Cohesion/friction ratio used for c-ϕ soil = $q_u/(kL_o)$
q_u Limiting force per unit length for cohesive component in c-ϕ soil = $s_u BN_p$
r Eccentricity parameter = $L/(e+L)$
R Pile length ratio = L_o/L
r_b Meyerhof reduction factor for moment = 1/(1+1.4e/L)
r_o Outer radius of pile
S Pile centreline horizontal spacing
s_{bu} Meyerhof pile shape factor
S_p Pile spacing reduction factor
s_u Soil undrained shear strength
u Pile lateral displacement
u^* Pile threshold displacement at local soil yield
u_c Displacement of pile at ground level for 0.5 of H_u
u_o Pile displacement at ground level
u_y Pile ground level displacement at yield of soil at pile toe
u_{yd} Dimensionless u_y: for cohesive soil = $u_y/u^* = u_y E_s/P_u$
x Height of elastic soil above rotation centre for cohesive soil
z Depth below ground level
z_m Depth of maximum moment
z_o Guo slip depth in cohesionless soil (soil at yield stress from surface to this depth)
z_r Pile rotation depth below ground surface
z_{rd} Pile dimensionless rotation depth = z_r/L
z_t Depth of soil from surface with zero resistance (cohesive soil)
z_{td} Dimensionless $z_t = z_t/L$
z_w Depth of water table below ground level
α Pile soil adhesion factor
δ Interface friction between pile and soil
ε_c Strain amplitude at one-half the peak deviatoric stress in an undrained compression test
ϕ Soil friction angle
Φ_ϕ Strength reduction for cohesionless resistance
Φ_c Strength reduction for soil shear strength
γ' Soil effective unit weight
η, ξ Pile shape functions = 0.8 and 1.0 respectively for circular pile
σ_{vo} vertical overburden stress
τ_u Ultimate shear stress on pile surface
ω Pile rotation angle

IN SITU TESTING: CPT - Seismic - DMT

GROUND INVESTIGATION

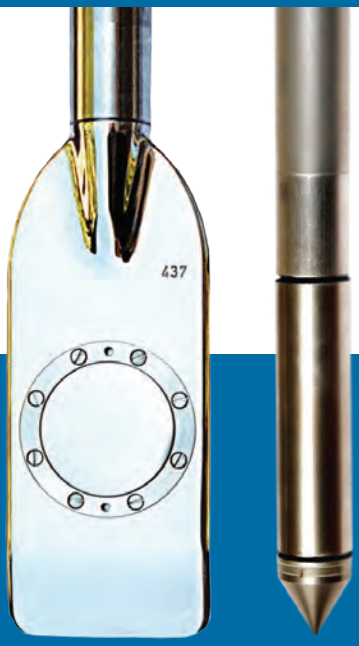

12, 18 & 20 TON TRUCK RIGS

SMALL & MEDIUM TRACKED RIGS

22 TON MOROOKA

MAN PORTABLE RIGS

Our Mission:
BEST POSSIBLE DATA

SPECIALISTS IN HIGH QUALITY IN SITU TESTING

- CPT, SCPT • DMT, SDMT • DPSH • HVSR
- Direct push cross-hole seismic testing
- Push-in piezometers • Push-in sampling

HVSR NEW!

Rapid, low cost assessment of Site Period and Subsoil Class using horizontal to vertical spectral ratio (HVSR) analysis of passive surface waves.

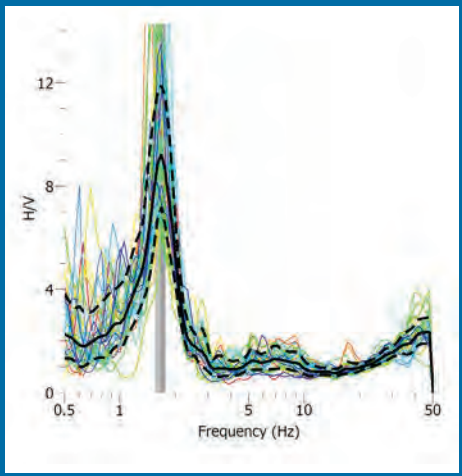

We provide a full service of collecting field data, analysing the results and reporting with comments on estimated site period and subsoil class. Please contact us for further information.

NORTH ISLAND
- Auckland
- Wellington

SOUTH ISLAND
- Christchurch
- Dunedin

0800 DMT CPT (368 278)
www.g-i.co.nz
info@g-i.co.nz

INITIA

GEOTECHNICAL SPECIALISTS

INITIA

GEOTECHNICAL SPECIALISTS

Eastland Port, Gisborne
Expansions to existing port including new slipway, wharf structure and channel dredging in Gisborne

Modal, Mt Albert
Five storey boutique apartment building in Mt Albert, Auckland

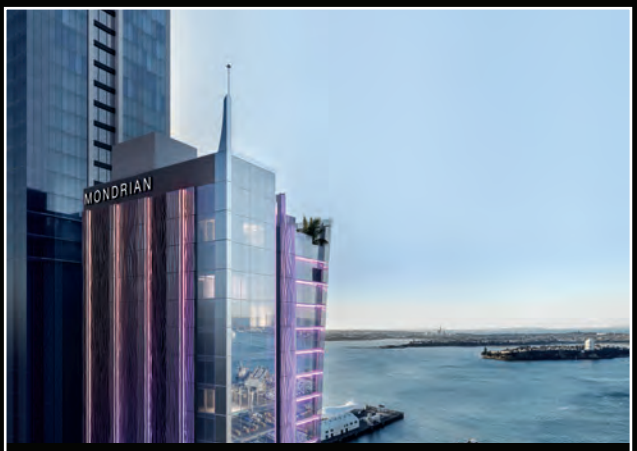

The Mondrian Hotel, Auckland
38 storey hotel with single level basement on Gore Street, Auckland CBD

Westside Healthcare, Hastings
Westside Healthcare Centre and Regional Cancer Treatment Facilities in Hastings

www.initia.co.nz

Geotechnical Investigation for the Scott Base Redevelopment Project

Tim McMorran, Latasha Templeton, Ben Higgs (Golder Associates NZ Limited), Matthew Jordan (Antarctica New Zealand)

Tim McMorran

Tim McMorran is an engineering geologist with thirty years of experience in geotechnical consulting. Tim is based in Christchurch and has worked throughout New Zealand, Australia, Fiji, Singapore, Antarctica, Indonesia and Papua New Guinea. Tim has experience in geotechnical investigation, design and construction monitoring for large civil and mining projects including dams, tunnels, open pits, transportation and high rise buildings. Tim has particular experience in seismic hazard assessment and slope stability assessment.

Latasha Templeton

Latasha Templeton is an Engineering Geologist at Golder with experience in New Zealand, Antarctica, West Africa, Canada, Fiji and Australia. She has worked on tunnel design and construction, slope stabilisation and natural hazard assessment. She has experience in field operations for geotechnical projects and has been involved in multiple large-scale projects.

Ben Higgs

Ben Higgs is an Engineering Geologist at Golder, who specializes in seismic hazard analysis. Ben also has experience in geophysical surveying as well as a range of data analysis and probabilistic modelling techniques to benefit data-driven geotechnical engineering projects.

Matthew Jordan

Matt Jordan is a Project Management Professional and Civil Engineer with over ten years' experience in major engineering and construction projects. Matt works for Antarctica New Zealand on the recently funded Scott Base Redevelopment Project. He is a Board Director for the US based Antarctican Society, where he chairs the outreach committee. Matt has been based in Christchurch for the last four years, having moved from his hometown of Perth, following over six years in the Australian mining and power generation industries.

INTRODUCTION

The Scott Base Redevelopment Project (SBR) aims to modernise the facilities at Antarctica New Zealand's Scott Base with extensive reconstruction of most of the current infrastructure. Golder was engaged to provide a geotechnical assessment to support detailed design of the proposed redevelopment. This article summarises the findings of two phases of geotechnical investigation and several site visits completed by Golder staff since 2015.

Scott Base currently comprises seven primary buildings interconnected by all-weather corridors and located over approximately 300 m x 200 m on Pram Point, Ross Island, in the Ross Dependency of Antarctica. The original buildings at Scott Base were constructed during the late 1950s as part of the International Geophysical Year. Additional buildings have been added over the subsequent decades to accommodate expansion of the base to support further scientific programmes.

The Scott Base Redevelopment (SBR) project will be the largest project ever undertaken by Antarctica New Zealand. It is a complex multi-year project that will significantly underpin New Zealand's research programme and strategic interests in Antarctica. The purpose of the rebuild is to fully address known risks and issues with the current infrastructure and provide a fit for purpose, environmentally sustainable research base that will support New Zealand's physical presence in the Ross Sea region of Antarctica.

GEOLOGICAL SETTING

Ross Island is formed from volcanic rocks of the McMurdo Volcanic Group, comprising basaltic rocks including lava flows and scoria deposits. Hut Point Peninsula is a southward extension of Ross Island and, at its southern end, is largely free of persistent thick ice. It is the site of the 1901-1904 Discovery Expedition's hut and is the site of McMurdo Station (USA) as well as Scott Base. Most of the volcanic cones on Hut Point Peninsula are centered on a prominent lineation that strikes NNE along the western side of the peninsula. The volcanic rocks are predominantly Quaternary age basalts, with minor flow banded trachyte at Observation Hill and autoclastic and pyroclastic breccias at Castle Rock and Boulder Cones (Cole et al. 1971) (Figure 1). Scott Base is located on the south eastern flanks of Crater Hill, a parasitic volcano on the south side of Hut Point

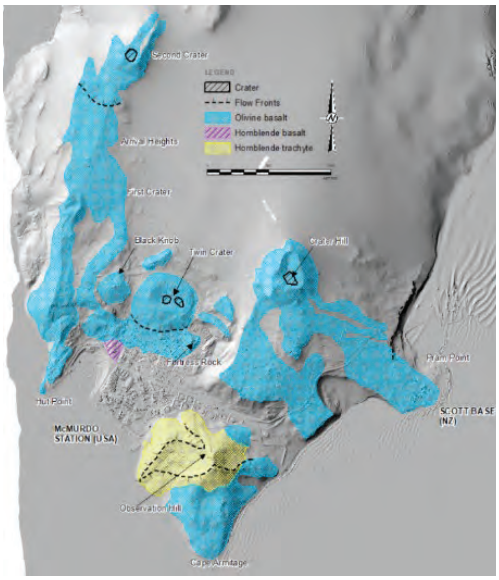

FIGURE 1: Geological Map of the Hut Point Peninsula adapted after Cole et al. 1971.

FIGURE 3: Permafrost deformation features around the road between Scott Base and McMurdo Station.

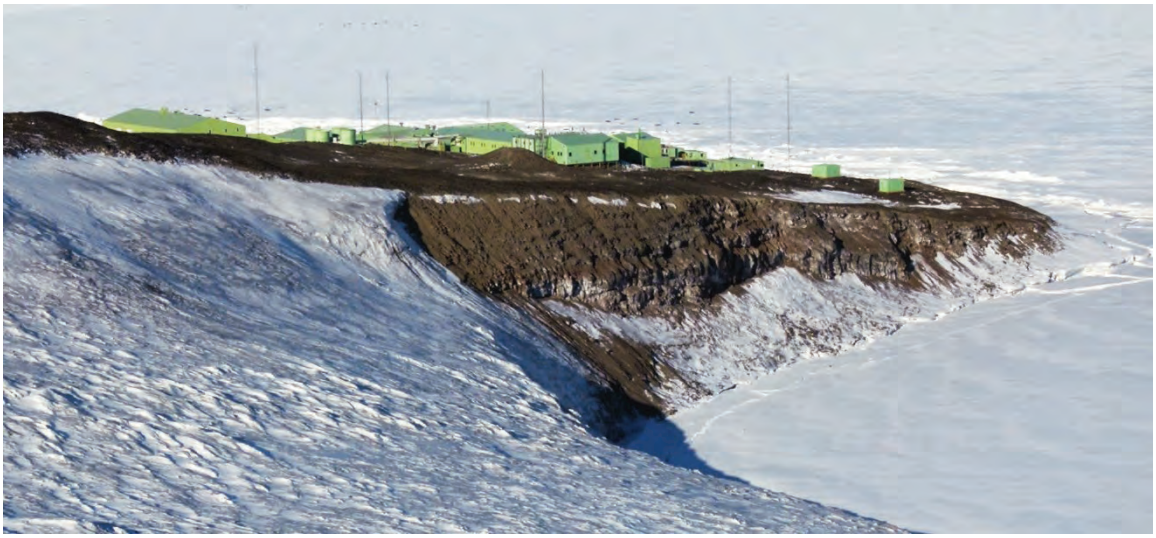

FIGURE 2: Scott Base geomorphic setting viewed from McMurdo Station Road west of Scott Base.

Peninsula. Less than 40 km from the site is Mt Erebus, which is the largest mountain on Ross Island at 3,794 m above sea level and is one of the few continuously active volcanoes on Earth. The volcanic rocks near Scott Base are geologically young, with the youngest estimated to be approximately 50,000 years old (Cox et al. 2012).

Scott Base is constructed on a gently sloping site 15 m to 30 m above sea level. The adjacent coastline is approximately 60 m from the existing main buildings and 30 m from the nearest out-buildings. The sloping surface on which Scott Base is located is interpreted to be the uppermost of a series of basaltic lava flows. The flows slope down from Crater Hill, located 1500 m northwest of Scott Base, which reaches an elevation of about 240 m above sea level. The stratigraphy is exposed in cross section in adjacent slopes, and typically comprises basalt flows estimated to be 1 to 10 m thick. The lava flows appear to dip at a flatter angle than the general ground surface, suggesting that the upper, youngest rocks, sourced from Crater Hill, thin downslope away from the vent (Figure 2). The extent to which glacial activity has shaped the landscape is unknown. The surface of the slope has been slightly eroded by some surface water channels.

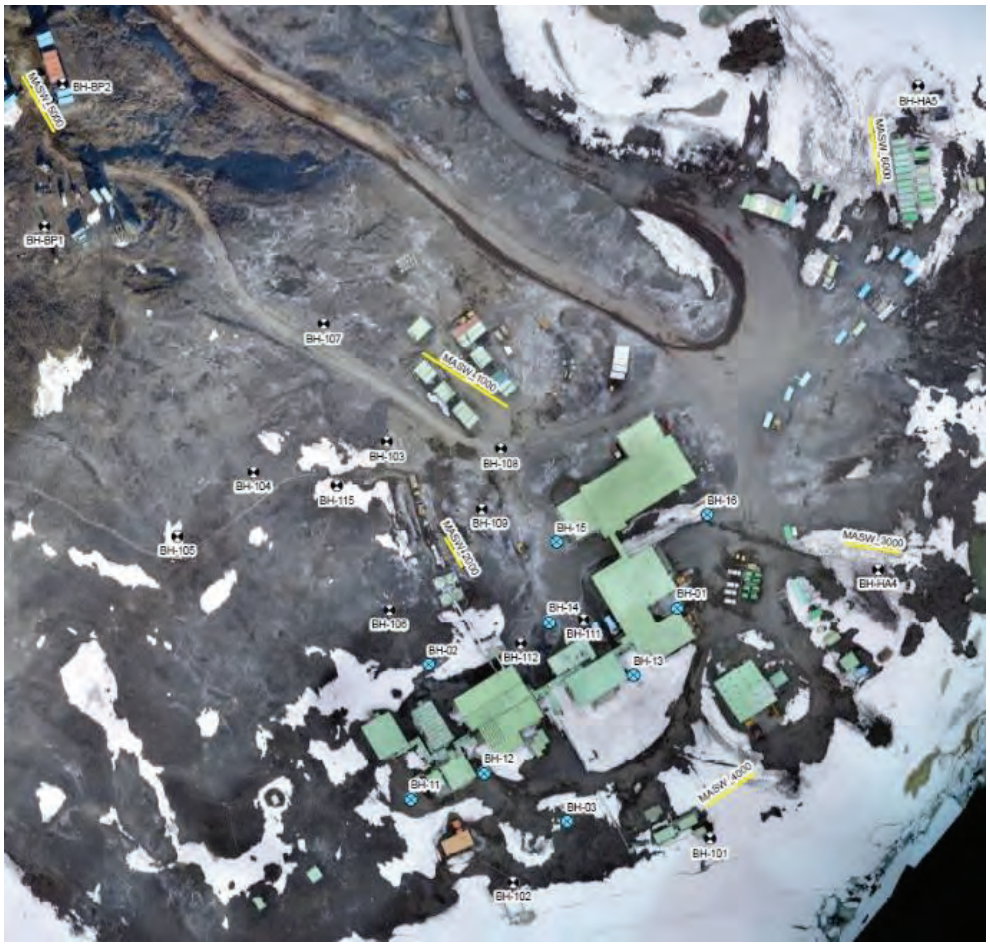

FIGURE 4: Drill hole investigations for 2019 (black and white circles) and 2015 (blue circles).

FIGURE 5 (OPPOSITE) : Webster's air flushed coring rig configured to recover continuous 55 mm diameter core located on the slope above Scott Base.

On the steeper ground above the McMurdo Station Road, permafrost deformation features ('patterned ground') can be seen in aerial images and on the ground. These features relate to expansion and contraction of the near surface ground due to seasonal freeze and thaw (Figure 3).

GEOTECHNICAL INVESTIGATIONS

Twenty-five drill holes were completed on site around Scott Base in October 2015 and October 2019 (Figure 4) by Webster Drilling and Exploration Limited (Webster), using a purpose built air flushed coring rig configured to recover continuous 55 mm diameter core (Figure 5).

A key aim of the site investigations was to recover the best possible samples of frozen ground including ice, frozen soil and rock. Webster's rig used radiators to chill the compressed air as cold as possible before flushing the bore hole annulus. This method proved highly effective and recovered high quality samples with very little core loss. It was observed that melting of the ice in the recovered core increased when ambient air temperatures reached above a threshold of about -7°C. Golder supervised the drilling of all drill holes and undertook the logging onsite as the holes progressed. Thermistors were installed in three of the drill holes (BH-01, BH-02, BH-03) to measure variations in ground temperature at a range of depths throughout the year and to assist in determining

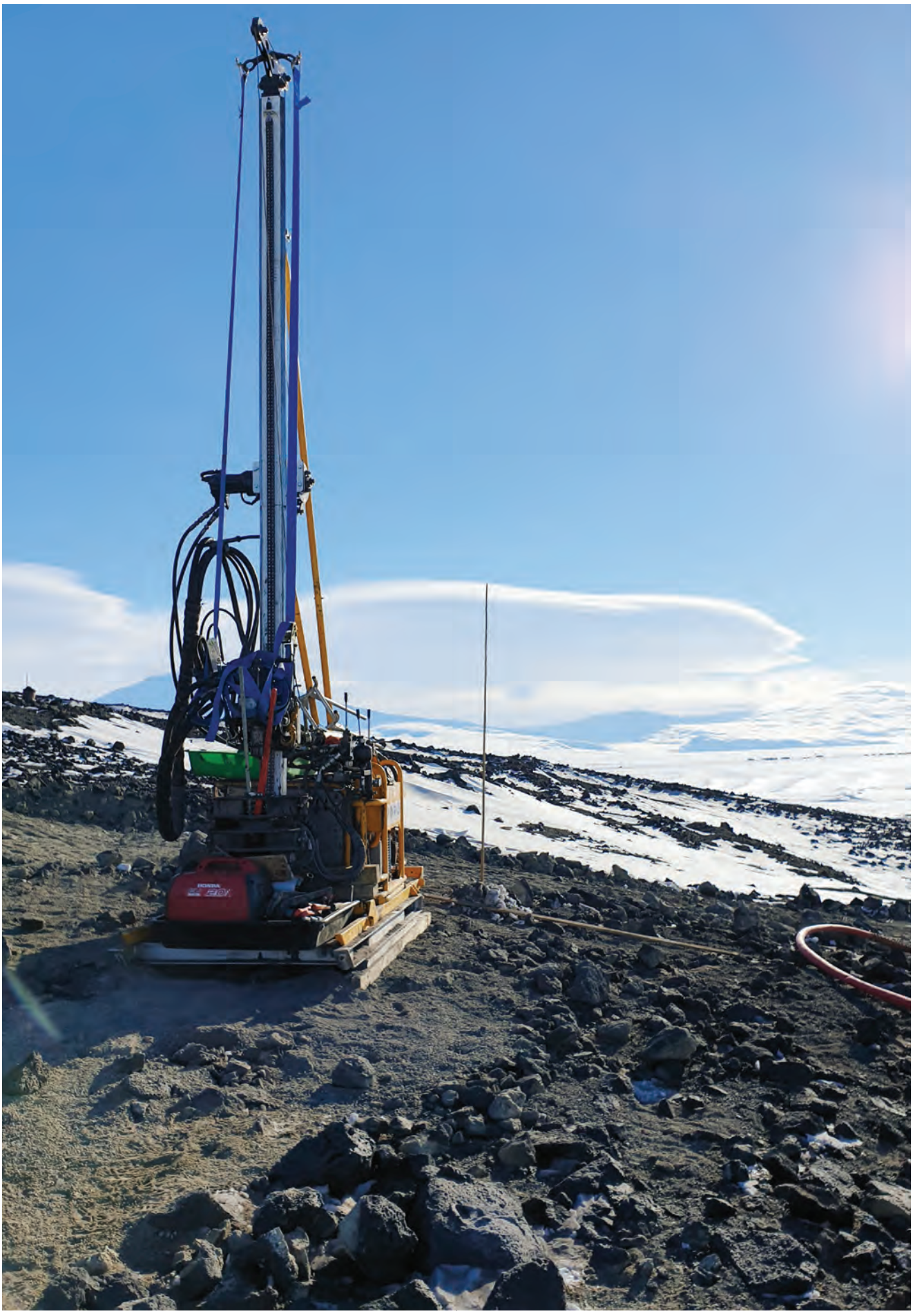

FIGURE 6: Image from the video inspection of a borehole on the slope above Scott Base. Image shows horizontal and vertical discontinuities and a small void.

FIGURE 7: MASW layout on site

FIGURE 8: GPR set up

the depth zone that could be affected by seasonal freeze and thaw (as discussed later in this paper).

A SeeSnake microReel video inspection system was utilized to produce high quality images of the borehole walls. The imagery identified sections of the drillholes that were highly fractured, small to large voids and sharp changes in geology (Figure 6).

Geophysical techniques were used to investigate the subsurface, in particular investigating the potential presence of any significant ice that could affect the redevelopment. Six Multi-channel Analysis of Surface Waves (MASW) profiles were completed around the base (Figure 7). The MASW lines that were completed along the shoreline are interpreted to measure shear wave velocity of 2000 to 2300 m/s in the upper ground profile. This approximates the shear wave velocity of ice suggesting that the stratigraphy contains abundant ice. The MASW lines that were completed further from the shoreline indicate lower shear wave velocity (800 to 1400 m/s) suggesting the presence of highly fractured rock with little ice.

Ground penetrating radar (GPR) was also used to investigate for subsurface ice (Figure 8). The GPR used at Scott Base was a USRadar Quantum Q4-300 that has three radar antenna with a frequency range of 220 MHz, 300 MHz and 380GHz. The interpretated GPR data identified areas where fill had been placed to develop roads or building platforms underlain by basalt.

GEOTECHNICAL TEST RESULTS

POINT LOAD TESTS

To characterise rock and frozen soil strength 391 Point Load Tests (PLT) of core samples were undertaken in the field to evaluate point load strength index ($I_{s(50)}$). The results show that the ice bonded sandy gravel soils have a point load strength index value approximately equivalent to a weak rock. The basaltic scoria and basalt are predominately strong to very strong, which correlates to an approximate unconfined uniaxial compressive strength of 50 to 250 MPa. All $I_{s(50)}$ results are shown in Figure 9.

UNCONFINED COMPRESSIVE STRENGTH

Unconfined compressive strength (UCS) tests were completed on 21 core samples. The samples were selected to represent the range of rock materials encountered on site. We selected 4 samples for each rock type; non-vesicular basalt, slightly vesicular basalt, moderately vesicular basalt, highly vesicular basalt and scoria. The non-vesicular basalt and slightly vesicular basalt returned UCS results between 60-120 MPa,

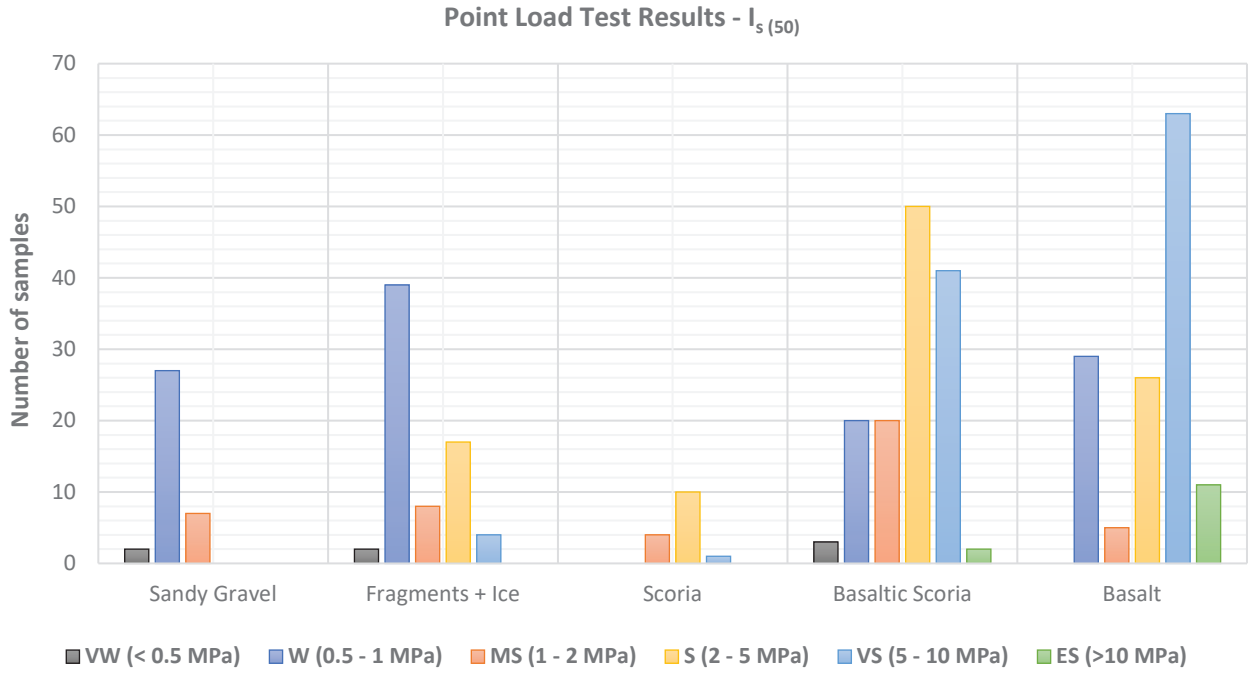

FIGURE 9: Point Load Strength Test (Is(50) results of frozen soil and rock samples from Scott Base.

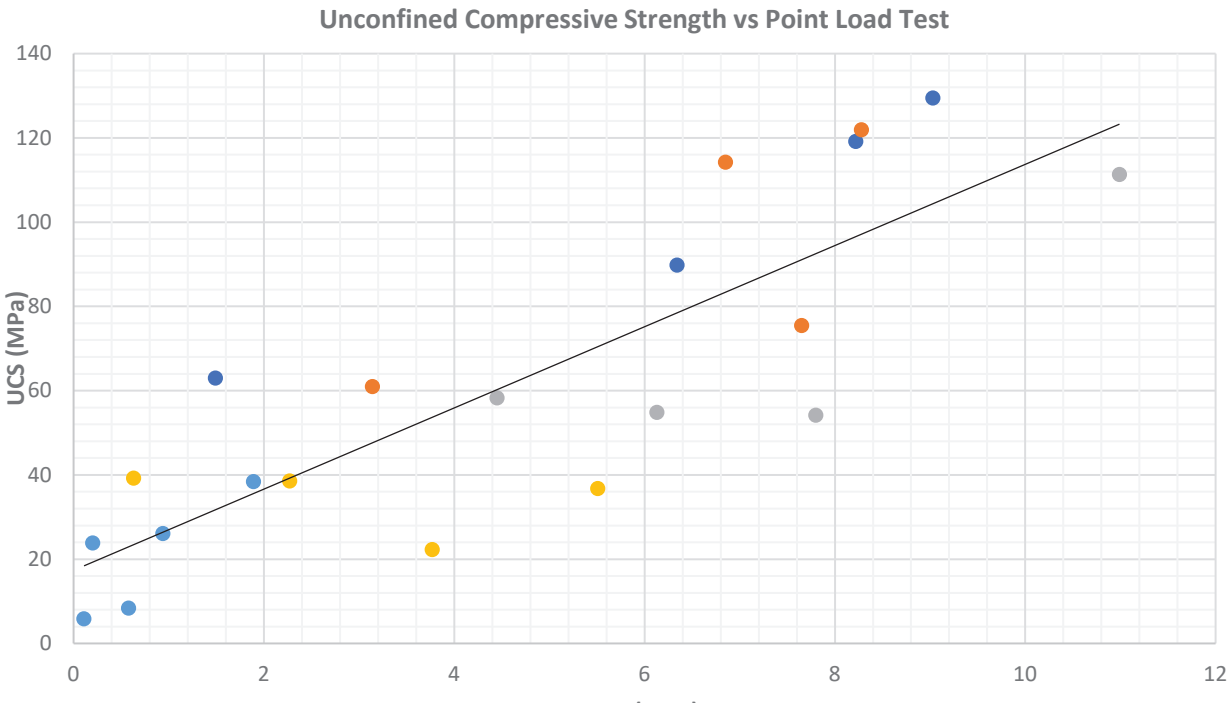

FIGURE 10: Unconfined Compressive Strength and Is50 results for a range of vesicle content in basalt samples from Scott Base.

moderately vesicular basalt ranged between 50-100 MPa, highly vesicular basalt and scoria ranged between 8-40 MPa. These results indicate a correlation of reducing compressive strength with increasing vesicularity.
UCS was plotted against the closest PLT results taken adjacent to the UCS samples to estimate a conversion factor between UCS and $I_{s(50)}$ to help represent the $I_{s(50)}$ results as inferred UCS. Figure 10 graphically summarises the UCS and $I_{s(50)}$ results and illustrates that a conversion factor of 17 is suitable.

MOISTURE CONTENT AND DENSITY

All the samples that underwent strength testing had moisture content measured along with bulk and dry density. The moisture content varied between 0.4 to 10.3 % with the moisture content generally increasing with vesicularity. The samples ranged from 1.9 t/m^3 to 2.91 t/m^3 for bulk density and 1.76 t/m^3 to 2.89 t/m^3 for dry density. As expected, the density in both cases decreased with increasing vesicularity.

FIGURE 11: Evidence of man-made ramps, roads and pads behind Scott Base with drilling rig to the right of the image. The dozing of snow into piles and tracking on roads shows how snow and ice can be incorporated into the fill (photograph supplied by Antarctica New Zealand).

FIGURE 12: Core run on site showing the different geology encountered. Ground surface is at the top right of the core box which is a layer of fresh snow, the upper 0.5 m is ice underlain by a moderately weathered basalt with moderate vesicularity moving into a slightly weathered basalt. The intact piece of core is a 1.5 m fully intact core run in the slightly weathered basalt. The core is fully covered in ice along all discontinuities and defects.

Table 1: Engineering Properties for the Basaltic Volcanic Material.

	Parameter	Non-vesicular			Slightly Vesicular			Moderately Vesicular			Highly Vesicular			Scoria		
Measured Results	Uniaxial Compressive Strength (MPa)	Min	Mean	Max	Min	Mean	Max	Min	Mean	Max	Min	Mean	Max	Min	Mean	Max
		62	99	129	61	67	121	54	69	111	22	33	39	5.8	20	38
	Point Load Strength (Is_{50} – MPa)	5 - >10			5 - 10			2 - 5			1 - 5			0.5 - 1		
	RQD (%)	80 - 100			70 - 100			70 - 95			25 - 60			0 - 50		
	Discontinuity Spacing	600 mm - >2 m			600 mm - >2 m			600 mm - >2 m			200 mm - 600 mm			200 mm - 600 mm		
	GSI	95 - 90			90 - 85			80 - 75			75 - 70			70 - 65		
Estimated Results	Mi	30			28			25			20			17		
	Disturbance Factor*	0			0			0			0			0		
	Intact Modulus (MPa)	44550			23450			20700			8250			4000		
	Modulus Ratio	450			350			300			250			200		

Notes: *the disturbance factor is based on the material as recovered in core. The material will be disturbed in a blasting scenario and consideration for the impacts will need to be considered.

GENERAL GROUND CONDITIONS

The subsurface geology at Scott Base generally comprises fill, scoria, basalt fragments in ice matrix and basalt bedrock (Figure 12). Ice is also evident in much of the core either as visible ice or inferred from ice bonded material where the ice is not visible to the unaided eye.

FILL

Uncontrolled fill was encountered in topographical lows near the shoreline and adjacent to buildings or roads. The fill is typically light brown in colour and comprises basalt gravel, silt and buried snow. The fill is typically well bonded with ice. Although significant ice lenses are uncommon within the fill material itself, the base of the fill is typically marked by thin ice lenses or buried snow (Figure 11).

BASALTIC VOLCANICS

The natural ground at Scott Base is predominantly composed of basaltic rocks of varying vesicularity, ranging from dense basalt to scoria with varying ice content. We have divided the recovered core into five different classes of vesicularity to help characterise the engineering properties of the material based on visual assessment of the relative proportion of vesicles: non vesicular basalt (0-10 % vesicles), slightly vesicular basalt (10-20 % vesicles), moderately vesicular basalt (20-30 % vesicles), highly vesicular basalt (30-40 % vesicles) and scoria (<50 % vesicles). Each class of basalt has been characterised below with a description of the geology, the range of UCS and $I_{s(50)}$, the Geological Strength Index (GSI) (Hoek, 1994) and Hoek Brown criterion (Hoek & Brown, 1980) values that can be used to determine the shear strength parameters as required. This summary is intended to be used to characterise the rock for foundation design and other engineering design requirements. A summary of the engineering properties for the basaltic volcanics is present in Table 1.

ICE

Ice was encountered to some degree in all the drill holes across Scott Base. The presence of ice, when not visible, was inferred by bonding of soil grains. Ice bonding ranging from friable (i.e., easily disaggregated when scraped with the point of rock hammer) to well-bonded (i.e., requiring a firm blow of the rock hammer to break). Where visible, ice ranging from sub-millimetre sized discrete crystals disseminated in the core to lenses of ice with no other soil or rock constituents. Ice also ranged from cloudy, white and granular ice to clear, hard and glassy ice. Very thick accumulations of white, granular ice are interpreted to be buried snow underlying fill. In general, the thickest (0.8 m) accumulations of ice were observed near the shoreline.

FIGURE 13: Proposed location of the redeveloped Scott Base buildings (supplied by Antarctica New Zealand).

GROUND CONDITIONS ACROSS THE REDEVELOPMENT SITE

The proposed Scott Base Redevelopment comprises three large buildings that are connected via hallways. The three buildings will be accommodation (Building A), science labs, offices and event staging (Building B) and store, cargo and workshops (Building C). The proposed building locations are upslope from the current Scott Base buildings (Figure 13). The ground profile at the location of the buildings will be formed by cut and fill to level off the building platforms.

The existing Scott Base is constructed on a gently sloping site interpreted to be the uppermost of a series of basaltic lava flows sloping gently to the southeast (Figure 2). Investigations determined that the properties of a basaltic rock changed across the site. The drillholes located on the upper slopes behind the current Scott Base buildings (Figure 13) encountered thaw sensitive sandy gravel (broken fragments of scoria/basalt) and weak, slightly weathered basalt/scoria with ice present in the vesicles or in an ice matrix.

Further down slope behind the current buildings the drill holes encountered similar material (weak to slightly weathered basalt/scoria with ice present), but lenses of moderately strong to very strong fine grained unweathered basalt were also present. These lenses of more competent basalt were more common further downslope towards the shoreline in varying thickness. The more competent basalt generally resulted in reduced drilling speed and improved core recovery. The ground conditions at the shoreline were found to comprise up to 1.5 m of fill consisting of sandy gravel, compacted snow and buried wood fragments underlain by natural ground (Figure 14).

The underlying natural ground was found to comprise strong basalt and weaker slightly weathered scoria. The core was filled with glassy, hard, clear to cloudy ice crystals in all vesicles and on discontinuities. We conclude that the ice content near the shoreline reflects the impact of seawater infiltrating the rock mass.

We infer from the distribution of materials that the upper slope above Scott Base may comprise local material sourced from Crater Hill and that the underlying material that outcrops closer to the shoreline may comprise a series of extensive flows, possibly from a separate source.

ACTIVE LAYER AFFECTED BY PERMAFROST PROCESSES

Three thermistor strings were installed during the 2015/2016 drilling season at Scott Base. The thermistor strings were installed in drillholes close to the existing base. Figure 16 shows the highest and lowest temperatures measured at each thermistor depth.

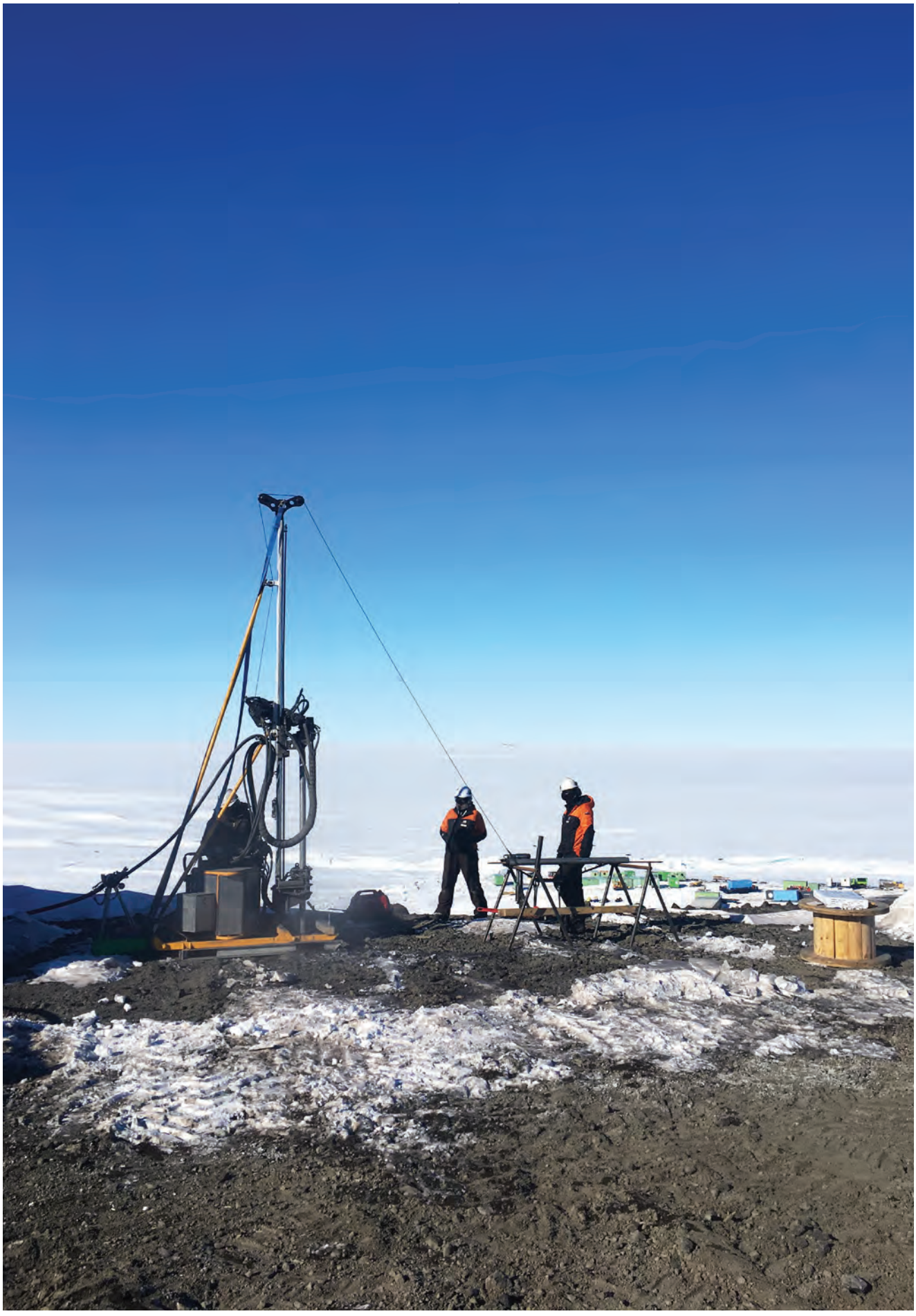

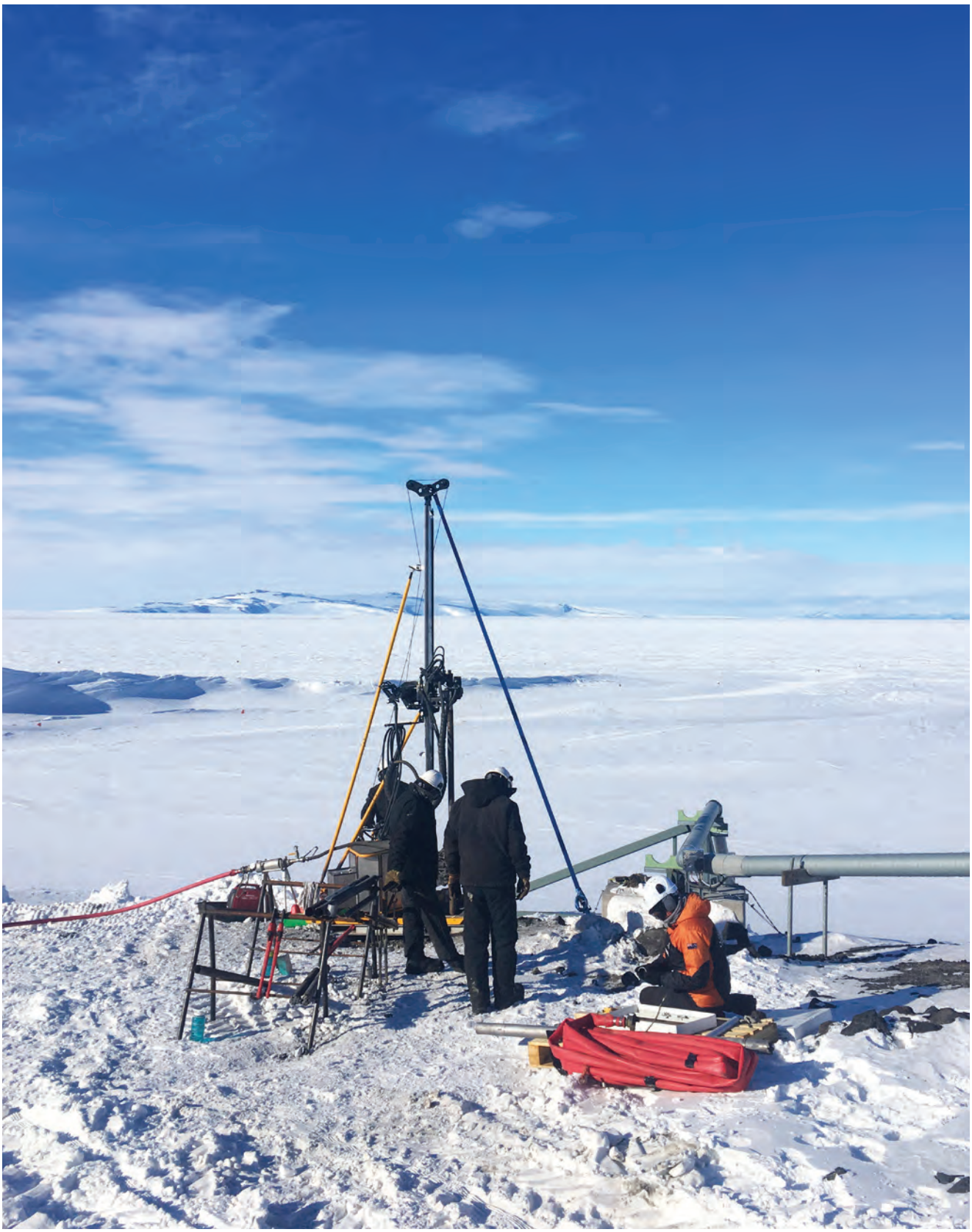

FIGURE 14 (LEFT): Drilling upslope of Scott Base (in the background). The material was predominately recovered as basaltic gravels with ice present (photograph supplied by Antarctica New Zealand)

FIGURE 15: Drilling near the shoreline and outlet pipe for Scott Base. The start of the pressure ridges are forming in the background (photograph supplied by Antarctica New Zealand).

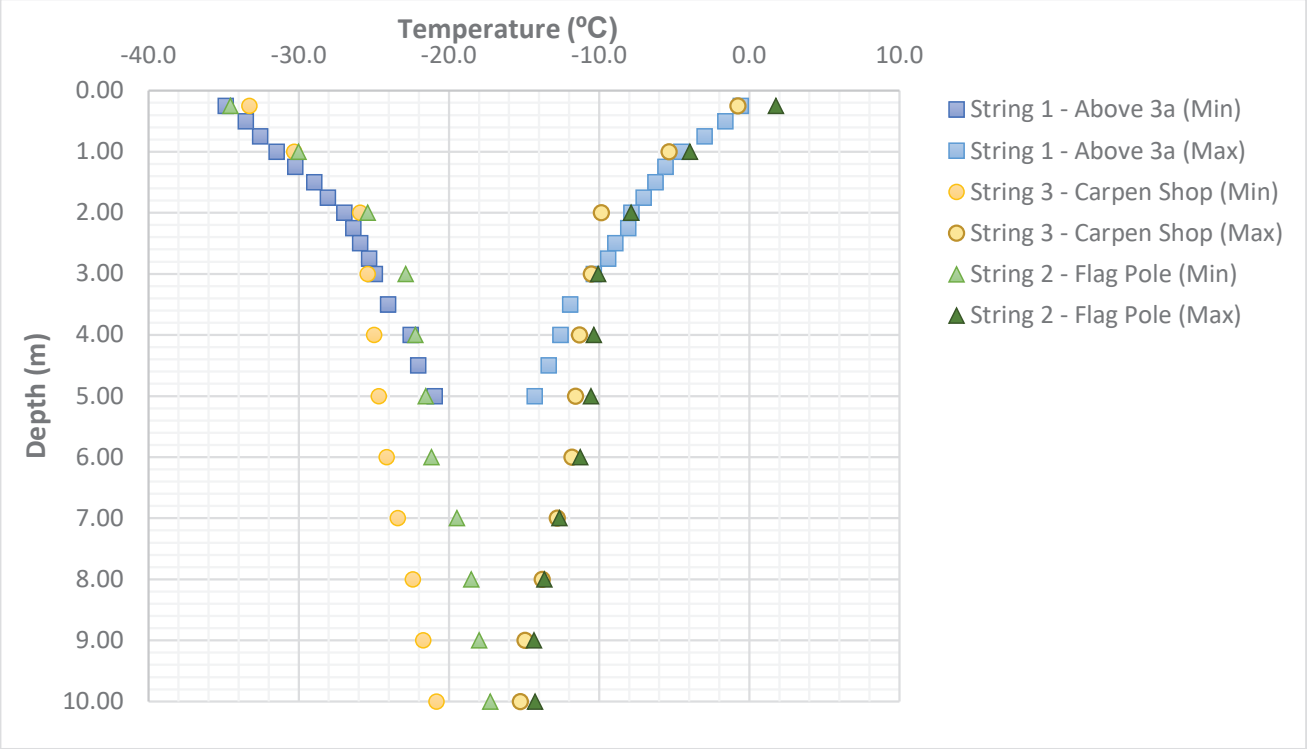

FIGURE 16: Summary of available temperature data from Scott Base.

The data collected between 30 January 2016 and 10 February 2020, presented in Figure 16, indicates that only shallow thermistors measure temperatures approaching 0 °C. We infer that the active layer that is affected by seasonal freeze and thaw processes extends to a depth of about 0.4 m below ground level at Scott Base.

CONCLUSIONS

Golder has completed two geotechnical investigation programmes at Scott Base in 2015 and 2019 for Antarctica New Zealand. During these investigations we have completed multiple drill holes, drill hole imagery, MASW, GPR and installed thermistors.

From these investigations we determined the site is underlain by man-made fill, basaltic volcanic rocks and ice. The fill is located to areas of previous construction, i.e. ramps and roads or building platforms. Ice is present within or under the fill and interpreted as buried compacted snow, or as ice crystals on defects in the basalt. There is no evidence of significant continuous ice lenses. The basaltic volcanic rock encountered was divided into 5 sub-categories based of the vesicularity of the material, non-vesicular basalt, slightly vesicular basalt, moderately vesicular basalt, highly vesicular basalt, and scoria. Each of these categories was found to have different engineering properties, which will influence engineering behaviour.

We infer that the more vesicular the basalt present on the slope above Scott Base may be local deposits sourced from Crater Hill and the more competent basalt present below Scott Base is part of a more extensive deposit, possibly from a different volcanic source.

REFERENCES

ASTM D4083-89 (2007), Standard Practice for Description of Frozen Soils (Visual-Manual Procedure), ASTM International, West Conshohocken, PA, 2007, www.astm.org.

Bannister, S., F. J. Davey, B. Kennett, (2003), Variations in Crustal structure across the transition from West to East Antarctica, Southern Victoria Land, International Journal of Geophysics, Volume 155, pages 870-884.

Cole, J.W., Kyle, P.R., and Neall, V.E., 1971: Contributions to Quaternary Geology of Cape Crozier, White Island and Hut Point Peninsula, McMurdo Sound Region, Antarctica. New Zealand Journal of Geology and geophysics, vol. 14 no. 3, 528 – 546.

Cox, S., Turnbull, I., Isaac, M., Townsend, D., Smith Lyttle, B. (2012). Geology of southern Victoria Land, Antarctica. IGNS 1:250 000 geological map 22.

Hoek, E. (1994). Strength or rock and rock masses. International Society of Rock Mechanics and Rock Engineering (ISRM) News Journal, 2 (2): 4-16.

Hoek, E., Brown E,T., (1980) Empirical Strength Criterion for Rock Masses. Journal of geotechnical and Geoenvironmental Engineering. Vol 109, Number GT9, Pp. 1013-1035.

Golder Associate (NZ) Limited (2016). Scott Base – Antarctica Geotechnical Assessment Report. Report Number 1413806_7407-003-R-Rev0, dated February 2016.

Golder Associates (NZ) Limited (2020). Scott Base Redevelopment Project Geotechnical Assessment Report. Report Number 19123189_7407-004-R-Rev0, dated July 2020.

New Zealand Standard (NZS) 4407:2015. Methods of sampling and testing road aggregates. ISBN 978-1-77551-962-1.

NZGS, (2005). Field Description of Soil and Rock, New Zealand Geotechnical Society, December 2005.

NZ Geotechnical Society

2021 PHOTO COMPETITION

The 2021 theme is

Anything Geotechnical

FIRST PRIZE WINS $250

ENTRIES CLOSE
30 September

SEND YOUR ENTRY TO

- Email to: editor@nzgs.org (send as jpgs)
- Entries close 30 September 2021
- Clearly mark your entry with your name and provide a caption for your photo

The winning photo and the top runners-up will be printed in the December 2021 issue of *NZ Geomechanics News*

CONDITIONS OF ENTRY

1. Only amateur photographers may enter.
2. Photos must be taken by the entrant.
3. No computer generated pictures.
4. Any photographs received may be published in subsequent NZ Geotechnical Society publications and material.
5. Winning entries will be final and no correspondence will be entered into.
6. NZ Geotechnical Society members only may enter.

Separation of pumice from soil mixtures

M.E. Stringer, Department of Civil and Natural Resources Engineering,
University of Canterbury, Christchurch, New Zealand

https://doi.org/10.1016/j.sandf.2019.05.004

Dr Stringer received the 2018-2021 JW Ridley Geomechanics Paper award, for his paper "Separation of Pumice from Soil Mixtures", originally published in Soils and Foundations in August 2019.

Mark Stringer

Dr Mark Stringer received his PhD from the University of Cambridge and is currently a Senior Lecturer at the University of Canterbury. Mark's current research interests lie in the cyclic behaviour of New Zealand soils, with a particular focus on the pumiceous soils of the North Island.

ABSTRACT

Pumice-rich deposits are found in a number of locations around the world, and in particular across large areas of the North Island of New Zealand. Pumice grains are commonly described as being lightweight, highly crushable, and vesicular in nature. These characteristics give rise to a unique set of behaviours under loading, and pumice-rich soils are highly problematic in terms of in-situ characterisation in large part due to their crushability. The presence of pumice within a soil mixture has the potential to completely alter the stress-strain behaviour of these soils as well as require a different interpretation of results from commonly used site characterisation technique. It is therefore important to be able to determine quantitatively the percentage of pumice within a given soil deposit. This paper proposes a methodology based on a gravity separation of pumice-bearing mixtures with a heavy fluid. The application of the method to artificial mixtures of fine pumice and non-pumiceous sands is shown to be sufficiently accurate for engineering purposes.

INTRODUCTION

Pumice is a particular type of pyroclastic material, and is described as "a white or pale gray to brown, highly vesicular, silicic or mafic glass foam which will commonly float on water" (Fisher & Schminke, 1984). The vesicular nature of pumiceous soil grains means that they are lightweight (hence larger particles will commonly float), and it is known that these particles have a low crushing strength. Orense et al. (2013) investigated the crushing strength of pumiceous sand grains and showed that while there is significant scatter, the crushing strength of single particles were typically one order of magnitude weaker than a typical silica sand grain, and that the crushing strength of the material reduced with increasing particle size. The relatively low crushing strength of these soil grains makes these soils problematic from a characterisation point of view. In particular, Wesley et al. (1999) showed that in calibration chamber tests, the cone penetration resistance of commercially available pumice was completely insensitive to the relative density of the soil as shown in Figure 1. This has significant implications for practicing engineers who routinely rely on the use of such tools to derive engineering properties from correlations to particular parameters.

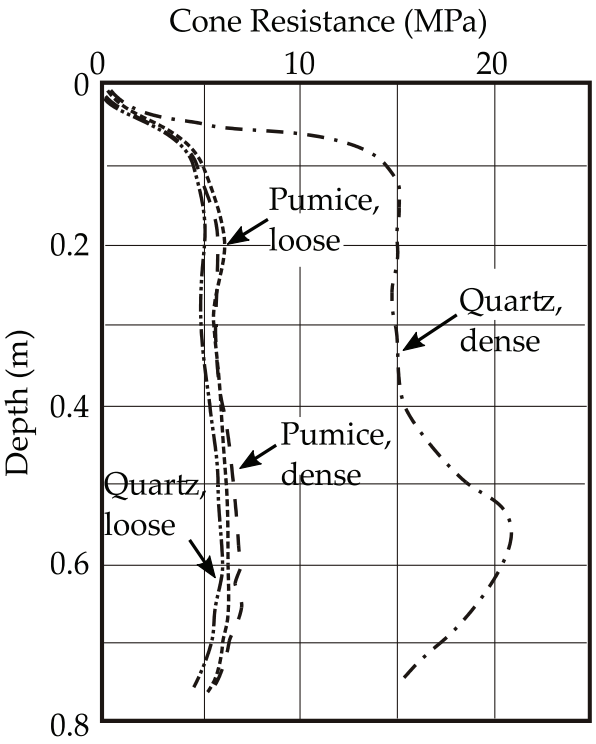

FIGURE 1: Calibration chamber testing on pumice and quartzitic sands (Wesley et al. 1999)

In addition to the issues associated with the in-situ characterisation of pumice-rich soils, the presence of pumiceous material is known to affect the response of a soil, in terms of compression characteristics (Hyodo et al., 1998; Miura et al., 2003), stiffness (Senetakis et al., 2016), stress-strain response (Orense & Pender, 2016, Senetakis et al., 2013), and liquefaction resistance (Hyodo et al., 1998; Orense & Pender, 2016). Additionally, volcanic materials can evolve significantly due to weathering or freeze-thaw effects, with implications for mechanical strength, cyclic resistance (Matsumura et al., 2015) and slope stability (Ishikawa et al., 2016). These studies indicate that if engineers are to make reasoned decisions regarding the behaviour of a pumice-bearing soil deposit, then a key property to evaluate is the percentage of pumice in a mixture.

Despite the importance of this parameter, it appears that there are currently few viable techniques that can be carried out in the laboratory. An obvious approach may include "spot-counting" where samples are examined under a microscope to determine the total number of pumiceous soil grains in a small sample. However, this process is generally too time consuming to be a reasonable tool for industry, as well as the issues related to the small numbers of particles being examined and the ability to convert numbers of particles into a percentage by mass or volume. In the absence of specific gravity (G_s) measurements, it is common to assume G_s in the range 2.65-2.7 for normal geotechnical materials, hence it is tempting to estimate the pumice content of a soil mixture based on the average specific gravity, noting that pumice has a low specific gravity due to its internal void structure. However, in the highly variable deposits containing pumiceous materials, G_s of the non-pumiceous component could be significantly different from 2.65. Additionally, Wesley (2001) discussed some of the issues associated with measuring specific gravity (G_s) in volcanic materials. In particular that when following the standard methods (i.e. ASTM D854-14), only part of the volume of gas in the internal voids is replaced with water so that the resulting G_s represents neither the actual mineral density, nor the bulk density of the grains. The G_s of pumiceous soil grains is generally size dependent, increasing with decreasing particle size. Therefore this simplistic method is unable to produce a satisfactory result.

Rogers & Sanderson (1954) described a method for commercial separation of pumice, where material is "jigged" - a process where water is introduced to the bottom of a vessel in a series of pulses, with the pumice being carried out of the vessel in the overflow. Recently, Asadi et al. (2019) attempt to apply the relative breakage index proposed by Hardin (1985) to estimate the percentage of pumice based on the change in particle size distribution when a soil sample is subjected to a vibratory load in a proctor compaction mold. However, while this latter approach may be closely linked to a parameter of interest to engineers (i.e. the strength of the particles), it is not known how robust the technique is in terms of particle sizes, previous stress history (i.e. previous crushing) and the effect of different particle strengths within the mixture. The determination of pumiceous content within a soil mixture therefore remains a question of interest.

In this paper, the author will present a methodology for determining the amount of pumiceous sands and gravels based on gravity separation, which aims to provide a robust test that can be replicated in a commercial laboratory.

PUMICE SAMPLES IN THIS STUDY

In this paper, pumiceous material has been obtained from a number of sites located on the North Island of New Zealand, with their locations marked on Figure 2 and noted in Table 1 along with key size properties, their mineral density ($G_{s,sk}$) and their geological formation. Particle size distributions are shown in Figure 3. The materials from Whakatane and Hamilton were obtained as part of wider research studies looking into the liquefaction resistance of natural pumiceous materials. The Whakatane samples were obtained from a site close to the Whakatane River and represent material which has been redeposited on a bend of the Whakatane river. The samples from two locations in Hamilton were obtained from several meters below the ground surface, and represent two very different depositional environments. The material from Tramway Road is taken from the Hinuera formation, while the material at

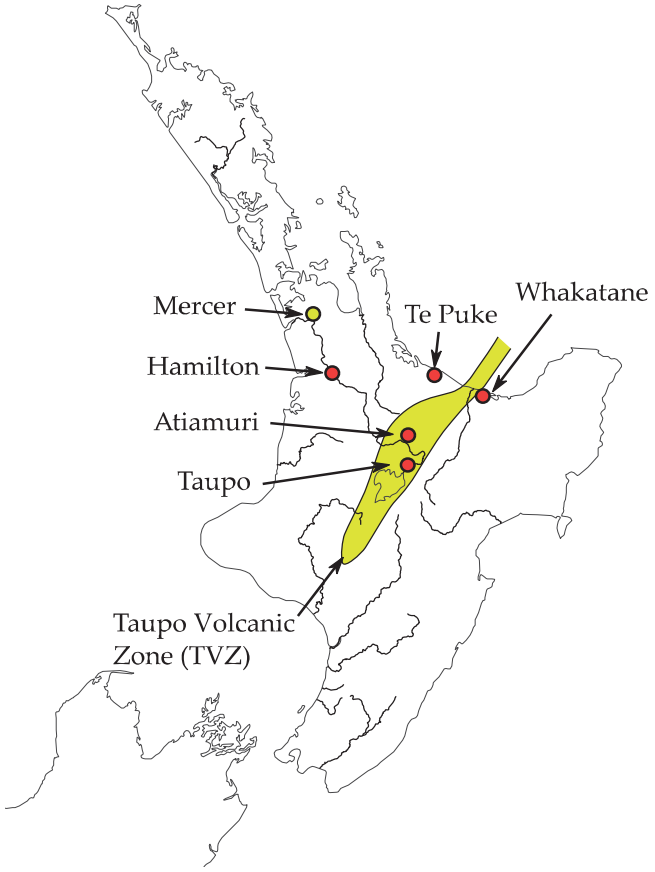

FIGURE 2: Location of samples used in this study.

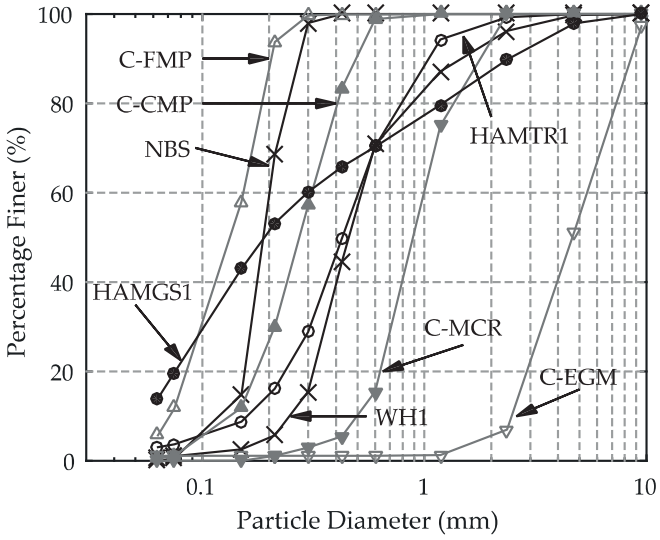

FIGURE 3: Particle size distributions of materials used in this study.

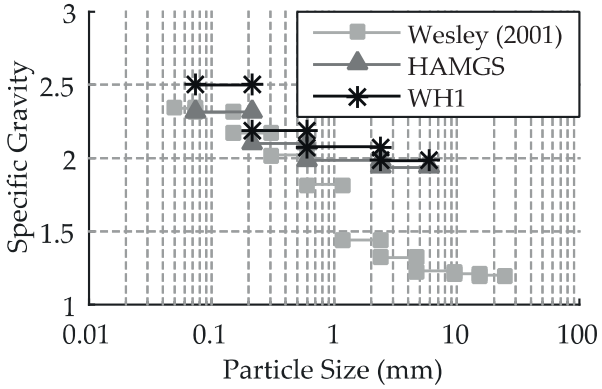

FIGURE 4: Specific gravity of pumice particles.

Grantham Street lies within the Taupō Pumice Alluvium (TPA). The Hinuera formation within the Hamilton Basin is described by Hume et al (1975) and the sediments are considered part of an alluvial fan created by the ancient braided Waikato River, with material being derived from volcanic eruptions in the central Taupō Volcanic Zone and deposited between 40,000 and 12,000 BP. The TPA is much younger, and were deposited rapidly when a pumiceous dam created during the Taupō eruption in 180 AD failed (Manville, 2002).

SPECIFIC GRAVITY OF PUMICEOUS MATERIALS

The three commonly quoted characteristics of pumice are vesicularity, low unit weights (as a result of internal voids) and crushability. In terms of determining the percentage of pumiceous material in a soil mixture, the low unit weight of pumice is appealing since it opens up the possibility of natural segregation through sedimentation, or a method based on the specific gravity of a mixture. As previously noted, the specific gravity of pumiceous materials tends to be size dependent, owing to the inability to replace the gas present within the internal voids of the grains with the fluid being used in the standard methods (i.e. using a pycnometer). A similar trend was observed in this study with the natural pumice samples from Whakatane (WH1) and Hamilton (HAMGS1). These results are shown in Figure 4 with those of Wesley (2001). While both of these samples appeared to be composed of pure pumice, it should be noted that the finest fraction (i.e. less than 75 µm) was significantly darker in colour and may represent a mixture of pumiceous material as well as hard-grained materials (i.e. the specific gravity may be higher in these fine fractions than the solid density of pumice).

In order to measure the mineral density ($G_{s,sk}$ in Table 1), individual gravel sized pumice particles were separated by hand, and then ground using a mortar and

Table 1: Gs measured on ground pumice material.

Formation	Sample ID (Location)	Location	$G_{s,sk}$	FC (%)	D_{50} (mm)	D_{95} (mm)	Density Separation
Hinuera formation	HAMTR1	Hamilton	2.340	4	0.43	1.31	Y
Taupō alluvium	HAMGS1	Hamilton	2.309	18	0.19	3.71	N
Taupō tephra	TPSH1	Taupō	2.295	0	N/A	N/A	N
Tauranga formation	WH1	Whakatane	2.335	1	0.46	2.16	Y
Taupō alluvium	C-CMP[a]	Atiamuri	2.395	1.2	0.27	0.55	Y
Taupō alluvium	C-FMP[a]	Atiamuri	-	12	0.13	0.23	Y
Tauranga formation	C-EGM[a]	Te Puke	2.294	0	4.67	9.21	N
Taupō alluvium	C-MCR[a,b]	Mercer	2.2	0	0.90	2.05	N
Christchurch formation	NBS[c]	Christchurch	2.65	1	0.19	0.29	Y

[a] Commercially available product.

[b] Solid density from CT-scanning, Orense & Pender (2016).

[c] Non-pumiceous beach sand from Christchurch, NZ.

pestle, to destroy the internal void structure. Grains were selected from natural materials in Hamilton (both sites), Taupō and Whakatane, as well as commercially available pumice. The results from these tests are summarised in Table 1 and varied between 2.29 and 2.40. The highest specific gravity came from the "milled" pumice - a product where naturally mined pumice is ground and then sieved to produce a more uniformly sized product for industrial applications. In this particular material, it was apparent that there was a noticeable amount of two additional components - both having the appearance of crystals and being either black in colour, or transparent and colourless. Similar materials were observed in the gravel sized particles from the sites in Hamilton, and testing on these particles indicated G_s is 2.65-2.67. Hence it is assumed that the higher value of G_s in the milled pumice is a result of the inclusion of these additional crystals. Excluding this result, the G_s of the ground pumiceous materials is 2.35 or less. In addition to the measurements on ground pumiceous material, Orense & Pender (2016) report a solid density (from CT-scanning) of 2.2 g/cm^3 for commercially available pumice grains sourced near the town of Mercer. The values of ground pumice and that of Orense & Pender (2016) are similar to the material density of 2.3 g/cm^3 assumed by Whitam & Sparks (1986) when attempting to estimate the internal void volume of Minoan pumice samples.

MICROSTRUCTURE OF PUMICEOUS SOIL GRAINS

To better understand the microstructure of these materials, the natural soil from the Grantham street site (HAMGS1) were sorted into size fractions corresponding to fine grained material (i.e. smaller than 75 µm), fine sand (i.e. 0.075 - 0.212 mm), medium sand (i.e. 0.212 - 0.6mm) and coarse sand (0.6 mm - 2.36 mm) and gravels. These particles were examined using a scanning electron microscope (SEM) and examples are shown in Figure 5.

The grains in Figure 5 display some of the commonly observed characteristics of these materials, namely that the surface is extremely irregular as a result of the vesicles. From the largest particles to the smallest particles, the overall characteristics remain similar until the finest materials in Figure 5, when they started to appear as plates. At the time of taking the SEM photographs, one grain (≈ 2.2 mm x 1.6 mm) was deliberately split with a scalpel, shown in Figure 6. Around the area of the cut, there are a number of very small plate like particles on the carbon mounting "dot", as well as a few fragments on the surface of the cut, two of which are visible in the expanded view. These photos suggest that when the pumice particles are broken to a sufficiently small size (i.e. smaller than 20 µm) , they are mainly composed of broken fragments of the walls between pumice cells.

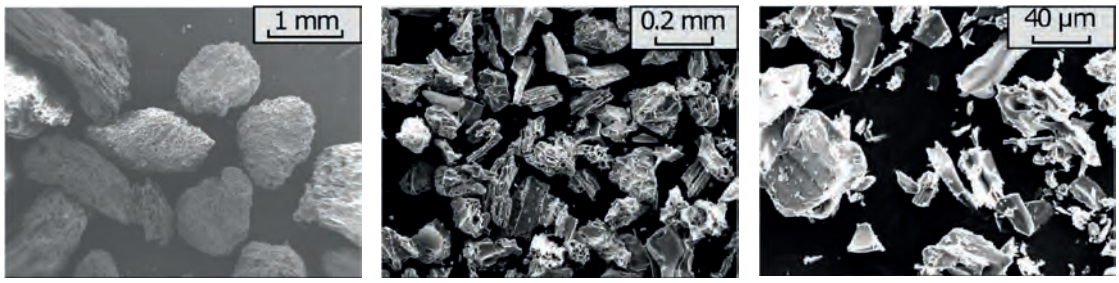

FIGURE 5: SEM images of pumiceous grains from Grantham Street, Hamilton.

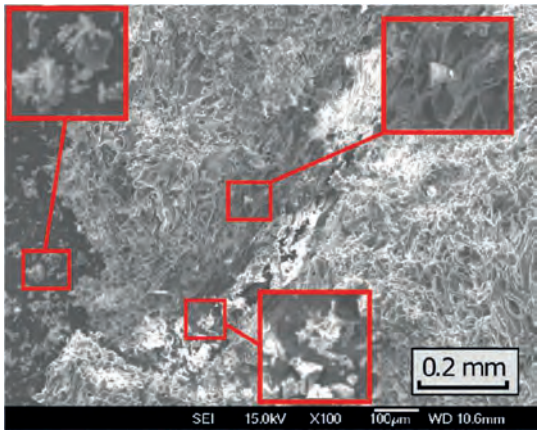

FIGURE 6: Split pumice grain. Zoomed view shows fragments of wall structure.

Ashby (1983) discusses that the strength of a cellular material is significantly lower than the parent material as a result of the fracturing of cell walls.

Additionally, it has been shown that the strength of porous ceramics is a function of porosity, with lower porosity materials displaying greater strength (i.e. Knudsen, 1959). Orense et al. (2013) have shown that the crushing strength of pumiceous grains increases with decreasing particle size. It is hypothesised that the low crushing strength of pumiceous soil grains comes as a result of their cellular structure, and that once broken down into platelike fragments the strength of the individual fragments would become significantly larger.

Hence if the aim is to identify the effect of pumice content on the engineering properties of a soil (i.e. as a result of the increased compressibility), it may be sufficient to develop a separation technique which concentrates on the coarse silt, sand and gravel sized particles within a soil mixture.

DENSITY SEPARATION USING HEAVY LIQUIDS

Despite the wide range in potential specific gravities of different rocks, the G_s of ground pumice is sufficiently low that separating the component of pumiceous material from a mixed soil sample remains an attractive approach. In the ideal scenario, the unit weight of the separating fluid would be set just above the mineral density of pumice (i.e. 2.35), and when a soil sample is mixed into the fluid, the pumice component will tend to float (recall also that the G_s of pumice reduces with increasing particle size), while other materials will sink.

Initial approaches considered the use of concentrated brine solutions, however the heavier brines (i.e. Sodium, calcium or zinc bromides) typically have a number of health and safety concerns, making them unsuitable for routine laboratory analysis methods. Attempts were made with lighter brines (i.e. calcium chloride, $G_s \approx 1.4$ at 40 % concentration), where the slightly elevated unit weight compared with water might allow separation of similarly sized particles of pumice from other materials due to differences in settling velocity. In this approach, the soils were pre-sieved into different size fractions (by sieving) and then placed in measuring cylinders filled with brine. However, it was found that when soil samples were introduced into the brine solutions, turbulent eddy currents were formed as the soil material settled, which caused a significant proportion of the pumiceous fraction to remain mixed with the non-pumiceous material. Separation of the pumice by "jigging" in a tube filled with calcium chloride brine was attempted using sieved fractions of the soil sample and an example of the resulting separation (medium sand sized particles) is shown in Figure 7. While some clear sorting has occurred, close inspection revealed that an appreciable amount of pumice remained in the "non-pumiceous" portion and vice-versa. This particular experiment had been sieved into size fractions prior to jigging, and it is expected that if the whole sample was tested at the same time, the separation would have been less effective still as a result

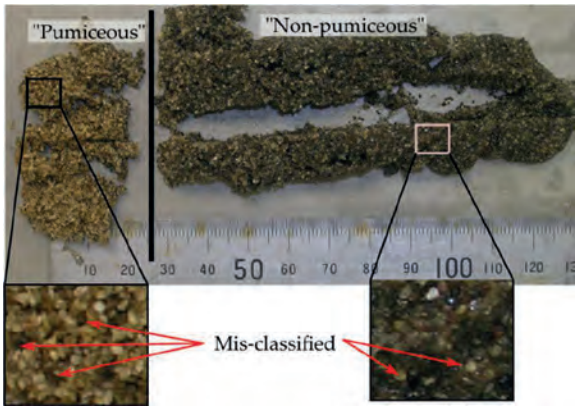

FIGURE 7: Separation of pumice by "jigging".

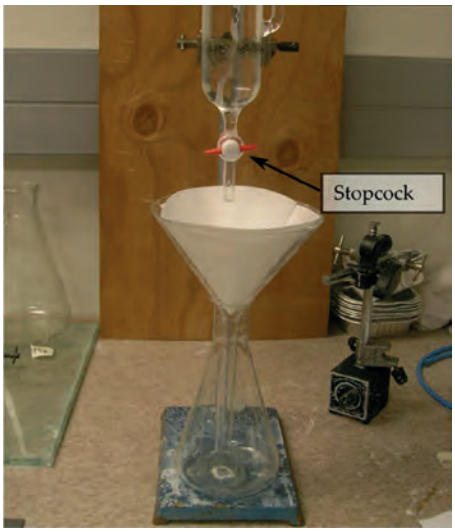

FIGURE 8: Glass separating cylinder.

of the finer non-pumiceous soil grains settling more slowly than the coarser pumiceous grains.

In geological studies, "sink/swim" analyses have been used to separate foramanifera from soil mixtures for many years, traditionally using bromoform as the heavy liquid. The use of bromoform was discontinued when non-toxic aqueous solutions of sodium metatungstate (SPT) became available, with specific gravities up to 3.1 (Gregory & Johnston, 1987; Munsterman & Kerstholt, 1996). More recently, aqueous solutions of lithum heteropolytungstates (LST) have been used, and as described by Leipe et al. (2018), they have two advantages over SPT: first, they are thermally stable above 60 ^{o}C, such that their density can be quickly increased by boiling to evaporate excess water. Second, they have a slightly lower viscosity, meaning separations occur slightly quicker. In this study, an aqueous solution of lithium heteropolytungstate (LST) was used to perform sink/swim analyses on the soil mixtures. It should be noted that LST solutions react with metals to form a dark blue coloured solutions. To avoid this, the experiments are carried out with glassware.

A glass separating cylinder was fabricated at the University of Canterbury, as shown in Figure 8. The main body of the separating cylinder is approximately 180 mm high and 45 mm inside diameter. A spout is fashioned near the top of the cylinder, with inner diameter 16mm, while a stopcock is placed at the base. A side arm (extending above the top of the main cylinder body by approximately 35 mm) is placed approximately half-way up the body of the cylinder with an inner diameter of 7 mm. Additionally, a modified glass stirring rod was made where the end of the rod was pressed into a paddle shape.

During the experiments, the density of the LST solution was set at 2.35kg/l by dissolving concentrated LST solution (supplied at G_s = 2.85) with deionised water (DI). The density of the solution was verified using a hydrometer, and at the specific gravity of 2.35, the kinematic viscosity was estimated (by measuring the velocity of falling soda glass spheres) as 2.86 cSt. The solution was added to the separating cylinder such that it filled approximately half of the cylinder. At this point, a 25 g or 50 g soil sample was added to the solution, thoroughly mixed using a stirring rod and left for 1 hour. The cylinder was then slowly filled via the side arm so that a gap of approximately 1cm was left below the spout. This second filling allows material which has floated inside the side arm to be washed back in the main chamber. If the soil is prevented from entering the side arm (i.e. placing a porous plastic filter at the base of the side arm, attaching filter paper across the base of the side arm, or redesigning the sidearm geometry) then the second filling stage would not be necessary. At this point, a clear separation of the sunken components and floating components would typically be apparent. It is possible that in the initial separation of the material, some pumice may become trapped in the sinking grains, while some non-pumiceous material may have become trapped in the floating grains. Hence, the raft of pumiceous material and the sunken material were both stirred gently to release any trapped grains. The soil was again allowed to separate for at least 4 hours. Photos showing the separation of KM04 are shown in Figure 9 and the clear separation of material is visible. It should be noted that there is some pumice in the side arm of this experiment. This material can be moved into the main body of the cylinder by the addition of more LST solution through the side arm, or placing a filter at the base of the side arm.

Soil was removed from the device in one of two ways, depending on the perceived grain size of the materials. In cases where the sinking material did not contain gravels, the separation took place by carefully opening the stop-cock and slowly drawing off both fluid and the material which had sunk. Where the material contained

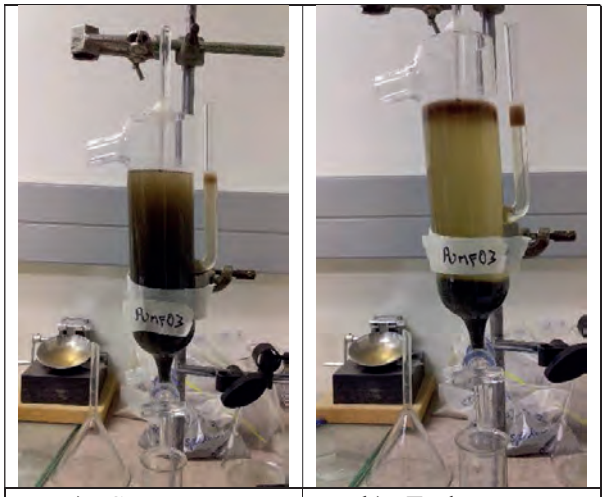

FIGURE 9: Separation of KM04.

gravel sized particles, it was not possible to draw the soil through the stop-cock, hence additional fluid was added via the side arm to raise the fluid level such that floating material would exit the cylinder via the spout. In the case of larger floating material (i.e. gravel sized pumice grains), the paddle on the end of the modified stirring rod was used to push the large particles into spout, whereafter the flow of fluid would carry the particles out of the spout.

The LST solution used in these experiments is relatively expensive (approximately $ 1000 / litre) so that a key element of these tests is the recovery of the LST. Whether the final separation takes place through the spout or stop-cock, the material is captured in a funnel lined with filter paper which has a pore size of 11 µm. The fluid which passes the filter is considered "clean" and can be directly re-used in the next analysis. After storing the "clean" LST fluid, the filter paper and contents are rinsed a further 3 times using DI water. In each rinse, the filter cone is filled, and allowed to completely empty prior to refilling. It should be noted that the rinse water contains an appreciable quantity of LST, hence this solution should be captured, stored and eventually concentrated (i.e. by evaporation in a soil oven) for re-use.

The remaining fluid and either floating or sunk material in the separating cylinder can then be carefully transferred to another filter cone, and treated in a similar way. The rinsed filter papers and soil grains are placed in a beaker and allowed to completely dry in a soil oven for 24 hours at 105 oC. The masses of the pumiceous soil grains ($M_{floating}$) and the remaining soil ($M_{sinking}$) can then be obtained and used to obtain the percentage of pumice by mass (P) of the sand and gravel portion using Equation 1.

$$P = \frac{M_{floating}}{M_{floating} + M_{sinking}} \quad (1)$$

The dilute LST solution from the rinse water is transferred to a large volume beaker (i.e. 5 l) and periodically placed in a conventional soil oven to concentrate the solution so that the G_s is greater than 2.35. At this point the solution can be re-diluted to G_s =2.35 using DI water. In cases where all of the fluid is evaporated, the LST will crystallise, but can be re-dissolved in DI water.

The aim of the filtration is to return the LST to its virgin state. If particles smaller than 11 µm are present within the soil, then they may pass through the filters and begin to contaminate the LST solution. As previously noted, the strength of pumiceous particles increases with reducing size so that pumice "fines" may play a lesser role in affecting the behaviour of a pumice bearing material compared with the larger particles. Hence in this method, it is recommended that the finest soil particles are removed from the sample prior to separation by wet sieving. If a user specifically wishes to retain silt sized particles (or if the soil sample contains a significant proportion of fines), it would be possible to wash the soil sample over a filter paper which is slightly coarser than the final filtation used to recover the LST. Note that in this paper, the soil samples were not pre-filtered, and there was no noticeable deterioration of the LST from the retention of fine grained material passing through the filter paper.

SEPARATION OF ARTIFICIAL SOIL MIXTURES

To test the efficacy of the method, a series of soil mixtures were created using commercially available milled pumice (C-FMP) and New Brighton sand (NBS). The particle size distributions for these two materials are shown in Figure 3, while the compositions of the soil mixtures are shown in Table 2. The separation of materials occurs due to the density difference of the materials relative to the fluid density. As shown in Figure 4, the apparent G_s of the material reduces as particle diameter increases. Stoke's law (Equation 2) governs the speed at which particles settle and examination of Equation 2 indicates that the most challenging situation in terms of separation occurs with small sized particles with the lowest difference in specific gravity relative to the fluid. For this reason, a "fine" grade of milled pumice was selected.

$$v = \frac{2}{9}\frac{\rho_s - \rho_f}{\mu} g R^2 \quad (2)$$

where v: settling velocity, ρ_s: density of solid, ρ_f: density of fluid, μ: dynamic viscosity, g: acceleration due to gravity, R: particle radius.

In order to create a separation of the materials, any pumice in the bottom half of the separating cylinder should have moved to the top half, and vice-versa. For the dimensions of the separating cylinder, a clear separation would be observed with a settling distance

Table 2: Separation of known mixtures of fine milled pumice (C-FMP) and New Brighton Sand (NBS) using LST solution with G_s = 2.35.

ID	Mass of soil (g)		Pumice Content (%)			Error (%)
	Initial	Final	Initial	Corrected	Separated	
KM01	25.1	25.3	100	84	84	0
KM02	50.0	49.9	75	63	64	1
KM03	50.0	49.8	50	42	39	-3
KM04	50.0	50.2	25	21	20	-1
KM05	50.0	25.2	0	0	0	0

of 100mm. Assuming that the solid phase of the pumice particles have a specific gravity of approximately 2.3, then with the kinematic viscosity of 2.9 cSt, it is possible to estimate the smallest particle that will have "separated" in the mixture after a given time. For the tests being described, there would be separation of particles greater than 27 μm after 4 hours.

Table 2 summarises the tests on known mixtures, expressing the pumice content as a percentage of the total soil mass. In some cases the final total mass of soil after the experiment is slightly larger than the initial mass. This observation implies that in those tests, there was a limited amount of LST that was not properly filtered out of the material. The amount of pumice being measured is consistently lower than that in the original mixture, and is particularly obvious in the case of KM01, where the mixture was 100 % milled pumice. During the separation with KM01, it was apparent that the sinking portion of KM01 was visibly different to the floating portion, appearing as either black crystals or clear, colourless crystals. Careful examination of the raw milled pumice revealed the existence of both components. These crystals (often volcanic quartz) are not uncommon and are found as phenocrysts within pumice grains (Fisher & Schminke, 1984; Hume et al., 1975). In undisturbed sampling carried out by the authors (in Hamilton and Whakatane), these crystals were also observed within the soil samples, often as individual soil grains. It is assumed that these particles would typically be attached to (or incorporated within) a large pumice particle, but that during the milling to reduce the particle sizes, these can become detached, or form a significant proportion of the smaller sand sized grains. The specific gravity of the volcanic glasses/quartz in the undisturbed specimens was 2.65 and hence they would be expected to sink in the LST solution with G_s equal to 2.35. Accepting that the sinking portion of KM01 is composed of these crystal particles, then the starting mass of pumice should be decreased by 16 % in each of the tests, and the mass of the non-pumiceous component increased by the corresponding amount. The "corrected" starting pumice content is shown in Table 2 and agreement within 3 % is obtained for all of the separated mixtures.

SEM photography was carried out on both the sinking and floating components of the material in KM01, with representative photos shown in Figure 10. An SEM image of the New Brighton sand is shown for comparison in Figure 11. On initial inspection it was surprising that the components of KM01 are not more obviously different. However, on close inspection, it is apparent that the grains from the floating component have internal voids which are visible on many of the particle faces, as well as a number of the grains displaying the expected surface vesicularity. In general these features were not apparent on the particles in the sinking component, which appear

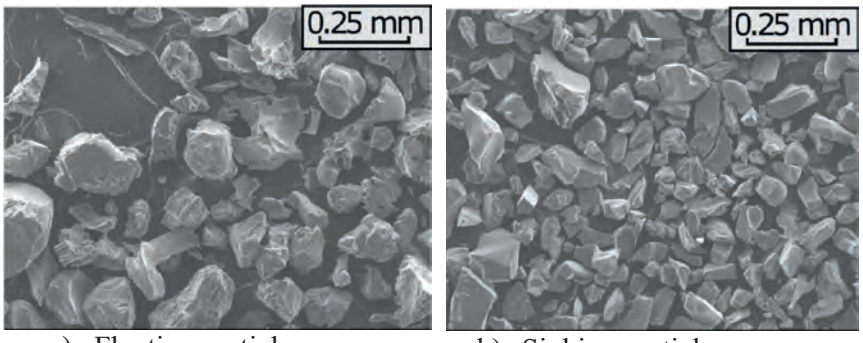

a) Floating particles b) Sinking particles

FIGURE 10: SEM photographs showing separated components of "milled pumice" from KM01.

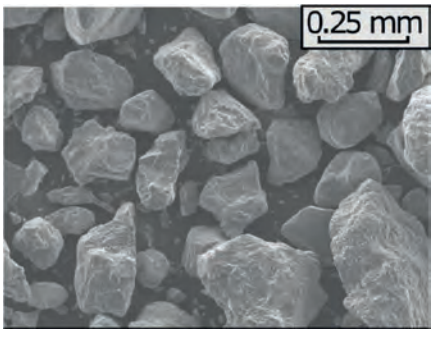

FIGURE 11: SEM photograph of New Brighton Sand (non-pumiceous)

Table 3: Separations with increasing fluid G_s.

ID	Fluid G_s	Starting Mass (g)	Separated Mix (g)		Description
			Floating	Sinking	
KM01	2.35	25.1	21.3	4.00	
KM01-S1	2.40	3.7	0.57	3.13	Sinking fraction of KM01
KM01-S2	2.45	3.1	0.24	2.74	Sinking fraction of KM01-S1
KM01-S3	2.50	2.7	0.25	2.62	Sinking fraction of KM01-S2

Table 4: Separation of natural soil samples.

ID	Location	Depth (m)	Initial Mass (g)	Separated Mix (g)		Pumice (%)	
				Floating	Sinking	P_{11}	P_{75}
HAMTR1	Hamilton	12.5	54.3	18.5	35.9	34.0	34.0
			43.6	14.1	29.1	32.6	32.6
			42.5	14.9	28.3	34.5	34.5
WH1	Whakatane	5.5	50	24.1	25.9	47.8	47.8

Note depths refer to the location of the soil sample below the ground surface.

to have smooth faces, devoid of vesicles. It should be noted that a small number of particles in the sinking component did however have some vesicles, meaning that there is some minor mis-separation. However, within the context of engineering requirements, the accuracy of the method is considered satisfactory.

A key question to consider is how sensitive the results of the method are to the specific gravity being selected. The decision to use a fluid with G_s equal to 2.35 was based on the specific gravities of ground pumice material listed in Table 1. It is now understood that there can be small crystals of volcanic glass/quartz attached to particles of pumice. If the pure pumice material were to have a specific gravity of approximately 2.30, and the glass/quartz a specific gravity of 2.65, then once a particle has more than about 15 % quartz/glass (by mass) and is ground up, it would be expected to have a specific gravity more than 2.35, and would be classified as non-pumiceous. This is over-simplified in the sense that the presence of voids within the particle will have an important effect - if the voids of a particle do not get completely filled with LST, then they will act to reduce the specific gravity of the particle, such that the quartz/glass would need to be a major proportion of the combined particle before it made the particle sink in the LST. It is also the case that in a "typical" pumice particle, the phenocrysts would be expected to take up a small percentage of the overall volume, such that pumice particles would still have a specific gravity less than 2.35. If the pumice particles get crushed, then it is expected that many of the phenocrysts would also be released, such that they form their own particles, and hence would not be considered pumiceous.

To partially investigate the sensitivity of the separation with the milled pumice to the specific gravity of the fluid, the sinking portion of the soil mixture from KM01 was subjected to additional separations, with the specific gravity being gradually increased each time. These tests (KM01-S1 to KM01-S3 in Table 3) were performed in the same way as before, with the sinking portion being re-used in the next experiment after being dried. From these experiments, it can be seen that as the specific gravity is increased, there is a small amount of additional material which floated, while the majority continued to sink. At G_s = 2.40, only an additional 15 % of the material which sank at a G_s of 2.35 became floating. This implies that G_s = 2.35 is a reasonable choice for this method.

SEPARATION OF NATURAL MATERIALS

In the previous section, artificial mixtures of commercially available "milled" pumice and natural soil from Christchurch (non-pumiceous) were separated using the LST solution. To check the performance of the method for more realistic soil mixtures, an additional set of separations were undertaken using the HAMTR1 and WH1 soil samples. The results of these separations are shown in Table 4, and included three independent tests on the HAMTR1 material. As shown, the tests on the HAMTR1 material show agreement within 2 % for the three samples, highlighting the good repeatability of this method.

After performing the separations, a series of SEM photographs were taken on the floating and sinking portions respectively, with representative photographs shown in Figure 12 and Figure 13. Image comparisons

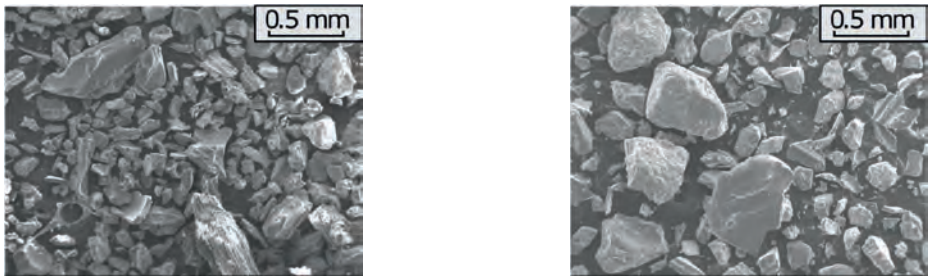

a) Floating particles b) Sinking particles

FIGURE 12: SEM photographs showing separated components of natural sample from Hamilton site, HAMTR1.

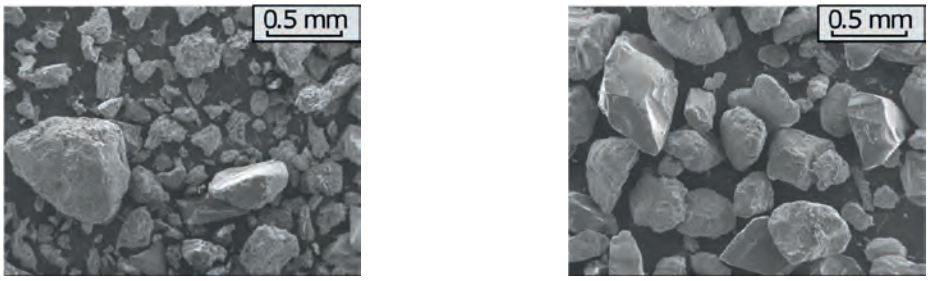

a) Floating particles b) Sinking particles

FIGURE 13: SEM photographs showing separated components of natural sample from Whakatane site, WH1.

must always be qualitative, however it is clear that there are marked differences in the appearances of the grains in the floating and sinking images. In the case of the floating particles, it is observed that there are a number which show the highly vesicular nature previously shown in Figure 5. There are also particles which don't display the obvious vesicularity, but appear highly curved and plate-like, with many appearing to have features which make the particules appear like the fragments of a broken cellular structure. These particles match the "bubblewall shards" description of Fisher & Schminke (1984). On the other hand, the sinking particles appear to have surface texture similar to the New Brighton sand (i.e. Figure 11) or to be smooth and lacking the vesicularity displayed by the floating particles. Similar to the artificial mixtures, there appear to be a small number of particles which might be thought of as being pumiceous but sinking, or non-pumiceous and floating. However, the number of these particles is generally small. The photos therefore appear to show that the separation technique has successfully separated the lightweight pumiceous grains from the main soil sample.

Having successfully separated the pumice material from the soil mixture, it is possible to consider the particle size distributions of the pumiceous and non-pumiceous components, as well as their relative proportions. This however raises an interesting point that should be considered by engineers and researchers alike. Namely, that it is generally assumed that the particle size distributions by mass are equivalent to size distributions by volume. If however, there are significant differences in the specific gravities of the constituent particles, then this equivalence is lost. This is particularly the case for pumice-rich deposits, and it may be necessary to consider whether proportions by mass are the best basis for comparison.

It is important to recall that in the separation of artificial soil mixtures, it was estimated that after 4 hours, only particles greater than 27 μm would be expected to have separated in the cylinder. On the basis of the increasing particle strength with reducing diameter, and the desire to preserve the purity of the LST solution, it was recommended that the materials be wet-sieved or filtered prior to performing the separation. For materials wet-sieved to either 63 μm or 75 μm, it is recommended that the separation time be at least 2 hours. For materials filtered to approximately 30 μm, the separation time should be at least 4 hours, and materials filtered to 11 μm should have a separation time of 24 hours.

When presenting the results, it is essential that users state the diameter of the sieve or filter used in the initial steps, hence the parameter *P* should be followed by the sieve or filter size in microns (i.e. results on materials filtered to 11 μm would be represented by P_{11}.) Note that for unfiltered materials, the final filtration will be an implicit filter, hence for these tests where the material was not pre-filtered, the appropriate parameter is P_{11} due to the washing of the material over an 11 μm filter paper. Given the prevalence of "fines" in geotechnical engineering practice, it is recommended that the parameter P_{75} be stated for all tests. Users retaining smaller particles than 75 μm and calculate P_{75} by sieving the dried components to determine the percentage of pumice which would have been obtained if wet sieving had been performed with a

75 µm sieve. In the cases of the natural materials tested here, the fines contents of the WH1 sample was 0.8 % and 0.6 %, while the HAMTR1 sample had fine contents of 4.2 % and 4.5 % for the pumiceous and non-pumiceous components respectively. The similarity in the fines contents for the pumiceous/non-pumiceous materials meant that there is no difference between the values of P_{11} and P_{75} in these cases.

It should be noted that over time it is possible for small amounts of fine grained material (i.e. those which weren't fully removed in the wet-sieving or initial filtration stages) to accumulate in the "cleaned" LST. As part of the procedure, the specific gravity of the LST solution is adjusted before separation, such that the separation itself is not affected by these fine particles. However, these very fine grained particles may then be retained in a future soil sample, such that they might begin introduce an error into future analyses. These fine grained particles can be removed by centrifugation followed by careful decanting of the clean liquid. During this process, pumice particles could potentially float, so it is recommended that centrifugation is performed after diluting the LST solution to a specific gravity of a maximum 2.0 so that all particles will sink. The purified LST can then be placed in an oven to increase the specific gravity as required.

The soils tested in this paper were typically dominated by sand and fine gravel sized particles, hence a representative sample can be obtained with relatively small amounts of material (i.e. 50 g for natural soils) due to the binary result of the test. The separation technique described in this paper will work for mixtures containing coarser gravels, however the sample size will need to be increased to ensure a representative value is obtained. If larger samples sizes are being used, then the physical size of the separating device will need to be increased.

Finally, the method has only been tested on New Zealand soils, in a relatively limited number of locations, hence when using this method in a new area, researchers should pay attention to whether there are unexpected components (i.e. mis-classification of the grains) in either the floating or sinking portions of the mixture. Prior to using this technique for the first time in a new area, it is recommended that users measure the specific gravity on a small sample of hand-separated, crushed pumiceous grains. If the specific gravity of the crushed pumiceous grains is larger than 2.3, then the specific gravity of the LST solution in the analysis should be raised.

CONCLUSIONS

In this paper, a gravity separation technique using aqueous solutions of LST has been proposed for the quantitative determination of pumice content by mass in the sand and gravel fraction of soil mixtures. A high-level summary of the method is shown in Figure 14.

The method has been developed for mixtures containing predominantly sand to fine gravel sized particles, but can also be applied to soils containing coarser gravel components. A sample size of 50 g is recommended for sand-fine gravel mixtures, and a repeatability of 3 1 % was obtained for a natural mixture using this sample mass.

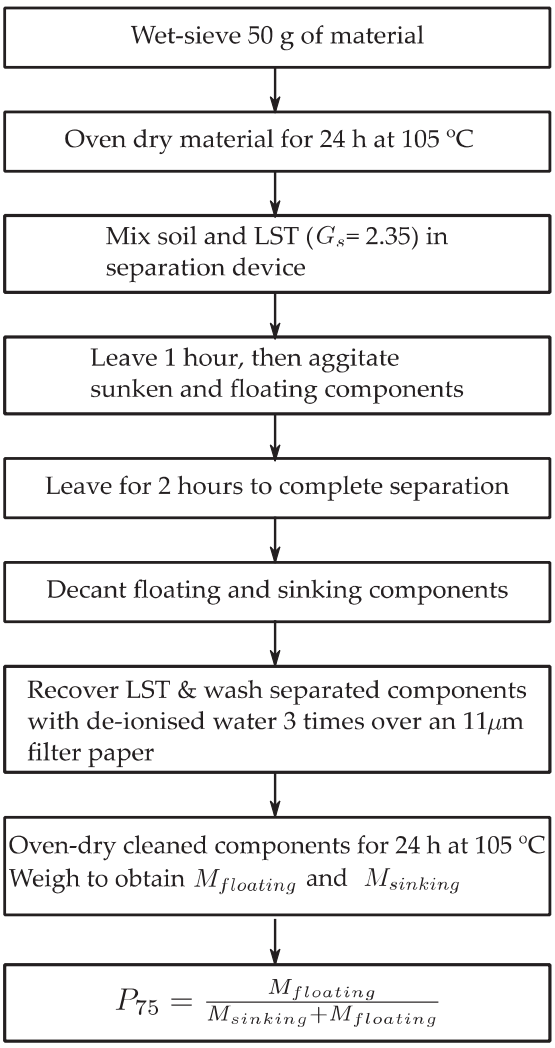

FIGURE 14: High-level summary of proposed method for determining pumice content by mass.

In the development of the method, it was found that the specific gravity of ground pumice samples taken from a number of locations across New Zealand was typically less than 2.35, though the presence of volcanic quartz/glass within the pumice grains could act to increase the apparent specific gravity. A specific gravity of 2.35 was therefore adopted in this paper, though when the technique is being applied in a new region or to previously untested deposits users may need to adjust the specific gravity to suit local conditions.

The method requires that the samples separate over a period of time, and it is recommended that the final separation take place over a minimum of 2 hours for materials washed across a 63 µm or 75 µm sieve. Materials which have been filtered to include particles up to 30 µm should be allowed to separate for at least 4 hours, and materials filtered to 11 µm should separate for 24 hours. In sieving or filtering the material, the method explicitly only estimates the percentage of pumice in the

part of the distribution coarser than the finest particles and the *P* parameter should include the minimum particle size as a subscript. The direct or back-calculated P_{75} parameter should be reported for all tests. For the natural materials tested in this paper, there was no difference between the P_{11} and P_{75} values.

The technique has been applied to a series of known mixtures of commercially available "milled" pumiceous material and non-pumiceous beach sand. After correcting for the presence of the volcanic (quartz) crystals, it was found that the method was able to separate pumiceous material from mixtures of fine sands with an apparent accuracy of around 3 %.

The presence of phenocrysts (volcanic quartz) within grains of pumice can increase the specific gravity of the pumice grain, and pumice grains which contain a significant proportion of quartz will not be included within the "pumice" fraction of the soil using the proposed technique. In the artificially milled pumice particles tested, the uniform fine sand particle size accentuated this error and increasing the specific gravity of the LST solution towards 2.65 caused an increasing proportion of these grains to float. SEM photographs of the natural soils collected by the author to date suggest that this is not a major source of error for unprocessed materials.

Confidence in the method has been gained through the examination of SEM photographs of the sinking and floating components of artificial and natural soil mixtures. The photographs showed that the majority of floating particles contain features associated with pumice soil grains (i.e. presence of voids/or ridge features which suggest that the grain previously formed part of a larger pumiceous particle), while photos of the sinking grains tended to be dominated by particles without obvious internal pores or ridge structures, suggesting successful separation of the pumiceous component.

It is expected that this method will be used by practicing engineers as part of routine site characterisation in pumiceous deposits, where existing in-situ characterisation techniques (such as the CPT) may require different interpretation depending on the pumice content.

ACKNOWLEDGEMENTS

The author would like to acknowledge the technical staff at the University of Canterbury, and in particular Rob McGregor for fabricating the separating cylinder, and Chris Grimshaw for discussions and demonstration regarding the use of heavy liquids in geology. Additionally, the author would like to thank Prof. Cubrinovski, Assoc. Prof. Orense and the reviewers of this paper for their helpful suggestions and advice.

This project was partially supported by QuakeCoRE, a New Zealand Tertiary Education Commission-funded Centre. This is QuakeCoRE publication number 0333. Additional support was provided by the University of Canterbury.

REFERENCES

Asadi, M., Orense, R.P., Asadi, M., Pender, M.J., 2019. Maximum dry density test to quantify pumice content in natural soils. *Soils & Foundations*. 59 (2), 532–543.

Ashby, M.F., 1983. Mechanical properties of cellular solids. *Metallurgical Transactions A*. 14A (9), 1755–1769.

ASTM, 2014. Standard test methods for specific gravity of soil solids by water pycnometer. D854-14. West Conshohocken, PA.

Fisher, R., Schminke, H., 1984. *Pyroclastic Rocks*. Springer-Verlag, Berlin Heideberg, Germany.

Gregory, M.R., Johnston, K.A., 1987. A nontoxic substitute for hazardous heavy liquids - aqueous sodium polytungstate (3Na2WO4.9-WO3.H2O) Solution. *NZ Journal of Geology and Geophysics.* 30 (3), 317–320.

Hardin, B.O., 1985. Crushing of soil particles. *Journal of Geotechnical Engineering.* ASCE. 111(10), 1177–1192.

Hume, T.M., Sherwood, A.M., Nelson, C.S., 1975. Alluvial sedimentology of the upper pleistocene Hinuera formation, Hamilton basin, New Zealand. *Journal of the Royal Society of New Zealand.* 5 (4), 421–462.

Hyodo, M., Hyde, A.F.L., Aramaki, N., 1998. Liquefaction of crushable soils. *Géotechnique.* 48 (4), 527–543.

Ishikawa, T., Tokoro, T., Miura, S., 2016. Influence of freeze–thaw action on hydraulic behavior of unsaturated volcanic coarse-grained soils. *Soils & Foundations.* 56 (5), 790-804.

Knudsen, F.P., 1959. Dependence of mechanical strength of brittle polycrystalline specimens on porosity and grain size. *Journal of the American Ceramic Society.* 42 (8), 376–387.

Leipe, C., Kobe, F., Müller, S., 2018. Testing the performance of sodium polytungstate and lithium heteropolytungstate as non-toxic dense media for pollen extraction from lake and peat sediment samples. *Quaternary International.* 516, 207-214

Manville, V., 2002. Sedimentary and geomorphic responses to ignimbrite emplacement: Readjustment of the Waikato River after the AD 181 TaupōEruption, New Zealand. *Journal of Geology.* 110 (5), 519-541.

Matsumura, S., Miura, S., Yokohama, S., Kawamura, S., 2015. Cyclic deformation-strength evaluation of compacted volcanic soil subjected to freeze-thaw sequence. *Soils & Foundations.* 55 (1), 86–98.

Miura, S., Yagi, K., Asonuma, T., 2003. Deformation-strength evaluation of crushable volcanic soils by laboratory and in-situ testing. *Soils & Foundations.* 43 (4), 47–57.

Munsterman, D., Kerstholt, S., 1996. Sodium polytungstate, a new non-toxic alternative to bromoform in heavy liquid separation. Review of *Paleobotany and Palynology.* 91 (1–4), 417–422

Orense, R.P., Pender, M.J., 2016. From micro to macro: An investigation of the geomechanical behaviour of pumice sand. *Volcanic Rocks and Soils.* 45–62.

Orense, R.P., Pender, M.J., Hyodo, M., Nakata, Y., 2013. Micro- mechanical properties of crushable pumice sands. *Géotechnique Letters.* 3, 67–71.

Rogers, J., Sanderson, F., 1954. The separation of pumice from sand. *New Zealand Engineering.* 9 (4), 106–109.

Senetakis, K., Anastasiadis, A., Pitilakis, K., 2013. Normalized shear modulus reduction and damping ratio curves of quartz sand and rhyolitic crushed rock. *Soils and Foundations.* 53 (6), 879–893.

Senetakis, K., Madhusudhan, B.N., Anastasiadis, A., 2016. Wave propagation attenuation and threshold strains of fully saturated soils with intraparticle voids. *Journal of Materials in Civil Engineering.* 28 (2).

Wesley, L.D., 2001. Determination of specific gravity and void ratio of pumice materials. G*eotechnical Testing Journal.* 24 (4), 418–422.

Wesley, L.D., Meyer, V., Prantoto, S., Pender, M.J., Larkin, T.J., Duske, G., 1999. Engineering properties of a pumice sand. In: Vitharana, N., Colman, R. (Eds.). 8*th ANZ Conference on Geomechanics.* Vol 2. Australian Geomechanics Society, Hobart, Australia, pp. 901-907.

Whitam, A., Sparks, R., 1986. Pumice. *Bulletin of Vulcanology.* 48, 209-223.

GEOLOGY AND THE CLYDE DAM

Simon Nathan (s.nathan@xtra.co.nz)

This article was previously published in the Geoscience Society of New Zealand Journal of the Historical Studies Group 68, January 2021

Simon Nathan

Simon Nathan worked for 30 years for the NZ Geological Survey/GNS on a variety of projects, mainly on the West Coast of the South Island. In 2003 he became science editor of Te Ara, the online Encyclopedia of New Zealand, and has subsequently written on aspects of New Zealand's scientific history. In this article he recalls the geological issues involved with construction of the Clyde Dam.

The Clyde Dam on the Clutha River (Fig. 1), which started generating power in 1993, was the last major hydro-electric scheme to be completed in New Zealand. It was a controversial project, with widespread opposition from local residents and environmentalists. Geological advice and assistance before and during construction was provided by members of the New Zealand Geological Survey (later DSIR Geology & Geophysics, then the Institute of Geological & Nuclear Sciences, now GNS Science). As well as the normal engineering geological issues that arise in a project of this size, there were delays because of the fractured nature of the rock at the dam site, the discovery of active faults, and the drainage and remediation of landslides in the reservoir area.

During the 20-year life of the project, from about 1974-1993, there were major conceptual changes in a number of geoscience areas intertwined with political decisions. This article has been prepared as a summary of the geological issues that arose during investigation and construction of the Clyde Dam, based on written records and interviews. It is an interesting case study with lessons that I hope may be useful in considering future projects involving large-scale landscape modification.

ENGINEERING AND POLITICAL BACKGROUND

After World War 2 there was a nationwide shortage of electricity – for example, residents of Otago had to endure regular power cuts until the Roxburgh dam began to generate power in 1956. The government started an urgent programme of hydro-electric development with a series of dams planned along the Waikato River in the North Island, and a similar programme in the South Island along the upper reaches of the Waitaki River. A skilled workforce was developed, and when one dam was completed they would move on to the next project. The growing demand for electricity overrode environmental concerns. But by the late 1960s there was a change in public opinion when the Manapouri power scheme was being developed to provide electricity for the Tiwai aluminium smelter near Bluff, which would have raised the level of Lake Manapouri. After widespread protests, led by the 'Save Manapouri' campaign, the Kirk Labour government agreed in 1973 that the lake level would not be changed.

FIGURE 1. View of the Clyde dam, looking upstream along Lake Dunstan. Photo: Scott Barnard (AECOM, Christchurch)

As the hydro-electric schemes in the Waitaki catchment were completed, it was planned to build a series of dams along the Clutha River that would include a dam in the Cromwell gorge near Clyde. Preliminary investigations included ground surveys and a number of drillholes (McKellar 1967). A number of options were considered, and in 1975 the Labour government opted for scheme H, a low dam that would minimise the size of the reservoir, with a second low dam further upstream.. After an election later that year, the incoming Muldoon National government decided to proceed with scheme F, a much higher dam that would generate more power but flood established orchards, the railway and road as well as parts of Cromwell. Protests were ignored, and the high dam became part of the government's 'Think Big' policy, with the aim of using surplus power for a second aluminium smelter.

Design and construction of the Clyde Dam was the responsibility of the Ministry of Works and Development (MWD, later Works Consultancy Services Ltd). As had happened in the past, members of New Zealand Geological Survey provided consultancy advice on geological matters and were actively involved in on-site investigations under the supervision of Chief Engineering Geologist Les Oborn, then by Graham Hancox after Les retired. Royden Thomson (Fig 2), an experienced engineering geologist who had previously worked on the Manapouri project was appointed site geologist, and moved to Cromwell in 1974. Initially he was told that the project would last two or three years, but it

FIGURE 2. Site geologist Royden Thomsen examining rock exposed in a drainage tunnel at the No 5 Creek slide in August 1989. Dominion Post collection, Alexander Turnbull Library

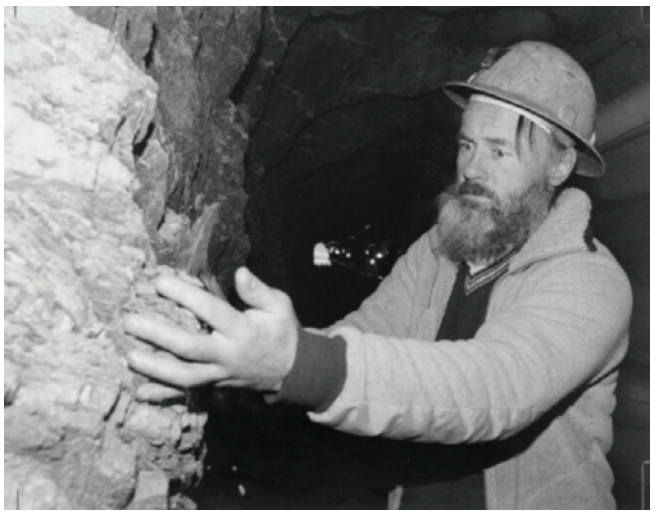

was almost 20 years until he could hand over the dam completion report (Thomson 1993). At different times he was assisted by other site geologists including Jim McLean, Mark Foley, Graham Salt and many visiting geoscientists.

DAMSITE INVESTIGATIONS

The geology of central Otago was reasonably well known in the early 1970s as it had been covered by regional 1:250,000 geological mapping only a decade earlier. Ian Turnbull had started more detailed mapping of the Cromwell area which covered the area around the damsite, and provided copies of his field maps as investigations. got underway. The dam site (DG3) was in hard Otago schist at the lower end of the Cromwell gorge, and it was assumed that construction would be straightforward. Some landslides had been identified in the reservoir area (including the Clyde landslide at the dam site), but were not anticipated to cause major problems.

The schist at the dam site was foliated (or layered), and had undergone several phases of deformation. As a consequence there were common shear zones, both parallel to and oblique to foliation, some of which contained layers of low-strength clayey gouge. The foliation itself was almost horizontal or gently dipping. Angled drilling showed the presence a narrow zone of crushed rock at right angles to axis of the dam which subsequently became known as the River Channel Fault. Other smaller faults and joints were mapped by the site geologists as excavation proceeded. Although the rock appeared hard in handspecimen and drill core, once excavated it was more broken and permeable than anticipated.

As a consequence of the defects in the rock, many excavations on varying scales were required in the dam foundations, especially in areas where adversely oriented foliation shears caused concern that part of the dam might slide. Crushed material was excavated out of the River Channel Fault, to be replaced by concrete. Widespread cement grouting was needed to fill voids and avoid leakage around the dam.

In 1982 a contract for construction of the dam was awarded to the Zublin-Williamson consortium. The original contract provided for excavation of 14,000 cubic metres of rock to provide a solid foundation. But eventually the contractors had to dig out almost twenty times that amount of weak rock. The specified concrete pour was 650,000 cubic metres, but the amount poured was 870,000 cubic metres, a third more than specified (Ministerial Review Committee 1990, p 41). One of the final events of the dam construction phase was a long and complicated arbitration case where the contractor claimed for additional costs. Royden Thomson provided expert evidence and underwent lengthy cross examination.

CHANGING IDEAS ABOUT FAULTING

From earlier geological mapping, it was realised that the Dunstan Fault separated Otago schist from younger sediments in the Manuherikia depression to the north of the damsite, but the faulting was believed to be ancient. In the early 1960s it was generally believed in the geological community that central Otago was seismically inactive – the 1:250,000 maps of the 1960s did not show a single active fault between the Alpine Fault in the west and the Akatore Fault near Dunedin (which was regarded as an oddity).

Work started on the DG3 site in 1976. From study of aerial photographs Royden Thomson was intrigued by a faint linear feature on a late Quaternary surface north of the dam site close to the Dunstan Fault. He and Ian Turnbull were able to get a trench excavated across the feature which revealed that sediments beneath the surface had been offset by fault movement (Fig 3). It was the first indication of young fault activity in central Otago, with the implication that the region might not be as seismically inactive as previously thought. This was the start of intensive seismotectonic studies of the area around the dam site and further afield in the upper Clutha catchment. The evidence for young faulting was not easy to detect, but was assisted by extensive low-level aerial photography by Lloyd Homer. Royden Thomson, Ian Turnbull and a group of earthquake geologists investigated possible faults, with trenching of selected sites, and this work was integrated with geological mapping. This showed that there were several active traces along the Dunstan Fault (Fig 4), although all were several kilometres north of the dam site. Despite the huge increase in knowledge of active faulting in the region over the next five years, this was not satisfactorily communicated to the dam design engineers.

In early 1982 the site was visited by Don Deere, an US engineering geologist with experience in dam construction who was engaged by MWD to advise on grouting the dam foundations. As well as reviewing the excavated dam site, he raised concerns about the possibility of a future earthquake on the Dunstan Fault that might activate the River Channel Fault. MWD requested an immediate synthesis of the work on active faulting and seismotectonic hazard so that they could evaluate the potential effects on the proposed dam..

The revelation that seismic activity was a possibility coincided with a political crisis. There was a public hearing into the final stages of the water-right hearing for the high dam, and the government was forced to pass amending legislation to allow the project to proceed. There was intense public interest in the issue of future seismic activity, and the Director of the Geological Survey, Pat Suggate, decided that the report sent to MWD must also be publicly released. Realising that he would have to defend the conclusions, he took an active role in the final preparation of the report (Officers of the NZ Geological Survey, 1983). One of the main conclusions was that the Maximum Credible Earthquake likely on the Dunstan Fault was between 7.0 and 7.5, with a return period of 12,500 years. The

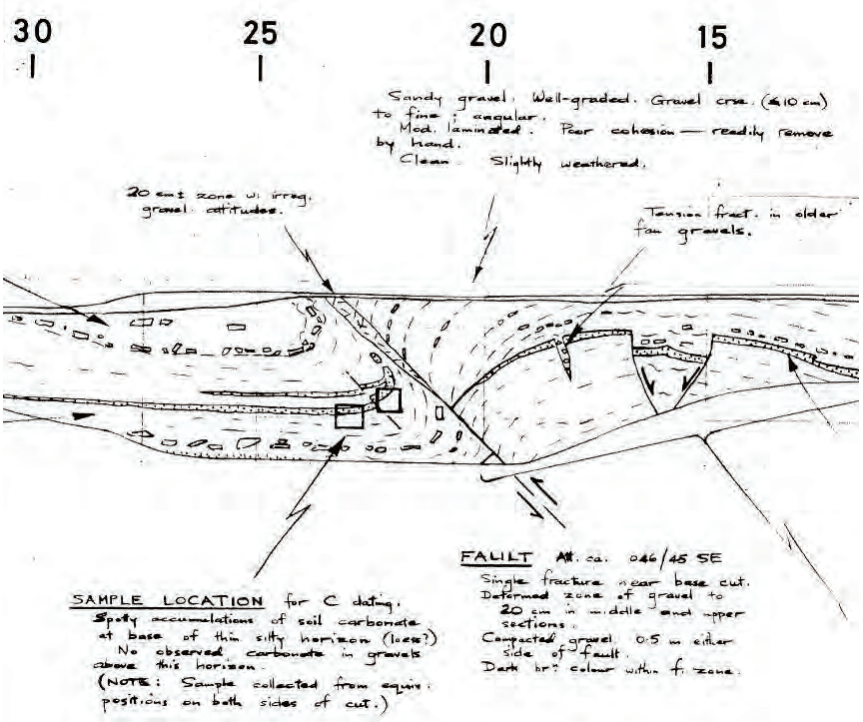

FIGURE 3. Log of first trench excavated across a suspected fault scarp at Waikerikeri valley in August 1977. Provided by Royden Thomson.

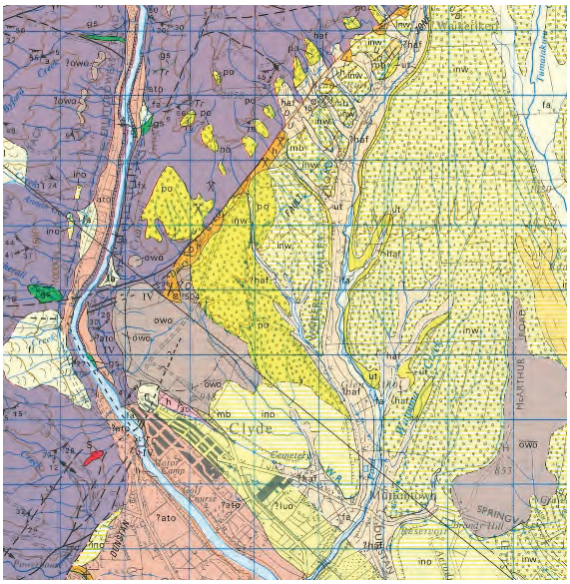

FIGURE 4. Section of the 1:63,360 geological map covering the area around the Clyde Dam (Turnbull 1987). This map shows the active fault traces identified during investigations in orange-brown.

probability of this occurring in the next 100 years was estimated to be low to very low, but if it did happen there might be some sympathetic movement on the River Channel Fault.

Because of widespread interest and concern within the geoscience community, the report was reviewed by a subcommittee set up by the Geological Society of New Zealand. (R.J. Norris, C.A. Landis and D.H. Bell). While generally supporting the NZGS report, they felt that the estimated return period of surface displacement was too low. Their report and a response from NZGS were published in *GSNZ Newsletter 63* (February 1984), pp 14-18.

As a consequence of the information on the seismotectonic hazard, the dam design was modified, including a slip joint to incorporate 1-2 metres of movement on the River Channel Fault. The redesign led to a decrease in generating capacity of the dam from 612 to 464 megawatts (Hatton, Foster & Thomson 1991).

Following the general election in 1984 a Labour government was elected. Although they had opposed the concept of the high dam, construction was too advanced by that time to abandon construction without huge financial penalty, so work continued.

In 1987, as part of major government reorganisation, the ownership of the electricity generation capability, previously controlled by the NZ Electricity Department, was transferred to the Electricity Corporation of New Zealand (ECNZ), a state-owned enterprise. This was to

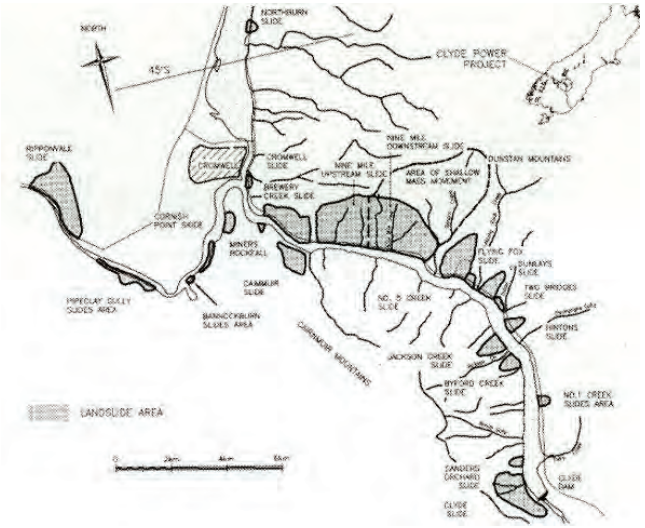

FIGURE 5. Map showing the main landslide areas surrounding the Cromwell gorge (now Lake Dunstan), from Macfarlane and Silvester (2019).

have a major impact on the final stages of the Clyde Dam project. By late 1988 the construction of the dam was nearly complete, and plans were underway to start filling the reservoir.

LANDSLIDE PROBLEMS

The presence of landslides in the Cromwell gorge had long been known and shown on geological maps (Turnbull 1987), but were not believed to pose major problems as they were thought to be ancient and inactive (Fig 5). Objectors to the Clyde Dam, however, pointed to the Vajont Dam in Italy where a landslide in the reservoir in 1963 caused a seiche that overtopped the dam, causing almost 2000 deaths downstream.

Until the early 1980s it was believed that only the Clyde, Cromwell and Cairnmuir slides were of concern, and would need remedial action. All the known landslides were monitored during the construction phase, and it was discovered that some 'dormant' slides in the Cromwell gorge were slowly moving downhill. Exploratory drilling for the new highway led to the discovery of a complex, high-pressure groundwater system near the base of the No 5 Creek slide, and this led on to an extensive drilling programme on other landslides. By 1989, when filling of the reservoir was due to start, an external review recommended further investigation and remediation of the landslides.

A strategy was developed for a fast-track stabilisation program, based primarily on the use of tunnels for both investigation and drainage. All known landslides were re-mapped in detail, combined with drilling and tunnelling (Gillon & Hancox 1981). Up to 40 geologists worked on the landslides over a two-year period (Fig 6) – it was the largest engineering geological investigation ever undertaken in New Zealand. Gravity drainage was the main method of remediation combined with grouting, buttressing, some pumped drainage and continuous monitoring.

The filling of Lake Dunstan behind the dam commenced in 1992 when the four diversion sluices were closed. The reservoir reached its maximum operating level in September 1993 after a series of intermediate steps to check the continuing stability of the landslides.

Monitoring and visual observations over the last 27 years indicate that the landslides are behaving as predicted – they have been classified as either dormant (<2 mm/year) or creeping (2-5 mm/yr) (Macfarlane and Silvester (2019).

GEOLOGICAL LESSONS FROM THE CLYDE DAM

Construction of the Clyde Dam took much longer than anticipated, with a final cost more than 45% above the original estimate. It was a controversial project from the start, with continuous public scrutiny and criticism through the whole construction period. I had a personal taste of this in 1989 when, as Acting Director of the Geological Survey, I had to take part in a press conference explaining that filling of the dam would be delayed for several years due to the need to investigate and remediate landslides in the reservoir area. I was worried that geologists would be blamed, but on the day the reporters were only interested in questioning ECNZ about financial management of the project.

In 1990 the government called for review of the whole Clyde Dam project, and particularly for the reasons for the cost blowout and delays, and I refer readers to this for a frank appraisal of the decision making process (Ministerial Review 1990). But to conclude this short review, I would comment on several geological/geotechnical issues.

One of the major conclusions of the review was that there was a lack of a proper investigation process prior to the start of construction. The DG3 site was selected essentially for political reasons, and had less investigation than other sites preferred by engineers. Only 2.8% of the expenditure by DSIR geoscientific team occurred prior to the final commitment of the project. While the need for a higher level of investigation is unarguable, it is important to realise that some of the issues that arose could not have been reasonably foreseen. For example, while it is tempting to suggest that more investigation would have revealed the presence of active fault traces along the Dunstan Fault and elsewhere, it has to be remembered that there was a widespread belief within the geological community that there were no active faults in central Otago. The first fault traces were not identified by the specialists in the Geological Survey who studied active faults nor by university colleagues, but by site geologist Royden Thomson scanning aerial photographs outside the immediate damsite area. Subsequent work identified more active fault traces in different parts of central Otago.

FIGURE 6. Group of engineering geologists working on landslides in the Cromwell Gorge during the summer of 1991-92. [This probably represents less than half the geologists who worked on the Clyde dam project]. Photographer: Gary Randall, MWD.

Back Row: Richard Justice, Richard DeLuca, David Stewart, Jeff Bryant, Royden Thomson, David Barrell, Graeme Halliday, Peter Brooks, Bruce Riddolls, Dean Fergusson, Virginia Cunningham.

Front: Tim Coote, Glen Coates, Neil Crampton, Guy Grocott, Dick Beetham, Don Macfarlane, Gary Smith, Peter Wood, Mark McKenzie, Charlie Watts.

[Others who worked on the project include Paul Horrey, Linda Price, Kelvin Moody, Mark Stirling, Gabrielle Bell, Bill Leask, Peter Manning, Stuart Read, Elizabeth Sowerbutts, Mary-Clare Delahunty, Mark Foley, Graham Salt, Angela Smith, David Ker, Graham Hancox, Ian Brown – with apologies to anyone omitted from the list].

The discovery of active faults in 1976 led to concentrated investigations over the next five years that included trenching and C14 dating that allowed the history of past fault movements to be worked out, developing a methodology for fault investigation that is still being used today. Strangely, however, this work appears to have had virtually no impact on the design of the dam because of lack of communication between geologists and engineers until visiting US geologist Don Deere raised concerns in 1982.

The Clyde dam site was excavated in the foliated schist that is widespread in Otago. It was assumed that excavation would be straightforward, but in fact there turned out to be widespread shear zones both parallel and oblique to foliation as well as faults and open joints. The combination of these defects in the rock mass meant that the amount of excavation and concrete remediation was much larger than anticipated. While this was difficult to anticipate in advance, it is a lesson for future excavations in schist.

Initially it was assumed that the landslides upstream from the dam site were inactive, but continued monitoring during the life of the project showed that some were creeping downhill very slowly, and investigations along the road line showed locally elevated water pressures. There was a debate about the amount of drainage and remediation needed to stabilise the landslides, but ECNZ elected to take a conservative approach, with continuing monitoring since the dam was filled in 1993.

The above paragraphs are illustrations of the sort of geological problems that arise in a major civil engineering project of this size and complexity. Although more preliminary investigation may have allowed some of them to be minimised, it is realistic to expect that there will always be unanticipated problems in dealing with complex geology.

The concentrated work on landslides involved large groups of engineering geologists, all of whom gained experience on the project. As they dispersed around New Zealand, many have become leaders in the geotechnical profession. There were several important advances as part of the landslide work, including the development of GIS technology for geotechnical work, the project-wide use of 3D modelling, and the development of a computer-based monitoring system, still used 30 years later for all major New Zealand dams.

Bearing in mind the controversy over the construction of the Clyde Dam, it is interesting to realise that it is now accepted as part of the natural environment in central Otago. I recently saw a sign advertising “Lake Dunstan – the jewel of the Clutha”, and power companies are proud to advertise that their electricity is 100% renewable.

REFERENCES

Gillon MD, Hancox GT 1992. Cromwell landslides – a general overview. Proceedings Sixth International Symposium on landslides. Ballema, Rotterdam: 83-102.

Hatton JW, Foster PF, Thomson R 1991. The influence of foundation conditions on the design of the Clyde Dam. Commission International Des Grands Barrages, XVI Congress, Vienna, 157-77.

Macfarlane D, Silvester P 2019. Performance and management of Cromwell Gorge landslides, Clyde Dam reservoir. ANCOLD 2019 Conference, 9-12 October, Auckland, 1-9.

McKellar IC 1967. Clutha River Power Development. Geological report on Clyde damsites DG3/1 and DG3/2. *NZ Geological Survey Engineering Geological Report 196.*

Ministerial review committee report to Cabinet (1990). Clyde Dam Project decision making.

Officers of the New Zealand Geological Survey 1983. Seismotectonic evaluation of the Clyde dam site (2 volumes). *NZ Geological Survey Engineering Geological report EG375.*

Thomson R 1993. Clyde Dam engineering geological completion report (2 volumes). *Institute of Geological & Nuclear Sciences contract report C-1992/18.*

Turnbull IM 1987. Sheet S133 – Cromwell. Geological Map of New Zealand 1:63360, map (1 sheet) + notes. Wellington, Department of Scientific & Industrial Research.

ACKNOWLEDGEMENTS

In preparing this article, I have consulted many colleagues who worked on different aspects of the Clyde Dam project. In particular I am pleased to thank Kelvin Berryman, Ian Brown, Graeme Hancox, Don Macfarlane, Royden Thomson and Ian Turnbull for reading draft versions and providing useful comment. I am also very grateful to Kristin Garbett (GNS Science) for her help locating reports and other documents.

Royden Thomson worked as site geologist based at Cromwell through the 20-year life of the project. Many of those interviewed commented on Royden's thorough work, wide knowledge and wise counsel – one person described him as "a quiet voice of sanity when problems arose". This paper is dedicated to him.

Earthquake Hydrology and Liquefaction

Sometimes research, like wine and other good things, matures over time

Simon Cox

Simon Cox

Dr Simon Cox is a Principal Scientist at GNS Science in Dunedin. His early career was dominated by interest in tectonics, the Southern Alps, Antarctica and mineral exploration. During the past decade he has focussed on geological hazards - characterising landslides, the Alpine Fault, earthquake hydrology and shallow groundwater systems. He is an avid skier, mountain biker and climber, and still plays a bit of 'old man' football.

AS THEY FLEW along the newly formed Greendale Fault in September 2010, there were many things that Dr Simon Cox and his GNS Science colleagues could see were clearly awry during the first aerial reconnaissance. But among the offset roads, bent hedgerows and fences, torn and cracked fields, and damaged houses, there was one curiosity that specifically caught Simon's attention. Many of the wells now had groundwater flowing out of them where normally it would have been at least 40 metres underground. Having worked on the formation of quartz veins and exploration of gold deposits, which are developed by earthquakes deep in the earth's crust, here was a real-life example of processes he had studied for his PhD and worked on for years, but never actually observed as they happen deep in the earth's crust. Not only that, but he was seeing it in full realisation there would be many recordings of what had happened in monitoring bores all over the Canterbury plains. While there was much to do initially for earthquake recovery, this was a serendipitous opportunity for new science that rarely comes along.

The weird things that seemed to happen to groundwater during the earthquakes also caught the attention of Dr Helen Rutter from Aqualinc, as well as many people from Environment Canterbury and regional councils throughout New Zealand. Emails quickly brought collaborators together and observations gathered. One of the first things that seemed apparent was the earthquakes generated a rapid increase in groundwater pressures immediately during the shaking, followed by a drop in the deeper aquifer levels and rise in shallow aquifers immediately after the earthquake. In many places there had been an upwards flow that coincided with emergence of new springs and a pulse of water flowing down the rivers. The effects were also far-reaching, affecting aquifers over 1000 km-away in Northland and throughout New Zealand. In a paper[1] in the New Zealand Journal of Geology and Geophysics, which subsequently won the New Zealand Geophysics Prize, Cox and his colleagues postulated that release of artesian groundwater pressure and groundwater flow also played pivotal roles in Christchurch liquefaction.

With support from the Royal Society Marsden fund and the Natural Hazards Research Platform, a portfolio of 'Earthquake Hydrology' research began to grow. Hydrologic responses in groundwater are a well-

'Haywire hydrology' as seen from an earthquake reconnaissance flight on 4 September 2010. Offset on the Greendale fault disturbed the flow of Hororata River. Photo: Richard Jongens/GNS Science.

An irrigation channel dammed and partially offset by the Greendale Fault. As as seen from an earthquake reconnaissance flight on 4 September 2010. Photo: Richard Jongens/GNS Science.

Liquefaction at Kirstens Place as a results of the Mw6.2 Christchurch earthquake, 22 February 2010. Photo: Alun Davies/simplicitywebdesign.co.nz.

documented phenomenon, observed for thousands of years, but of renewed interest due to implications for water supplies, engineering and hazards[2]. But although it appears permeability is best considered a dynamic variable that can change with stress and strain, exact causal mechanisms are yet to be perfectly understood[3,4]. The density of groundwater and seismic monitoring networks in New Zealand, combined with regular earthquake activity, was a unique opportunity for local research to contribute to internationally. Albeit dominated by observations in permeable young aquifers, events of the 2009 Fiordland, 2010-2011 Canterbury, 2013 Cook Strait and 2016 Kaikoura earthquakes have now been particularly well-documented[1,5-7], shown to produce changes to groundwater throughout New Zealand lasting locally for many years[8]. Other impactful New Zealand studies, all enabled through collaborations and support of regional councils and the GeoNet facility, include large 'multiple-earthquake at multiple-site' datasets of earthquake-responses that enable causative variables to be controlled and examined[9,10], and the first international attempt to derive probabilistic models of groundwater change given varied levels of shaking[11].

With aquifer leakage and compromised aquitards postulated to have somehow been involved in liquefaction[1,6,12], Sjoerd van Ballegooy and other engineers from Tonkin & Taylor became involved in the research. One of the first challenges for understanding liquefaction was to map out exactly what happened within, across and between the aquifers throughout the earthquake sequence. A collaboration contributed maps of the water table position to help inform the Christchurch rebuild[13]. Mapping pressure changes during the earthquakes, the team found groundwater in aquifers beneath Christchurch rose locally in pressure an equivalent of > 5 m in hydraulic head during the Mw6.3 earthquake. This added substantially to the +5-10 m 'above ground' pressures that were normally contained by the overlying impermeable aquitard layers. The spatial correlations also appeared very clear – much of the worst liquefaction and surface flooding coincided with the areas that experienced highest groundwater pressures. But 'correlation is not proof of causation' so initial reviews of the work were critical that spatial relationships could have been coincidental because the highest pressures were also where the greatest thickness

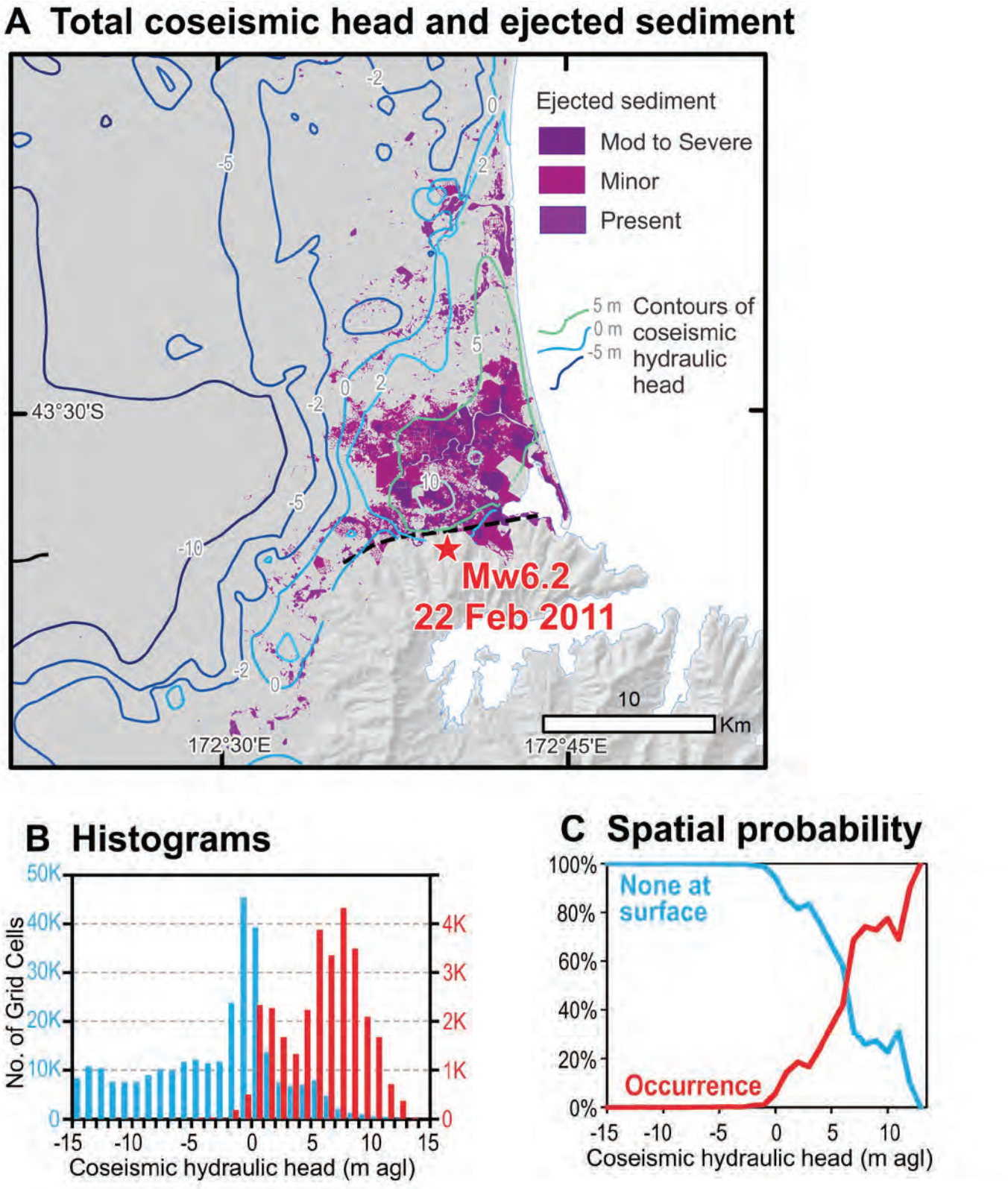

Graphic figure: (A) Map of the occurrence of liquefaction as ejected to the surface after the 22 Feb 2011 Mw6.2 earthquake, overlain with coloured contours of total coseismic hydraulic head in aquifers. (B) Histograms of the number of 50 x 50 m grid cells of ejected sediment occurrence (red, left scale) and not observed (blue, right scale) within 1 m intervals of aquifer hydraulic head. (C) Spatial probability distributions for ejected sediment 'occurrence' and 'not observed' derived from the relative proportion of classified grid cells within each 1 m groundwater level in the study area. Reproduction of Figure 4 from Cox et al. (2021).

of liquefaction-prone sandy-silt were found. The science was still premature, and a new approach was needed.

Enlisting further expertise of statistician David Harte, the team began unpicking the relationships between the geotechnical tests carried out by engineers on liquefaction vulnerability, actual observations of liquefaction during the earthquakes, and groundwater pressure changes that had occurred in aquifers about 20-40 m below each site. Where the first approach had been only at a regional-scale, relationships between liquefaction and groundwater, deliberately including areas of the Canterbury Plains to the west of Christchurch to span a wide range of aquifer pressures, it had potentially caused non-causative covariations in the data. The reanalysis looked only within the Christchurch urban area. When tests were grouped on the basis of liquefaction vulnerability and soil strength, irrespective of location, places where 'minor' and 'moderate-severe' liquefaction occurred during the 22 February Mw6.2 earthquake, had distinctly higher aquifer pressure than sites where liquefaction was not observed. Now with immediate relevance to engineering, a series of manuscripts were written and rewritten for the Journal of Engineering Geology.

'It was an incredibly frustrating and long road that was bad for morale at the time' says Simon Cox 'but ultimately a process that greatly strengthened the science. Although it took a decade from initial observations, developing the hypothesis then teasing all the details out, it now seems unequivocal leakage of artesian groundwater contributed to near-surface liquefaction-induced ground damage.'

The final paper[14] was published on the 10th anniversary of the Canterbury earthquake. It argues leakage and upwards flow from artesian aquifers promoted the ejection of liquefied sediment in Christchurch. It showed that hazard assessments need to consider hydrogeological setting and conditions, that Christchurch may have been one of the worst-case examples ever experienced, and there is a need to re-evaluate other examples of liquefaction worldwide. The paper can be downloaded for free from https://doi.org/10.1016/j.enggeo.2020.105982, while the associated data archive can be found at http://doi.org/10.5281/zenodo.4391461.

REFERENCES

1. Cox, S.C., Rutter, H.K., Sims, A., Manga, M., Weir, J.J., Ezzy, T., White, P.A., Horton, T.W., Scott, D., 2012. Hydrological effects of the Mw 7.1 Darfield (Canterbury) earthquake, 4 September 2010, New Zealand. New Zealand Journal of Geology and Geophysics 55(3), 231-247.
2. Wang, C-Y., Manga, M. 2010a. Earthquakes and water: Lecture Notes in Earth Sciences, v. 114, Springer, New York 235 pages.
3. Ingebritson, S.E., Manga, M., 2019. Earthquake hydrogeology. Water Resources Research 55, 5121-5216 doi:10.1029/2019WR025341.
4. Manga, M., Beresnev, I., Brodsky, E.E., Elkhoury, J.E., Elsworth, D., Ingebritsen, S.E., Mays, D.C., Wang, C-Y., 2012. Changes in permeability caused by transient stresses: Field observations, experiments, and mechanisms. Reviews in Geophysics 50, RG2004.
5. Cox, S.C., Menzies, C.D., Sutherland, R. Denys, P.H., Chamberlain, C., Teagle, D.A.H. 2015. Changes in hot spring temperature and hydrogeology of the Alpine Fault hanging wall, New Zealand, induced by distal South Island earthquakes. Geofluids, 15(1/2): 216-239
6. Gulley, A., Dudley Ward, N.F., Cox, S.C., Kaipio, J.P., 2013. Groundwater responses to the recent Canterbury Earthquakes: a comparison. Journal of Hydrology 504, 171-181.
7. Weaver, K.C.; Cox, S.C.; Townend, J.; Rutter, H.; Hamling, I.J.; Holden, C. 2019. Seismological and hydrogeological controls on New Zealand-wide groundwater level changes induced by the 2016 Mw7.8 Kaikōura earthquake. Geofluids, A9809458.
8. Rutter, H.K., Cox, S.C., Dudley Ward, N.F., Weir, J.J., 2016. Aquifer permeability change caused by a nearfield earthquake, Canterbury, New Zealand. Water Resources Research 52, 8861-8878
9. O'Brien, G.A.; Cox, S.C.; Townend, J. 2016 Spatially and temporally systematic hydrologic changes within large geoengineered landslides, Cromwell Gorge, New Zealand, induced by multiple regional earthquakes. Journal of Geophysical Research. Solid Earth, 121(12): 8750-8773.
10. Weaver, K.C., Doan, M.-L., Cox, S.C., Townend, J., Holden, C., 2019. Tidal behavior and water-level changes in gravel aquifer in response to multiple earthquakes: a case study from New Zealand. Water Resources Research 55, doi:10.1029/2018WR022784.
11. Weaver, K.C.; Arnold, R.; Holden, C.; Townend, J.; Cox, S.C., 2020. A probabilistic model of aquifer susceptibility to earthquake-induced groundwater-level changes. Bulletin of the Seismological Society of America 110(3), 1046-1063.Dudley Ward, N. 2015. On the mechanism of earthquake induced groundwater flow. Journal of Hydrology 530, 561-567.
12. Dudley Ward, N. 2015. On the mechanism of earthquake induced groundwater flow. Journal of Hydrology 530, 561-567.
13. van Ballegooy, S.; Cox, S.C.; Thurlow, C.; Rutter, H.K.; Reynolds, T.; Harrington, G.; Fraser, J.; Smith, T. 2014. Median water table elevation in Christchurch and surrounding area after the 4 September 2010 Darfield Earthquake. Version 2. Lower Hutt, NZ: GNS Science. GNS Science report 2014/18. 79 p. + appendices.
14. Cox, S.C., van Ballegooy, S., Rutter, H.K., Harte D.S., Holden, C., Gulley A.K., Lacrosse V., Manga M. (2021) Can artesian groundwater and earthquake-induced aquifer leakage exacerbate the manifestation of liquefaction? Engineering Geology, 281: article 105982; doi:10.1016/j.enggeo.2020.105982.

EXPERIENCED INSTALLERS OF ROCKFALL PROTECTION

+ DELIVERING

VEGETATION MANAGEMENT
ANCHOR SYSTEMS
EROSION CONTROL
ROCK BARRIERS
SOIL NAILS
EXPLOSIVES

We minimise your risks!

AVALON

// ROPE ACCESS SERVICES

PO BOX 5187, 94 HIGH STREET, FRANKTON, HAMILTON 3204

P 07 846 1686 **E** admin@avalonltd.co.nz **W** avalonltd.co.nz

EXPERIENCE // INNOVATION // PERFORMANCE

AUP Groundwater Take and Diversion

Nick Speight & Matthew Wansbone,
Senior Geotechnical Engineers, Initia Limited

Nick Speight
Nick Speight CPEng, CMEngNZ, APEC Engineer, is a Senior Geotechnical Engineer and Director of Initia – a specialist geotechnical consultancy. He has over 20 years' experience in geotechnical engineering and advisory services, predominantly supporting projects in the Auckland Region. Nick specialises in buildings – both large scale industrial and commercial/residential multi-storey buildings with basement levels.

Matthew Wansborne
Matthew Wansbone CPEng, CMEngNZ, is a Senior Geotechnical Engineer and Director of Initia – a specialist geotechnical consultancy. He has over 17 years' experience in geotechnical engineering predominantly including buildings and civil infrastructure in New Zealand and internationally.

INTRODUCTION

The Auckland Unitary Plan (AUP) introduced new regulations for groundwater take and diversion in the Auckland Region. Whilst the authors of the rules unquestionably had the correct intentions, the interpretation and application of the regulations has been overly conservative and lacking in context. The unfortunate effect of this has been to add significant additional time, cost, and complexity to projects at a time when society requires the opposite from the engineering profession.

This article has been prepared to outline the key issues with the AUP (from a groundwater perspective) and propose minor revisions to the AUP standards for groundwater take (AUP Section E7.6.1.6). We have also proposed changes to the assessment of groundwater related effects during the consenting process which we believe would both simplify the regulatory requirements and increase certainty for all parties.

AUCKLAND UNITARY PLAN GROUNDWATER DRAWDOWN AND DIVERSION STANDARDS

Section E7 of the AUP relates to taking, using, damming and diversion of water [and drilling]. The relevant permitted activity standards for groundwater diversion and take associated with excavations are as follows:

- **Section E7.6.1.10** - *Diversion of groundwater caused by any excavation (including trench) or tunnel.*
- **Section E7.6.1.6** – *Groundwater Take for dewatering or groundwater level control associated with a groundwater diversion permitted under Standard E7.6.1.10.*

A summary of the permitted activity standards for each is outlined below for context.

Section E7.6.1.10 – Diversion of Groundwater caused by any excavation.

Under E7.6.1.10 of the AUP, a consent is required unless the following permitted activity standards are met:

2) Any excavation that extends below natural groundwater level, must not exceed:
   (a) 1ha in total area; and
   (b) 6 m depth below the natural ground level.

3) The natural groundwater level must not be reduced by more than 2m on the boundary of any adjoining site.
4) Any structure, excluding sheet piling that remains in place for no more than 30 days, that physically impedes the flow of groundwater through the site must not:
   (a) impede the flow of groundwater over a length of more than 20m; and
   (b) extend more than 2 m below the natural groundwater level.
5) The distance to any existing building or structure on an adjoining site from the edge of any;
   (a) trench or open excavation that extends below natural groundwater level must be at least equal to the depth of the excavation.
   (b) tunnel or pipe with an external diameter of 0.2 – 1.5 m that extends below natural groundwater level must be 2m or greater; or
   (c) a tunnel or pipe with an external diameter of up to 0.2 m that extends below natural groundwater level, has no separation requirement.
6) The distance from the edge of any excavation that extends below natural groundwater level, must not be less than;
   (a) 50 m from the Wetland Management Areas Overlay:
   (b) 10 m from a scheduled Historic Heritage Overlay; or
   (c) 10 m from a lawful groundwater take.

   Pile foundations, pipes, and trenching works (associated with linear infrastructure) are exempt from the above standards.

The above rules consider the risk and associated effects from potential groundwater drawdown, particularly where compressible soils are present (as they are in some areas of the Auckland Region) in combination with elevated groundwater levels. However, under the AUP, groundwater diversion associated with an excavation can only occur in combination with '*Dewatering or Groundwater Level Control*'. Therefore, even when an excavation meets permitted activity criteria under E7.6.1.10, the related **Standard E7.6.1.6** for 'Dewatering or Groundwater Level Control' must also be considered, as outlined below.

Section E7.6.1.6: Dewatering or groundwater level control associated with a groundwater diversion (permitted under Standard E7.6.1.10)

Under E7.6.1.6 - Dewatering or Groundwater level control (associated with a groundwater diversion under E7.6.1.10) is a permitted activity only of it meets all of the following standards:

1. The groundwater take is not geothermal water
2. The groundwater take is only for a period of 10 days (in peat soil) or 30 days (in other soils or rock); and
3. The groundwater take must only occur during construction.

IMPLICATIONS FOR THE AUP STANDARDS FOR GROUNDWATER TAKE AND DIVERSION

The implication of **E7.6.1.6** is that, unless an excavation is wholly above the 'natural groundwater level' (i.e., there is no dewatering or groundwater level control associated with the excavation), then a consent is required unless the works can be completed within 10 days for peat or 30 days for other soils. In practice this means that a groundwater consent is required for any excavation below the 'natural groundwater level' for any basement or other substantial below ground structure as it is not practical to excavate and construct in less than 30 days.

In our view, the key issue with the above lies with the following:

1. There is no clear definition of "natural groundwater level" in the AUP. In the absence of a clear definition, Council's present interpretation is that any free water present within the soil matrix is "natural groundwater". For the reasons we outline below, this is not incorrect for most Auckland sites with elevated topography;
2. While E7.6.1.10 presents a rational, risk-based approach to determining whether an activity is permitted or not, E7.6.1.6 "overrides" this risk-based approach. Accordingly, the permitted activity criteria for dewatering or groundwater control (E7.6.1.6) effectively means that any excavation extending even nominally (say 100 mm) below 'natural groundwater level' (for the purposes of constructing a basement or any other substantial below ground structure) requires a consent, unless full groundwater cut off is provided to prevent drawdown. In addition, we have found that when a consent is required because this permitted activity standard is not met, Council reviewers require a full and detailed assessment of effects for all magnitude of groundwater diversion/ drawdown, not just where it exceeds the limits in E7.6.1.10. The reason for this is not clear.

WHAT DOES THIS MEAN FOR CONSENTING EXCAVATIONS AND BASEMENT STRUCTURES IN THE AUCKLAND REGION?

The implications of the AUP rules under E7.6.1.6 and E7.6.1.10 are that almost all projects in Auckland which have basement levels or often even just nominal excavations to form building platforms, require a consent. Unfortunately, it is also our experience, that both the interpretation of the permitted activity standards, as well as Council's requirements for assessing the effects of groundwater drawdown, are becoming more onerous with time. These requirements are usually disproportionate to the potential risks or effects associated with groundwater drawdown. The outcome of this is:

1. Significantly increased costs associated with additional geotechnical investigation and installation of expensive groundwater monitoring instrumentation which is arguably not needed for shallow excavations.

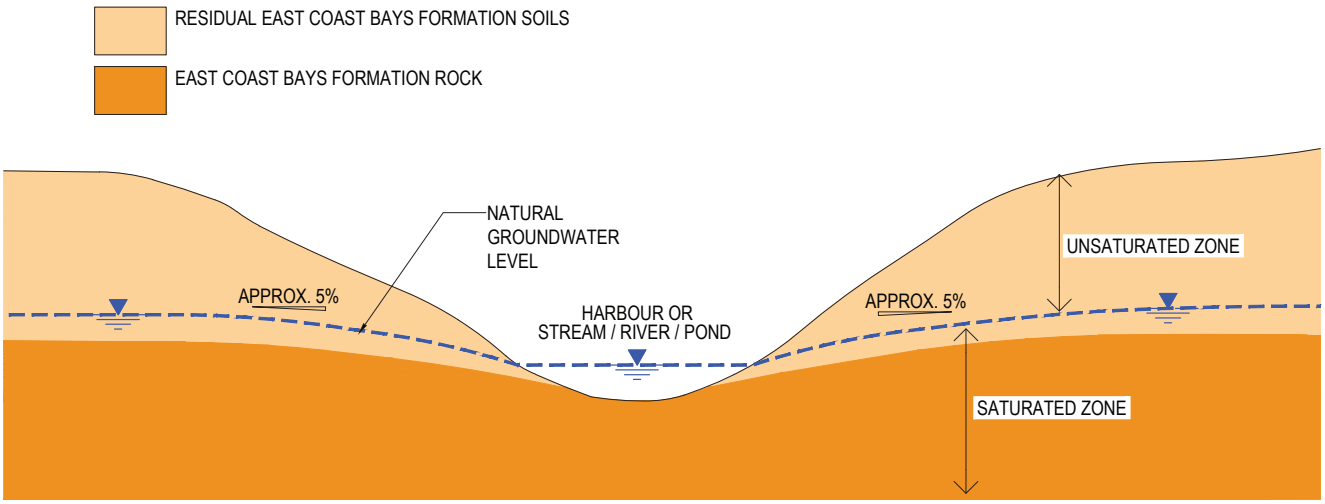

FIGURE 1: Typical Groundwater Conditions of elevated Auckland sites

2. Increased professional services (consulting) fees, consent application, and Council review fees.
3. Delays in obtaining consent for applicants, particularly given the scope for interpretation of the AUP rules and groundwater conditions at a site.
4. Higher compliance/monitoring costs during construction as relatively rigid, standardised monitoring regimes are imposed by default as a condition of consent.
5. Potential construction delays due to 'alert level' triggers in groundwater levels.

However, one of more concerning outcomes of the AUP groundwater consenting requirements is that, in our experience, geotechnical engineering professionals are implementing overly conservative design and construction solutions to mitigate the 'apparent' risk of groundwater drawdown. In extreme cases, the authors of this article have observed the detailing of secant piled walls for single level basements, often for sites positioned on or near to ridgelines where elevated groundwater levels and soil types that could lead to consequential settlement effects do not exist. We can only surmise that such decisions have been made in the interest of programme, consultant budgetary constraints or because of protracted debates of technical issues with Council reviewers. Regardless, the cost implications of such decisions can extend into the hundreds of thousands of dollars, and potentially upwards of $1M in extreme cases.

While these outcomes are clearly in part the responsibility of the geotechnical professional, it is not surprising that such outcomes are occurring on projects where geotechnical engineers, unfamiliar with the unique regulatory environment in Auckland and the "unwritten rules" regarding groundwater consenting, are defaulting to "easier to consent", expensive solutions. These sorts of outcomes are highly undesirable and contribute to increased construction costs at a time when the industry needs to reduce the cost of construction.

Before we can propose how the AUP rules could be modified (or clarified), it is important to consider the geology and hydrogeology of the Auckland Region.

AUCKLAND HYDROGEOLOGICAL AND GEOLOGICAL CONDITIONS

With Auckland located at the isthmus of the Waitemata and Manukau Harbours, much of the land is proximal to coastal regions or other bodies of water (streams, rivers, swamps, lakes etc). Near surface 'natural groundwater levels' persist near the coastline, around lakes and streams and near to wetland areas. Furthermore, it is in these areas that compressible soils tend to be prevalent (e.g. Marine Sediments, Peats and other Holocene Age alluvial deposits). The primary risk associated with groundwater drawdown in these areas is almost always the potential for ground settlement which can affect surrounding buildings, land, and infrastructure. Where near surface, permanent, hydrostatic groundwater levels are present in combination with soft and compressible soils, this is a significant risk that needs to be addressed carefully. The permitted activity criteria for groundwater diversion (E7.6.1.10) is therefore appropriate for these sites. It is also accepted that it is not possible to accurately delineate (by way of GIS overlays) the areas of Auckland where compressible soils are present. Therefore, it is appropriate that the E7.6.1.10 permitted activity standards apply to the wider Auckland Region. This minimises the risk of groundwater drawdown effects (principally settlement) on land, property, and infrastructure.

However, Auckland is also a region with significant topographic highs. In these areas, permanent hydrostatic groundwater levels are generally not present. Such conditions persist across vast swathes of high intensity development areas in the Auckland Region - the CBD, city periphery areas (Parnell, Ponsonby, Newton, the Great North Road ridgeline) and many other urban areas of the city (Remuera, Grey Lynn, St Marys Bay, the

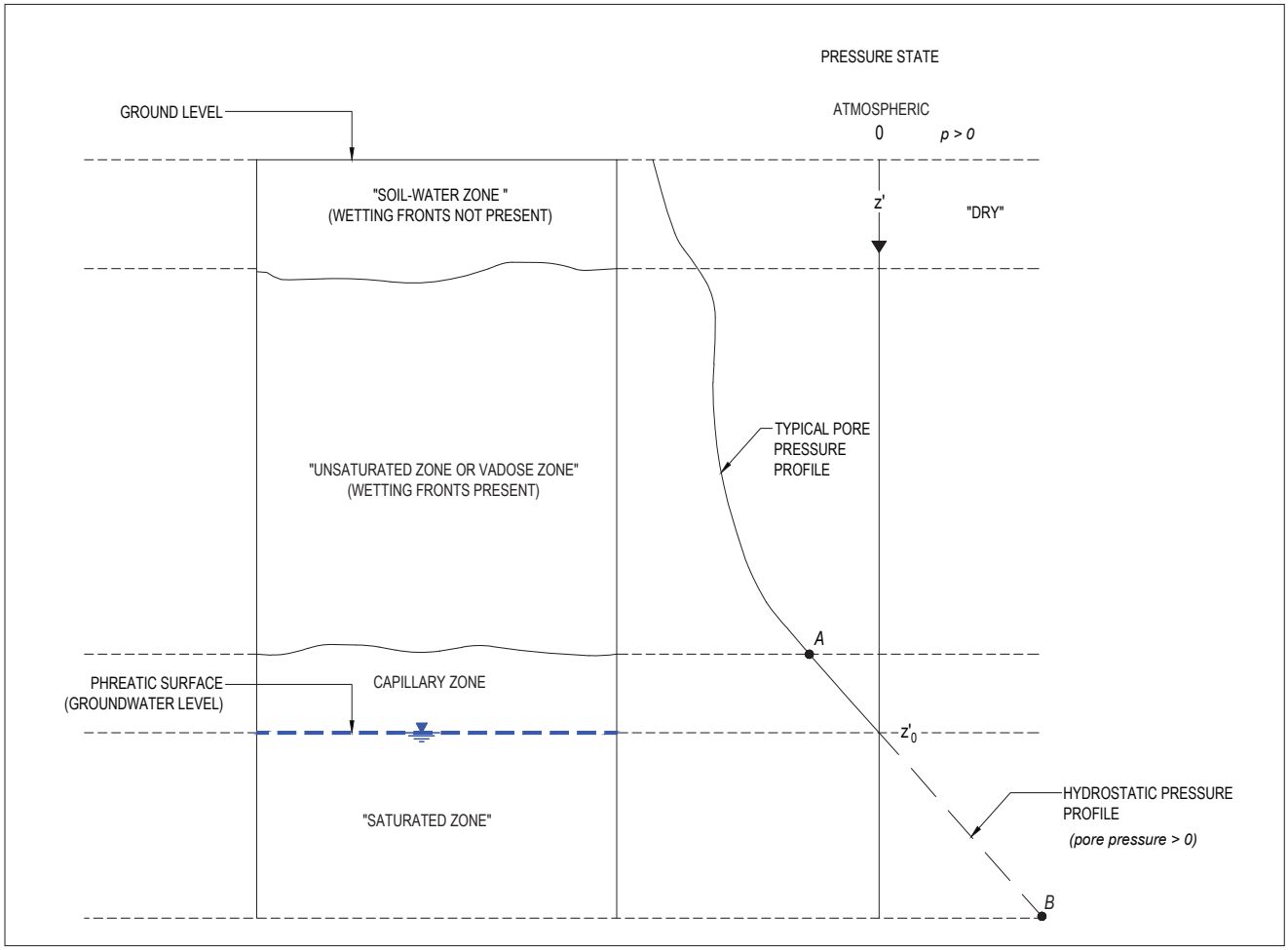

FIGURE 2: Groundwater Zones

Eastern Bays, and much of the North Shore to name just a few). In these areas, where ground surface levels are elevated well above sea level, and where sites are remote from lakes, streams, creeks and other bodies of water, permanent hydrostatic groundwater levels are often well below ground level and below the influence of most developments. In addition, ground conditions in these areas usually consist of residual soils, sometimes capped with volcanic ash & tuff or stiff, old, over-consolidated Puketoka Formation deposits – i.e. soils which are not known to be significantly impacted by groundwater drawdown. Historical investigations on the Auckland Isthmus have indicated that "regional" groundwater levels within the East Coast Bays Formation soils and rock of the Auckland Region have a gradient of between approximately 2 and 5% toward the coastline or other bodies of static water. Figure 1 presents the typical groundwater conditions of an elevated site in Auckland (i.e., located above the coastal zone and/or other bodies of water).

In general, the groundwater conditions of most sites can be defined with the following 'zones':

- The **Soil-Water Zone** – often in the upper 1-2 m below ground surface levels where trees and other vegetation extract water from the pores of the soil matrix and/or where the ground surface is sealed with pavements and other impermeable surfaces preventing recharge by rainfall and stormwater runoff.
- The **"Unsaturated Zone"** (also referred to as the 'Vadose Zone') where 'wetting fronts' are present. Groundwater is present within this zone – occurring as water within the pores of the soil matrix - however, the soil is not fully saturated and porewater pressures are less than atmospheric pressure.
- The **"Capillary Zone"** where soils are fully saturated but capillary forces causes a negative pore water pressure component, i.e., the porewater pressure is less than atmospheric pressure.
- The **"Saturated Zone"** where the pores of soil are permanently and fully occupied by water, the porewater pressure is greater than atmospheric pressure and a hydrostatic groundwater profile exists. The surface of the "Saturated Zone" is often referred to as the 'phreatic surface' or more commonly just the groundwater level. This surface will fluctuate throughout the year – varying due to rainfall conditions, being elevated in winter and depressed in summer. The 'groundwater level' often follows the surface topography but with smaller relief.

Figure 2 presents the various zones of groundwater beneath most sites.

'NATURAL GROUNDWATER LEVEL'

In the absence of any clear definition of the 'natural groundwater level' within the AUP, it is reasonable to assume that Council intended it to relate to a 'groundwater level' which, if reduced by dewatering, would cause ground settlement. It therefore follows, that the 'natural groundwater level' must be the 'phreatic surface' or the level at which porewater pressure (p_w) is equivalent to atmospheric pressure (p_a) as presented on Figure 2 and is permanently saturated. In addition, within the context of groundwater drawdown induced settlements, this should be a "permanent" groundwater level which has been present since the deposition of the soil/rock unit.

In our experience groundwater conditions above the phreatic surface (i.e. above the permanent, hydrostatic groundwater level) are complex in the Auckland Region. Standpipe piezometers on sites with elevated relief (e.g. on ridgelines or cliff tops) in Auckland often collect groundwater within the 'Vadose Zone', above the permanent, hydrostatic groundwater level. In our view, the measured groundwater levels in shallow piezometers relates to the collection of downwardly percolating groundwater. Standpipe piezometers act as a high permeability zone within the soil profile, effectively providing a path of least resistance and a "sump" that intercepts downward groundwater seepage flowing toward a lower permanent, hydrostatic groundwater level. This is similar to conditions often observed behind shallow retaining walls, where outlet drains are blocked – the drainage aggregate behind the walls is highly permeable and preferentially collects groundwater seepage. In some cases, groundwater pressures (head) can build up within the drainage; however, such water levels do not have any relationship to permanent, hydrostatic groundwater levels.

The above interpretation is also consistent with our observations of seepage within excavations at these sites during construction; inflows are often limited to a trickle at most. These minor seepages are most likely vertically and horizontally percolating groundwater migrating through the 'Vadose Zone' toward the 'Saturated Zone' or the permanent, hydrostatic groundwater level.

The type of situation described above is often attributed to a "perched" groundwater level by Council (and/or their reviewers), which is subsequently interpreted as the 'natural groundwater level'. In our opinion, this is a misinterpretation in the context of the Unitary Plan. While a true "perched" groundwater level could represent a permanent "natural groundwater level" in specific hydrogeological settings (i.e. an aquifer overlying a low permeability aquiclude, which in turn sits above a deeper groundwater level), this does not appear to be a relevant model for the typically low permeability soils in Auckland.

MEASURING THE 'NATURAL GROUNDWATER LEVEL' FOR ANALYSIS AND CONSENTING PURPOSES

The reality is that there is no "one size fits" all approach to investigating and assessing groundwater conditions and hydrogeology for all sites. In areas of low-lying relief – in proximity to the coastline or lakes, rivers, streams and other bodies of water – determining the groundwater level will not be difficult. This requires little more than a common-sense approach. However, in areas of higher relief, one or more of the following methods could be considered:

1. Installation of a series of nested vibrating wire piezometers installed over the depth range of the excavation and down toward the anticipated permanent, hydrostatic groundwater level" or at least one deep piezometer that extends into the permanent hydrostatic groundwater level. Vibrating wire piezometers, grouted into place, should be used. In this situation the hydrostatic groundwater level would be adopted as the 'natural groundwater level' at the site, unless there was evidence to suggest a true perched groundwater level is present.
2. Obtaining a series of core samples over the depth range of the excavation and completing laboratory (oedometer) tests to confirm where the soils are fully saturated, or
3. Carrying out cross-hole P-wave velocity testing.

Regardless of which method is adopted; the permanent hydrostatic groundwater level should meet the following criteria:

a) The porewater pressure is greater than atmospheric pressure; and
b) There is a permanent hydrostatic pressure profile present below the inferred groundwater level (temporarily higher transient/seasonal groundwater levels would not be captured by this criteria).

Confirming that the soils are fully saturated would also be beneficial, but this is implicit in the results of a) and b) above anyway.

RECOMMENDED CHANGES TO AUP GROUNDWATER RULES

To minimise unnecessary cost, time, and complexity, we recommend the following changes be considered for the AUP rules for **E7.6.1.6.**

E7.6.1.6. Dewatering or groundwater level control associated with a groundwater diversion permitted under Standard E7.6.1.10, all of the following must be met:

1) The water take must not be geothermal water;
2) The water take must not be for a period of more than 10 days where it occurs in peat soils, ~~or 30 days in other types of soil or rock; and~~
~~3) The water take must only occur during construction.~~

CONFERENCE RE-SCHEDULED TO 2ND-5TH MAY 2022

ICSMGE 2021 is coming to Sydney

The Australian Geomechanics Society's successful bid to host the 20th International Conference on Soil Mechanics and Geotechnical Engineering means that premiere conference in geotechnics will be held in Sydney, Australia, from 12 to 17 September 2021.

We can't wait to welcome our profession's best and brightest minds from across the world to our International Convention Centre (ICC Sydney) on the stunning Sydney Harbour.

It's an exciting time for our profession here in Sydney, with major redevelopment projects using new and innovative technology and techniques that will help to shape the future of geotechnical engineering.

Join us in the harbour city in September 2021 for a Geotechnical Discovery Down Under!

Visit us at www.icsmge2021.org for more information.

SEE YOU IN SYDNEY!

SYDNEY ICSMGE 2021

A GEOTECHNICAL DISCOVERY **DOWN UNDER**

20th International Conference on Soil Mechanics and Geotechnical Engineering
12-17 September 2021 | ICC Sydney Australia www.icsgme2021.org

AUSTRALIAN GEOMECHANICS SOCIETY

SIMSG ISSMGE

www.icsmge2021.org

In our opinion, Standard E7.6.1.6 (2) is unnecessary in non-peat soils as the risk based rules in E7.6.1.10 are already sufficient to pick up situations where consequential groundwater induced settlement could occur.

In addition, we consider Standard E7.6.1.6 (3) to be redundant, since by the end of construction (likely to be 6- least 12 months for typical basements), most groundwater drawdown related effects would be complete, and the potential effects of groundwater drawdown have already been considered under E7.6.1.10 (2), (3) and (5).

Secondly, the 'natural groundwater level' must be clearly defined. We recommend the following definition:

> **'Natural Groundwater Level'**
> The phreatic surface, where the pore pressure in the soil is equal to or greater atmospheric pressure, and below which a hydrostatic pressure profile exists with depth. This includes 'Perched Groundwater Levels' where the geological setting permits the presence of such.

RECOMMENDED CHANGES TO COUNCIL PROCESSING

In addition to the proposed changes and clarifications of permitted activity standards E7.6.1.6, we recommend Council, and their reviewers consider the following when processing consent applications for groundwater take/diversion:

1. Assessment of the 'natural groundwater level' at a site should include consideration of multiple information sources including, but not just limited to piezometer measurements, but also an assessment of the topography, geology, and hydrogeology in the vicinity of the site.
2. For determining if a consent is required and/or assessing settlement effects, the 'natural groundwater level' should be taken as the lowest measured groundwater level over the monitoring period. Consolidation settlement occurs where the stress in the soils exceeds the historical stress history of the soil, i.e. when the groundwater level has been lowest. Therefore, the "summer low" of the 'natural groundwater level' is the relevant level that should be used for assessing settlement effects.
3. Permissible settlement magnitudes from groundwater drawdown combined with the mechanical deformation effects of the excavation itself (usually retaining wall deformation) should relate to the 'tolerances or sensitivity' of neighbouring buildings, infrastructure, and property, not what the engineer has calculated from his/her unique design solution.

Council should consider publishing permissible total and vertical settlement magnitudes for roads, footpaths, buried services etc. Maximum permissible total and differential settlements for adjoining buildings should be assessed and confirmed by structural engineers based on a review of the structure type and foundation systems of each building. These could in turn be reviewed by Council or their appointed reviewers.

An effects-based assessment would enable the geotechnical professional to detail and design retaining systems (including drainage or tanking systems for control of groundwater levels) at detailed design stage, rather than at preliminary design (for resource consent) when other design elements are not sufficiently advanced to support the level of detail required.

Alert and Alarm level settlement magnitudes, and the required monitoring regime could be agreed at resource consent, effectively locking in the design criteria which the geotechnical professional subsequently refers to for detailed design.

In addition, consideration could be given to allowing publication by the industry of actual settlement monitoring results on dewatered sites so that effects assessments can be better calibrated and unnecessary conservatism avoided.

The above approach would significantly streamline the groundwater consenting process, without compromising the process or increasing the risk to Council and to neighbouring landowners or asset owners.

FEEDBACK AND NEXT STEPS

We are very interested in receiving feedback on the above article and invite you to share your own views with us. Please email either Nick or Matt at the email addresses below.

Nick Speight: nspeight@initia.co.nz
Matthew Wansbone mwansbone@initia.co.nz

Following receipt of industry feedback, and once we are satisfied that there is consensus, we propose to submit an opinion to Auckland Council for consideration and discussion.

GEOBRUGG®
BRUGG

Safety is our nature

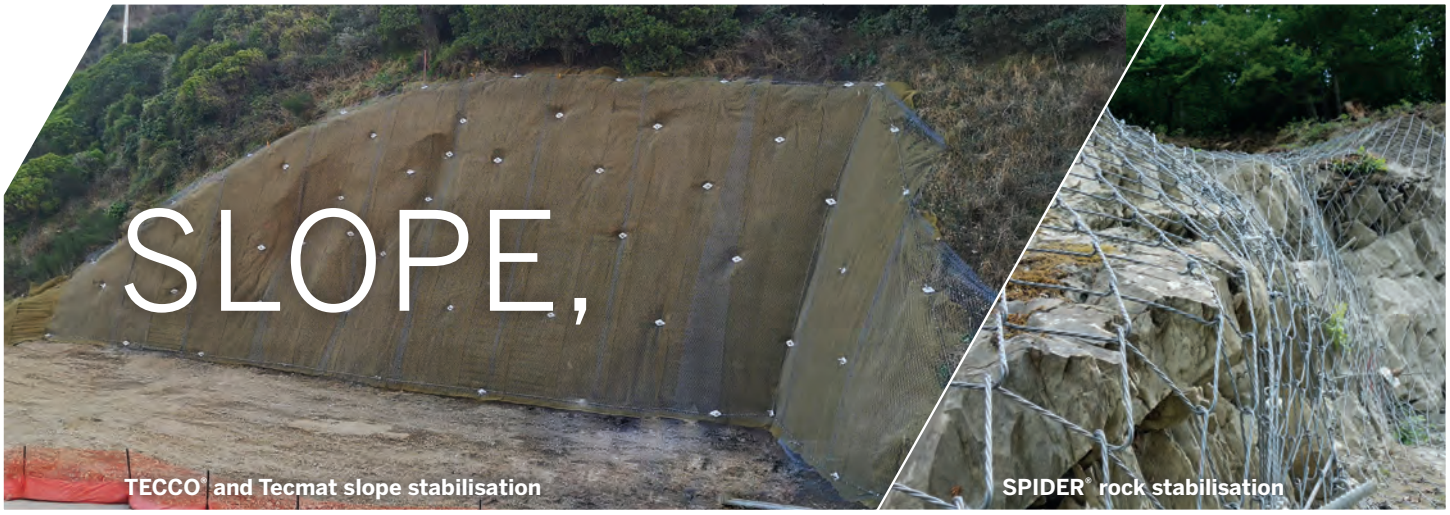

Your local Geobrugg specialist:
www.geobrugg.com/contacts

Geobrugg (NZ)
Christchurch
T: +64 220 499 897
stu.mason@geobrugg.com
www.geobrugg.co.nz

STUDENT POSTER COMPETITION WINNERS

Seismic and 1-D Compressibility Properties o

Civil Engineering Final Year Research Proje

Authors: O. E. Ross and J. M. Young

1. BACKGROUND

New Zealand produces over 5 million end-of life tyres (ELT) per year and disregards 70% of these in landfills, stockpiles or illegally[1]. A sustainable multi-disciplinary solution to this problem is to **re-use** and **re-cycle** ELTs. The geotechnical properties can be utilised through mechanically shearing ELTs for use in **Gravel-Rubber Mixtures** (GRM) for foundations.

Figure 1. ELTs in Waikato Landfill[1].

ERGSI: eco-rubber geotechnical seismic isolation foundation systems

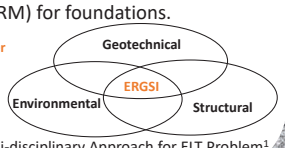

Figure 2. Multi-disciplinary Approach for ELT Problem[1].

2. OBJECTIVES

This study investigated the following, for varying volumetric rubber contents (VRC):

Properties	Method
Seismic properties	Impact testing
Long-term 1-D compressibility	1-D compression test with 1-day creep
Frictional and arching effects	Load cell analysis

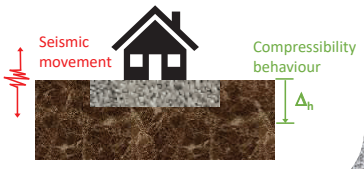

Figure 3. Schematic of Project Objectives.

3. MATERIALS

Rounded Gravel	$D_{50,G}$ = 6.0 mm	G_s=2.72
Tyre Rubber	$D_{50,R}$ = 4.0 mm	G_s=1.15

Rounded Gravel Large Rubber

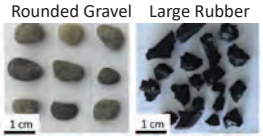

Figure 4. Material Used (left: gravel, right: rubber) [1].

The following VRC were selected for testing:

VRC (%)	0	10	25	40
Density (g/cm^3)	1.66	1.52	1.37	1.19

4. SEISMIC PROPERTIES

Method:

1. Hit the bottom of GRM specimen with an impact hammer.
2. Measure input and output accelerations (with accelerometers placed on the top and bottom of specimen).
3. Calculate frequency response functions (FRF) using cross power spectral density method.
4. Determine natural frequency and damping effects.

Apparatus:

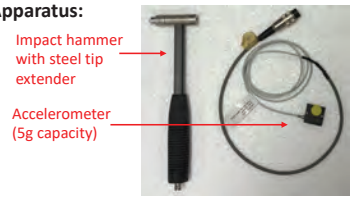

Figure 5. Impact Hammer and Accelerometers.

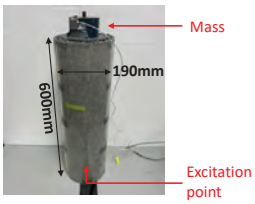

Figure 6. Specimen Set-Up.

Results and Discussion

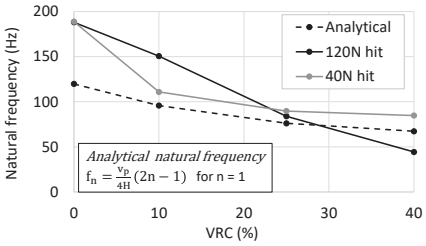

Figure 7. Natural Frequency versus VRC Showing the Isolation Effect.

- Increasing VRC increases the **effect of isolation**; this is proportional to a decrease in the natural frequency of the specimen.

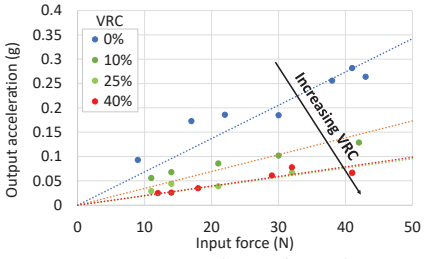

Figure 8. Input Force versus Output Acceleration Showing the Dissipative Effect.

- Increasing VRC increases the **dissipative effect**; this is proportional to a decrease in the output acceleration read by the accelerometer at the top of the specimen.

Figure 6 demonstrates the above results:

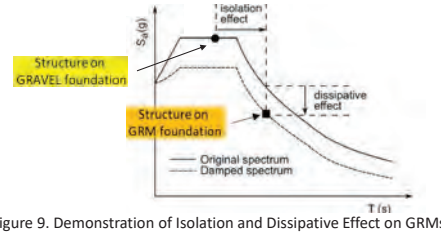

Figure 9. Demonstration of Isolation and Dissipative Effect on GRMs[1].

5. LONG-TERM 1-D PROP

Method:

1. Set-up rigid cell apparatus with G
2. Apply 20 kPa vertical load via a be cylinders. Use computer logging s and back pressure over time. Leav behaviour.
3. Repeat Step 2 for 50 kPa, 100 kPa

Apparatus:

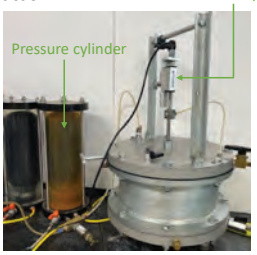

Figure 10. Long-Term 1-D Co

Results and Discussion:

Figure 11 shows the total strain (ε_t) and long-term strain (ε_c) for different VRC at each pressure increment. The difference between total and long-term strain represents instantaneous strain.

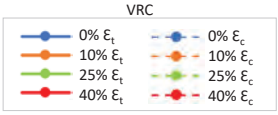

- Increasing VRC is proportional:
  - to an increase in total strain.
  - to an increase in long-term str
  - to an increase in the rate of lo vertical stress.

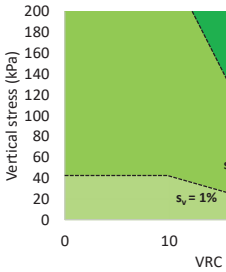

Figure 12. VRC versus Vertical Stress Show

- Green-shaded zones show allowab
- Increasing VRC is proportional to in vertical stress.

Supervisors: Dr. G. Chiaro and Dr. A. Tasalloti

f Gravel-Rubber Mixtures

ect

UNIVERSITY OF CANTERBURY
Te Whare Wānanga o Waitaha
CHRISTCHURCH NEW ZEALAND

D COMPRESSIBILTY PERTIES

RM layered in 20 mm layers.
ellofram, connected to two pressure ystem to record axial displacement ve for 24 hours to observe creep

and 200 kPa.

acement rod

ompressibility Test Set-Up.

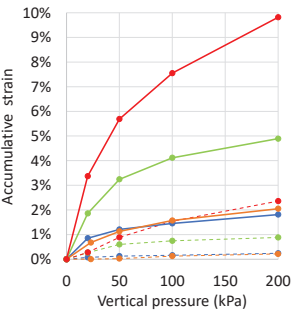

Figure 11. Vertical Stress versus Strain Showing 1-day Creep Behaviour.

ain and **creep behaviour**.
ng-term strain for any applied

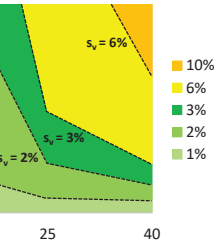

wing Settlement Zones For 1-day Creep.

le settlement regions for each VRC. ncreasing settlement for a given

6. FRICTIONAL AND ARCHING EFFECTS

The load transfer efficiency (LTE) of each specimen used in the 1D compressibility tests can be estimated using a load cell, placed at the bottom of the apparatus. A porous stone was placed on top of the load cell to ensure even distribution of stress (Figure 13).

Method:

1. Place a known mass on top of the porous stone/load cell.
2. Record and plot voltage output.
3. Repeat Steps 1 & 2 with various known masses.

Apparatus:

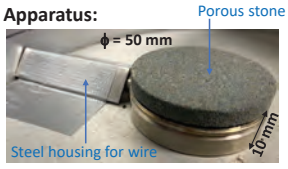

Figure 13. Load Cell and Porous Stone Configuration.

Results and Discussion:

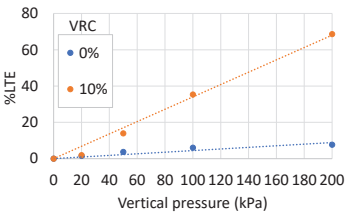

Figure 14. LTE for Various Specimens.

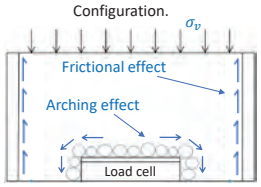

Figure 15. Schematic of Frictional and Arching Effects.

- Increasing VRC is proportional to a higher LTE.
- Possible reasons for inefficiencies:
  - **Frictional effects:** Interface behaviour between particles and apparatus reduces the pressure experienced by the load cell and lower particles.
  - **Arching effects:** Interlocking of particles surrounding the load cell redistributes the pressure via arching action, towards the base of the apparatus and away from the load cell.

7. RECOMMENDATIONS

- Undertake further impact tests using a specimen with a larger area, to mitigate and quantify possible boundary effects.
- Perform impact tests with incremental layer heights and relate to real life applications.
- Use a force-application mechanism to ensure the same input load is applied for each impact test.
- Evaluate frictional and arching effects for all GRM specimens.
- Use the LTE analysis results to correct 1D compressibility data.

8a. REFERENCES

1. Chiaro, G., Tasalloti, A., Banasiak, L.J., Palermo, A., Granello, G., Rees, S. (2020). "Sustainable recycling of end-of-life tyres in civil (geotechnical) engineering applications: turning issues into opportunities in the New Zealand context." 99, 38-47.

8b. ACKNOWLEDGEMENTS

The authors wish to thank Dr. Gabriele Chiaro and Dr. Ali Tasalloti for providing guidance and advice throughout the project. Thanks is also given to Dr. Sean Rees, Dr Gabriele Granello and Mr. Siale Faitotonu for contributing greatly to the success of the project.

1ST PLACE

A LARGE NUMBER of very high-quality posters were submitted to the annual competition. After careful evaluation and much discussion, the judges decided that the winning posters for 2020 are:

1ST PLACE

Olivia ROSS / Julia YOUNG: Seismic and 1-D Compressibility Properties of Gravel-Rubber Mixtures (BE(Hons) student, University of Canterbury)

2ND PLACE

Baqer ASADI: Liquefaction assessment of pumiceous soil: shear wave velocity-based method (PhD student, University of Auckland)

3RD PLACE

Amelia LIN: Validation of a Geospatial Liquefaction Model (PhD student, University of Auckland)

Congratulations to all of you.

And our thanks to all other entries; we are continually amazed by the high standard of the posters we receive.

2ND PLACE

Liquefaction assessment of pumiceous soil: shear wave velocity-based method

Mohammad Bagher Asadi I PhD student

THE UNIVERSITY OF AUCKLAND
Te Whare Wananga o Tamaki Makaurau
NEW ZEALAND

1 - INTRODUCTION

Pumice sands are originated from volcanic eruptions in the Taupo Volcanic Zone.

- The pumice sands are then mixed with normal soils and deposited across central of the North Island, and they are frequently encountered in many engineering projects.
- Pumice particles are vesicular, crushable and lightweight (Figure1) leading in difficulties to accurately characterise the properties of Natural Pumiceous (NP) sands.
- Per literature, the current practice correlations using penetration tests can not provide a reliable estimate of cyclic resistance ratio (*CRR*) of NP sands (Orense et al. 2020).
- Surprisingly, the existing correlations from shear wave velocity (V_s) based methods, a non-destructive test, are also found to be not appropriate for liquefaction analysis of NP sand (Asadi et al. 2018).

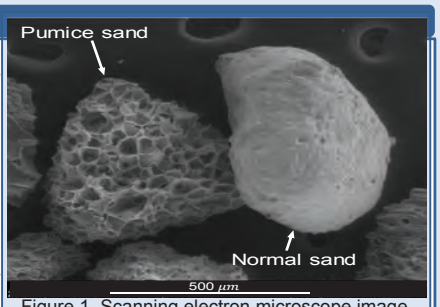

Figure 1. Scanning electron microscope image.

2 - RESEARCH OBJECTIVES

- To obtain high-quality undisturbed pumiceous samples from different locations in Waikato Basin and Bay of Plenty.
- To perform advanced laboratory testing.
- To estimate the pumice content of the pumiceous sands.
- To establish a simplified method for liquefaction assessment of pumiceous sands following V_s-based method.

3 - LABORATORY TESTING

✓ Sample preparation

- The frozen undisturbed samples of Dames & Moore and Gel-push were trimmed to 63mm diameter and 126mm hight for multi-stage triaxial testing (Figure 2).


Figure 2. Undisturbed samples.

✓ Bender element (BE) test

- BE tests were performed on the saturated samples at effective confining pressure of (σ'_c) 100 kPa with different levels of frequencies, i.e. 2, 4, 6, 8 kHz (Figure 3).
- The maximum shear modulus of the samples are then estimated using $G_{max}=\rho V_s^2$, where ρ is sample's bulk density.

✓ Undrained cyclic triaxial test

- After BE testing, stress-controlled cyclic loading was applied on the specimens at frequency of 0.1 Hz under different levels of cyclic stress ratio, *CSR* (Figure 3).
- Cyclic resistance ratio (*CRR*) is defined as a level of *CSR* where 5% double amplitude axial strain occurred in 15 cycles.

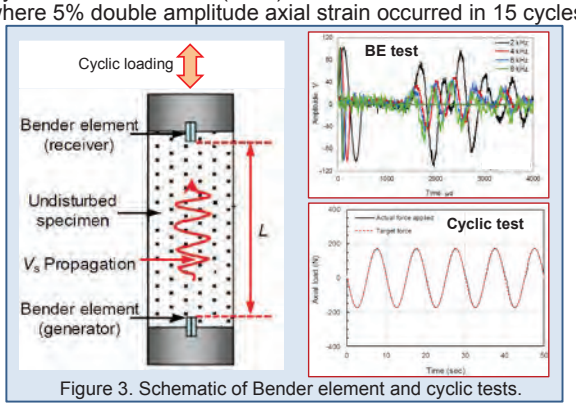

Figure 3. Schematic of Bender element and cyclic tests.

✓ Pumice content (*PC*) quantification test

- The methodology proposed by Asadi et al. (2019) was used for *PC* quantification (based on particle crushing potential).
- The materials showed significant different, i.e. *PC*≈15 - 95%.

4 - TEST RESULTS

- NP sands have considerably lower G_{max} compared with normal sands (Figure 4).
- NP sands have soft cyclic behaviour as well as have higher liquefaction resistance (Figure 4).
- Toward the end of the test, NP sands are able to subject to considerable number of cycles at high excess pore water pressure (EPWP) with slow increase in deformation; this is in contrast with normal sands (Figure 4).

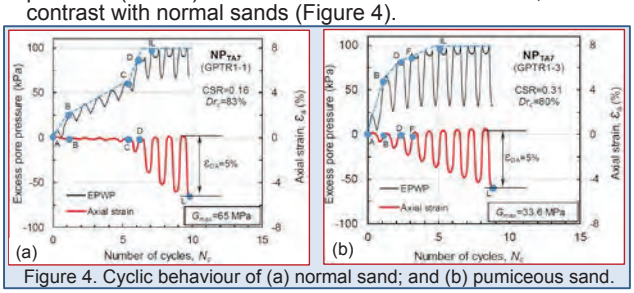

Figure 4. Cyclic behaviour of (a) normal sand; and (b) pumiceous sand.

- Due to lower V_s (G_{max}) and higher *CRR* of NP sands, their *CRR*-V_s relations plot far to the left of the correlations developed for normal sands (Figure 5).
- The established *CRR*-V_s relations are found to be dependent on the *PC* (Figure 5).
- Three *CRR*-V_s relations are established for NP sands with *PC* of about 15%, 50% and >70% using the laboratory data while converted to the field condition.

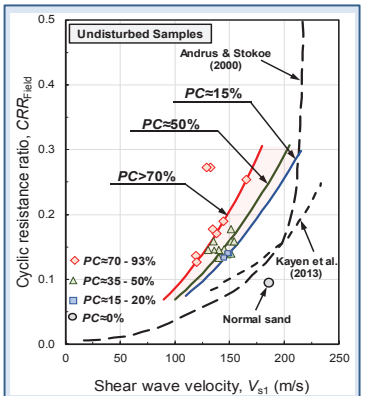

Figure 5. CRR_{Field} – V_{s1} relations.

5 - CONCLUSIONS

- The NP sands obtained from Waikato Basin and Bay of Plenty showed significant different pumice content (*PC*).
- The G_{max} ($=\rho V_s^2$) and *CRR* of NP sands was found to be significantly different than that of normal sands, and they are highly dependent on the level of *PC*.
- The existing V_s-based correlations from normal sands would considerably underestimate the *CRR* of NP sands.

ACKNOWLEDGEMENTS

The author wish to acknowledge the supervisions of A/Prof Rolando Orense and Professor Michael Pender, and the assistance of Jeff Melster for Laboratory testing. The author also gratefully acknowledges the PhD scholarship support from NHRP and QuakeCoRE.

REFRENCES:

- Andrus, R. D., and Stokoe, K. H. (2000). "Liquefaction resistance of soils from shear-wave velocity." *Journal of Geotechnical and Geoenvironmental Engineering*, 126(11), 1015-1025.
- Asadi et al. (2018). "Shear wave velocity-based assessment of liquefaction resistance of natural pumiceous sands." *Geotechnique Letters*, 8(4), 262-267
- Asadi et al. (2019). "Maximum dry density test to quantify pumice content in natural soils." *Soils and Foundations*, 59(2), 532-543.
- Kayen et al. (2013). "Shear-wave velocity-based probabilistic and deterministic assessment of seismic soil liquefaction potential." *Journal of Geotechnical and Geoenvironmental Engineering*, 139(3), 407-419.
- Orense et al. (2020). "Evaluating liquefaction potential of pumiceous deposits through field testing: case study of the 1987 Edgecumbe earthquake." *Bulletin of the New Zealand Society for Earthquake Engineering*, 53(2), 101-110.

VALIDATION OF A GEOSPATIAL LIQUEFACTION MODEL

USING OBSERVATIONAL DATA FROM THE 2016 KAIKŌURA EARTHQUAKE

Earthquake induced liquefaction and lateral spreading can cause **major damage** to buildings and infrastructure. Common procedures to identify exposed areas such as cone penetration testing require extensive resources. **Statistical models based on geospatial variables** offer an alternative approach, allowing for a time and cost efficient estimation of liquefaction.

GEOSPATIAL LIQUEFACTION MODEL*

Using logistic regression, Zhu et al. (2017) correlated observational data from 27 earthquakes around the globe with geospatial data on soil properties that are related to liquefaction manifestation. They found that the most promising results were achieved with a combination of

- peak ground velocity (**PGV**) in cm/s,
- shear wave velocity in the upper 30 m ($\mathbf{Vs_{30}}$) in m/s,
- annual precipitation (**PRECIP**) in mm,
- distance to the closest water body (**DW**) in km and
- water table depth (**WTD**) in m.b.g.l.

The model performed well for the 2010 Darfield and 2011 Christchurch event. However, both events were used in the calibration process, suggesting that the **performance might be overstated**.

RESEARCH GOAL

In order to better understand its prediction potential, the geospatial model is evaluated using liquefaction observational data from the **2016 Kaikōura earthquake**.

*Zhu J, Baise LG, & Thompson EM (2017). An updated geospatial liquefaction model for global application. *Bulletin of the Seismological Society of America, 107*(3),1365-1385.

OBSERVATIONAL DATA

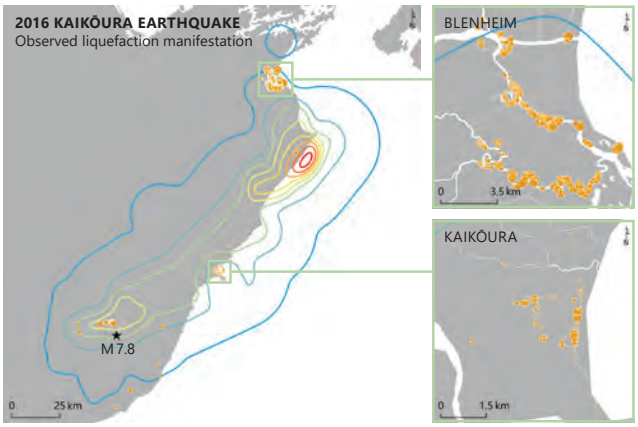

83% of liquefaction manifestation was observed in Blenheim and Kaikōura.

3RD PLACE

RESULTS & DISCUSSION

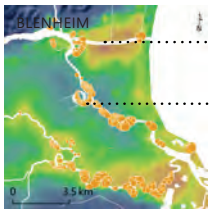

Overestimation of liquefaction severity.

Underestimation of liquefaction severity.

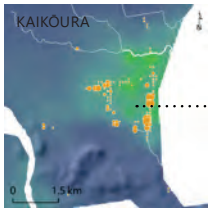

Overall **good representation** of liquefaction severity.

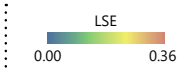

The **liquefaction spatial extent** (LSE) describes the areal coverage (in percent) of surface manifestation.

The comparison with the observational data indicates that the model performs well for the Kaikōura cluster but poorly for the Blenheim cluster.

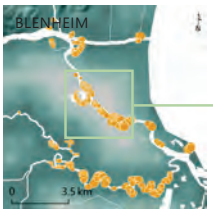

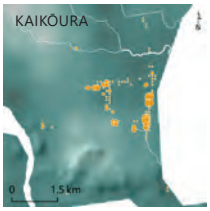

In the Blenheim cluster, DW is relatively high in the centre leading to the false assumption of a larger distance to the nearest water body.

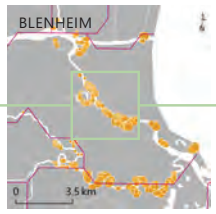

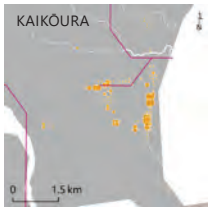

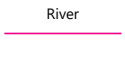

DW is defined as the minimum of the distance to the closest river and the distance to the nearest coastline. The **river streams** seem to be oversimplified.

The low resolution of the (global) river dataset leads to **spatial inaccuracy**, which contributes to the underestimation of liquefaction for the Blenheim cluster.

While the input variables are appropriate for large-scale hazard assessments as they provide global coverage, they might **not be suitable for regional or local application**.

Further research needs to evaluate the quality of the input variables across New Zealand and potentially consider the **use of national (high resolution) datasets**.

CONCLUSION

Despite showing promising prediction potential in some areas (e.g. Kaikōura), the geospatial model seems to be unsuitable for regional or local liquefaction assessments due to low resolution input variables (e.g. Blenheim).

AMELIA LIN | University of Auckland

This research is supervsied by Liam Wotherspoon (University of Auckland) and funded by the University of Auckland Doctoral Scholarship, QuakeCoRE and EQC.

NZGS Symposium 2021

Eleni Gkeli

CLOCKWISE FROM TOP LEFT: Eleni Gkeli and Ross Roberts opening the Symposium. Morning of Thursday 24 March – The main event begins!! The first online keynote speech by Sissy Nikolaou. MBIE and the Geotechnical Module update project panel answer the questions of the delegates.

THE 2021 NZGS Symposium in Dunedin on 25 and 26 of March 2021 will remain in our memories as one of the most eventful in the history of NZGS. Due to the impacts of the COVID-19 pandemic, the in-person event was uncertain throughout 2020 and eventually had to be postponed from its original date in October 2020. But in my view, it will also remain as one of the most anticipated, with engagement and enthusiasm by the delegates and supporters that humbled the organisers.

Due to the ban on international travel, the Symposium trialled a hybrid format including online and live presentations, with all international invited and keynote speakers (and some of the delegates) joining online. This was a first-time experience for the NZGS Symposium that I am sure will find more application in the future. In the times of the pandemic, our industry showed its resilience and adaptability to different ways of working and this format seemed to be well received by the delegates.

The theme of the Symposium was "Good grounds for the future" inspired by the profound changes that our world has been experiencing. It was a call for reflection on what our future will look like and how we can learn from the successes and the failures of our past to shape a better future for us and the generations to come.

The Symposium started with a pre-symposium event perfectly aligned with its theme. A half day workshop on the 23rd of March in Queenstown discussed landslides and current and future trends in slope monitoring. A mix of in-person and virtual presentations from Chris Massey and Peter Amos from New Zealand and Joseph Wartman, Michael J. Olsen and Mark Vessely from the United States provided valuable insight into the state of practice of slope monitoring both now and in the future. The workshop was oversubscribed with around 80 participants, and concluded with the promise that the discussion will continue.

The following day, the group of 80 split into two and loaded into buses for a field study with one

group heading to Macraes Mine and the other to the Clyde Dam through Kawarau and Cromwell Gorges. There were stops along the way to look at slope hazards and features of interest.

The Macraes Mine trip was led by David Stewart and involved a brief stop at the Deadmans Point rockslide near Cromwell, then through the Maniototo to Macraes Gold Mine. There, the group attended a presentation from Oceana Gold staff on the mine site and various pits that have been mined over the years. They then travelled into the 280m deep Frasers Pit for a first-hand look at the scale of the mine and the operations and activities being undertaken.

The Clyde Dam trip was led by Don Macfarlane with support from David Barrell of GNS. Contact Energy provided a tour of the dam and one the slope monitoring tunnels. The group was lucky enough to observe a test of the dam spillway gates, while the buffet lunch at a local café was certainly one of the highlights. Thank you to David and Don for organising, as well as to Contact Energy and Oceana Gold for making these field trips possible.

At the completion of the field trips, the two groups met at Hindon Siding to board the spectacular Taieri Gorge Railway, enjoy refreshments, catch up on the day and travel into Dunedin for the Welcome Reception, which took place at the Toitu Otago Settlers Museum. A tour through the museum exhibition, which is full of Dunedin and Otago Region history, was offered to the reception attendees, whose turnout on the evening was exceptional!

The main Symposium event officially kicked off on the 25th of March. The Dunedin Centre, the venue in the heart of the city with the unique baroque style and architecture hosted us for two full-on days of technical program. Apart from the keynote talks, the special sessions and the interactive plenary sessions, the Symposium included about 60 oral presentations and 23 poster presentations.

The exhibition was held in the impressive Town Hall decorated by 'Norma', the symphonic organ built in 1919. The organising committee was pleased to see all the exhibition spaces taken by the industry representatives, who finally had the opportunity to interact with the delegates in person in the breaks of the intensive technical program. The organising committee and NZGS sincerely value the commitment and patience of our exhibitors and all the sponsors through the bumpy journey of organising; the event would not have been possible without their support.

Four keynote talks by renowned international experts, delivered virtually, were focused on hot topics of our profession and attracted the interest. Dr. Sissy Nikolaou, in the opening keynote talked about the future of engineering resilience and functional recovery. Professor Ross Boulanger demonstrated the use of numerical modelling and a new user-defined strain-rate dependent constitutive model to provide reasonable approximations of undrained creep behaviours that can be important for static slope stability evaluations.

The keynote of George Gazettas discussed the performance and design of rigid gravity walls under strong seismic shaking; the talk revealed some of the limitations of the pseudo-static methods of analysis and investigated the main causes of the poor performance of these walls when they constitute quaywalls in harbours. Dr. Chris Haberfield discussed the design of retention systems for basements in rock in tight urban environments.

A good part of the Symposium was focused on regulation and guidance. The Chief Engineer of MBIE Mike Kerr and Kieran Saligame discussed balancing between regulation, community risk and community impact and informed us about MBIE's upcoming projects. Mike Stannard and Misko Cubrinovski updated us on the Geotechnical Modules finalisation project and in particular on the proposed changes to the Module 1 and the earthquake hazard.

Collaboration with our colleague structural engineers was the focus of a panel discussion on the second day of the Symposium. A lively and stimulating debate on our collaboration and soil structure interaction for the best outcome of the project was led by a panel of experts including the SESOC President Hamish McKenzie, Dr Alexei Murashev, Stuart Palmer and Dejan Novakov. The duration of the session was not enough to cover all the questions from the delegates. These remain in our agenda and NZGS will seek opportunities to organise future similar events in various centres to continue the discussion.

Our Symposium made a first step in exploring the role of our profession regarding climate change and sustainable geotechnical engineering with a few papers on environmentally sustainable solutions. NZGS, however, aims to continue this discussion with the industry, and looks forward to more fora and Symposia in the future exclusively devoted to sustainable geotechnical engineering practice.

The gala dinner of the Symposium, another oversubscribed part of the event, was delightful. The NZGS Chair Ross Roberts presented their well-deserved Life Member awards to Stuart Read and John Scott and the JW Ridley Geomechanics Paper Award to Dr. Mark Stringer for his paper on "Separation of pumice from soil mixtures".

I want to close this report with a special reference to the presentations delivered by the four young geotechnical professionals Jessie Beetham, Christoph Kraus, David Rowland and Michelle Willis in the YGP special breakfast on the second day. These papers were voted as best papers in the mini-Symposia that the local NZGS branches organise around the country and NZGS supported the four to attend and present in the main Symposium. I was impressed by the quality, the ingenuity, the empathy and the high technical level of all four presentations. By listening to these, I felt very confident that the geotechnical profession in New Zealand has definitely laid some *good grounds for its future*.

CLOCKWISE FROM TOP LEFT: The Clyde dam group observing the test of the spillway gates carried out on the day; The Clyde Dam group inside the dam structure; The infamous slip joint that will enable the dam to move if the secondary River Channel fault ruptures in a Dunstan fault event; Macraes Mine – bus; Macraes Mine Fieldtrip Group at Deadmans Point Rockslide.

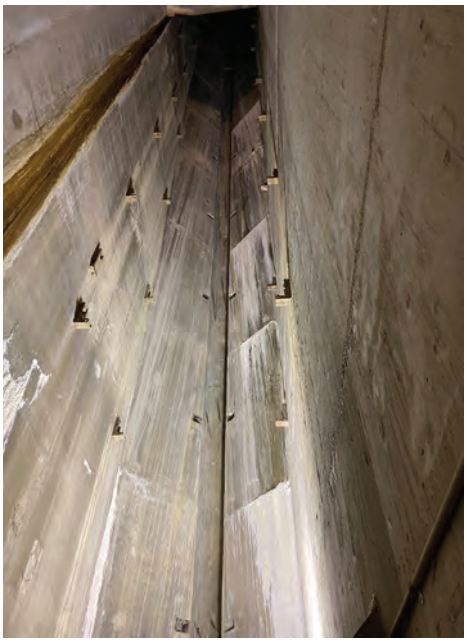

LEFT: Frasers pit is a huge 280m deep hole in schist bedrock, where very large active failures are managed through monitoring with slope radar. The portal for the underground portion of the mine is visible to the left.

ABOVE: The mists parted for us to have a clear view down into the Frasers pit and slope failure (this drone image is from the day before)!

LEFT: We were extremely fortunate to be able to finish our bus trips by historic train from Hindon to Dunedin through the scenic Taieri Gorge. The train is a victim of Covid – indications are that we may have been on the penultimate trip before it is retired for good!

Awards & Scholarship Report

Rolly Orense

2021 JW RIDLEY GEOMECHANICS PAPER AWARD (EVERY 3 YEARS)

THE CALL FOR nominations ended in 20 December 2020, and we received 6 papers for consideration. These were sent to the panel consisting of Mick Pender, Kevin McManus and CY Chin. Based on careful assessment, the panel was unanimous in recommending the following paper by Dr. Mark Stringer (Univ of Canterbury) as the recipient of the award:

- Stringer, ME (2019). Separation of pumice from soil mixtures. Soils and Foundations, 59(4): 1073-1084 (August 2019).

On 18/03/2021, a copy of the paper and the feedback from the panel members were circulated to the Management Committee members.

STUDENT POSTER COMPETITION (ANNUAL)

The registration deadline was 11 December 2020, while posters were due 31 January 2021. We received 6 submissions, and they were assessed by a panel consisting of: Sally Hargraves, Tony Fairclough and Robert Hillier. Per the panel's recommendation, the winners are:

1st Olivia ROSS / Julia YOUNG: Seismic and 1-D Compressibility Properties of Gravel-Rubber Mixtures (BE(Hons) student, University of Canterbury)

2nd Baqer ASADI: Liquefaction assessment of pumiceous soil: shear wave velocity-based method (PhD student, University of Auckland)

3rd Amelia LIN: Validation of a Geospatial Liquefaction Model (PhD student, University of Auckland)

NZGS SCHOLARSHIPS (BIENNIAL)

There were 4 applications received; 1 withdrew and 2 were shortlisted by the panel (consisting of CY Chin, Eleni Gkeli & Sally Dellow). The two applicants were interviewed by the panel separately last 11 February. Following the interview, the panel requested further clarifications/ refinements of the submitted research proposals. Last 10 March, one of the applicants withdrew due to work commitments. And on 16 March, the remaining applicant submitted her response to the panel's request.

As of this writing, the panel is still considering if the remaining candidate (applying to support further research post-PhD) will be given the scholarship (or not) with/ without conditions. Update will be provided once a decision is made.


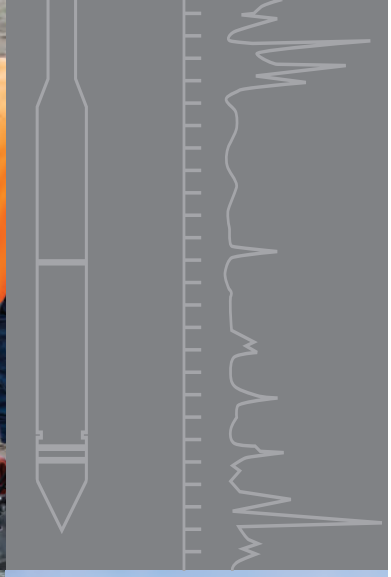






Geocivil is a IANZ accredited testing laboratory that provides services for the geotechnical and civil engineering industry.

Services we offer are;

- Full suite of soil classification testing
- Direct shear
- 1D consolidation
- CPT testing
- NDM compaction testing
- Static plate load and light weight deflectometer

Get in touch:

Otago
Joe@geocivil.co.nz
0276565231

Canterbury
Nick@geocivil.co.nz
0276565317

Wellington
Tony@geocivil.co.nz
0276565220

Northland
Darcy@geocivil.co.nz
0276565226

GEO CIVIL

TEST RIGHT • BUILD RIGHT

www.geocivil.co.nz

Tom Arnold

THE GEOTECHNICAL COMMUNITY has sadly been hit by tragedy in the last few weeks, with rope access contractor Tom Arnold falling victim to a fatal rockfall incident in Fiordland on April 20. Tom was undertaking geotechnical work in the Fiordland National Park when he died. He was 40 years old.

Tom was first exposed to rope access and rockfall slope stabilisation in Christchurch's Port Hills, following the 2011 Canterbury Earthquake sequence. He brought a healthy attitude to health and safety and positive working environment from his Franz Josef Glacier guiding days, and his field safety work in Antarctica. He was well known both in the rope access industry and within the geotechnical community – particularly in the South Island. He was closely involved with rock fall mitigation and worked on multiple projects over many parts of the Port Hills. His geotechnical rope access work took him all over New Zealand, including work in the mountainous regions of Mt Hutt, Arthurs Pass, Mt Cook National Park.

Tom became a familiar face to many of the geotechs and geologists in the South Island following the 2016 Kaikoura Earthquake. His experience and skillset were highly sought after for some of the trickier jobs that came up on the slopes above State Highway One. If you needed a tricky rock blasted – you'd get Tom, if you needed someone to dangle off a long line below a helicopter to get to a hard to reach spot, you'd get Tom. Although if it was summer you may have had to wait, as summers were usually spent working with Antarctica New Zealand as a field trainer and guide. On his return to New Zealand he would have plenty of stories to tell about his escapades on the ice. Tom had a thirst for adventure, but was extremely safety conscious. He did things properly. When you were up on a cliff working with Tom, you knew you were in good hands. He was good company too, and clearly loved his work. Losing Tom is a big loss to the not only his friends and family, but to the rope access, Antarctic, and geotechnical communities. Slope stabilisation won't be the same, or as safe, without him....

Dr Peter Kirkwood

Engineer, Tonkin + Taylor

DR PETER BRIAN KIRKWOOD, 33, was born and raised in Cardiff, Wales. The son of Paul and Katrina, brother to Beth, Matthew, and Edith.

He met his wife-to-be, Kerrie Ann, in the University of Cambridge Hillwalking Club, while completing a PhD in geotechnical engineering. After graduation, they spent time working, skiing, and climbing based out of Boulder, Colorado, before moving to New Zealand in 2018.

The mountains were central to Peter's life. He was a skilled and experienced tramper, mountaineer and backcountry skier, who had climbed numerous peaks in the European Alps, the Scottish Highlands, the North American Rockies, and the New Zealand Southern Alps.

He had recently become a father, and was looking forward to introducing his baby daughter, Elaine Sierra, to the mountains that he and Kerrie Ann loved so much.

A competent, careful engineer, who tackled complex geotechnical problems with relish, Peter was held in high esteem by his colleagues at Tonkin & Taylor.

He was a loyal and adventurous soul, who will be dearly missed by his friends in the UK, the US, and in Christchurch, where he and Kerrie Ann had made their home.

Richard Philips

Engineering Geologist, Tonkin + Taylor

To be attributed to the family of Richard Phillips

RICHARD ANTHONY PHILLIPS, 46, was a man dedicated to his family – his partner Jacqueline and their teenage daughters Freya and Indy.

He met Jac while travelling in Nepal in 1997. Together with their daughters, they made the move from the UK to New Zealand in 2008, and they have brought their girls up to share their love of the outdoors.

Rich was happiest in the hills with his family and his beloved dog Betsy. He was an experienced climber, hiker, mountain biker and diver who had travelled widely before settling in New Zealand. He was the sort of person who could turn his hand to anything, including having a hands-on role in building the family's home on the Port Hills in Christchurch.

He was a loyal and loving friend who would never fail to go the extra mile for anyone. He earned the respect and admiration of those he met at home, at work, on his travels and even on the sidelines of his girls' sporting events.

An engineering geologist, Rich joined Tonkin & Taylor in 2008. His colleagues will remember him for his technical expertise, his willingness to help, and his positive outlook on life.

He was the rock of his family and they are devastated by his loss, as are his parents Roy and Valerie, and his brother Stewart. His family appreciate all the support they have received as they come to terms with the loss of their most incredible father, partner, son, brother, and friend.

International Society for Soil Mechanics and Geotechnical Engineering (ISSMGE)

Vice President - Regional Report for Australasia

Philip Robins

Philip is a Technical Director – Geotechnical with Beca based in Wellington, with over 20 years' experience specialising in geotechnical analysis and design. He has been involved in the design and construction of major infrastructure projects in New Zealand, California, Hong Kong and Southern Africa. Philip was Chair of the NZGS Management Committee from 2009 to 2010.

THE ISSMGE IS the pre-eminent professional body representing the interests and activities of Engineers, Academics and Contractors all over the world that actively participate in geotechnical engineering.

See the ISSMGE website – http://www.issmge.org/ for full details of all ISSMGE activities.

1. INTRODUCTION

I am writing this report just following the announcement that the long awaited Tasman bubble is here. While the Covid-19 pandemic rages around the world, we can be justly proud of the lifestyle we have in New Zealand and Australia. Due to the pandemic, the ISSMGE Board Meeting was held via Zoom on 29 January 2021. The following is a summary of recent highlights of ISSMGE activities regionally and internationally.

2. BRIEF REPORT FROM THE PRESIDENT

The ISSMGE President asked all present to join him in expressing their condolences on the passing of Gavin Alexander, former ISSMGE Vice-President for Australasia. I thanked everyone for the outpouring of condolences which were collated, printed and pasted into a book, which was presented to Gavin's wife and two sons at a special ceremony.

The President confirmed that Antonio Gens would deliver the Terzaghi Oration at the 20ICSMGE and also noted that the pandemic had forced conference organisers to alter plans for their events. Some conferences were postponed, some changed to mixed-mode (partial attendance by generally local delegates and others participating via online broadcasts) and others forced to have a fully online virtual conference.

3. 20TH ICSMGE SYDNEY 2022

The ISSMGE Board agreed that the 20ICSMGE should be rescheduled to 2 – 5 May 2022 with the Council Meeting taking place on 1 May 2022. It was hoped that a full in-person conference and Council Meeting would be possible. It was noted that there would be no further change to the timing of the 20ICSMGE and that the conference and Council Meeting would take place on those dates as either in-person, hybrid or virtual events depending on travel restrictions in place at the time. Find out more on the 20thICSMGE Website (https://www.icsmge2021.org/).

The President invited the Board and Board-Level Committee Chairs to continue in their present posts until the new Board elections are completed in May 2022. All agreed to continue. The duration of next Board will still be approximately 4 years starting from May 2022.

4. NZGS SYMPOSIUM 2021

On behalf of the ISSMGE President and Board, I would like to congratulate the NZGS on a very successful Symposium in March. With over 250 live registrations, it was wonderful to see old friends and make new ones in Dunedin. Thank you for your attendance at the conference. A face to face conference is a rare event these days.

Thank you to all those who attended the Symposium and prepared technical papers. The organising committee, led by Eleni Gkeli, did an excellent job organising a wonderful event. Thanks also to the Conferences & Events team lead by Kerry South and the NZGS sponsors and exhibitors who hung on for the "wild ride" during the various lockdowns and alert level changes.

Photograph courtesy of Ross Roberts.

5. ISSMGE VIRTUAL UNIVERSITY

Mounir Bouassida gave an update on courses being assembled for the Virtual University, which now includes an almost complete Course 9 on "Landslides". L M Zhang has added a lecture for Course 10: "Risk analysis and machine learning" and Mounir has invited Chairs of TC304 (Engineering Practice of Risk Assessment and Management) and TC309 (Machine Learning and Big Data) to prepare lectures.

6. YMPG PROPOSAL – FUTURE OF GEOTECHNICS EVENT

The YMPG proposes to create an event that would be engaging for young geotechnical engineers and would attempt to imagine what the world and the field of geotechnics would look like in 40 years' time. Lucy Wu and her team are organising several events and these would conclude by September 2021. Outputs from the event would be edited and made suitable for the Time Capsule project.

7. ISSMGE TIME CAPSULE

At the ISSMGE board meeting Sukumar provided an update on the project. The time capsule now has a section on the ISSMGE website and blogs are being added. For further information, or to offer your support, please contact sukumar.pathmanandavel@gmail.com.

8. YGP NZGS

The NZGS has taken the unusual step of creating roles for YGPs to specifically be our liaison with each of the international societies. In the past our Young Geotechnical Professional rep did all of the internal NZ coordination, as well as linking with the international societies. The NZGS decided that more could be achieved with individuals specific to each society, and that it would also help increase the activity of young professionals to the NZGS and the international societies. I am pleased to welcome Nima Taghipouran as the NZGS ISSMGE liaison. You can find out more here: https://www.nzgs.org/new-ygp-roles-announced/

9. NEXT BOARD MEETING

The next ISSMGE Board Meeting will be held online in May 2021.

Philip Robins
ISSMGE Vice President for Australasia
philip.robins@beca.com

International Society for Rock Mechanics and Rock Engineering (ISRM)

Report for New Zealand – May, 2021

Paul Horrey

Paul Horrey is a principal and engineering geology specialist with Beca and manages the company's Southern Geotechnical Team based in Christchurch. He has worked extensively in New Zealand and overseas in infrastructure, mining and hydropower and has a particular interest in natural hazard mitigation and risk management.

THE REPORT ADDRESSES ISRM matters since the December 2020 edition of *NZ Geomechanics News*.

NEW NZGS YGP COORDINATOR FOR ISRM

It is a pleasure to welcome Romy Ridl as our very first ever NZGS YGP coordinator for ISRM in New Zealand. Romy was appointed to the role by NZGS following a selection process earlier in the year. Romy joins the other international society YGP coordinators Nima Taghipouran (ISSMGE) and Sarah Barrett (IAEG), all of whom will work alongside NZGS's overall YGP representative Helen Hendrickson.

Romy will also work closely with our Australasian VP for ISRM, Sevda Dehkhoda, who also leads the ISRM Young Engineers group.

BOARD AND COUNCIL MEETINGS:

The next ISRM Council and Board meetings will be held in conjunction with the Eurock Symposium in September 2021. Deadline for agenda items of the Council meeting is 22 June 2021.

ISRM AWARDS:

Nominations for the Rocha Medal 2022 are to be received by the ISRM Secretariat by 31 December 2021. The winner will be announced during the 2022 ISRM International Symposium, LARMS 2022 in Asuncion, Paraguay, and will be invited to receive the award and deliver a lecture at the ISRM International Congress in 2023.

YOUNG PROFESSIONALS WEBINARS

Some Young Members of different ISRM National Groups (France, Italy, Paraguay, and Spain) started working in the organization of a series of international webinars on rock mechanics, with the aim of involving young researchers and practitioners in a series of short presentation focussed on professional development.

We are current investigating whether a similar event could be run in New Zealand and Australia.

INTERNATIONAL SYMPOSIA 2021 AND 2022

- The 2021 ISRM International Symposium will be held in Torino, Italy 20-25 September 2021. This is now confirmed as a fully virtual event.

- The AusRock Conference 2022, the 6th Australasian Ground Control in Mining Conference, an ISRM Regional Conference will be held in Melbourne and online between 29 November and 1 December 2022. Abstract submissions are now open until 25 February 2022.

- The 2022 International Symposium will be held in conjunction with the IX Latin American Congress on Rock Mechanics, Rock Testing and Site Characterization in Asuncion, Paraguay on October 12-19 2022. Abstract submissions are open until 30 June 2021.

COVID19 EFFECTS

The ongoing effects of the pandemic continue to result in a number of changes to both timing and format of upcoming events. Please refer to the ISRM website for updated information.

TRAINING OPPORTUNITIES

ISRM ON-LINE LECTURES

Two on-line lectures have been given since the last report:

These have been recorded and are available on the ISRM website.

December 2020	**Empirical Design Methods in Underground Mining**	Prof. Antonio Samaniego
March 2021	**The role of rock mechanics in the safe and economic development of oil fields**	Prof. Sergio Fontoura

ONLINE COURSES

Four online courses have been added the ISRM website (https://www.isrm.net/gca/?id=912) in 2022 as follows:

Course name	Presenter/ co-ordinator	Sections
Prevention methods in Rock Mechanics and Rock Engineering	Prof. Zhong-qi Quentin YUE	• Understanding landslides in rock mass • Methods for quantifying rock mass • Methods for landslide potential of rock mass • Measures for preventing landslides in rock mass
Empirical Methods in Rock Mechanics and Rock Engineering: Tunnelling, Rock Joints, Rock Masses, and Rock Slopes, Cliffs and Mountain	Dr. Nick Barton	• The many faces of Q • Shear Strength of Rock, Rock Joint, etc • Failure Modes in Rock Masses • TBM Performance and Prognosis
Course on Monitoring Data Interpretation	Prof. Wulf Schubert	• Geotechnical monitoring for tunnels • Prediction on displacements and check of system behaviour with geofit • Use and important of deflection or state lines • Displacement vectors in cross and longitudinal section • Evaluation of displacement vector orientations and ratios of displacement components • Evaluation and prediction of lining utilization from displacement measurements
Rock Mass Characterization and Monitoring based on Advanced Remote Sensing Techniques	Prof. Leandro Alejano	• Introduction of advanced survey methods for rock mass characterisation and monitoring • Methods for automatic or semi-automatic discontinuity traces sampling on digital rock mass • Rock mass characterization and monitoring based on advanced remote sensing techniques • SAR interferometry in rock mechanics

OTHER ITEMS

Sadly, Professor Milton Kanji passed away on 12 February 2021. Details of Professor Kanji's life and work may be found in tributes on the IRSM website. The ISRM and the rock mechanics community deeply regret his loss.

Paul Horrey
NZGS ISRM Liaison
May, 2021

IAEG Report
June 2021

DOUG JOHNSON

Doug has a Master's degree in Engineering Geology from the University of Canterbury NZ (1984). He has worked on many mining, quarrying and civil engineering projects across a range of complex geological terrains, geographies and on both green and brown field site developments. Doug is currently Managing Director of Tonkin + Taylor and is passionate about people, the client experience, and technical solutions providing long term benefits to the community and the environment.

THE IAEG EXECUTIVE Committee met via Zoom on 23 April 2021. This was first meeting of the executive since the 2019 September Meeting in Jeju South Korea. The activities of the IAEG have been widely impacted by Coivd-19 and the annual 2020 executive and council meetings were not held. The committee is presently working through the re-establishment of the IAEG activities as travel and local, regional, and international conferences are starting to happen again in one form or another. Noting with the shift to new way of operating and to a revised programme of activities the bylaw and rules by which IAEG are governed are not designed for the current world context. A review of the IAEG bylaws and governance is being undertaken by a sub group of the IAEG Executive. A review of the commission supported by IAEG is also underway.

IAEG Membership in 2021 remains stable at 4294 paid members from 44 active National Groups. There have been new national groups established in South America and Europe, and these are to be ratified at the 2021 council meeting. 43.4% of IAEG membership comes from only 4 countries (China 13.6%, Germany 11.2%, NZ 10.7% and Australia 7.9%).

The finances of the IAEG remain stable with a surplus reported in 2020 due to reduced operational cost (mostly related to restricted travel of the Executive and reduced conference attendance). A neutral budget is forecast for 2021.

The most active part of the IAEG in 2020 has been the YGP groups and this was recognised and congratulated. Greater promotion and support to the YGP programme was discussed and it was encouraged that each National Group have a YGP sub-group or liaison person. NZGS already has this in place. The introduction of the YGP webinar series and posting of recorded conference key notes and lectures to the IAEG website has been well received. Noting the next event in YGP webinar series is the 9th with invited talks from Prof. Jordi Corominas Dulcet (Spain) & Dr. Anika Braun (Germany) on Rock Hazard and Future Considerations for 21 May at 12:00 GMT (Path: search for YEG IAEG's Zoom Meeting or subscribe to IAEG YEG on Youtube.com). A link to previous talks can also be found the IAEG Webpage.

The IAEG bulletin has again lifted its impact factor and now one the more highly sited technical journals and is now fully on-line. The success of the Bulletin as leading publication is celebrated. However, concerns over the bulletin content (highly computational and geotechnical biased and skewed contribution with over 90% of submitted papers from Asian countries) does not reflect the wider geologic and global representation of the IAEG membership. The falling contribution on geology, limited global case studies and the limited value of the papers to non-academic readers is concern for the Executive. A sub-group of the Executive have been asked to review the scope and nature of the IAEG publications (to report back in October). ailed weekly directly to members.

More work has been completed on the IAEG website and in particular the activity to upload and make more accessible IAGE lectures and YGP content. A request for more content was made.

An update on progress for the 2022 Congress was given. This remains in planning and progressing well. A call for papers will be issued soon. The Executive is expected to have further zoom meetings prior to the annual Executive and Council meeting in October 2021 (currently to linked to the European Regional Conference in Athens via a combination of physical and virtual attendance).

Branch Reports

SEE THE EVENTS DIARY OR WWW.NZGS.ORG FOR FUTURE EVENTS

GEO-NEWS WEEKLY E-NEWSLETTER
Our new weekly email lists all notices and Branch announcements normally sent to members, but in one email. Please send items to include to **secretary@nzgs.org**

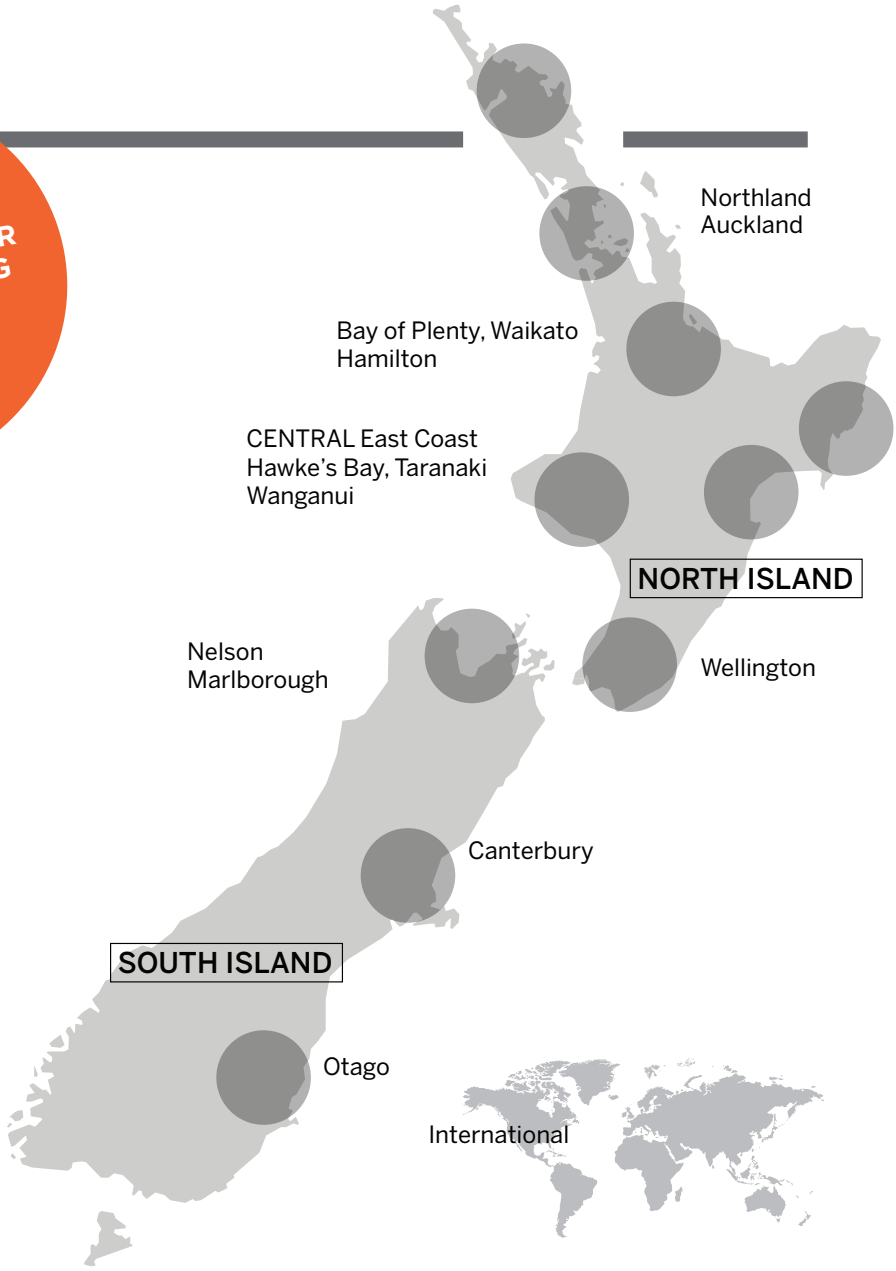

Auckland branch

The Auckland Branch kicked off the year with an online presentation by Dr. Robert Pyke from California on the Limitations of Simplified Methods for Estimating Seismic Settlements. The event was attended by more than 200 members. Yet another lockdown ensued in March, and our first in-person event for 2021 had to be delivered online. Dougal, Kyle and Julie from GNS presented on the fantastic work GNS has been doing on updating the geology of South Auckland.

The Branch is currently busy organising a number of in person and online events for the remainder of 2021 – these will include both NZ and international speakers. Although not an Auckland Branch organised event, a recent highlight was the exaugural lecture by Professor Michael J. Pender, which was keenly attended by a large audience that filled the room and networked before and after the talk. It was great to see so many geotechnical professionals coming together to celebrate the career of one of NZ's best geotechnical minds, and to recognise the influence that Mick has had on so many people's careers.

Ben & Jay would also like to welcome ex-Hawkes Bay Branch coordinator Sirini De Silva to the Auckland team, who will assist with organising and running events. If you would like to present to the Branch or have a specific topic you'd like to see covered, please touch base with the team.

Waikato Branch

Big changes afoot in the Hamilton branch - both Andrew Holland and Kori Lentfer are stepping down as branch coordinators after 10 and 12 years in the role respectively! Kori initially looked after both Waikato and BoP (from 2009) but when he moved to the Waikato in 2011, the branches split back into separate Waikato and BoP branches, with Kori taking over the Waikato branch, initially with Ken Read and then from late 2011 with Andrew Holland. Along with a number of local technical presentations on local ground conditions and projects, they have organised visits to various projects including the Te Uku windfarm, the Karapiro Gully Viaduct and the upgrades at the Waikato Hospital to name but a few. We would like to thank them both for all their endeavours over the last decade (and a bit) and to wish their successors all the best. As their successors work in the same offices as both Kori and Andrew, we're sure their collective wisdom will be around for a while longer!

Bay of Plenty branch

Tauranga branch has a few events in the pipeline. We hope that some of our local members were able to enjoy the NZGS 2021 conference in Dunedin in March. We have arranged for the NZGS Geomechanics Award paper to be presented by Mark Stringer in late May. There have been and continue to be a number of very good online presentations and locally Engineering NZ site visits or presentations which have included large portions of geotechnical / geological work. If members have ideas on presentations or would like to contribute a presentation please get in touch with James or Kim.

Hawkes Bay branch

"Hawkes Bay partnered up with the Engineering NZ Branch for a site visit to a local Large Dam site currently under construction. The site was remote, it was evening and it was raining - so we were pleased to see a combined turn out of a dozen people. It was great to interact with other disciplines, including quantity surveyors, water, civil & transport engineers."

Wellington branch

The Wellington branch is pleased to announce that the 2nd Wellington YGP Symposium will take place on 21 July 2021. More details will be sending out in NZGS newsletters.

Recently the Wellington branch is looking at organising joint presentations or panel discussions with seismologists and structural engineers to promote collaboration between different disciplines.

Nelson branch

The Nelson region has had a slow start to the year in terms of functions. A few members attended the Symposium last month and there was a couple of engineering NZ events including a maritime simulator experience and winery building tour and tasting. The new Nelson Tasman Geological map has been released giving an updated model of the region with the previous mapping dated 1987. We are always looking for more discussion group, function and presentation ideas so get in touch if you are keen!

Canterbury branch

The Christchurch branch were involved in a series of 'lessons learnt' presentations commemorating the 10 year anniversary of the Christchurch earthquake.

Looking forward we are excited to host a presentation by Mark Stringer covering his paper 'Separation of pumice from soil mixtures', which was recently awarded the JW Ridley Geomechanics Paper Award at the NZGS symposium. This was initially planned for mid-May however has been postponed to a later, yet to be confirmed, date. We will also be hosting a YGP symposium in early June and have had a good response from our YGP members.

We have a few talks in the pipeline however are keen to hear from anyone who would be keen to give a presentation, or has an idea for one.

Otago branch

We kicked off our year with a really interesting presentation from Phil Glassey (GNS, Dunedin) about his work on updating the geological model for South Dunedin, as part of a wider body of work aiming to address the flooding issues in South Dunedin. Coming up in the near future, we are working on organising a talk about rockfall protection. Further out, we're planning to organise some more interesting talks for our local members. And, of course, we thoroughly enjoyed having so many of our colleagues from around the country in Dunedin for the symposium in March

Branch Coordinators

NORTHLAND

PHILIP COOK

I am a Chartered Professional Engineer. I have an interest in risk assessment, landslides, Northland Allochthon geology, liquefaction, and seismic assessment for earthquake resistant foundations, foundation settlement. I look forward to improving the geotechnical features of soils in Northland. I enjoy the coastal lifestyle of Northland

phil@coco.co.nz

AUCKLAND

JAY DODDABALLAPUR

Jay is a Chartered Principal Geotechnical Engineer with an MSc in Geotechnical Engineering from the University of Glasgow. He has worked in the UK, Middle East and New Zealand on buildings, infrastructure and marine projects. He has experience in design and management of temporary and permanent works with a particular focus on providing value engineered, sustainable and buildable solutions.

jay.doddaballapur@aecom.com

BEN FRANCIS

Ben is a geotechnical engineer with Tonkin & Taylor in Auckland and has a BE(Hons) and MEngSt(Geotech) from the University of Auckland. He has a broad interest in geotechnical engineering design, with a focus in liquefaction and geotechnical earthquake engineering. He works on technically challenging projects across NZ and internationally.

BFrancis@tonkintaylor.co.nz

SIRINI DE SILVA

Sirini works at RDCL's Newmarket office as an Engineering Geologist. She graduated with a BSc (hons) from UoA in 2017 and briefly worked in Kaikoura for the NCTIR project. Sirini is experienced in geotechnical site investigations, ground modelling, materials testing, geohazards and liquefaction assessments.

sdesilva@rdcl.co.nz

WAIKATO

LUKE STANLEY

Luke is an engineering geologist with CMW Geosciences in Hamilton. He graduated from the University of Plymouth, UK with BSc (Hons), 2016 and MGeol Geology, 2017 before moving into the geotech sector. After working in the south-west of the UK, he decided to chase warmer climates and gain experience working with the very variable soils in the Waikato. He has been working with CMW since 2019 on projects throughout the central north island.

lukes@cmwgeo.com

BEN SMITH

Ben is an engineering geologist with HD Geo in Hamilton. He graduated from the University of Waikato to complete a BSc in GeoSciences in 2013, and has since gained knowledge and experience working on projects through the central north island. Outside of work he enjoys the outdoors, surfing, music and the odd DIY renovation project.

ben.smith@hdgeo.co.nz

SHIMA SHEYBANI AGHDAM

Shima is a geotechnical engineer currently working at HDGeo in Hamilton. She studied for a bachelor's in structural engineering in Azarbaijan before graduating with a Masters in geotechnical engineering in 2015 from Shahid Rajaee University in southern Iran. She moved to New Zealand in 2016 and joined HFC in Canterbury before moving to join HDGeo in April 2019.

shima@hdgeo.co.nz

GEO-NEWS WEEKLY E-NEWSLETTER

Our new weekly email lists all notices and Branch announcements normally sent to members, but in one email. Please send items to include to **secretary@nzgs.org**

BAY OF PLENTY

JAMES GRIFFITHS

James is an Engineering Geologist with Beca in Tauranga. After a previous life working in outdoor education and guiding on the Fox Glacier for 7 years, James studied Geology at Otago University, graduating in 2014 with a BSc (Hons). James has worked on site hazard assessments, geotechnical site investigations and ground modeling for a broad range of clients and market sectors.

James.Griffiths@beca.com

KIM DE GRAAF

Kim is a Senior Lecturer at the University of Waikato and a Senior Geotechnical Engineer with ENGEO and is based in Tauranga. Kim's experience includes earthworks, detailed seismic assessments, building foundation design, 3Waters projects and resilience. Kim's research interests cross a broad range of geotechnical areas including the behaviour of pumiceous soils, ground improvement and soil-foundation-structure-interaction.

KDeGraaf@engeo.co.nz

GISBORNE

FRANCIS NEESON

Frances is an Engineering Geologist and Eastern region Geotechnical Manager with LDE Ltd in Gisborne. She has over 12 years of experience having previously worked in Auckland, Christchurch, and Kaikoura. She has previously held the role YGP Rep on the NZGS Management Committee from 2014-2017. Frances is looking forward to building momentum with the new Gisborne Branch and actively contributing to the NZGS community again.

f.neeson@lde.co.nz

HAWKE'S BAY

TOM GRACE

Tom is a geologist who has worked for consulting companies on a large range of projects - predominately mineral exploration, mining feasibility & development and geotechnical projects in Southeast Asia, Canada, Australia and New Zealand. Tom has a strong interest in ground testing (CPT, surface and downhole geophysics, downhole testing).

tgrace@rdcl.co.nz

WELLINGTON

AIMEE RHODES

Aimee is a graduate geotechnical engineer with Opus. She recently completed her Masters degree in Earthquake Engineering with the University of Canterbury. Aimee has experience with liquefaction analysis and soil characterisation having worked on modelling liquefaction in stratified soils for her Masters research.

aimee.rhodes@wsp.com

SHIRLEY WANG

Shirley is a Geotechnical Engineer with 8 years of experience working at Tonkin & Taylor Wellington Office. She graduated from Canterbury University with a BE(Hons) in 2009. She has experience in seismic assessment, geotechnical and environmental investigation, slope stability, foundation design and construction monitoring.

SWang@tonkintaylor.co.nz

SAFIA MONIZ

Safia is a Chartered Professional Engineer who has worked in the Caribbean and New Zealand since graduating from the University of the West Indies with a Degree in Civil Engineering (Hons) in 2004. She completed a Masters in Geotechnical Engineering at MIT in 2009. Recent projects include deep foundation design and ground improvement for buildings and bridges.

safia.moniz@holmesconsulting.co.nz

NELSON

KYLIE JOHNSON

I'm an Engineering Geologist working for CGW Consulting Engineers based in Nelson. I have been a NZ geologist for the past 9 years and a keen member of NZGS. I work closely with our Engineering NZ branch to bring events and functions to the nelson region. I have a strong interest in site investigations and mapping around the Top of the South Region.

kylie@cgwl.co.nz

CANTERBURY

SARAH BARETT

Sarah is an Engineering Geologist at Beca Ltd in Christchurch. She has experience in natural hazard assessments and completed a PhD and post-doctoral role researching geomorphic influences on observed liquefaction following the 2010-2011 Canterbury earthquakes and 2016 Kaikoura earthquake, and evidence for paleo-liquefaction. In her spare time Sarah enjoys riding her horse and working on her lifestyle property.

sarah.barrett@beca.com

SAM BURGESS

Sam is a geotechnical engineer at Tonkin and Taylor in Christchurch. She has over 4 years' experience in geotechnical engineering, predominantly based in tunnelling projects. Outside of work she enjoys rock climbing, mountain biking and skiing.

SBurgess@tonkintaylor.co.nz

OTAGO

NIMA TAGHIPOURAN

Nima is a chartered professional engineer based in the WSP-Opus office in Dunedin. Nima graduated from the University of Auckland in 2012. He has been involved in a wide range of medium to large scale projects throughout the lower North Island. His areas of interest include foundation and retaining wall design, slope stabilisation and earthquake engineering.

nima.taghipouran@wsp.com

MATT FITZMAURICE

Matt is an engineering geologist in GHD's Dunedin office. He has 9 years' experience working in both the Western Australian mining industry (predominantly underground), and in New Zealand consultancies. Matt's areas of interest typically revolve around rock mechanics, and he loves to get out of the office and walk around the hills looking at rocks.

matthew.fitzmaurice@ghd.com

QUEENSTOWN

PAUL JAQUIN

Paul is a Chartered Professional Engineer, and is Work Group Manager for Buildings and Structures in the WSP Queenstown office. He works across a range of disciplines, including building foundations, bridge assessment, retaining walls, rockfall and landslide analysis. Paul holds a PhD in unsaturated soil mechanics and is a recognised expert in mud brick construction, providing advice and engineering expertise internationally.

Paul.Jaquin@wsp-opus.co.nz

NEW ZEALAND GEOTECHNICAL SOCIETY INC

The New Zealand Geotechnical Society (NZGS) is the affiliated organization in New Zealand of the International Societies representing practitioners in Soil mechanics, Rock mechanics and Engineering geology. NZGS is also affiliated to the Institution of Professional Engineers NZ as one of its collaborating technical societies.

The aims of the Society are:

a) To advance the education and application of soil mechanics, rock mechanics and engineering geology among engineers and scientists.
b) To advance the practice and application of these disciplines in engineering.
c) To implement the statutes of the respective international societies in so far as they are applicable in New Zealand.
d) To ensure that the learning achieved through the above objectives is passed on to the public as is appropriate.

All society correspondence should be addressed to the Management Secretary (email: secretary@nzgs.org).

The postal address is NZ Geotechnical Society Inc, P O Box 12 241, WELLINGTON 6144.

WELCOME TO THE first issue of 2021.

The year has got off to a roaring start with our Dunedin Symposium in March.

It was great meeting familiar names and putting them to faces. Attendees at the Symposium were very happy to finally see this come to fruition, as were those that put in the hard work in bringing us this successful event with special thanks to the sponsors!

Teresa Roetman

Please remember to contact the Management Secretary (Teresa) if you wish to update any membership, address or contact details. If you would like to assist your Branch, as a presenter or sponsor, or to provide a venue, refreshments, or an idea, please drop a line to your Branch Co-ordinator or Teresa. If you require any information about other events or conferences, the NZGS Committee and NZGS projects, or the International Societies (IAEG, ISRM and ISSMGE) please contact the Secretary on secretary@nzgs.org You may also check the Society's website for Branch and Conference listings, and other Society news: www.nzgs.org

Management Committee 2019-2020

POSITION	NAME	EMAIL
Chair	Ross Roberts	chair@nzgs.org
Vice-Chair & Treasurer	Eleni Gkeli	treasurer@nzgs.org
Immediate Past Chair	Tony Fairclough	TFairclough@tonkin.co.nz
Elected Member	Sally Dellow	S.Dellow@gns.cri.nz
Elected Member	Sally Hargraves	sally@tfel.co.nz
Elected Member	Rolando Orense	r.orense@auckland.ac.nz
Elected Member	Jen Smith	jsmith@tonkintaylor.co.nz
Appointed Member	Teresa Roetman	secretary@nzgs.org
Co-opted Website Editor	Olivia Gill	Oliviag@cmwgeo.com
Co-opted NZ Geomechanics Editor	Don Macfarlane	don.macfarlane@aecom.com
NZ Geomechanics Editor Co-editor	Gabriele Chiaro	gabriele.chiaro@canterbury.ac.nz
Co-opted YGP Representative	Aine McCarthy	aineymcc@gmail.com
IAEG Australiasian Vice President	Doug Johnson	DJohnson@tonkintaylor.co.nz
ISRM Australiasian Vice President	Paul Horrey	Paul.Horrey@beca.com
ISSMGE Australasian Vice President	Phil Robins	Philip.Robins@beca.com

EDITORIAL POLICY

***NZ Geomechanics News* is a biannual bulletin issued to members of the NZ Geotechnical Society Inc.**

Readers are encouraged to submit articles for future editions of *NZ Geomechanics News*. Contributions typically comprise any of the following:

- technical papers which may, but need not necessarily be, of a standard which would be required by international journals and conferences
- technical notes of any length
- feedback on papers and articles published in *NZ Geomechanics News*
- news or technical descriptions of geotechnical projects
- letters to the NZ Geotechnical Society or the Editor
- reports of events and personalities
- industry news
- opinion pieces

Please contact the editors (editor@nzgs.org) if you need any advice about the format or suitability of your material.

Articles and papers are not normally refereed, although constructive post-publication feedback is welcomed. Authors and other contributors must be responsible for the integrity of their material and for permission to publish. Letters to the Editor about articles and papers will be forwarded to the author for a right of reply. The editors reserve the right to amend or abridge articles as required.

The statements made or opinions expressed do not necessarily reflect the views of the New Zealand Geotechnical Society Inc.

NEW ZEALAND GEOTECHNICAL SOCIETY INC

NZGS Membership SUBSCRIPTIONS

Annual subscriptions cost $135 per member. First time members will receive a 50% discount for their first year of membership; and student membership is free. Membership application forms can be found on the website http://www.nzgs.org/membership.htm or contact the NZGS Secretary on secretary@nzgs.org for more information.

Letters or articles for *NZ Geomechanics News* should be sent to editor@nzgs.org.

Advertisers' Directory

MEMBERSHIP

Engineers, scientists, technicians, contractors, students and others who are interested in the practice and application of soil mechanics, rock mechanics and engineering geology are encouraged to join.

Full details of how to join are provided on the NZGS website http://www.nzgs.org/about/

ADVERTISING

NZ Geomechanics News is published twice a year and distributed to the Society's 1000 plus members throughout New Zealand and overseas. The magazine is issued to society members who comprise professional geotechnical and civil engineers and engineering geologists from a wide range of consulting, contracting and university organisations, as well as those involved in laboratory and instrumentation services. NZGS aims to break even on publication, and is grateful for the support of advertisers in making the publication possible.

TYPE	BLACK AND WHITE	COLOUR	SPECIAL PLACEMENTS		SIZE
			INSIDE FRONT OR BACK COVER	OPPOSITE CONTENTS PAGE	
Double A3	-	$1400	$1600 (front A3)		420mm wide x 297mm high
Full page A4	$600	$700	$1000	$1000	210mm wide x 297mm high
Half page	$300	$350	-		90mm wide x 265mm high 210mm wide x 148mm high
Quarter page	$150	$175	-		90mm wide x 130mm high

Flyers/inserts	From $700 for an A4 page, contact us for an exact quote to suit your requirements as price depends on weight and size.

NOTES

1. All rates given per issue and exclude GST
2. Space is subject to availability
3. A 3mm bleed is required on all ads that bleed off the page.
4. Advertiser to provide all flyers
5. Advertisers are responsible for ensuring they have all appropriate permissions to publish. This includes the text, images, logos etc. Use of the NZGS logo in advertising material is not allowed without pre-approval of the NZGS committee.

National and International Events

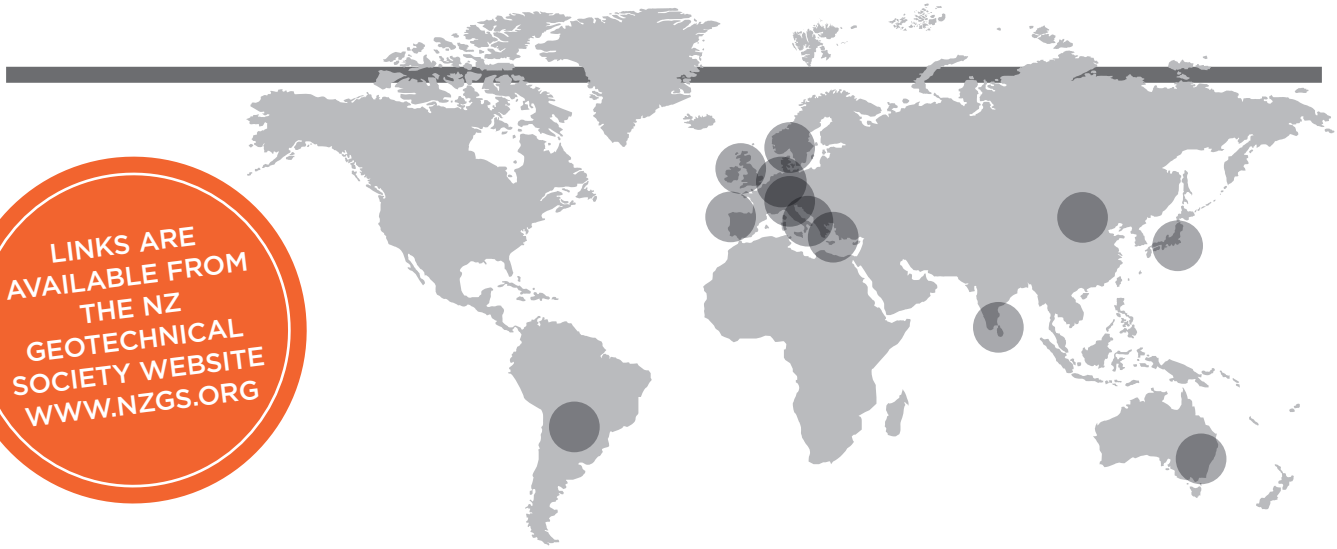

LINKS ARE AVAILABLE FROM THE NZ GEOTECHNICAL SOCIETY WEBSITE WWW.NZGS.ORG

2021

9-10 September
Fukuoka, Japan
5th International Workshop on Rock Mechanics and Engineering Geology in Volcanic Fields.

20-25 September
Virtual Symposium
EUROCK TORINO 2021

30 October
London, England
British Tunnelling Society Conference and Exhibition

21-25 October
Beijing, China
ARMS11 – 11th Asian Rock Mechanics Symposium – Challenges and Opportunities in Rock Mechanics

6 -7 December
Colombo, Sri Lanka
3rd International Conference on Geotechnical Engineering

2022

SYDNEY ICSMGE 2022
A GEOTECHNICAL DISCOVERY DOWN UNDER

1 – 5 May
Sydney, Australia
20th International Conference on Soil Mechanics and Geotechnical Engineering

15-18 May
Asuncion, Paraquay
LARMS2022 IX Latin American Congress on Rock Mechanics

8-10 June
Bologna, Italy
5th International Symposium on Cone Penetration Testing (CPT'22)

26-28 June
Chania, Greece
9th International congress on Environmental Geotechnics

27-29 June
University of Cambridge, England
TC204: Goetechnical Aspects of Underground Construction in Soft Ground

12-15 September
Helsinki, Finland
EUROOCK2022

20-23 September
Rotterdam, The Netherlands
11th International Conference on Stress Wave Theory and Design and Testing Methods for Deep Foundations

29 -1 November/ December
Melbourne, Australia
AusRock2022 - 6th Australasian Ground Control in Mining Conference

2023

9-14 October
Salzberg, Austria
15th ISRM International Congress on Rock Mechanics

2024

25-30 August
Lisborn, Portugal
XVIII European Conference on Soil Mechanics and Geotechnical Engineering





YOUR PARTNER FOR ALL GROUND ENGINEERING PROJECTS IN ANY ENVIRONMENT

An Engineering and Construction Company providing innovative restricted access solutions. Renowned for delivering complex projects safely in any environment operating Ground Engineering and Asset Integrity Management businesses.

- Ground Anchors
- Soil Nails
- Confined Space & Low Overhead
- Drilling
- Slope Stabilisation
- Rockfall Protection
- Debris Flow Systems
- Erosion Control Matting
- Grout Plant
- Reinforced Shotcrete
- Hyrdroseeding
- Ecocell Installation
- Retaining Walls
- Micro Piling
- Tunnel Remediation & Strengthening

www.geovert.com

Auckland Office
15 Kaimahi Rd, Wairau Valley
Auckland 0627, New Zealand
P: +64 3 837 7808 | F: +64 9 837 7809

GEOVERT
New Zealand | Australia | Singapore | United States

Christchurch Office
39 Francella St, Bromley
CHCH 8062, New Zealand
P: +64 9 962 5840 | F: +64 3 837 7809

menard

CentrePort, Wellington

We provided our specialist expertise and installed stone columns on a triangular grid pattern, to 20 m depth to create a stabilised landmass, prevent lateral displacement and control settlement within the main operational areas of the Port, in the event of future earthquakes.

Ground Improvement Specialists

Jet grouting

Soil Mixing

Stone columns

Grouting

Vibro compaction

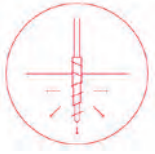

CMC

and more...

CHRISTCHURCH BRISBANE PERTH MELBOURNE SYDNEY

Contact us!

www.menardoceania.co.nz